Density Model for North Atlantic Right Whale (*Eubalaena glacialis*) for the U.S. East Coast: Supplementary Report

Duke University Marine Geospatial Ecology Lab*

Model Version 5.6 - 2016-04-21

Citation

When referencing our methodology or results generally, please cite our open-access article:

Roberts JJ, Best BD, Mannocci L, Fujioka E, Halpin PN, Palka DL, Garrison LP, Mullin KD, Cole TVN, Khan CB, McLellan WM, Pabst DA, Lockhart GG (2016) Habitat-based cetacean density models for the U.S. Atlantic and Gulf of Mexico. Scientific Reports 6: 22615. doi: 10.1038/srep22615

To reference this specific model or Supplementary Report, please cite:

Roberts JJ, Best BD, Mannocci L, Fujioka E, Halpin PN, Palka DL, Garrison LP, Mullin KD, Cole TVN, Khan CB, McLellan WM, Pabst DA, Lockhart GG (2016) Density Model for North Atlantic Right Whale (*Eubalaena glacialis*) for the U.S. East Coast Version 5.6, 2016-04-21, and Supplementary Report. Marine Geospatial Ecology Lab, Duke University, Durham, North Carolina.

Copyright and License

Revision History

Version	Date	Description of changes
1	2013-02-20	Draft model of spring season only, for NOAA internal meetings.
2	2013-04-30	All four seasons modeled; many improvements implemented, too numerous to list.
3	2013-05-08	Figures regenerated with improved label placement. No changes to models.
4	2014-05-28	Shrunk spring and fall seasons to two months, expanded summer to five. Reformulated density model using a Horvitz-Thompson estimator. Eliminated GAM for group size (consequence of above). Added group size as a candidate covariate in detection functions (benefit of above). Added survey ID as a candidate covariate in NOAA NARWSS detection functions. Took more care in selecting right-truncation distances. Fitted models with contemporaneous predictors, for comparison to climatological. Switched SST and SST fronts predictors from NOAA Pathfinder to GHRSST CMC0.2deg L4. Changed SST fronts algorithm to use Canny operator instead of Cayula-Cornillon. Switched winds predictors from SCOW to CCMP (SCOW only gives climatol. estimates.) Added DistToEddy predictors, based on Chelton et al. (2011) eddy database. Added cumulative VGPM predictors, summing productivity for 45, 90, and 180 days. Added North Atlantic Oscillation (NAO) predictor; included 3 and 6 month lags. Transformed predictors more carefully, to better minimize leverage of outliers. Implemented hybrid hierarchical-forward / exhaustive model selection procedure. Model selection procedure better avoids concurvity between predictors. Allowed GAMs to select between multiple formulations of dynamic predictors. Adjusted land mask to eliminate additional estuaries and hard-to-predict cells.

*For questions, or to offer feedback about this model or report, please contact Jason Roberts (jason.roberts@duke.edu)

5	2015-01-20	TODO: Describe this update.
5.1	2015-01-20	Updated the documentation. No changes to the model.
5.2	2015-03-06	Updated the documentation. No changes to the model.
5.3	2015-04-06	Updated the documentation. No changes to the model.
5.4	2015-05-14	Updated calculation of CVs. Switched density rasters to logarithmic breaks. No changes to the model.
5.5	2015-10-12	Updated the documentation. No changes to the model.
5.6	2016-04-21	Switched calculation of monthly 5% and 95% confidence interval rasters to the method used to produce the year-round rasters. (We intended this to happen in version 5.4 but I did not implement it properly.) Updated the monthly CV rasters to have value 0 where we assumed the species was absent, consistent with the year-round CV raster. No changes to the other (non-zero) CV values, the mean abundance rasters, or the model itself.

Survey Data

Survey	Period	Length (1000 km)	Hours	Sightings
NEFSC Aerial Surveys	1995-2008	70	412	36
NEFSC NARWSS Harbor Porpoise Survey	1999-1999	6	36	2
NEFSC North Atlantic Right Whale Sighting Survey	1999-2013	432	2330	1543
NEFSC Shipboard Surveys	1995-2004	16	1143	11
NJDEP Aerial Surveys	2008-2009	11	60	0
NJDEP Shipboard Surveys	2008-2009	14	836	2
SEFSC Atlantic Shipboard Surveys	1992-2005	28	1731	1
SEFSC Mid Atlantic Tursiops Aerial Surveys	1995-2005	35	196	5
SEFSC Southeast Cetacean Aerial Surveys	1992-1995	8	42	0
UNCW Cape Hatteras Navy Surveys	2011-2013	19	125	0
UNCW Early Marine Mammal Surveys	2002-2002	18	98	7
UNCW Jacksonville Navy Surveys	2009-2013	66	402	2
UNCW Onslow Navy Surveys	2007-2011	49	282	0
UNCW Right Whale Surveys	2005-2008	114	586	22
Virginia Aquarium Aerial Surveys	2012-2014	9	53	3
Total		895	8332	1634

Table 2: Survey effort and sightings used in this model. Effort is tallied as the cumulative length of on-effort transects and hours the survey team was on effort. Sightings are the number of on-effort encounters of the modeled species for which a perpendicular sighting distance (PSD) was available. Off effort sightings and those without PSDs were omitted from the analysis.

Season	Months	Length (1000 km)	Hours	Sightings
Winter	Nov Dec Jan Feb	237	1718	371
Spring	Mar Apr	188	1320	326
Summer	May Jun Jul	296	3005	845
Fall	Aug Sep Oct	176	2289	92

Table 3: Survey effort and on-effort sightings having perpendicular sighting distances, summarized by season.

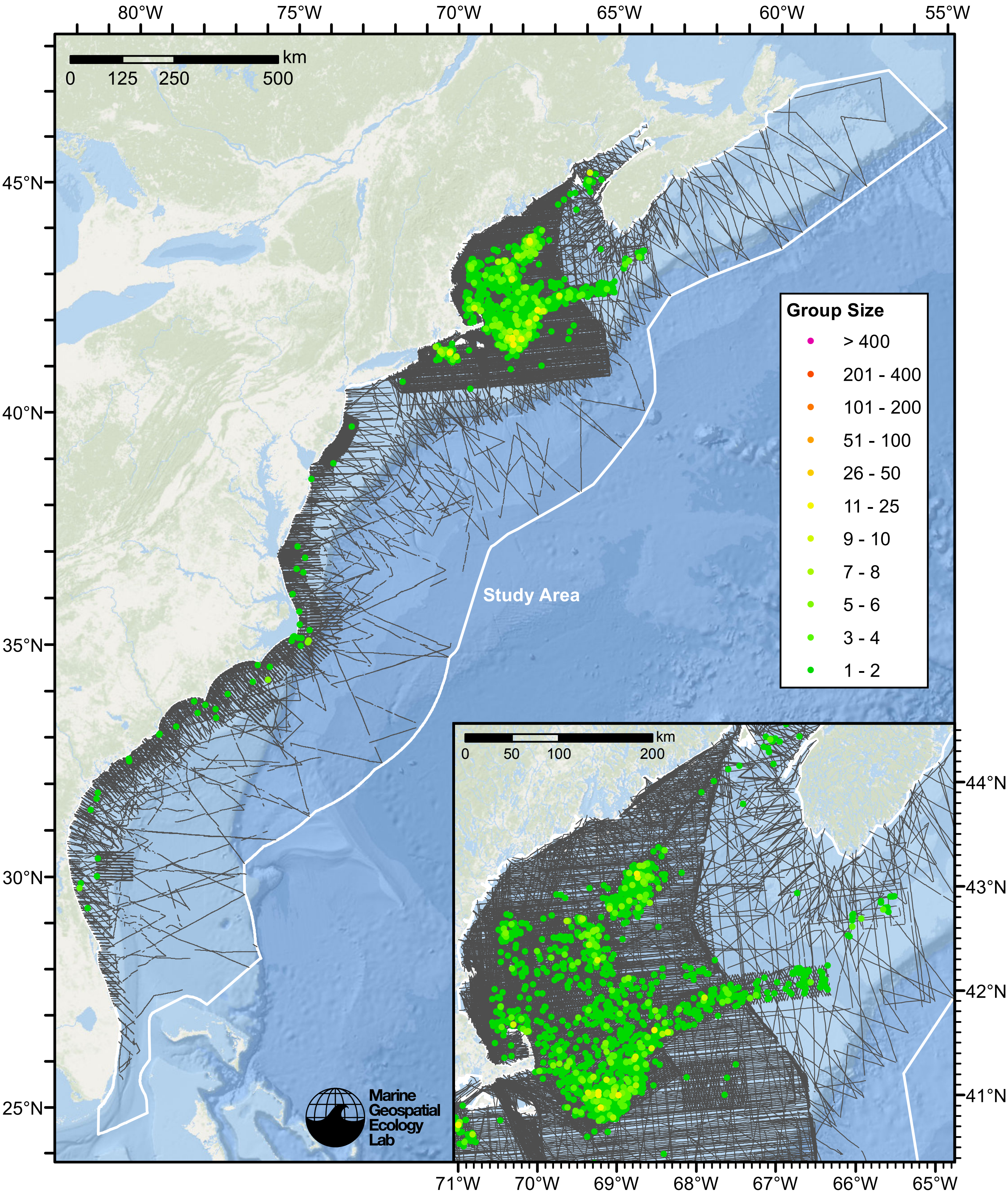

Figure 1: North Atlantic right whale sightings and survey tracklines.

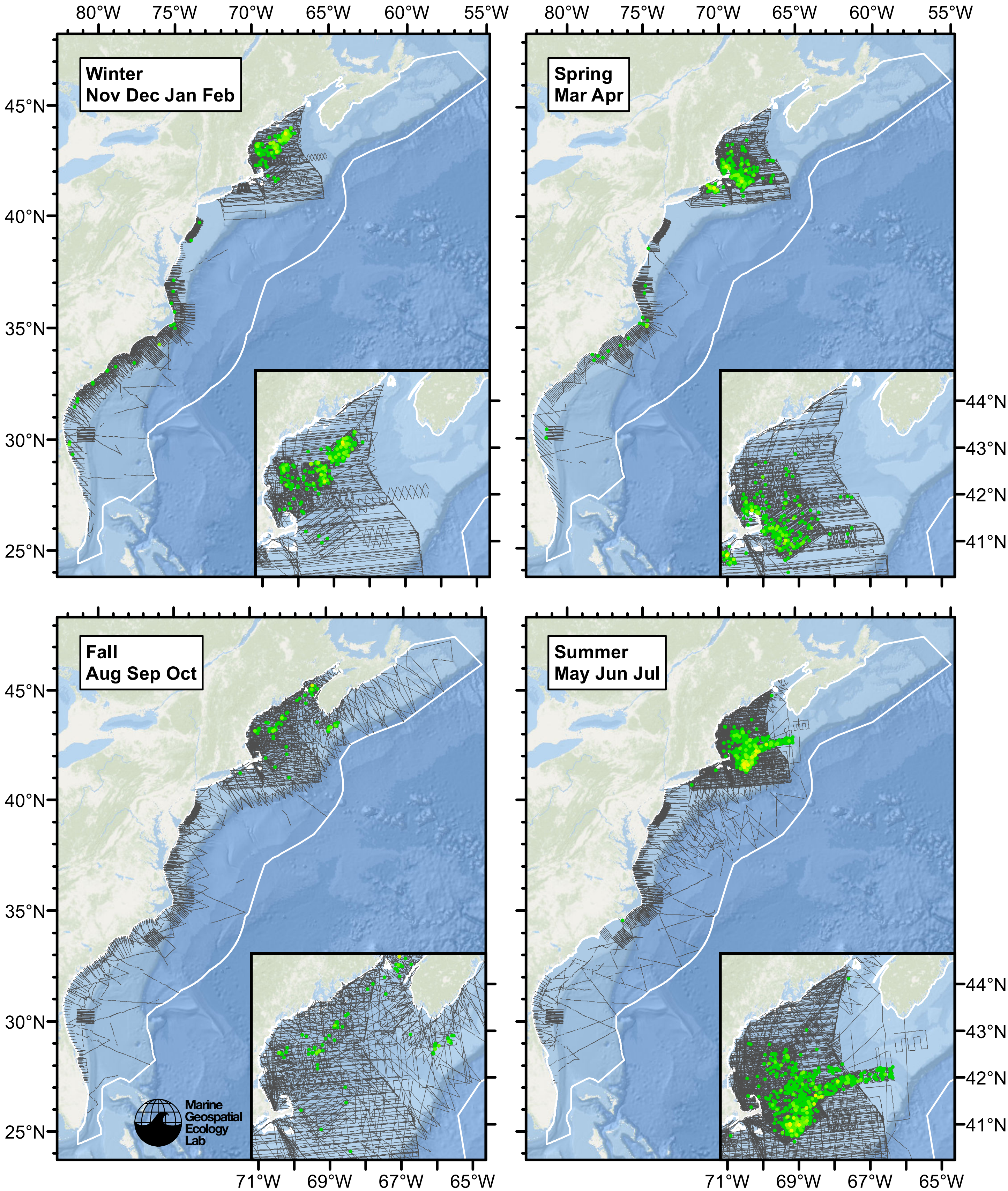

Figure 2: North Atlantic right whale sightings and survey tracklines, by season. Sighting colors are the same as the previous figure.

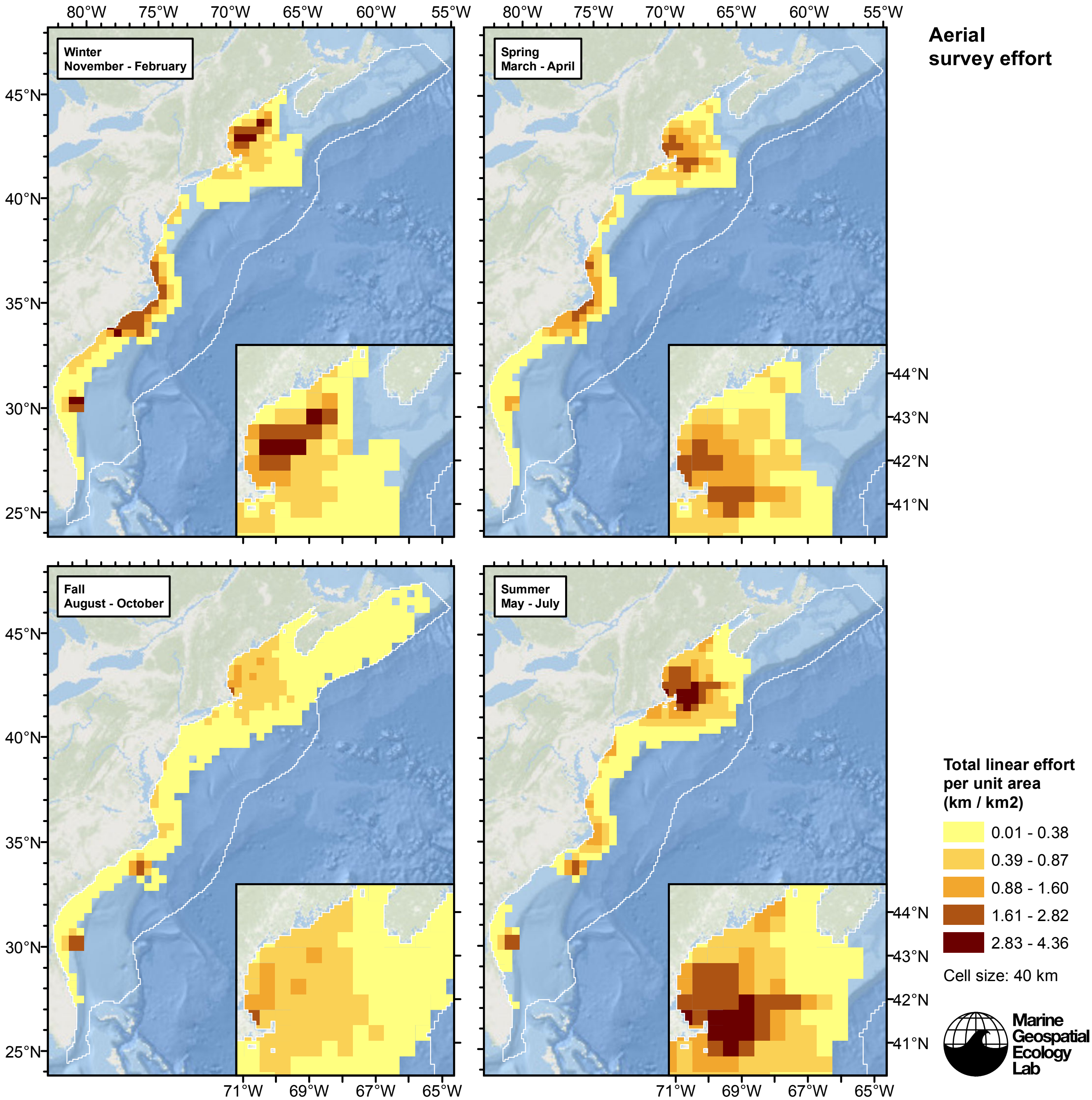

Figure 3: Aerial linear survey effort per unit area.

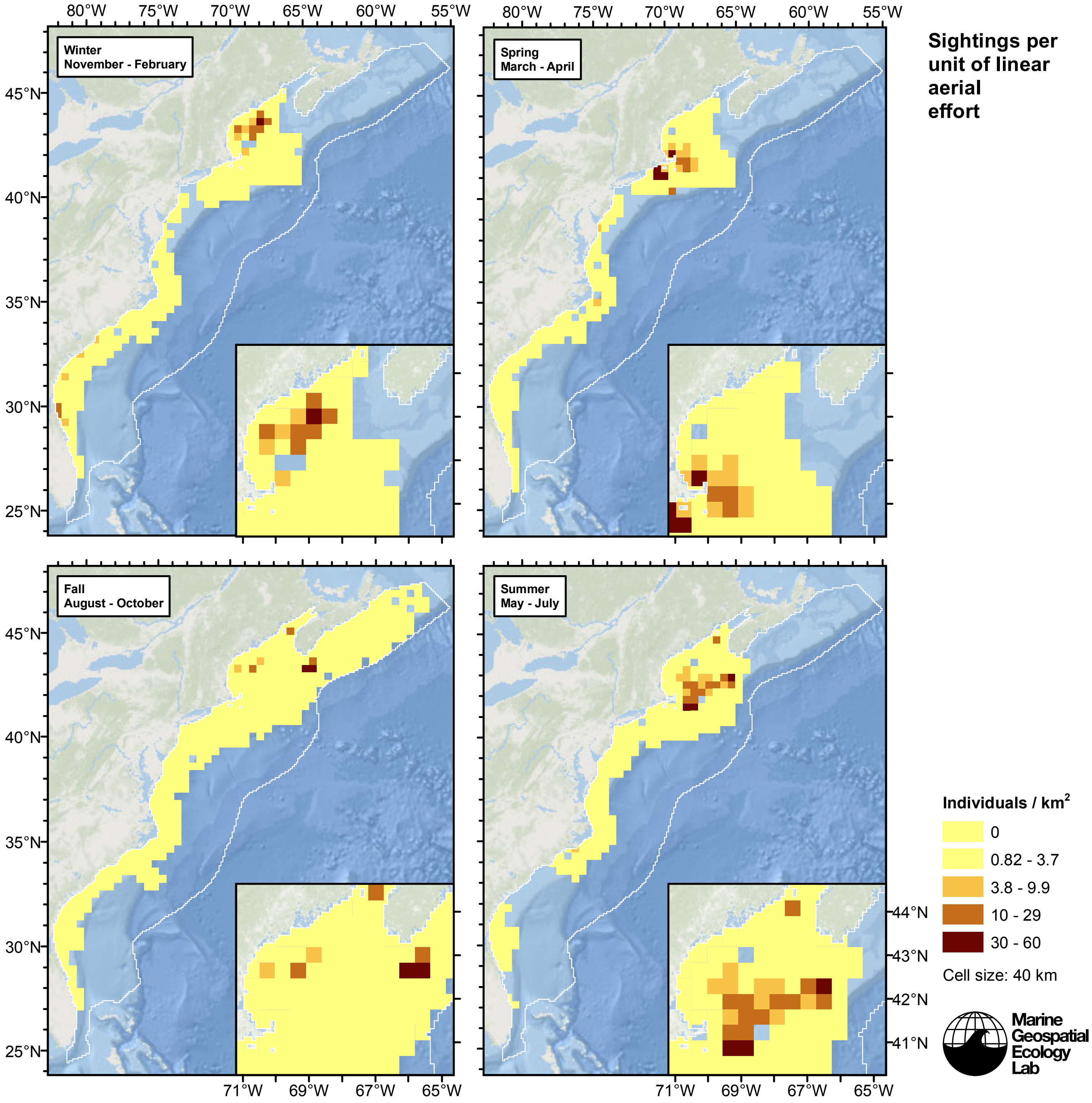

Figure 4: North Atlantic right whale sightings per unit aerial linear survey effort.

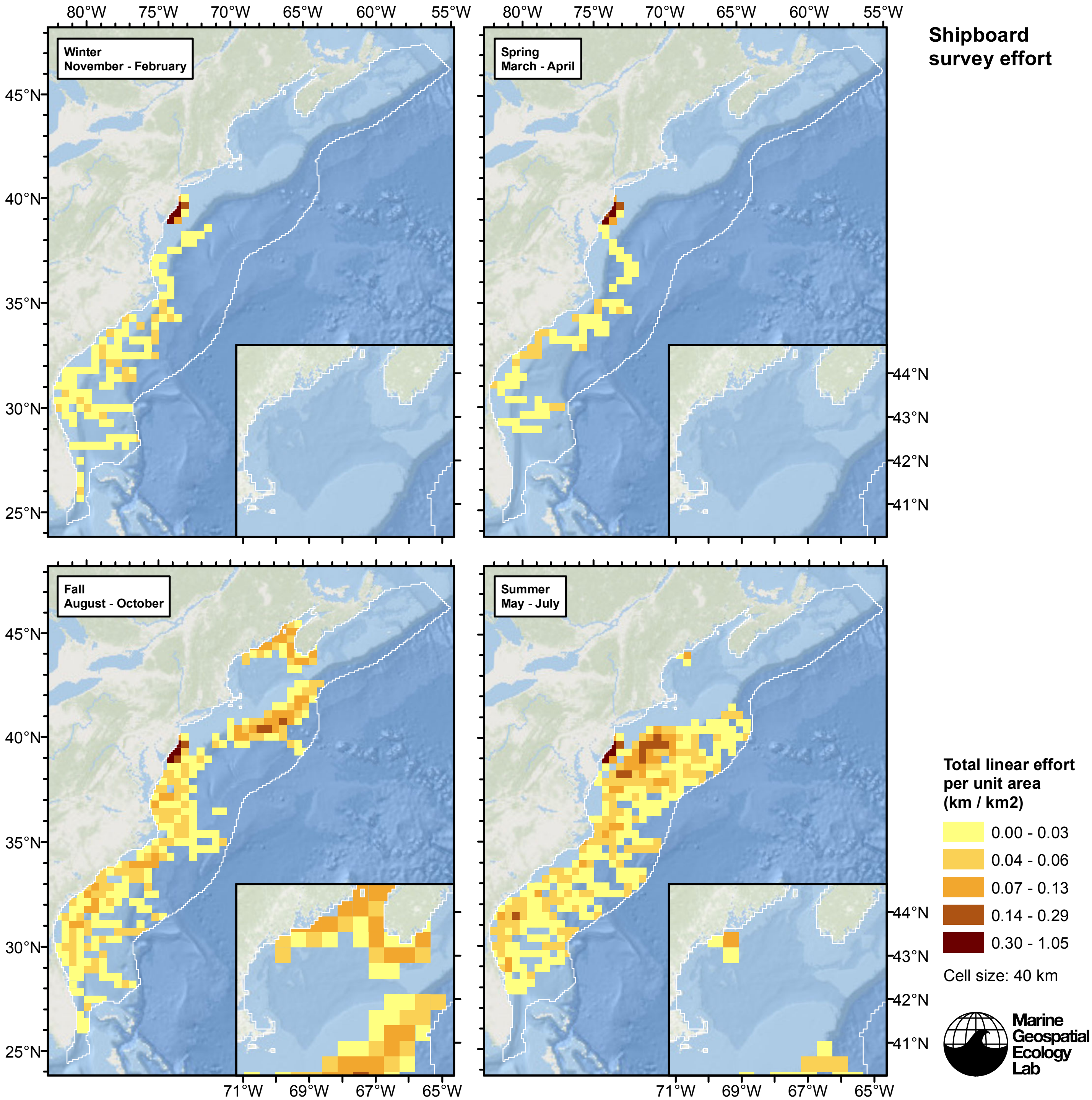

Figure 5: Shipboard linear survey effort per unit area.

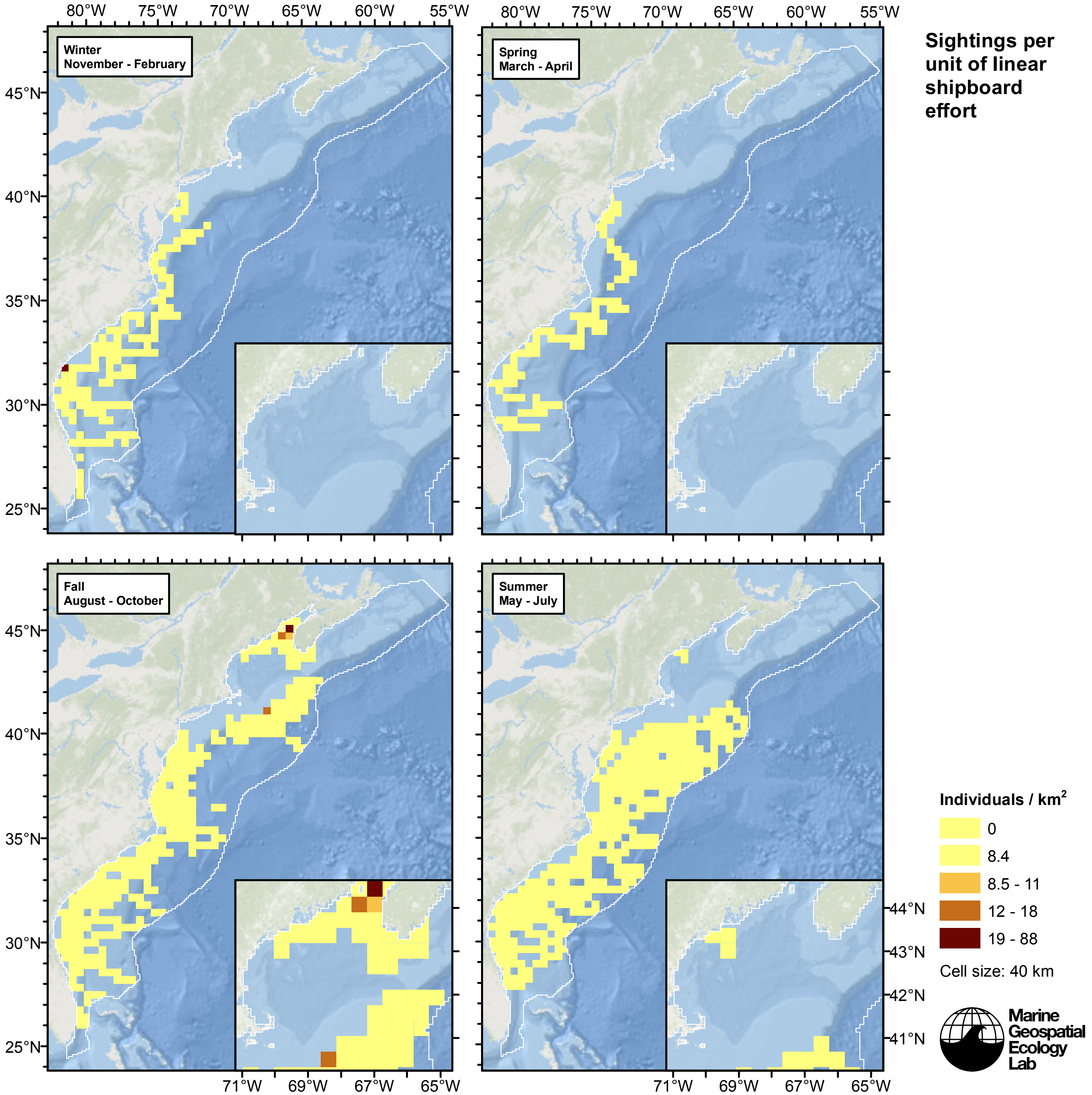

Figure 6: North Atlantic right whale sightings per unit shipboard linear survey effort.

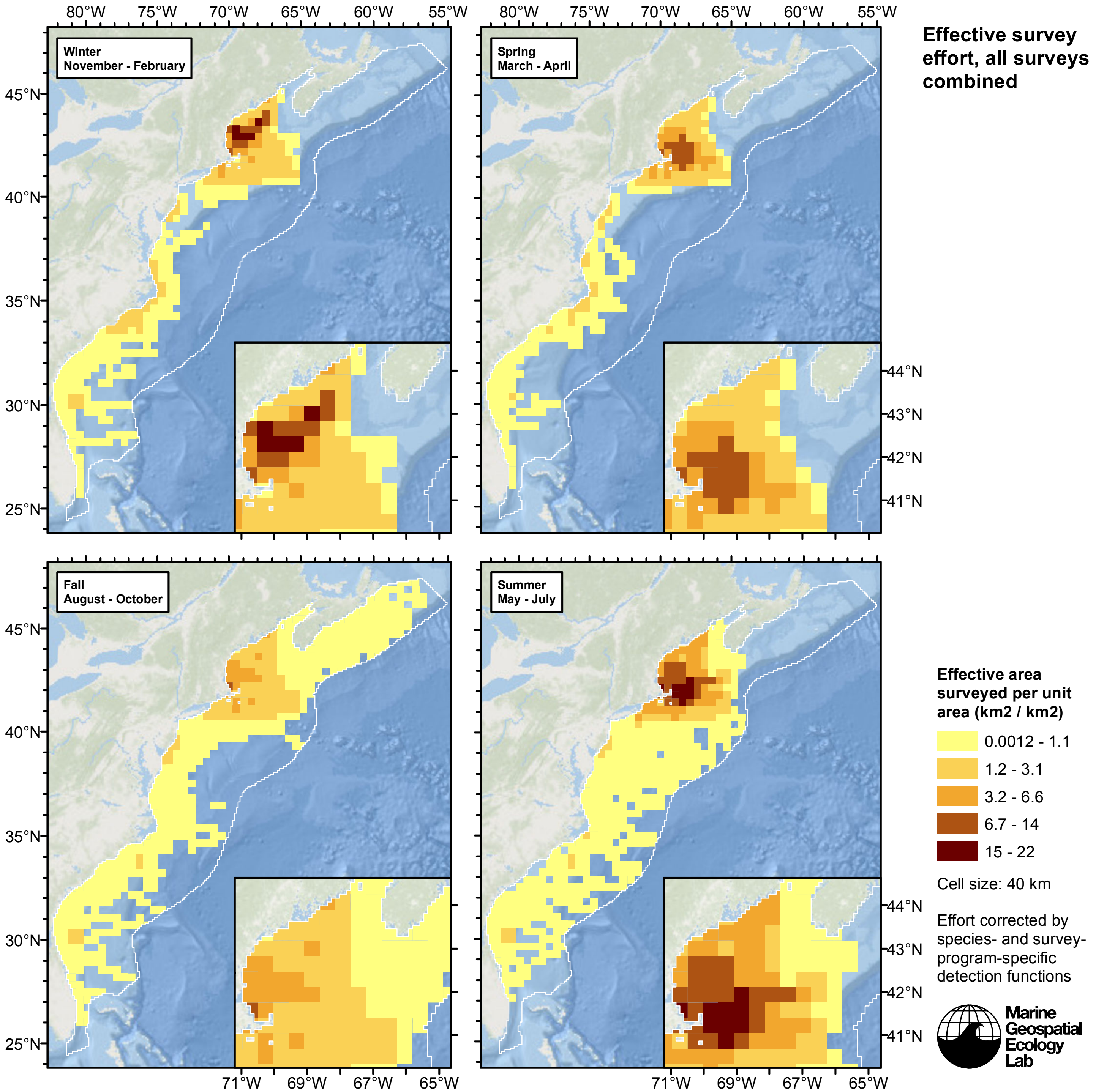

Figure 7: Effective survey effort per unit area, for all surveys combined. Here, effort is corrected by the species- and survey-program-specific detection functions used in fitting the density models.

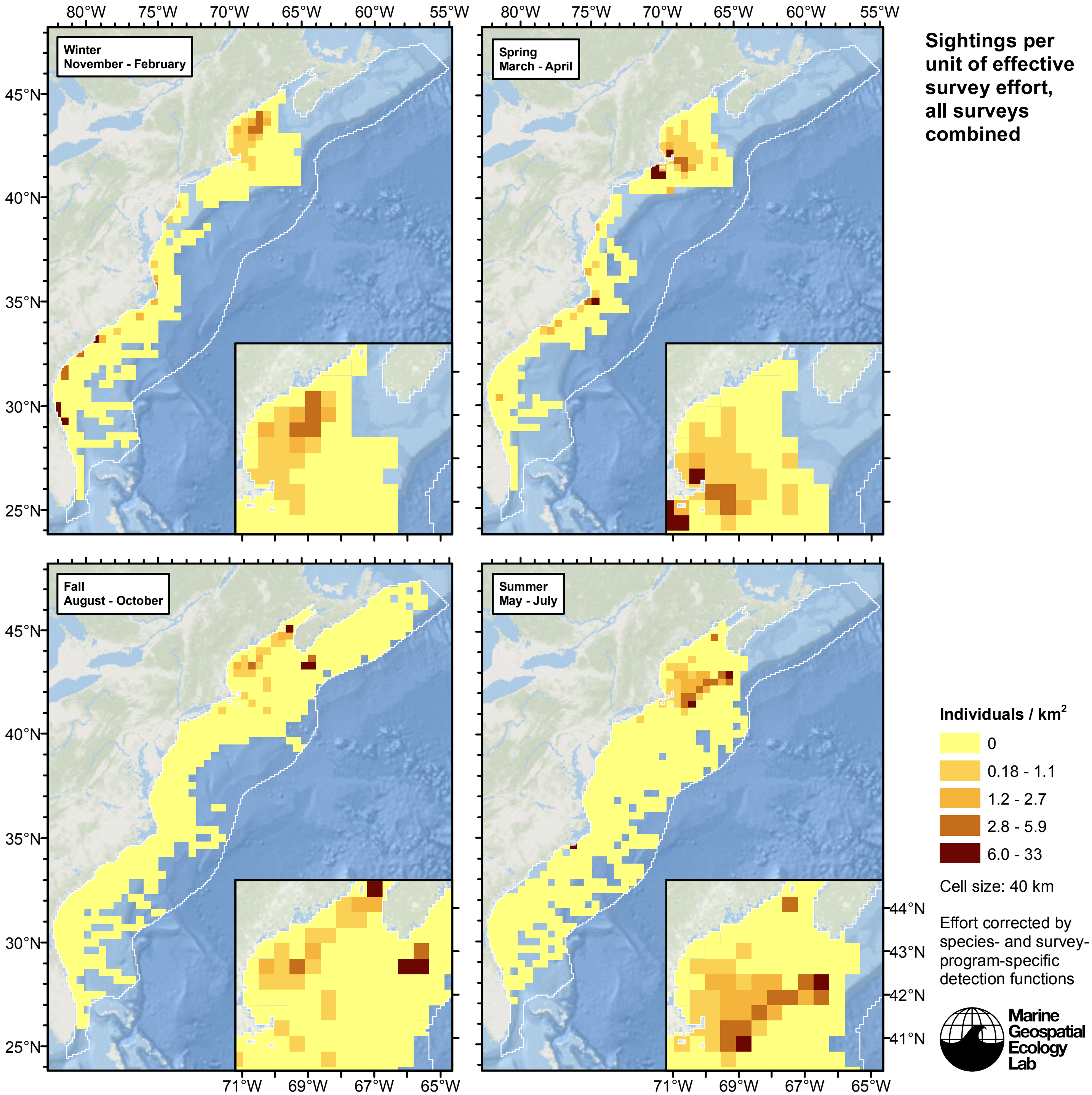

Figure 8: North Atlantic right whale sightings per unit of effective survey effort, for all surveys combined. Here, effort is corrected by the species- and survey-program-specific detection functions used in fitting the density models.

Detection Functions

The detection hierarchy figures below show how sightings from multiple surveys were pooled to try to achieve Buckland et. al's (2001) recommendation that at least 60-80 sightings be used to fit a detection function. Leaf nodes, on the right, usually represent individual surveys, while the hierarchy to the left shows how they have been grouped according to how similar we believed the surveys were to each other in their detection performance.

At each node, the red or green number indicates the total number of sightings below that node in the hierarchy, and is colored green if 70 or more sightings were available, and red otherwise. If a grouping node has zero sightings–i.e. all of the surveys within it had zero sightings–it may be collapsed and shown as a leaf to save space.

Each histogram in the figure indicates a node where a detection function was fitted. The actual detection functions do not appear in this figure; they are presented in subsequent sections. The histogram shows the frequency of sightings by perpendicular sighting distance for all surveys contained by that node. Each survey (leaf node) recieves the detection function that is closest to it up the hierarchy. Thus, for common species, sufficient sightings may be available to fit detection functions deep in the hierarchy, with each function applying to only a few surveys, thereby allowing variability in detection performance between surveys to be addressed relatively finely. For rare species, so few sightings may be available that we have to pool many surveys together to try to meet Buckland's recommendation, and fit only a few coarse detection functions high in the hierarchy.

A blue Proxy Species tag indicates that so few sightings were available that, rather than ascend higher in the hierarchy to a point that we would pool grossly-incompatible surveys together, (e.g. shipboard surveys that used big-eye binoculars with those that used only naked eyes) we pooled sightings of similar species together instead. The list of species pooled is given in following sections.

Shipboard Surveys

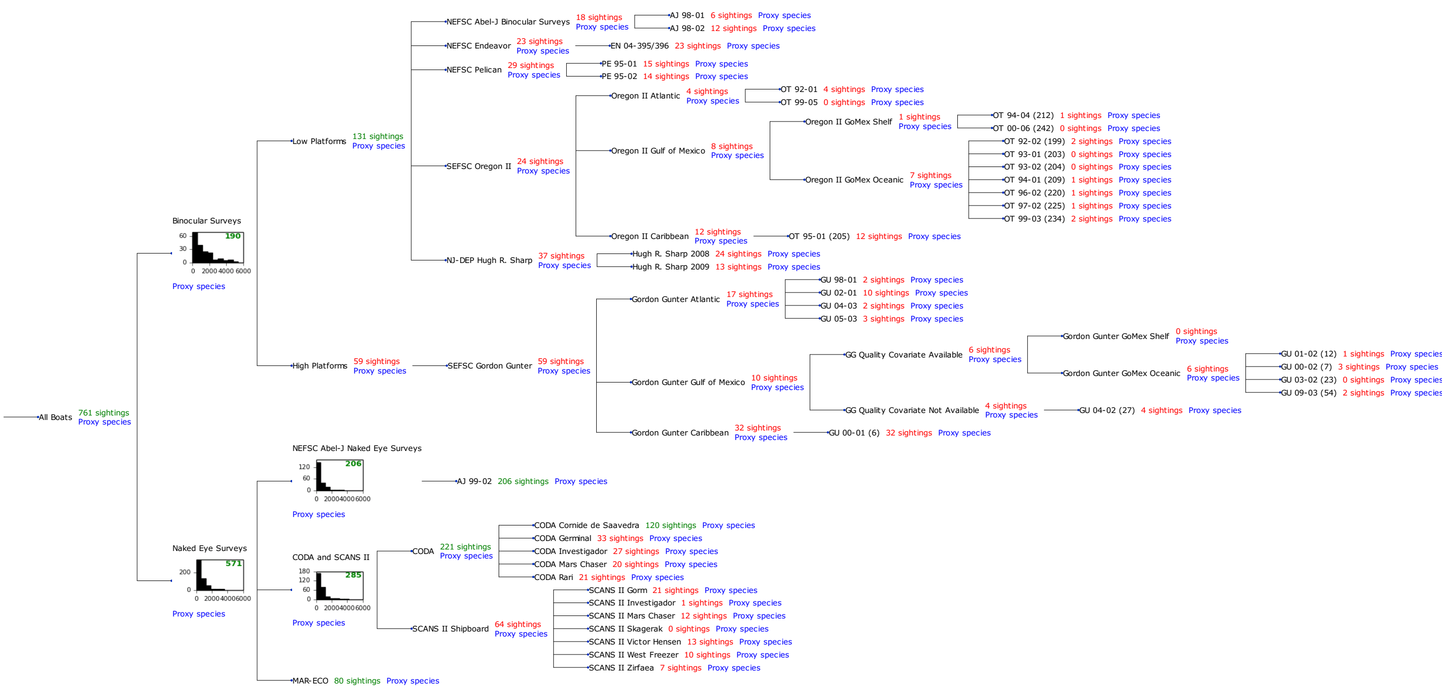

Figure 9: Detection hierarchy for shipboard surveys

Binocular Surveys

Because this taxon was sighted too infrequently to fit a detection function to its sightings alone, we fit a detection function to the pooled sightings of several other species that we believed would exhibit similar detectability. These "proxy species" are listed below.

Reported By Observer	Common Name	n
Balaenoptera	Balaenopterid sp.	8
Balaenoptera acutorostrata	Minke whale	4
Balaenoptera borealis	Sei whale	4
Balaenoptera borealis/edeni	Sei or Bryde's whale	6

Balaenoptera borealis/physalus	Fin or Sei whale	0
Balaenoptera edeni	Bryde's whale	21
Balaenoptera musculus	Blue whale	0
Balaenoptera physalus	Fin whale	98
Eubalaena glacialis	North Atlantic right whale	4
Eubalaena glacialis/Megaptera novaeangliae	Right or humpback whale	0
Megaptera novaeangliae	Humpback whale	46
Total		191

Table 4: Proxy species used to fit detection functions for Binocular Surveys. The number of sightings, n, is before truncation.

The sightings were right truncated at 5500m.

Covariate	Description
beaufort	Beaufort sea state.
size	Estimated size (number of individuals) of the sighted group.
vessel	Vessel from which the observation was made. This covariate allows the detection function to account for vessel-specific biases, such as the height of the survey platform.

Table 5: Covariates tested in candidate "multi-covariate distance sampling" (MCDS) detection functions.

Key	Adjustment	Order	Covariates	Succeeded	Δ AIC	Mean ESHW (m)
hr	poly	2		Yes	0.00	1309
hr	poly	4		Yes	0.47	1353
hr			size	Yes	0.78	1757
hr				Yes	0.80	1542
hn	cos	2		Yes	1.99	1802
hr			beaufort, size	Yes	2.64	1780
hr			beaufort	Yes	2.71	1553
hr			size, vessel	Yes	6.31	1920
hr			vessel	Yes	6.89	1605
hr			beaufort, size, vessel	Yes	8.03	1952
hr			beaufort, vessel	Yes	8.50	1675
hn	cos	3		Yes	9.91	1787
hn			size	Yes	11.86	2317
hn			beaufort, size	Yes	13.68	2319
hn			size, vessel	Yes	15.29	2299
hn			vessel	Yes	17.57	2301

hn				Yes	17.60	2311
hn			beaufort	Yes	19.19	2310
hn	herm	4		No		
hn			beaufort, vessel	No		
hn			beaufort, size, vessel	No		

Table 6: Candidate detection functions for Binocular Surveys. The first one listed was selected for the density model.

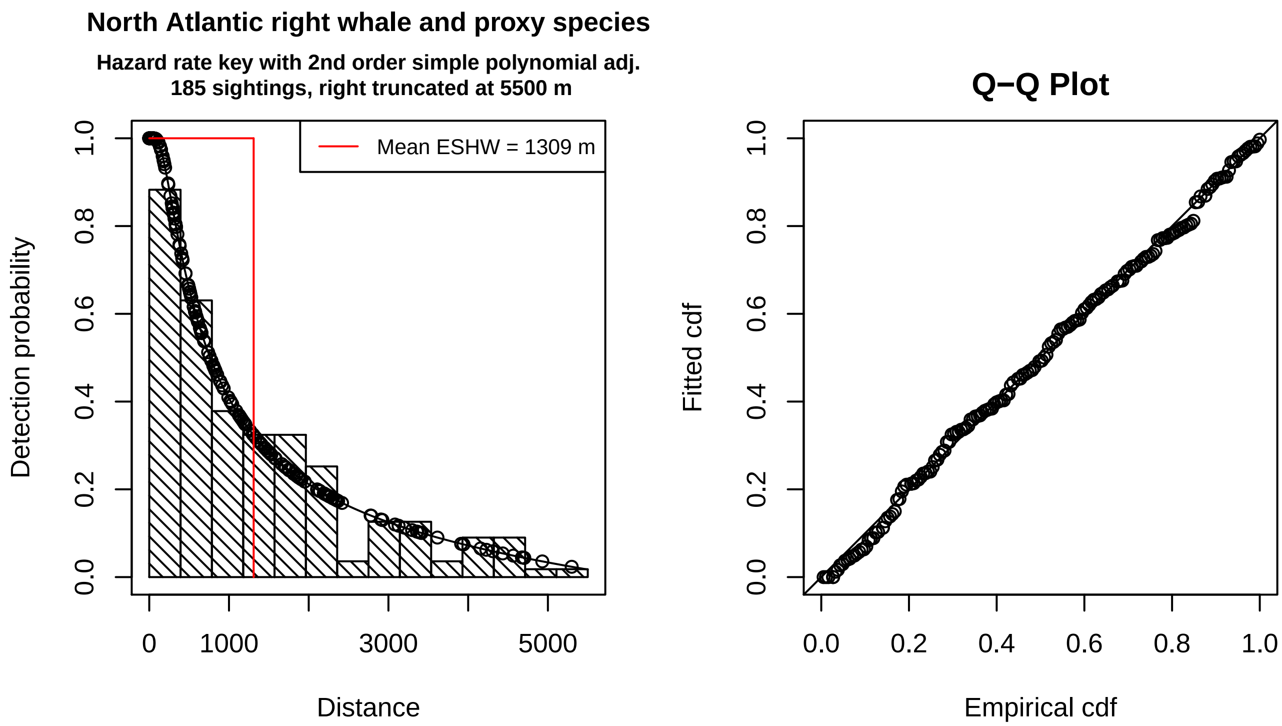

Figure 10: Detection function for Binocular Surveys that was selected for the density model

Statistical output for this detection function:

```
Summary for ds object
Number of observations :  185
Distance range         :  0  -  5500
AIC                    :  3029.944

Detection function:
 Hazard-rate key function with simple polynomial adjustment term of order 2

Detection function parameters
Scale Coefficients:
            estimate        se
(Intercept)  6.29521 0.4058206

Shape parameters:
                estimate        se
(Intercept) 1.102627e-07 0.2306009
```

```
Adjustment term parameter(s):
                estimate        se
poly, order 2 -0.8163341 0.2362982


Monotonicity constraints were enforced.
                      Estimate           SE        CV
Average p             0.238058   0.04195355 0.1762325
N in covered region 777.121670 145.75228225 0.1875540

Monotonicity constraints were enforced.
```

Additional diagnostic plots:

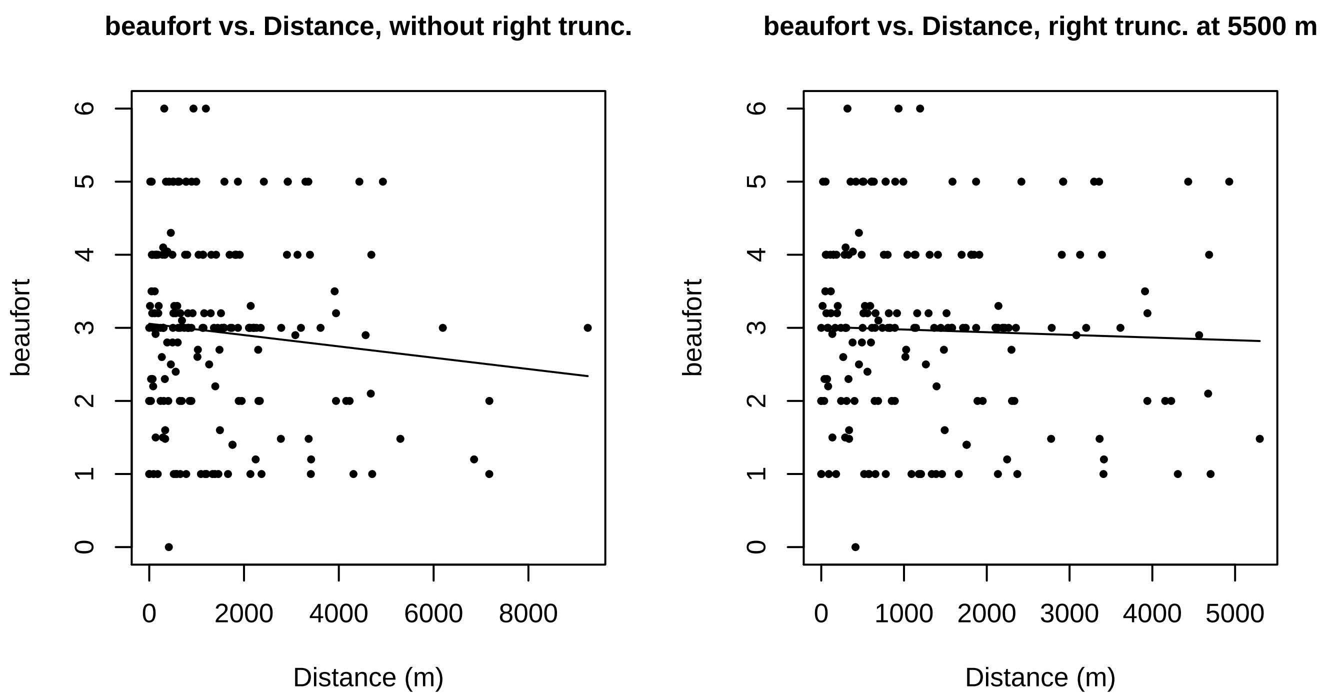

Figure 11: Scatterplots showing the relationship between Beaufort sea state and perpendicular sighting distance, for all sightings (left) and only those not right truncated (right). The line is a simple linear regression.

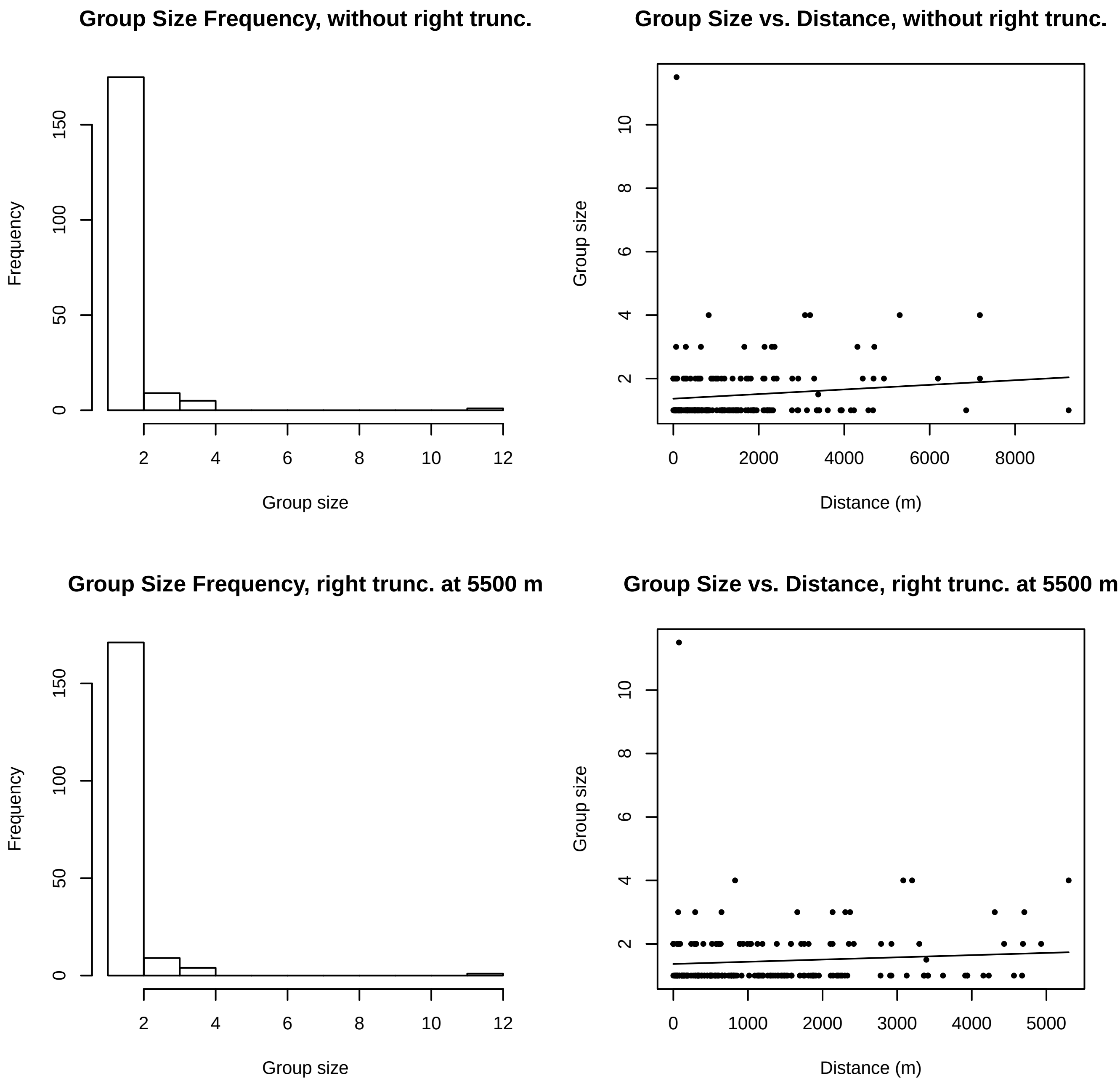

Figure 12: Histograms showing group size frequency and scatterplots showing the relationship between group size and perpendicular sighting distance, for all sightings (top row) and only those not right truncated (bottom row). In the scatterplot, the line is a simple linear regression.

Naked Eye Surveys

Because this taxon was sighted too infrequently to fit a detection function to its sightings alone, we fit a detection function to the pooled sightings of several other species that we believed would exhibit similar detectability. These "proxy species" are listed below.

Reported By Observer	Common Name	n
Balaenoptera	Balaenopterid sp.	7
Balaenoptera acutorostrata	Minke whale	177

Balaenoptera borealis	Sei whale	68
Balaenoptera borealis/edeni	Sei or Bryde's whale	0
Balaenoptera borealis/physalus	Fin or Sei whale	4
Balaenoptera edeni	Bryde's whale	1
Balaenoptera musculus	Blue whale	5
Balaenoptera physalus	Fin whale	261
Eubalaena glacialis	North Atlantic right whale	10
Eubalaena glacialis/Megaptera novaeangliae	Right or humpback whale	0
Megaptera novaeangliae	Humpback whale	38
Total		571

Table 7: Proxy species used to fit detection functions for Naked Eye Surveys. The number of sightings, n, is before truncation.

The sightings were right truncated at 2500m.

Covariate	Description
beaufort	Beaufort sea state.
size	Estimated size (number of individuals) of the sighted group.

Table 8: Covariates tested in candidate "multi-covariate distance sampling" (MCDS) detection functions.

Key	Adjustment	Order	Covariates	Succeeded	Δ AIC	Mean ESHW (m)
hn	cos	2		Yes	0.00	788
hr			size	Yes	0.23	881
hr	poly	2		Yes	4.00	802
hr	poly	4		Yes	4.09	816
hr				Yes	5.53	844
hn	cos	3		Yes	12.95	774
hn			size	Yes	17.09	953
hn			beaufort, size	Yes	19.06	953
hn				Yes	28.40	951
hn			beaufort	Yes	30.12	951
hn	herm	4		No		
hr			beaufort	No		
hr			beaufort, size	No		

Table 9: Candidate detection functions for Naked Eye Surveys. The first one listed was selected for the density model.

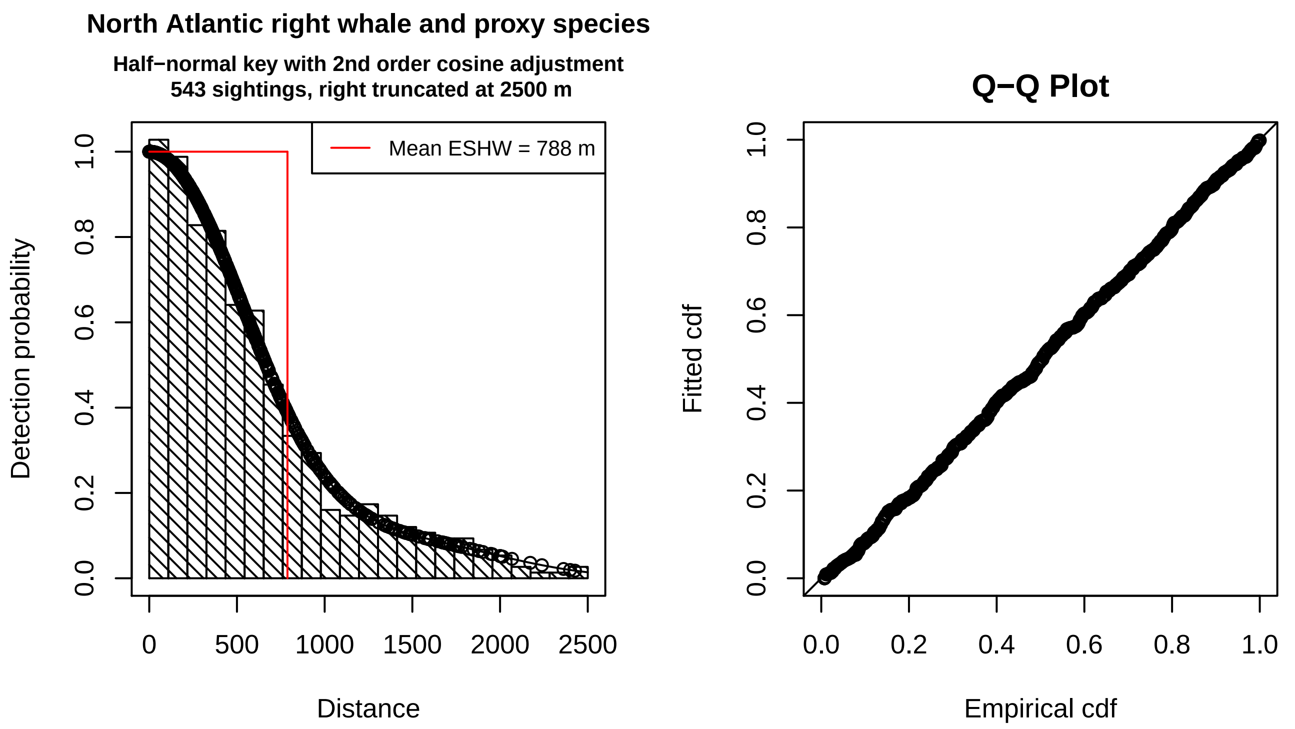

Figure 13: Detection function for Naked Eye Surveys that was selected for the density model

Statistical output for this detection function:

```
Summary for ds object
Number of observations :  543
Distance range         :  0  -  2500
AIC                    :  7957.87

Detection function:
 Half-normal key function with cosine adjustment term of order 2

Detection function parameters
Scale Coefficients:
            estimate         se
(Intercept) 6.752179 0.03907979

Adjustment term parameter(s):
             estimate         se
cos, order 2 0.410434 0.07032504


Monotonicity constraints were enforced.
                        Estimate          SE         CV
Average p              0.3152005  0.01193713 0.03787156
N in covered region 1722.7129529 89.43843211 0.05191720

Monotonicity constraints were enforced.
```

Additional diagnostic plots:

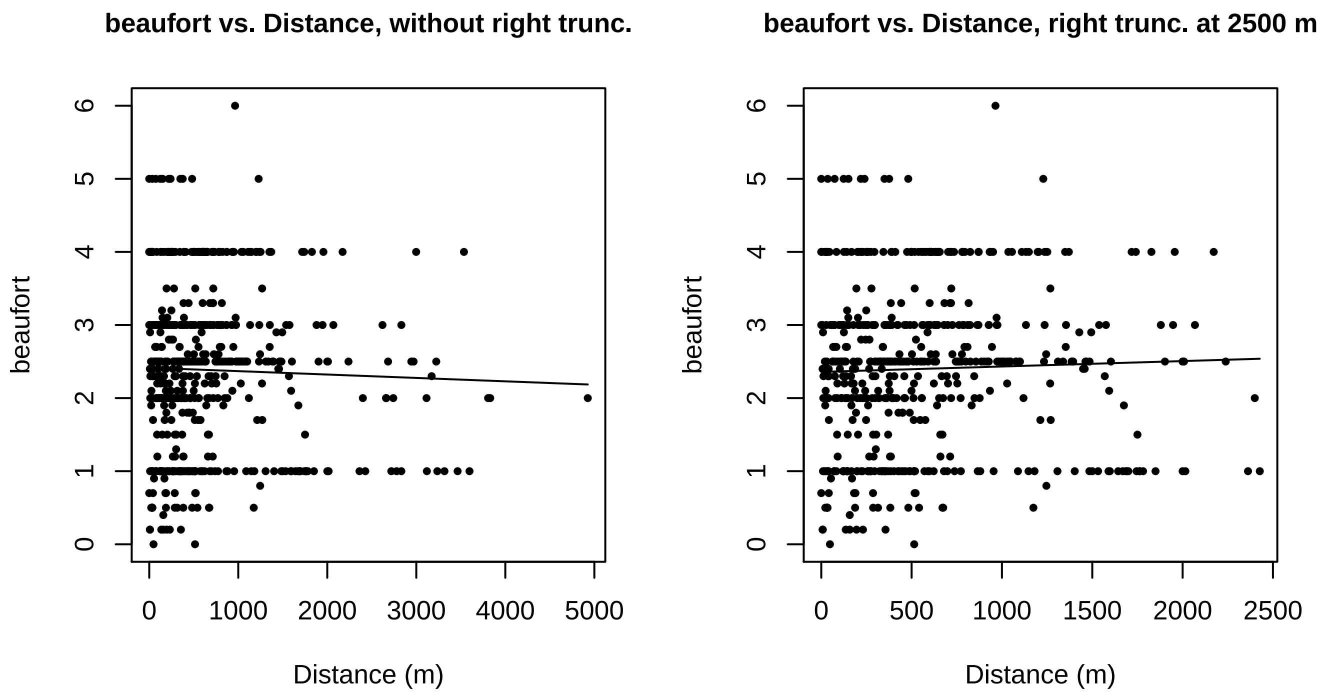

Figure 14: Scatterplots showing the relationship between Beaufort sea state and perpendicular sighting distance, for all sightings (left) and only those not right truncated (right). The line is a simple linear regression.

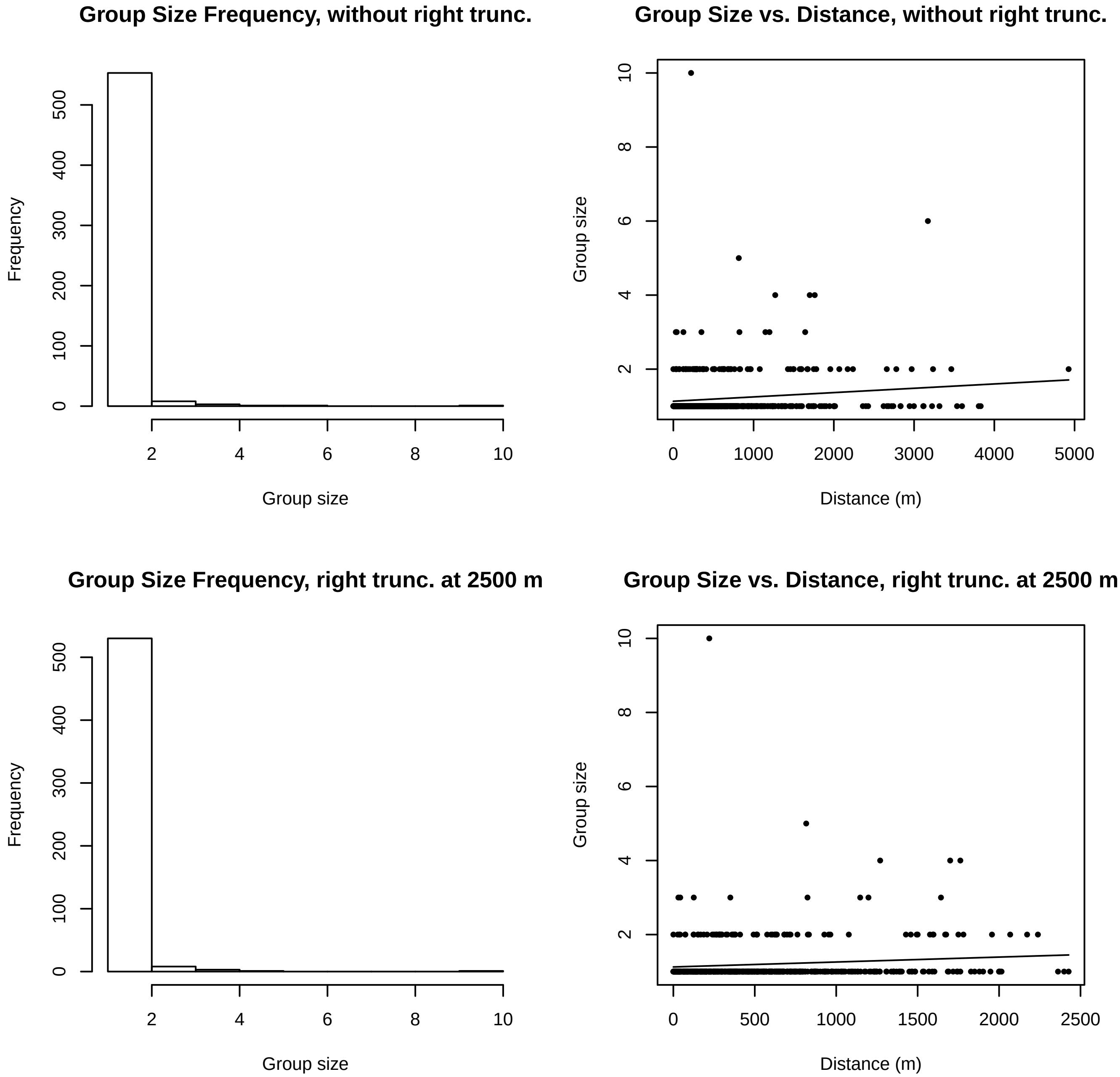

Figure 15: Histograms showing group size frequency and scatterplots showing the relationship between group size and perpendicular sighting distance, for all sightings (top row) and only those not right truncated (bottom row). In the scatterplot, the line is a simple linear regression.

NEFSC Abel-J Naked Eye Surveys

Because this taxon was sighted too infrequently to fit a detection function to its sightings alone, we fit a detection function to the pooled sightings of several other species that we believed would exhibit similar detectability. These “proxy species” are listed below.

Reported By Observer	Common Name	n
Balaenoptera	Balaenopterid sp.	0
Balaenoptera acutorostrata	Minke whale	100

Balaenoptera borealis	Sei whale	2
Balaenoptera borealis/edeni	Sei or Bryde's whale	0
Balaenoptera borealis/physalus	Fin or Sei whale	0
Balaenoptera edeni	Bryde's whale	0
Balaenoptera musculus	Blue whale	0
Balaenoptera physalus	Fin whale	57
Eubalaena glacialis	North Atlantic right whale	10
Eubalaena glacialis/Megaptera novaeangliae	Right or humpback whale	0
Megaptera novaeangliae	Humpback whale	37
Total		206

Table 10: Proxy species used to fit detection functions for NEFSC Abel-J Naked Eye Surveys. The number of sightings, n, is before truncation.

The sightings were right truncated at 2500m.

Covariate	Description
beaufort	Beaufort sea state.
quality	Survey-specific index of the quality of observation conditions, utilizing relevant factors other than Beaufort sea state (see methods).
size	Estimated size (number of individuals) of the sighted group.

Table 11: Covariates tested in candidate "multi-covariate distance sampling" (MCDS) detection functions.

Key	Adjustment	Order	Covariates	Succeeded	Δ AIC	Mean ESHW (m)
hn	cos	2		Yes	0.00	714
hr			size	Yes	0.04	799
hr				Yes	0.63	760
hr	poly	4		Yes	0.75	741
hr	poly	2		Yes	1.11	728
hn	cos	3		Yes	2.84	669
hn			size	Yes	5.20	855
hn			quality, size	Yes	6.85	854
hn				Yes	10.43	845
hn			quality	Yes	12.24	845
hn	herm	4		No		
hn			beaufort	No		
hr			beaufort	No		
hr			quality	No		
hn			beaufort, quality	No		

hr	beaufort, quality	No
hn	beaufort, size	No
hr	beaufort, size	No
hr	quality, size	No
hn	beaufort, quality, size	No
hr	beaufort, quality, size	No

Table 12: Candidate detection functions for NEFSC Abel-J Naked Eye Surveys. The first one listed was selected for the density model.

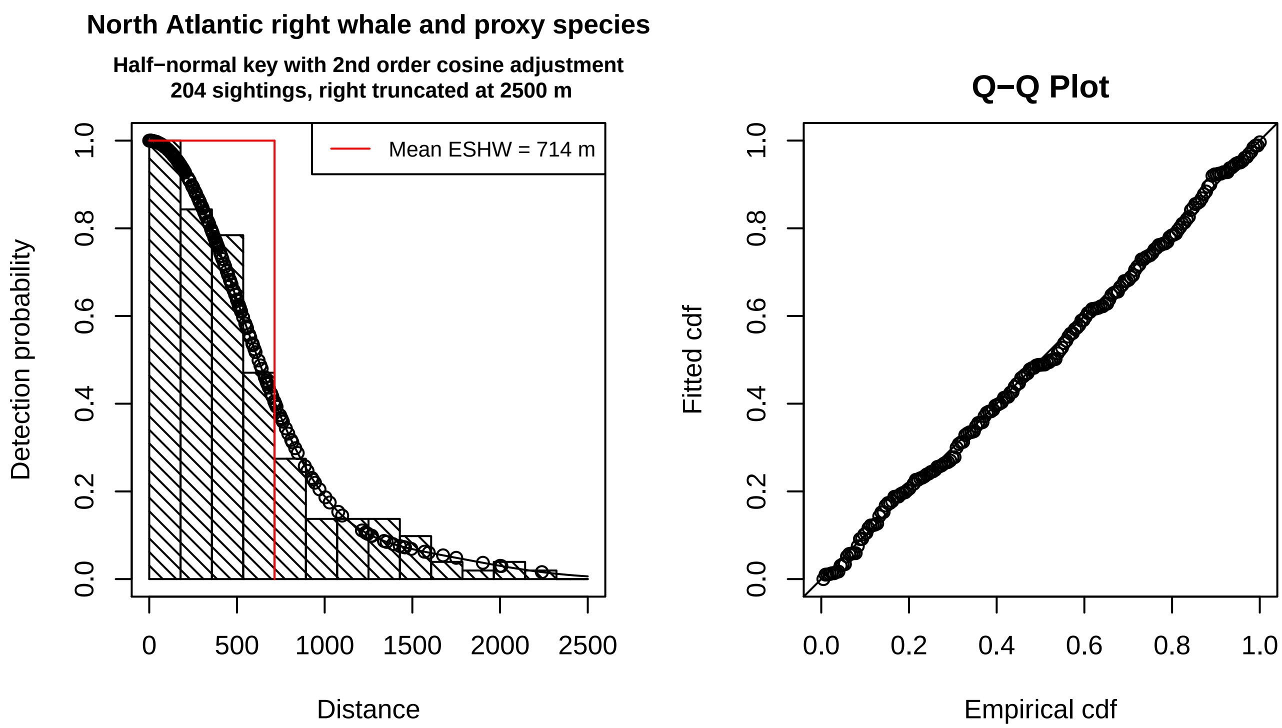

Figure 16: Detection function for NEFSC Abel-J Naked Eye Surveys that was selected for the density model

Statistical output for this detection function:

```
Summary for ds object
Number of observations :  204
Distance range         :  0  -  2500
AIC                    :  2944.665

Detection function:
 Half-normal key function with cosine adjustment term of order 2

Detection function parameters
Scale Coefficients:
            estimate         se
(Intercept) 6.665111 0.06962659

Adjustment term parameter(s):
```

```
              estimate        se
cos, order 2 0.4654074 0.1236342


Monotonicity constraints were enforced.
                       Estimate          SE         CV
Average p             0.2857526  0.01551915 0.05430975
N in covered region 713.9042289 57.33838258 0.08031663

Monotonicity constraints were enforced.
```

Additional diagnostic plots:

Figure 17: Scatterplots showing the relationship between Beaufort sea state and perpendicular sighting distance, for all sightings (left) and only those not right truncated (right). The line is a simple linear regression.

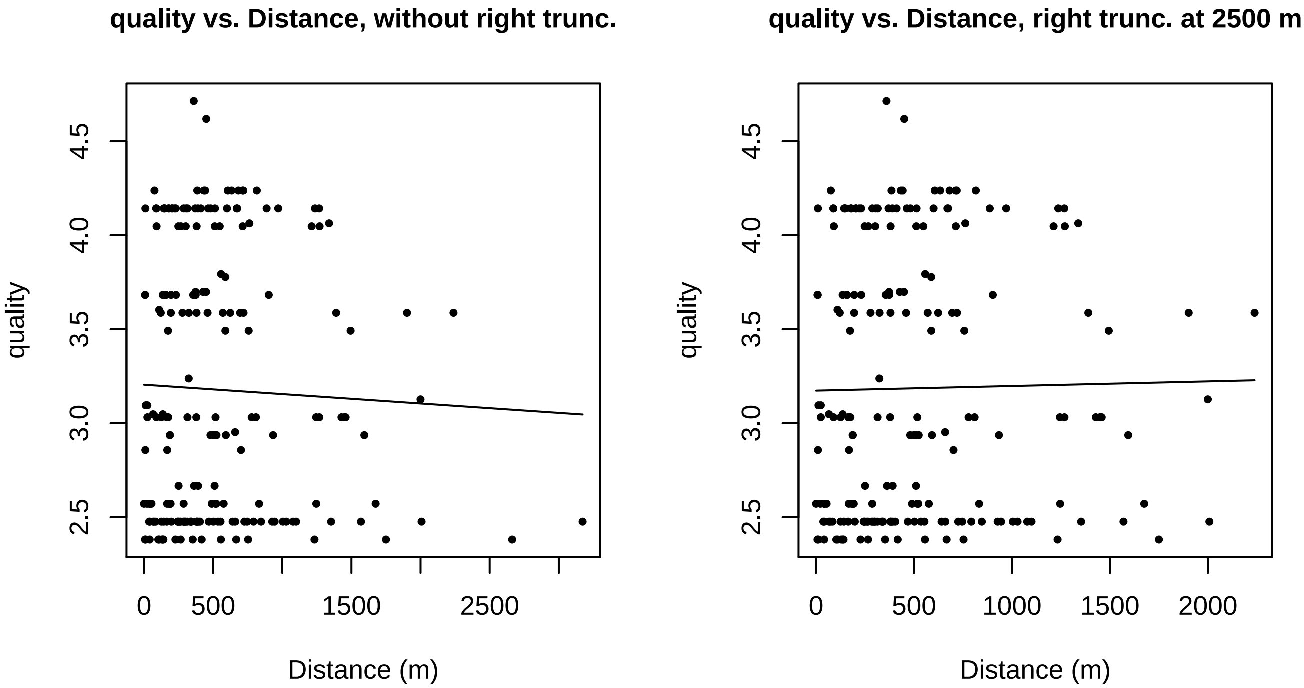

Figure 18: Scatterplots showing the relationship between the survey-specific index of the quality of observation conditions and perpendicular sighting distance, for all sightings (left) and only those not right truncated (right). Low values of the quality index correspond to better observation conditions. The line is a simple linear regression.

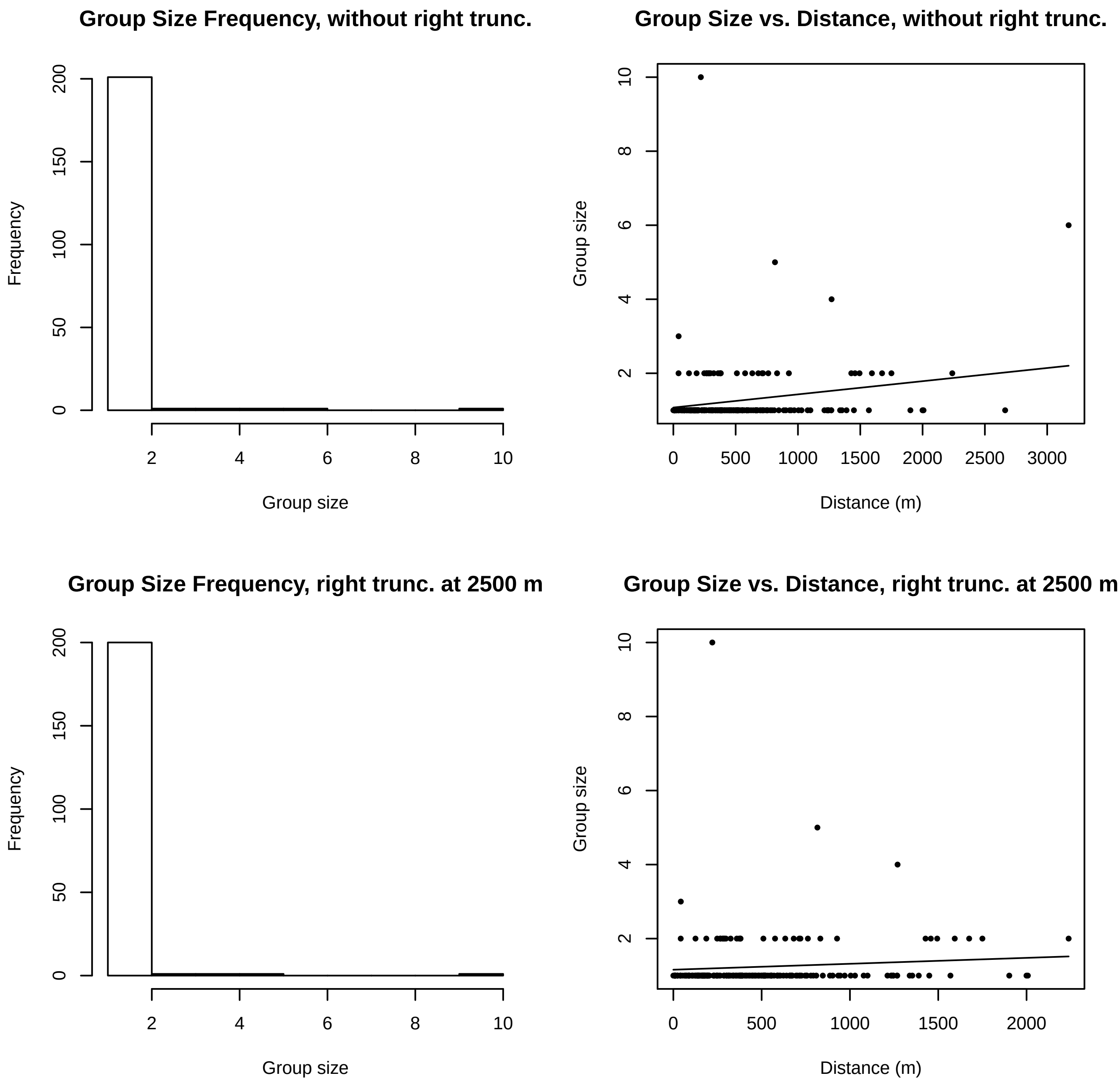

Figure 19: Histograms showing group size frequency and scatterplots showing the relationship between group size and perpendicular sighting distance, for all sightings (top row) and only those not right truncated (bottom row). In the scatterplot, the line is a simple linear regression.

CODA and SCANS II

Because this taxon was sighted too infrequently to fit a detection function to its sightings alone, we fit a detection function to the pooled sightings of several other species that we believed would exhibit similar detectability. These "proxy species" are listed below.

Reported By Observer	Common Name	n
Balaenoptera	Balaenopterid sp.	0
Balaenoptera acutorostrata	Minke whale	76

Balaenoptera borealis	Sei whale	12
Balaenoptera borealis/edeni	Sei or Bryde's whale	0
Balaenoptera borealis/physalus	Fin or Sei whale	4
Balaenoptera edeni	Bryde's whale	0
Balaenoptera musculus	Blue whale	1
Balaenoptera physalus	Fin whale	192
Eubalaena glacialis	North Atlantic right whale	0
Eubalaena glacialis/Megaptera novaeangliae	Right or humpback whale	0
Megaptera novaeangliae	Humpback whale	0
Total		285

Table 13: Proxy species used to fit detection functions for CODA and SCANS II. The number of sightings, n, is before truncation.

The sightings were right truncated at 2500m.

Covariate	Description
beaufort	Beaufort sea state.
quality	Survey-specific index of the quality of observation conditions, utilizing relevant factors other than Beaufort sea state (see methods).
size	Estimated size (number of individuals) of the sighted group.

Table 14: Covariates tested in candidate "multi-covariate distance sampling" (MCDS) detection functions.

Key	Adjustment	Order	Covariates	Succeeded	Δ AIC	Mean ESHW (m)
hn	cos	2		Yes	0.00	796
hn			size	Yes	3.86	900
hn				Yes	4.25	901
hn	cos	3		Yes	4.27	815
hr	poly	2		Yes	4.81	836
hr				Yes	5.06	929
hr	poly	4		Yes	5.80	872
hr			size	Yes	7.05	931
hn	herm	4		No		
hn			beaufort	No		
hr			beaufort	No		
hn			quality	No		
hr			quality	No		
hn			beaufort, quality	No		
hr			beaufort, quality	No		

hn	beaufort, size	No
hr	beaufort, size	No
hn	quality, size	No
hr	quality, size	No
hn	beaufort, quality, size	No
hr	beaufort, quality, size	No

Table 15: Candidate detection functions for CODA and SCANS II. The first one listed was selected for the density model.

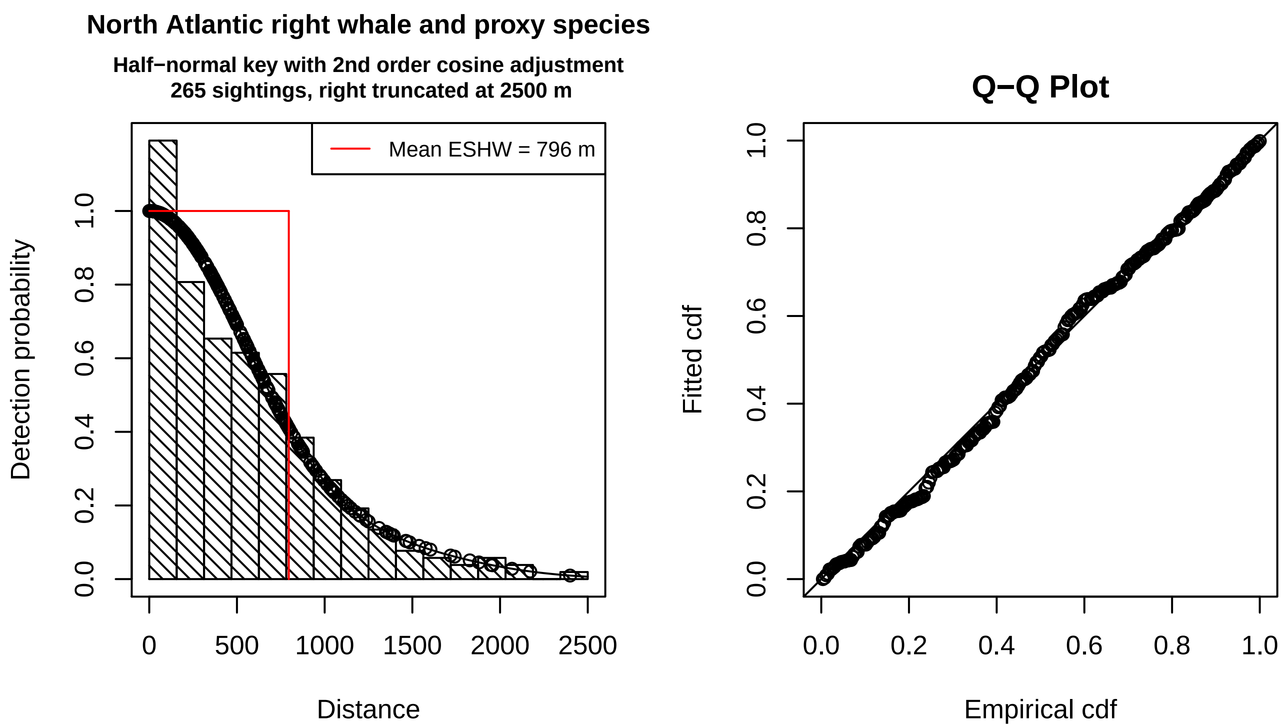

Figure 20: Detection function for CODA and SCANS II that was selected for the density model

Statistical output for this detection function:

```
Summary for ds object
Number of observations :  265
Distance range         :  0  -  2500
AIC                    :  3866.705

Detection function:
 Half-normal key function with cosine adjustment term of order 2

Detection function parameters
Scale Coefficients:
            estimate         se
(Intercept) 6.669744 0.05443106

Adjustment term parameter(s):
```

```
              estimate        se
cos, order 2 0.2900295 0.1074259


Monotonicity constraints were enforced.
                        Estimate          SE         CV
Average p              0.3182231  0.01860502 0.05846533
N in covered region 832.7490402 64.45573418 0.07740115

Monotonicity constraints were enforced.
```

Additional diagnostic plots:

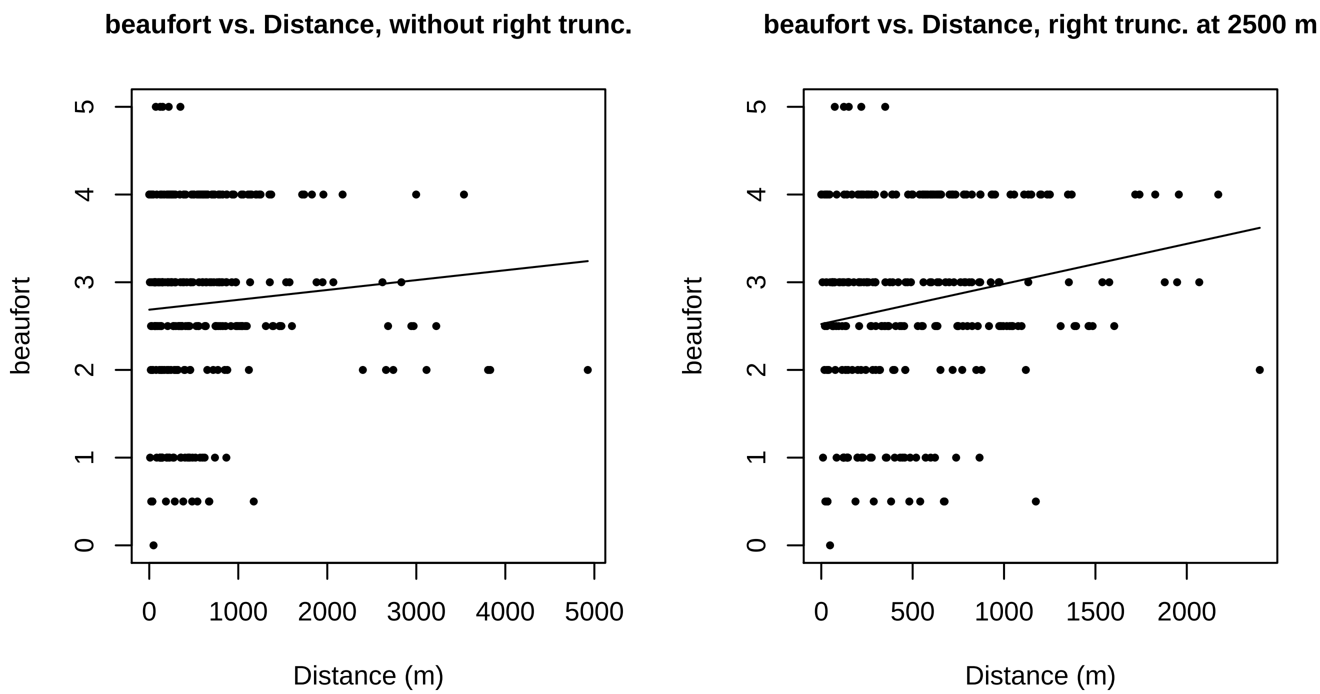

Figure 21: Scatterplots showing the relationship between Beaufort sea state and perpendicular sighting distance, for all sightings (left) and only those not right truncated (right). The line is a simple linear regression.

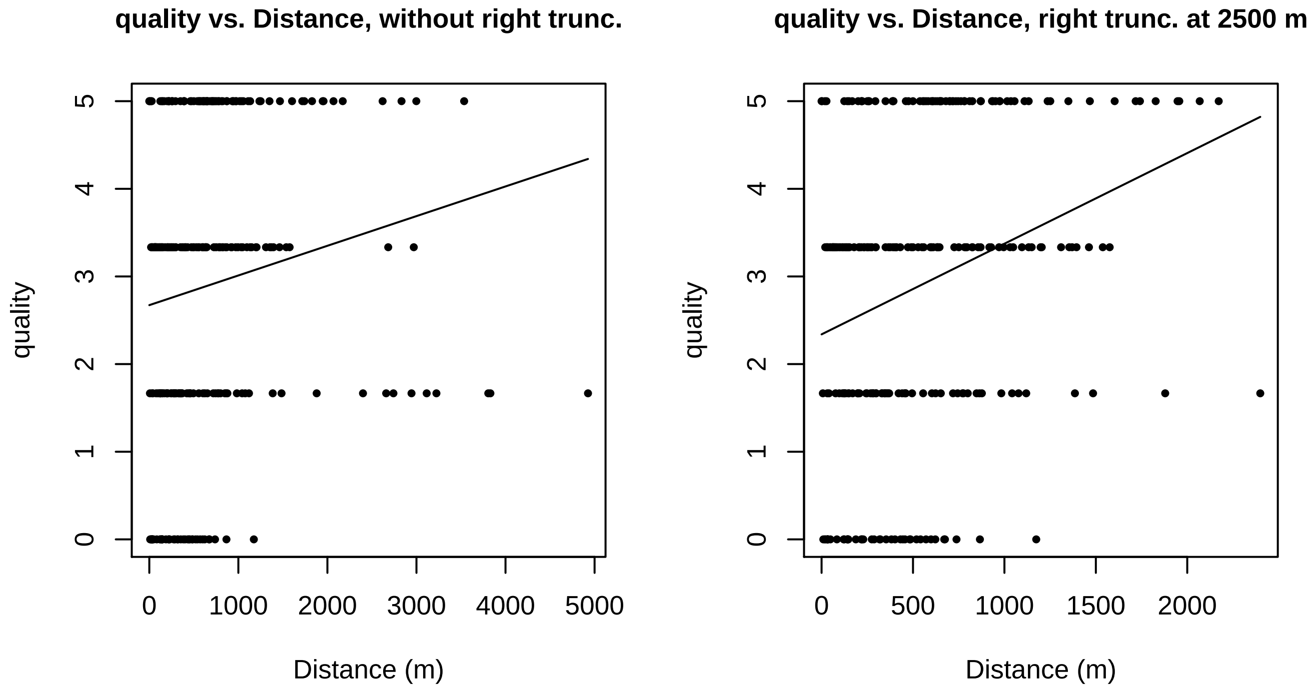

Figure 22: Scatterplots showing the relationship between the survey-specific index of the quality of observation conditions and perpendicular sighting distance, for all sightings (left) and only those not right truncated (right). Low values of the quality index correspond to better observation conditions. The line is a simple linear regression.

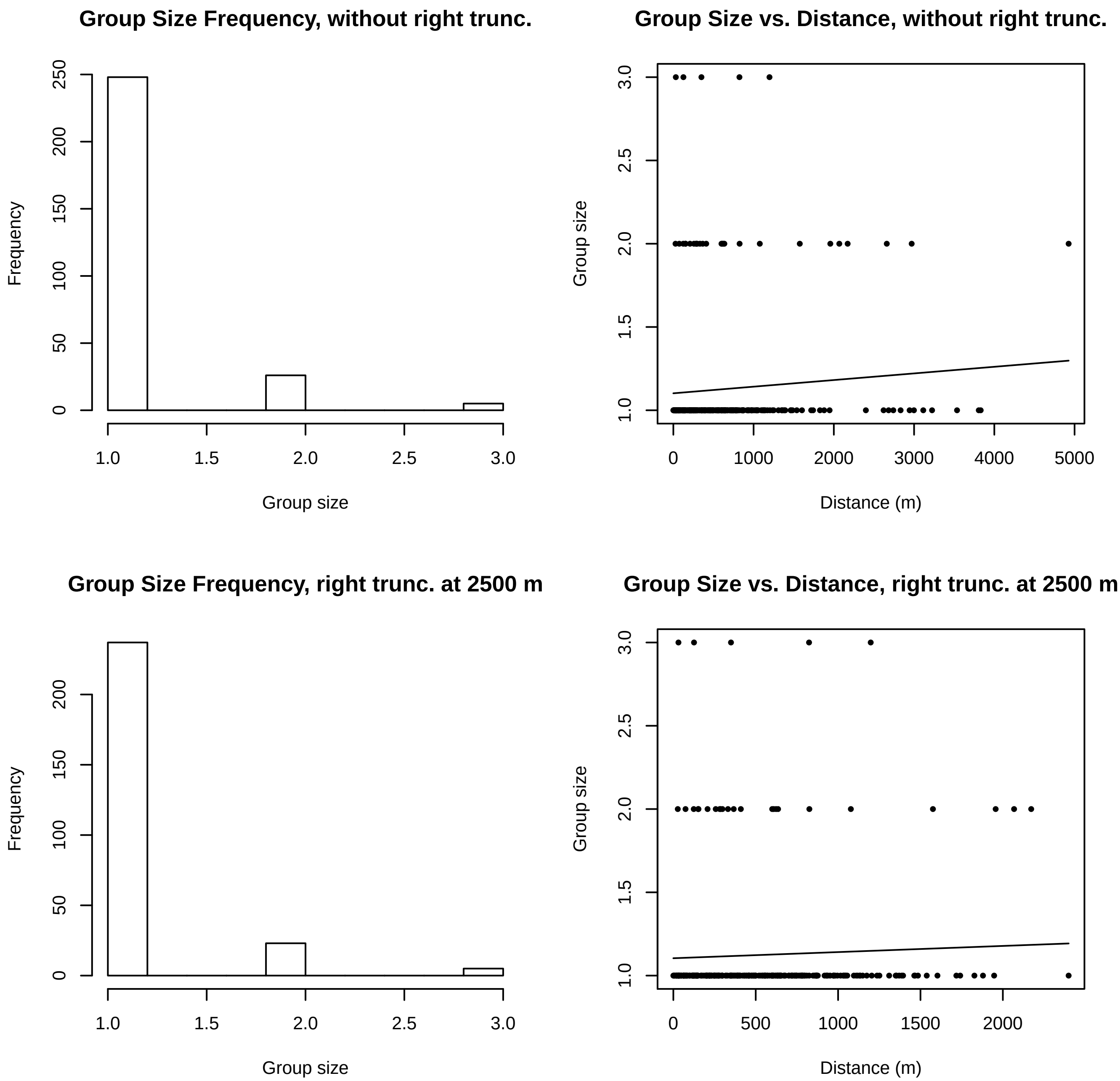

Figure 23: Histograms showing group size frequency and scatterplots showing the relationship between group size and perpendicular sighting distance, for all sightings (top row) and only those not right truncated (bottom row). In the scatterplot, the line is a simple linear regression.

Aerial Surveys

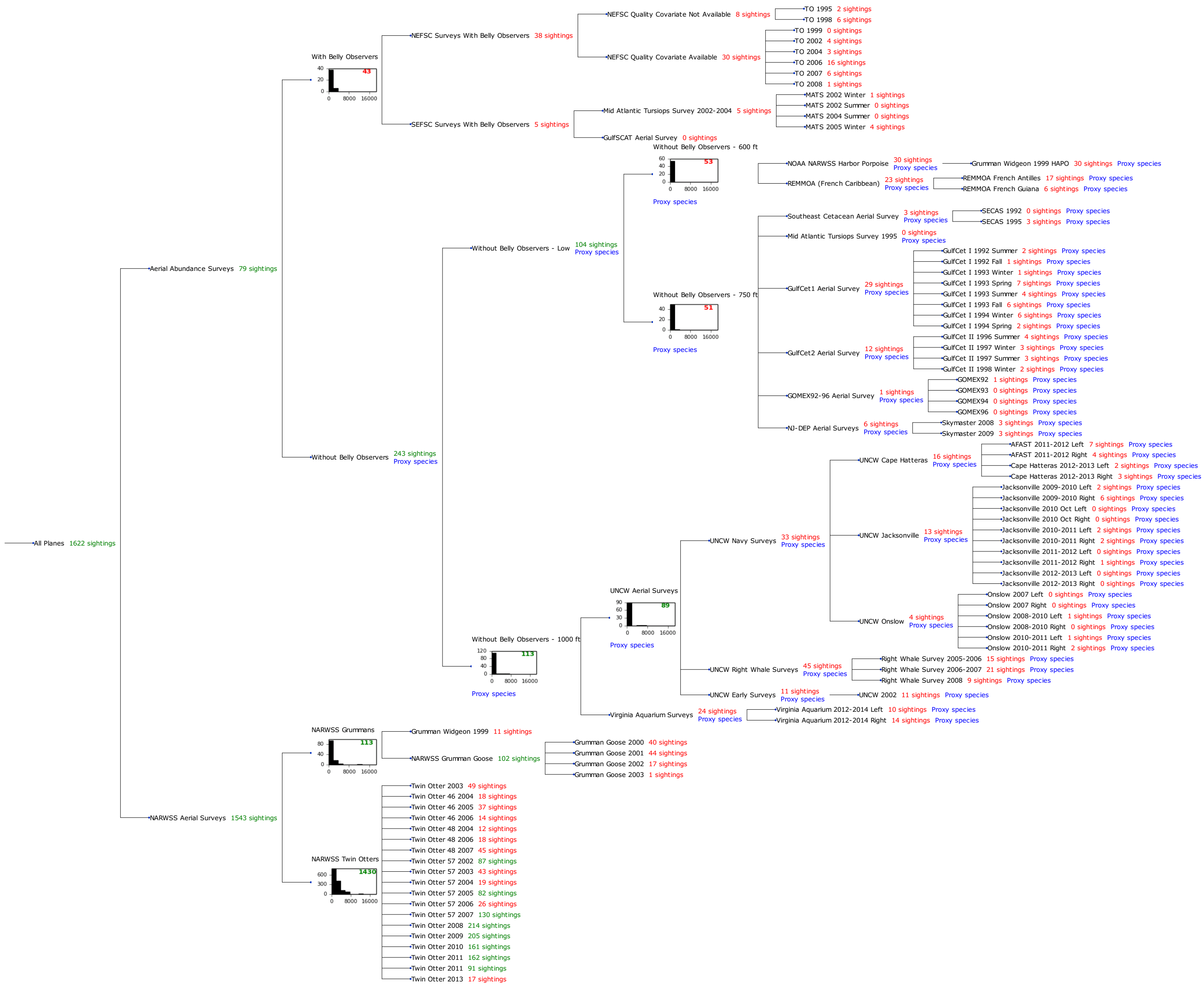

Figure 24: Detection hierarchy for aerial surveys

With Belly Observers

The sightings were right truncated at 2000m.

Covariate	Description
beaufort	Beaufort sea state.
size	Estimated size (number of individuals) of the sighted group.

Table 16: Covariates tested in candidate "multi-covariate distance sampling" (MCDS) detection functions.

Key	Adjustment	Order	Covariates	Succeeded	Δ AIC	Mean ESHW (m)

hn				Yes	0.00	785
hn	cos	2		Yes	0.71	898
hr			size	Yes	0.72	1125
hn			size	Yes	1.15	784
hn	cos	3		Yes	1.61	867
hr				Yes	1.73	1009
hr			beaufort, size	Yes	2.72	1121
hr	poly	4		Yes	3.20	996
hr			beaufort	Yes	3.72	1012
hn	herm	4		No		
hr	poly	2		No		
hn			beaufort	No		
hn			beaufort, size	No		

Table 17: Candidate detection functions for With Belly Observers. The first one listed was selected for the density model.

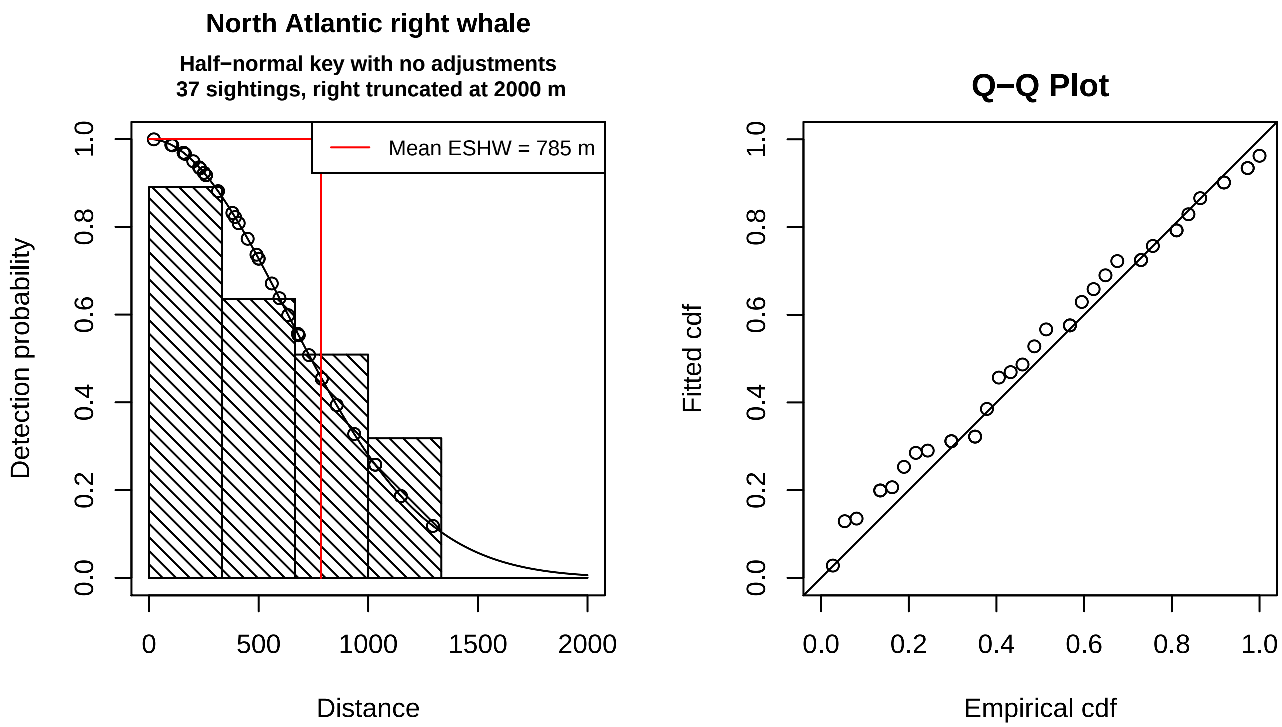

Figure 25: Detection function for With Belly Observers that was selected for the density model

Statistical output for this detection function:

```
Summary for ds object
Number of observations :  37
```

```
Distance range         :  0  -  2000
AIC                    :  531.6337

Detection function:
 Half-normal key function

Detection function parameters
Scale Coefficients:
            estimate        se
(Intercept) 6.440691 0.1511545

                      Estimate          SE        CV
Average p            0.3922558  0.05836055 0.1487818
N in covered region 94.3261980 18.52292673 0.1963710
```

Additional diagnostic plots:

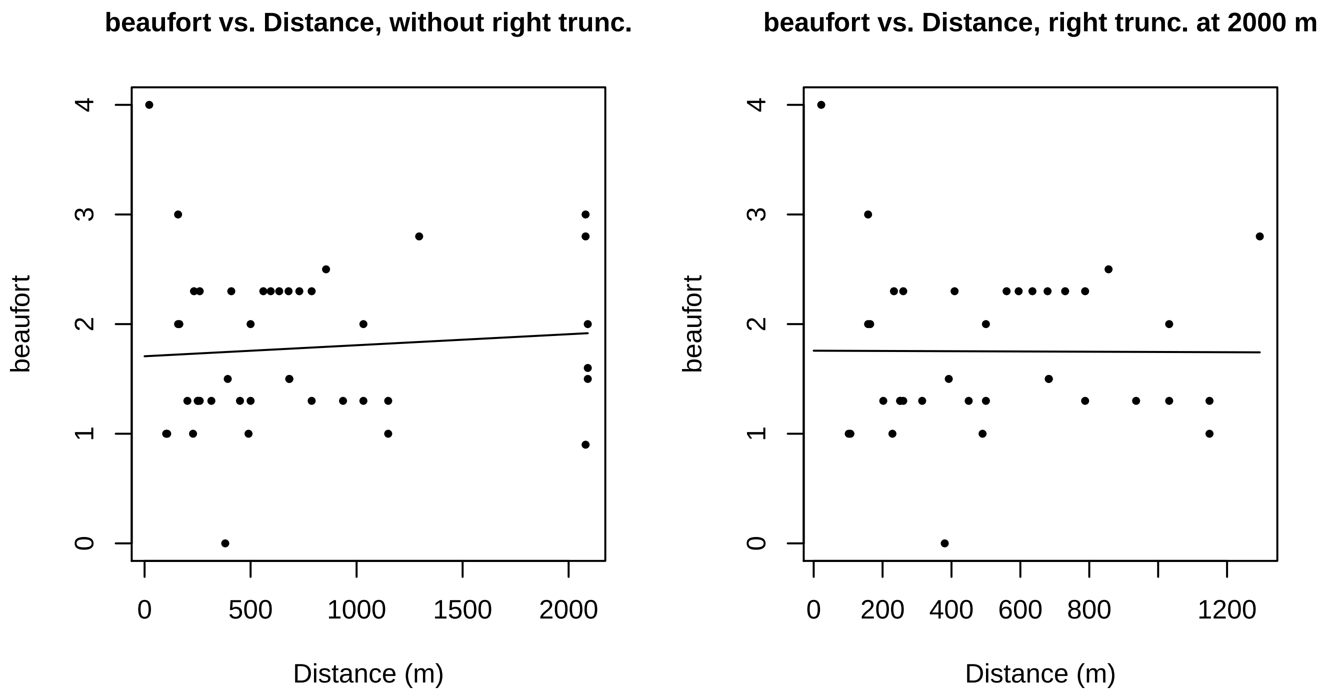

Figure 26: Scatterplots showing the relationship between Beaufort sea state and perpendicular sighting distance, for all sightings (left) and only those not right truncated (right). The line is a simple linear regression.

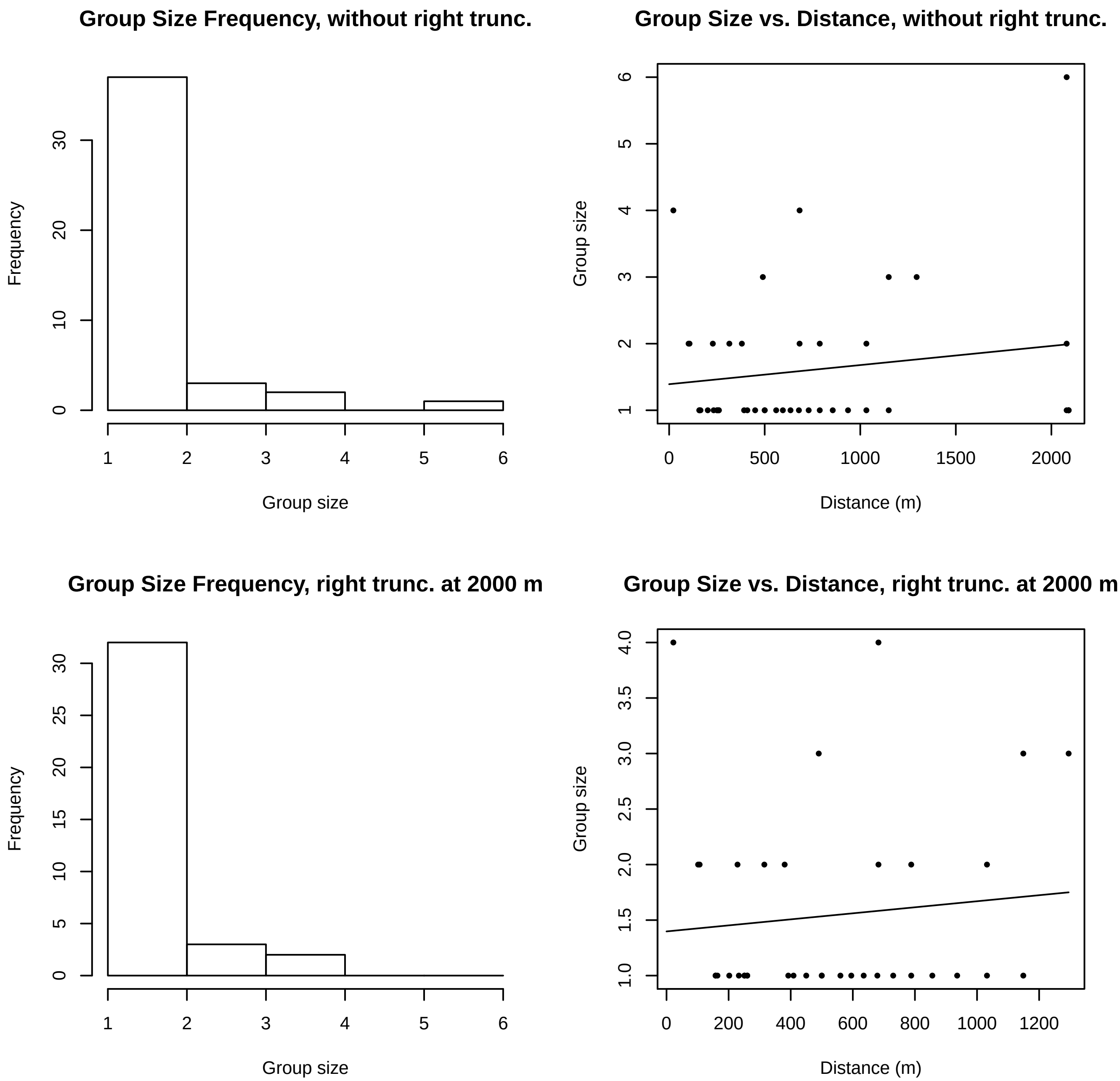

Figure 27: Histograms showing group size frequency and scatterplots showing the relationship between group size and perpendicular sighting distance, for all sightings (top row) and only those not right truncated (bottom row). In the scatterplot, the line is a simple linear regression.

Without Belly Observers - 600 ft

Because this taxon was sighted too infrequently to fit a detection function to its sightings alone, we fit a detection function to the pooled sightings of several other species that we believed would exhibit similar detectability. These "proxy species" are listed below.

Reported By Observer	Common Name	n
Balaenoptera	Balaenopterid sp.	2
Balaenoptera acutorostrata	Minke whale	8

Balaenoptera borealis	Sei whale	0
Balaenoptera borealis/edeni	Sei or Bryde's whale	0
Balaenoptera borealis/physalus	Fin or Sei whale	0
Balaenoptera edeni	Bryde's whale	0
Balaenoptera musculus	Blue whale	0
Balaenoptera physalus	Fin whale	15
Eubalaena glacialis	North Atlantic right whale	2
Eubalaena glacialis/Megaptera novaeangliae	Right or humpback whale	0
Megaptera novaeangliae	Humpback whale	16
Physeter macrocephalus	Sperm whale	10
Total		53

Table 18: Proxy species used to fit detection functions for Without Belly Observers - 600 ft. The number of sightings, n, is before truncation.

The sightings were right truncated at 600m. Due to a reduced frequency of sightings close to the trackline that plausibly resulted from the behavior of the observers and/or the configuration of the survey platform, the sightings were left truncted as well. Sightings closer than 32 m to the trackline were omitted from the analysis, and it was assumed that the the area closer to the trackline than this was not surveyed. This distance was estimated by inspecting histograms of perpendicular sighting distances.

Covariate	Description
beaufort	Beaufort sea state.
size	Estimated size (number of individuals) of the sighted group.

Table 19: Covariates tested in candidate "multi-covariate distance sampling" (MCDS) detection functions.

Key	Adjustment	Order	Covariates	Succeeded	Δ AIC	Mean ESHW (m)
hn				Yes	0.00	293
hr				Yes	1.14	318
hn			beaufort	Yes	1.57	293
hn	cos	3		Yes	1.65	311
hn	herm	4		Yes	1.93	291
hr			beaufort	Yes	1.97	326
hn	cos	2		Yes	1.97	283
hr	poly	2		Yes	3.14	318
hr	poly	4		Yes	3.14	318
hn			size	No		
hr			size	No		
hn			beaufort, size	No		
hr			beaufort, size	No		

Table 20: Candidate detection functions for Without Belly Observers - 600 ft. The first one listed was selected for the density model.

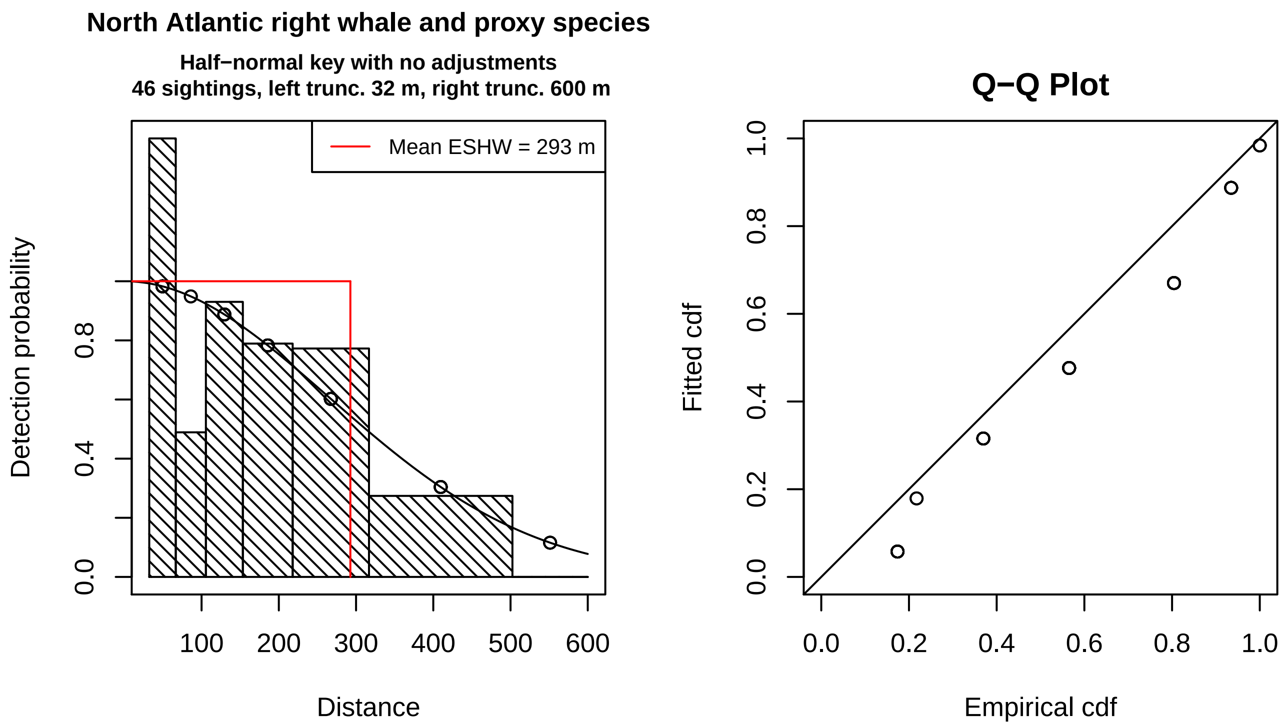

Figure 28: Detection function for Without Belly Observers - 600 ft that was selected for the density model

Statistical output for this detection function:

```
Summary for ds object
Number of observations :  46
Distance range         :  32.24668  -  600
AIC                    :  177.4011

Detection function:
 Half-normal key function

Detection function parameters
Scale Coefficients:
            estimate        se
(Intercept) 5.581559 0.1339955

                     Estimate          SE        CV
Average p            0.487738  0.06208134 0.1272842
N in covered region 94.312922 15.59372100 0.1653402
```

Additional diagnostic plots:

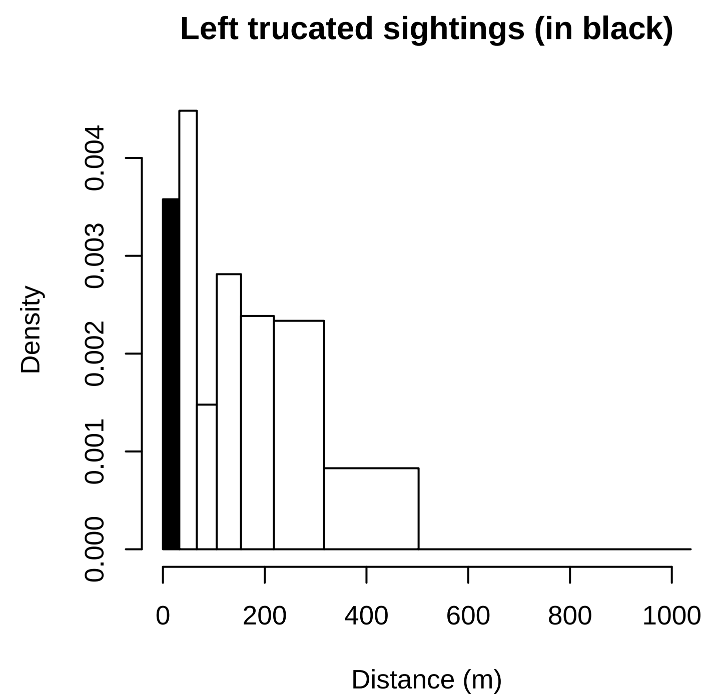

Figure 29: Density of sightings by perpendicular distance for Without Belly Observers - 600 ft. Black bars on the left show sightings that were left truncated.

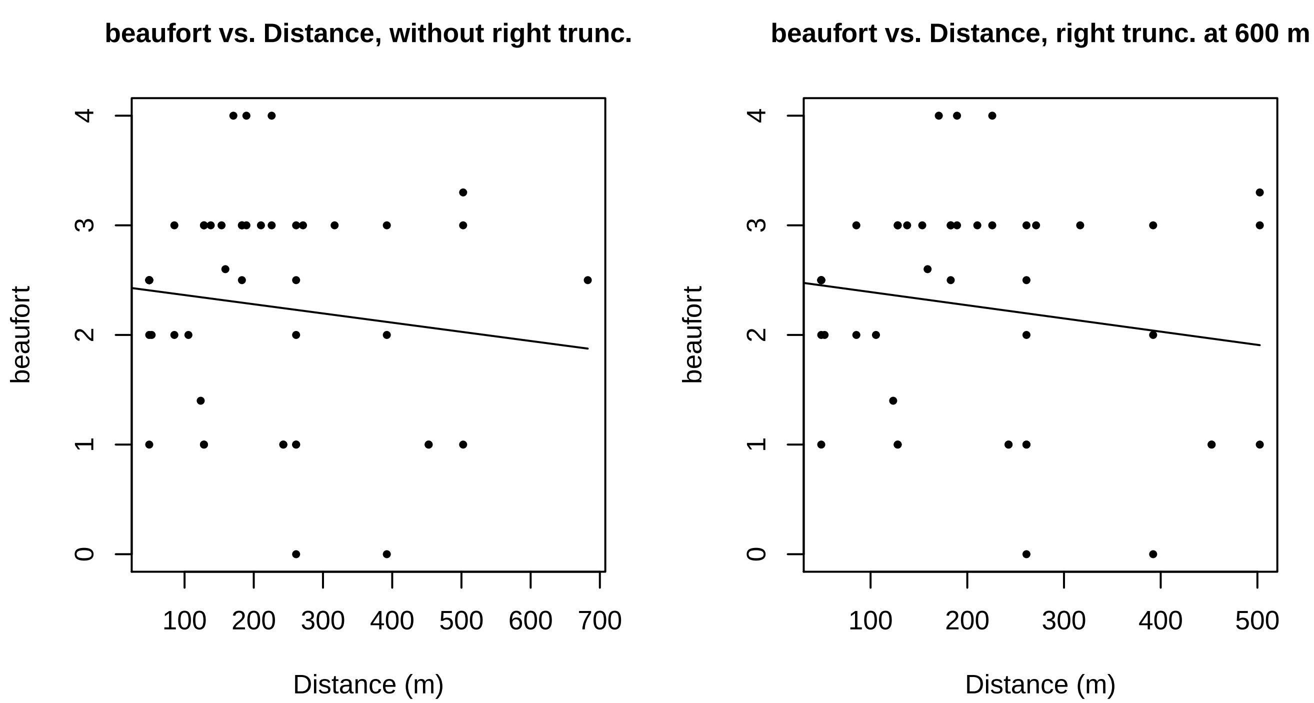

Figure 30: Scatterplots showing the relationship between Beaufort sea state and perpendicular sighting distance, for all sightings (left) and only those not right truncated (right). The line is a simple linear regression.

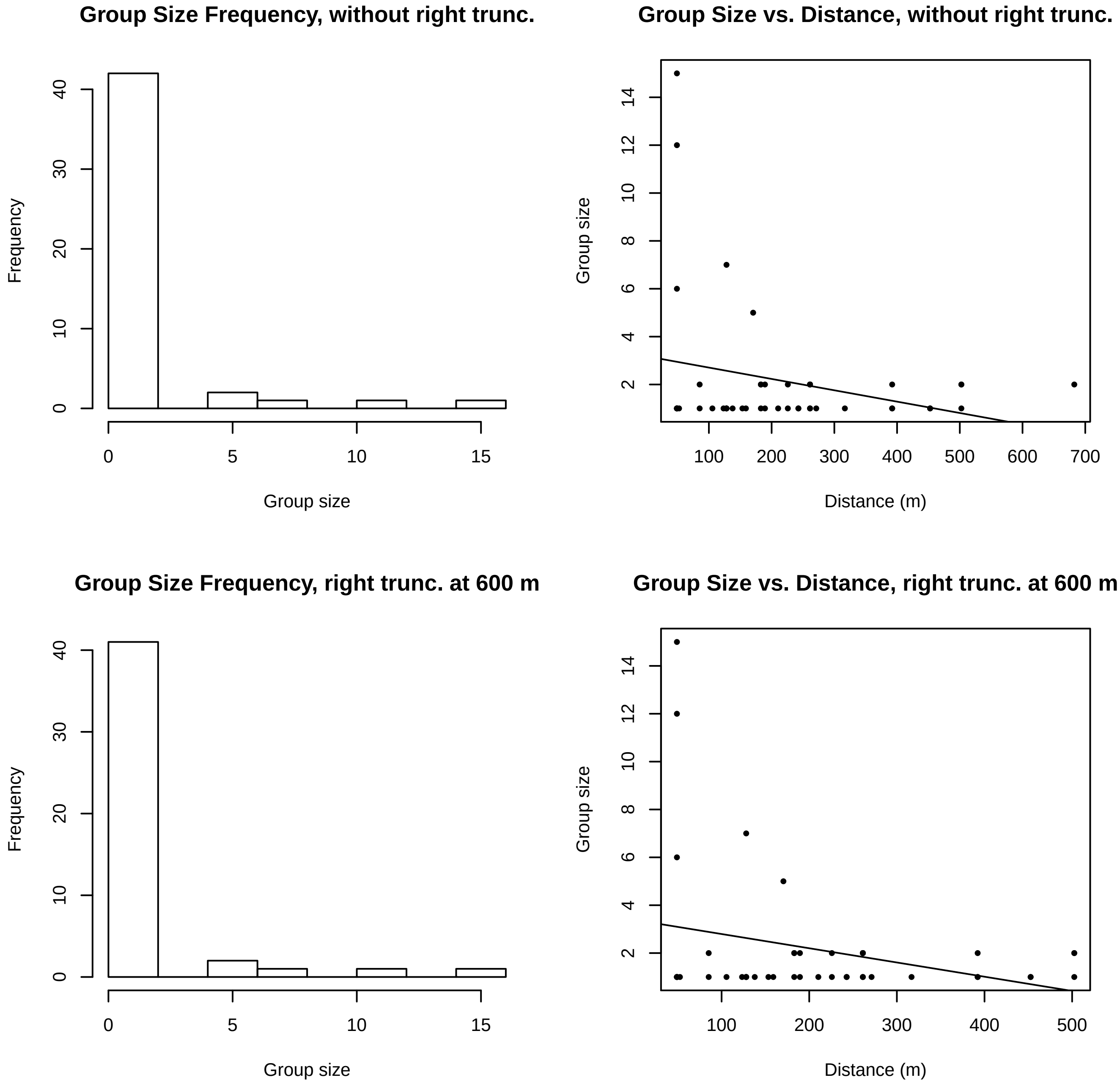

Figure 31: Histograms showing group size frequency and scatterplots showing the relationship between group size and perpendicular sighting distance, for all sightings (top row) and only those not right truncated (bottom row). In the scatterplot, the line is a simple linear regression.

Without Belly Observers - 750 ft

Because this taxon was sighted too infrequently to fit a detection function to its sightings alone, we fit a detection function to the pooled sightings of several other species that we believed would exhibit similar detectability. These "proxy species" are listed below.

Reported By Observer	Common Name	n
Balaenoptera	Balaenopterid sp.	1
Balaenoptera acutorostrata	Minke whale	0

Balaenoptera borealis	Sei whale	0
Balaenoptera borealis/edeni	Sei or Bryde's whale	2
Balaenoptera borealis/physalus	Fin or Sei whale	0
Balaenoptera edeni	Bryde's whale	3
Balaenoptera musculus	Blue whale	0
Balaenoptera physalus	Fin whale	2
Eubalaena glacialis	North Atlantic right whale	0
Eubalaena glacialis/Megaptera novaeangliae	Right or humpback whale	0
Megaptera novaeangliae	Humpback whale	6
Physeter macrocephalus	Sperm whale	37
Total		51

Table 21: Proxy species used to fit detection functions for Without Belly Observers - 750 ft. The number of sightings, n, is before truncation.

The sightings were right truncated at 600m. Due to a reduced frequency of sightings close to the trackline that plausibly resulted from the behavior of the observers and/or the configuration of the survey platform, the sightings were left truncted as well. Sightings closer than 40 m to the trackline were omitted from the analysis, and it was assumed that the the area closer to the trackline than this was not surveyed. This distance was estimated by inspecting histograms of perpendicular sighting distances. The vertical sighting angles were heaped at 10 degree increments, so the candidate detection functions were fitted using linear bins scaled accordingly.

Key	Adjustment	Order	Covariates	Succeeded	Δ AIC	Mean ESHW (m)
hn	cos	2		Yes	0.00	216
hr				Yes	0.59	251
hn	cos	3		Yes	2.31	255
hn	herm	4		Yes	2.46	316
hr	poly	2		Yes	2.59	251
hr	poly	4		Yes	2.59	255
hn				No		

Table 22: Candidate detection functions for Without Belly Observers - 750 ft. The first one listed was selected for the density model.

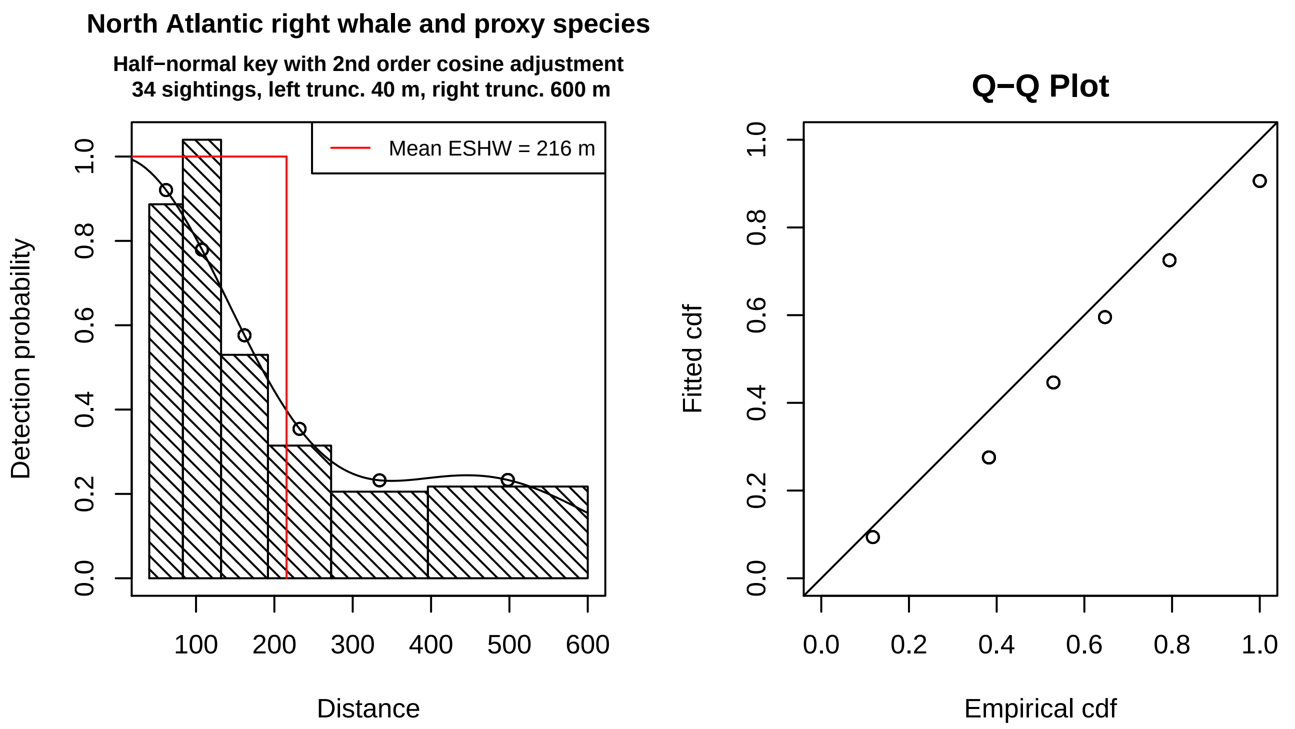

Figure 32: Detection function for Without Belly Observers - 750 ft that was selected for the density model

Statistical output for this detection function:

```
Summary for ds object
Number of observations :  34
Distance range         :  40.30835  -  600
AIC                    :  124.984

Detection function:
 Half-normal key function with cosine adjustment term of order 2

Detection function parameters
Scale Coefficients:
            estimate        se
(Intercept) 5.738325 0.1838281

Adjustment term parameter(s):
              estimate        se
cos, order 2 0.4333816 0.2422531


Monotonicity constraints were enforced.
                      Estimate          SE        CV
Average p            0.3592782  0.08709342 0.2424122
N in covered region 94.6341885 26.36346680 0.2785829

Monotonicity constraints were enforced.
```

Additional diagnostic plots:

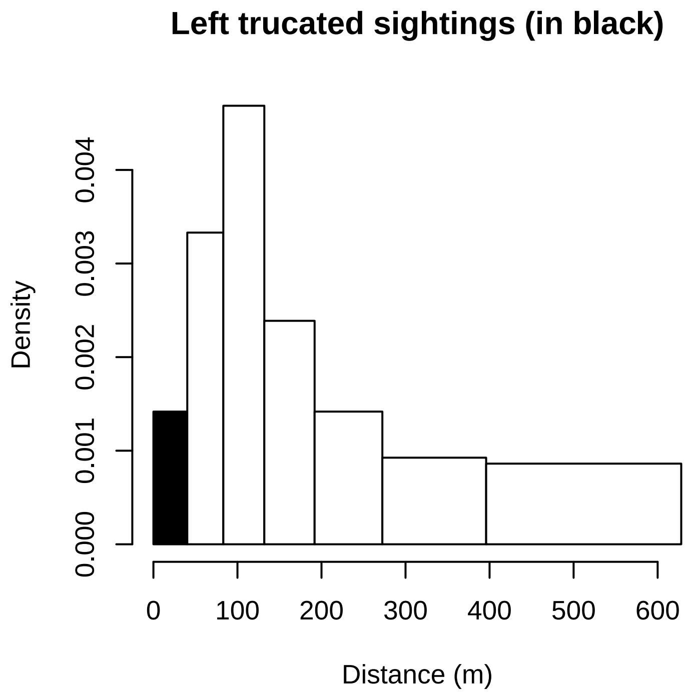

Figure 33: Density of sightings by perpendicular distance for Without Belly Observers - 750 ft. Black bars on the left show sightings that were left truncated.

Without Belly Observers - 1000 ft

Because this taxon was sighted too infrequently to fit a detection function to its sightings alone, we fit a detection function to the pooled sightings of several other species that we believed would exhibit similar detectability. These "proxy species" are listed below.

Reported By Observer	Common Name	n
Balaenoptera	Balaenopterid sp.	1
Balaenoptera acutorostrata	Minke whale	16
Balaenoptera borealis	Sei whale	0
Balaenoptera borealis/edeni	Sei or Bryde's whale	0
Balaenoptera borealis/physalus	Fin or Sei whale	0
Balaenoptera edeni	Bryde's whale	0
Balaenoptera musculus	Blue whale	0
Balaenoptera physalus	Fin whale	32
Eubalaena glacialis	North Atlantic right whale	34
Eubalaena glacialis/Megaptera novaeangliae	Right or humpback whale	0
Megaptera novaeangliae	Humpback whale	30
Total		113

Table 23: Proxy species used to fit detection functions for Without Belly Observers - 1000 ft. The number of sightings, n, is before truncation.

The sightings were right truncated at 1500m.

Covariate	Description
beaufort	Beaufort sea state.
quality	Survey-specific index of the quality of observation conditions, utilizing relevant factors other than Beaufort sea state (see methods).
size	Estimated size (number of individuals) of the sighted group.

Table 24: Covariates tested in candidate "multi-covariate distance sampling" (MCDS) detection functions.

Key	Adjustment	Order	Covariates	Succeeded	Δ AIC	Mean ESHW (m)
hr				Yes	0.00	434
hr	poly	4		Yes	1.58	424
hn	cos	2		Yes	1.71	462
hr	poly	2		Yes	1.92	427
hr			quality	Yes	1.96	433
hn	cos	3		Yes	3.64	418
hn				Yes	11.03	585
hn	herm	4		No		
hn			beaufort	No		
hr			beaufort	No		
hn			quality	No		
hn			size	No		
hr			size	No		
hn			beaufort, quality	No		
hr			beaufort, quality	No		
hn			beaufort, size	No		
hr			beaufort, size	No		
hn			quality, size	No		
hr			quality, size	No		
hn			beaufort, quality, size	No		
hr			beaufort, quality, size	No		

Table 25: Candidate detection functions for Without Belly Observers - 1000 ft. The first one listed was selected for the density model.

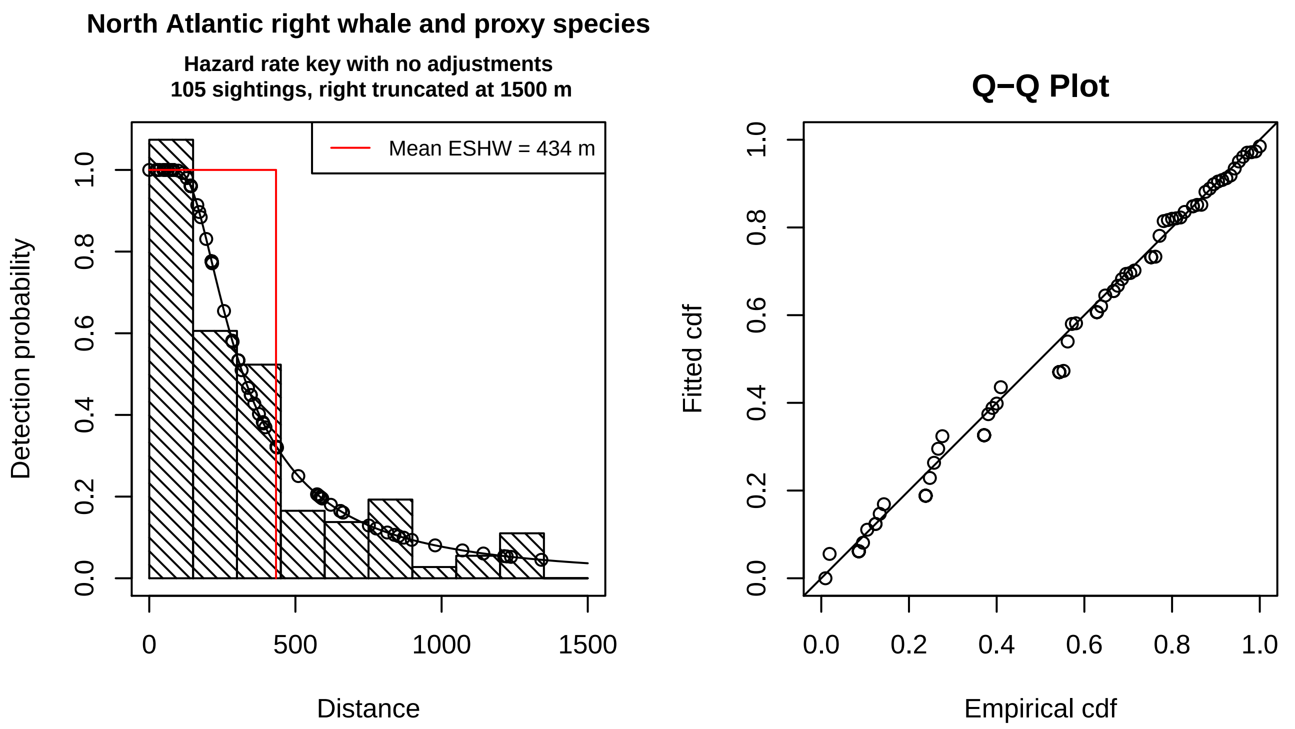

Figure 34: Detection function for Without Belly Observers - 1000 ft that was selected for the density model

Statistical output for this detection function:

```
Summary for ds object
Number of observations :  105
Distance range         :  0  -  1500
AIC                    :  1432.491

Detection function:
 Hazard-rate key function

Detection function parameters
Scale Coefficients:
            estimate        se
(Intercept) 5.576432 0.2232183

Shape parameters:
             estimate        se
(Intercept) 0.6374087 0.1752092

                        Estimate          SE        CV
Average p              0.2891295  0.03984493 0.1378100
N in covered region 363.1591175 58.28878285 0.1605048
```

Additional diagnostic plots:

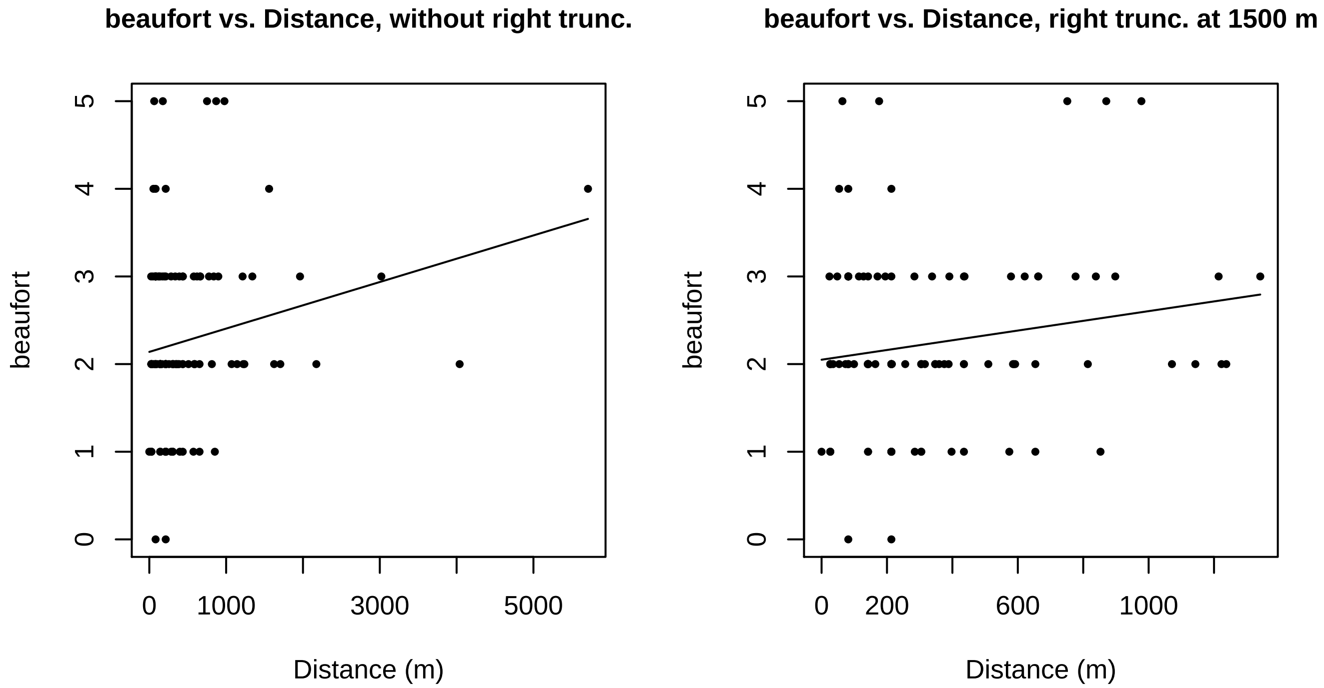

Figure 35: Scatterplots showing the relationship between Beaufort sea state and perpendicular sighting distance, for all sightings (left) and only those not right truncated (right). The line is a simple linear regression.

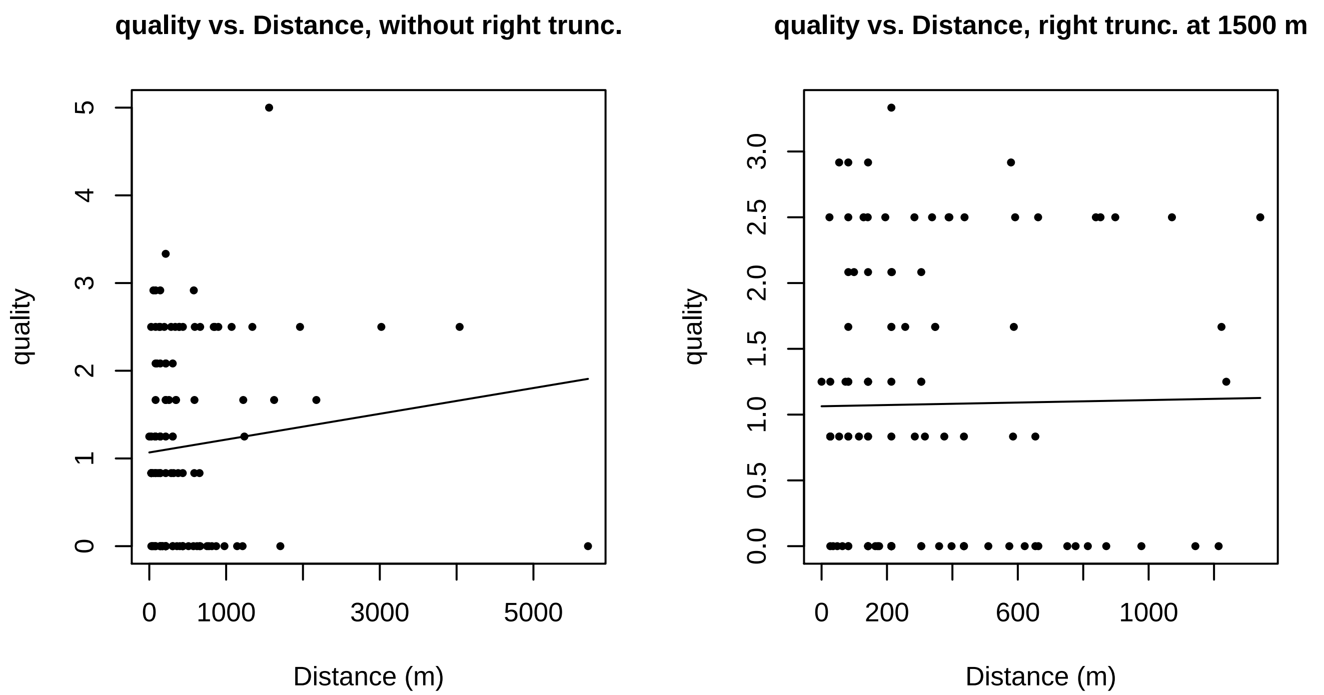

Figure 36: Scatterplots showing the relationship between the survey-specific index of the quality of observation conditions and perpendicular sighting distance, for all sightings (left) and only those not right truncated (right). Low values of the quality index correspond to better observation conditions. The line is a simple linear regression.

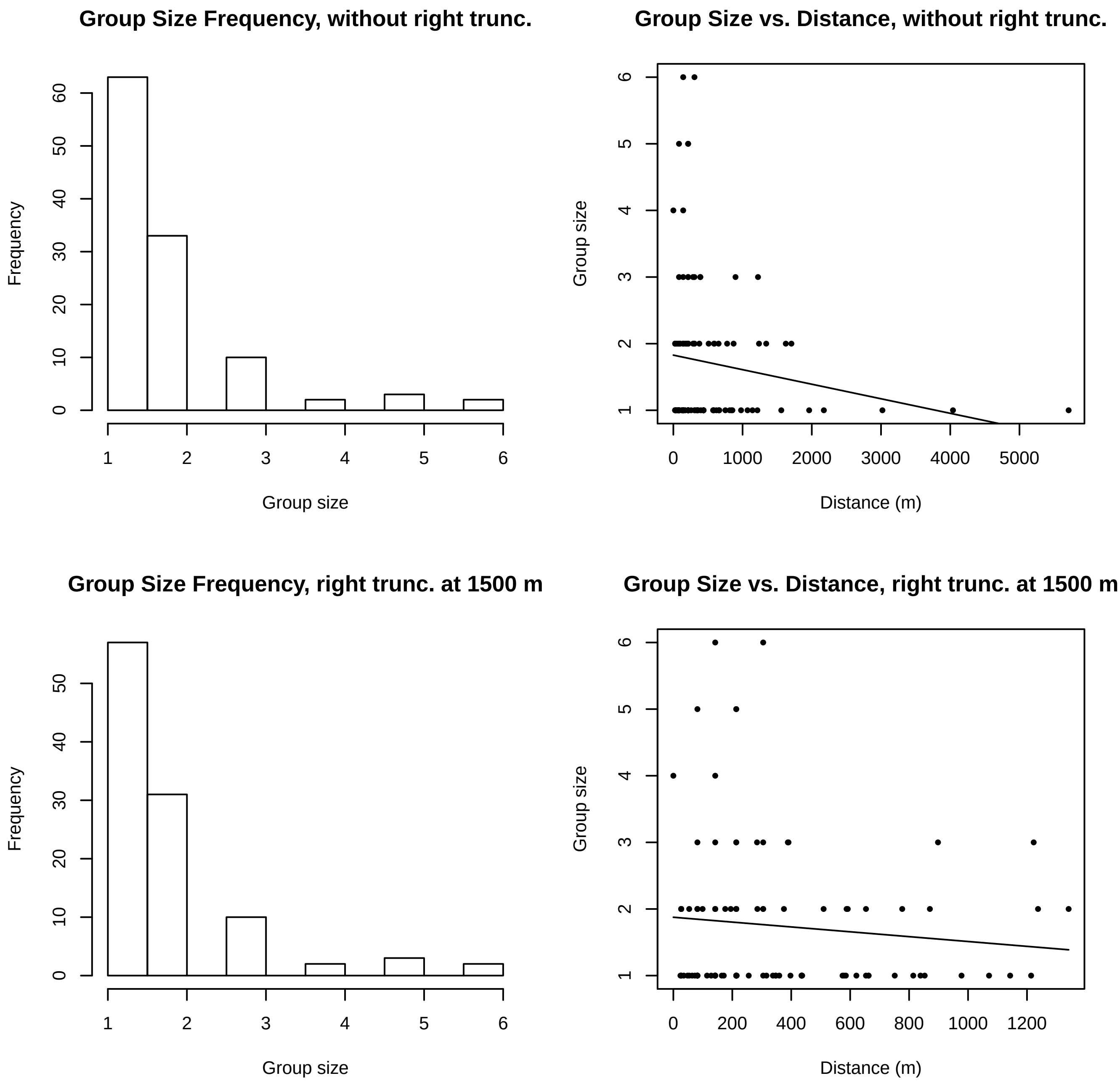

Figure 37: Histograms showing group size frequency and scatterplots showing the relationship between group size and perpendicular sighting distance, for all sightings (top row) and only those not right truncated (bottom row). In the scatterplot, the line is a simple linear regression.

UNCW Aerial Surveys

Because this taxon was sighted too infrequently to fit a detection function to its sightings alone, we fit a detection function to the pooled sightings of several other species that we believed would exhibit similar detectability. These "proxy species" are listed below.

Reported By Observer	Common Name	n
Balaenoptera	Balaenopterid sp.	1
Balaenoptera acutorostrata	Minke whale	15

Balaenoptera borealis	Sei whale	0
Balaenoptera borealis/edeni	Sei or Bryde's whale	0
Balaenoptera borealis/physalus	Fin or Sei whale	0
Balaenoptera edeni	Bryde's whale	0
Balaenoptera musculus	Blue whale	0
Balaenoptera physalus	Fin whale	19
Eubalaena glacialis	North Atlantic right whale	31
Eubalaena glacialis/Megaptera novaeangliae	Right or humpback whale	0
Megaptera novaeangliae	Humpback whale	23
Total		89

Table 26: Proxy species used to fit detection functions for UNCW Aerial Surveys. The number of sightings, n, is before truncation.

The sightings were right truncated at 1500m.

Covariate	Description
beaufort	Beaufort sea state.
quality	Survey-specific index of the quality of observation conditions, utilizing relevant factors other than Beaufort sea state (see methods).
size	Estimated size (number of individuals) of the sighted group.

Table 27: Covariates tested in candidate "multi-covariate distance sampling" (MCDS) detection functions.

Key	Adjustment	Order	Covariates	Succeeded	Δ AIC	Mean ESHW (m)
hn	cos	3		Yes	0.00	358
hr				Yes	0.01	397
hr	poly	4		Yes	0.85	391
hr	poly	2		Yes	1.03	386
hn	cos	2		Yes	1.24	409
hr			quality	Yes	1.55	396
hn				Yes	5.53	480
hn			quality	Yes	7.53	480
hn	herm	4		No		
hn			beaufort	No		
hr			beaufort	No		
hn			size	No		
hr			size	No		
hn			beaufort, quality	No		
hr			beaufort, quality	No		

hn	beaufort, size	No
hr	beaufort, size	No
hn	quality, size	No
hr	quality, size	No
hn	beaufort, quality, size	No
hr	beaufort, quality, size	No

Table 28: Candidate detection functions for UNCW Aerial Surveys. The first one listed was selected for the density model.

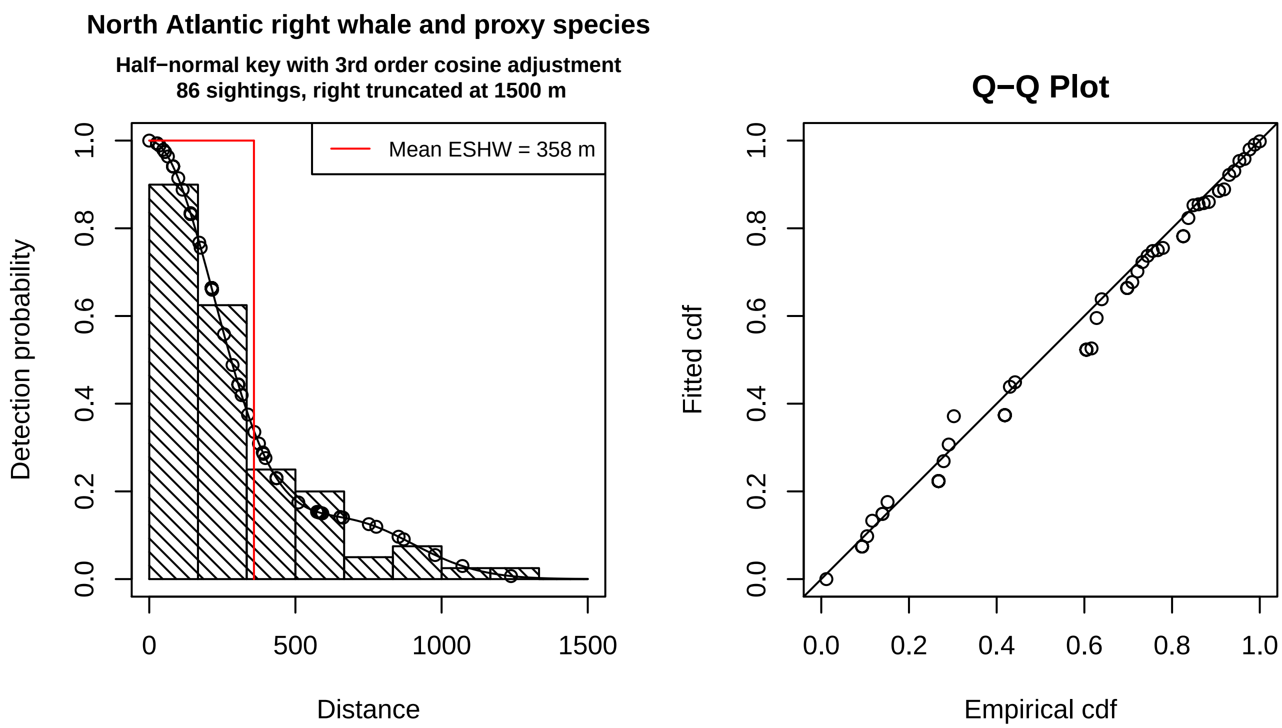

Figure 38: Detection function for UNCW Aerial Surveys that was selected for the density model

Statistical output for this detection function:

```
Summary for ds object
Number of observations :  86
Distance range         :  0  -  1500
AIC                    :  1144.166

Detection function:
 Half-normal key function with cosine adjustment term of order 3

Detection function parameters
Scale Coefficients:
            estimate         se
(Intercept) 6.006457 0.06897782

Adjustment term parameter(s):
```

```
               estimate        se
cos, order 3 0.4451316 0.1512901


Monotonicity constraints were enforced.
                        Estimate          SE        CV
Average p             0.2387636  0.02505433 0.1049337
N in covered region 360.1889782 50.76321627 0.1409350

Monotonicity constraints were enforced.
```

Additional diagnostic plots:

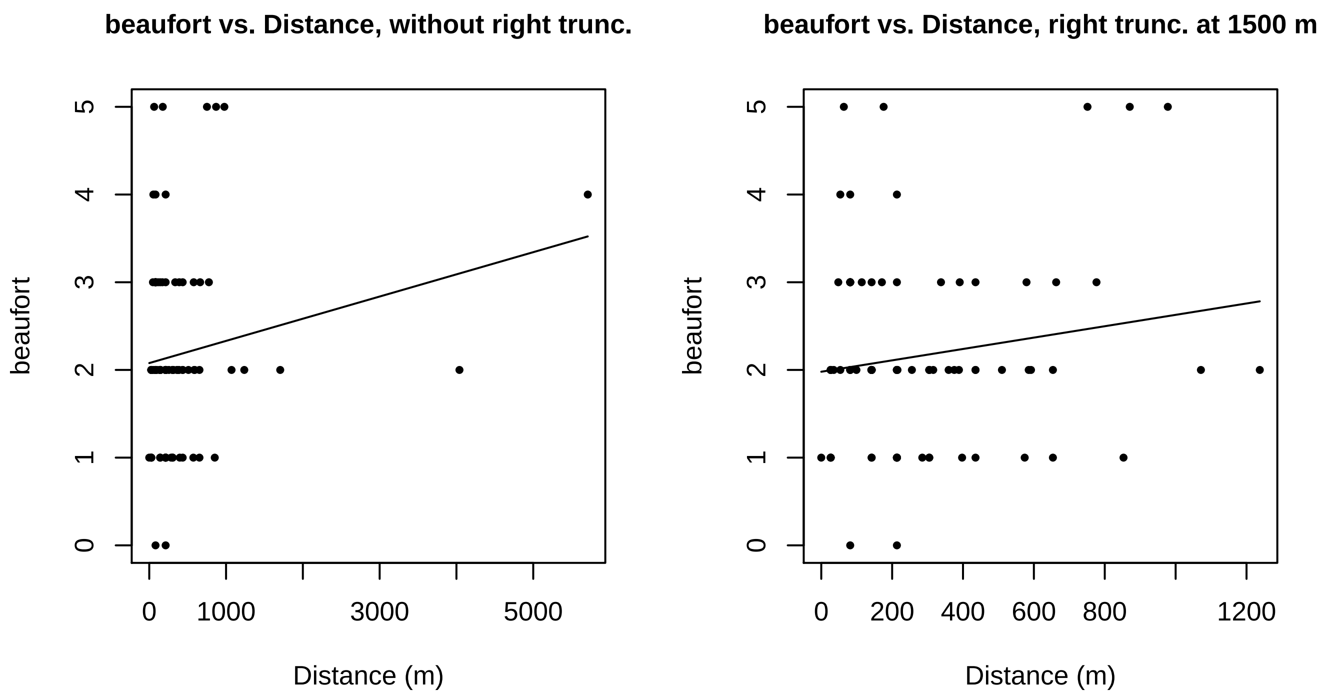

Figure 39: Scatterplots showing the relationship between Beaufort sea state and perpendicular sighting distance, for all sightings (left) and only those not right truncated (right). The line is a simple linear regression.

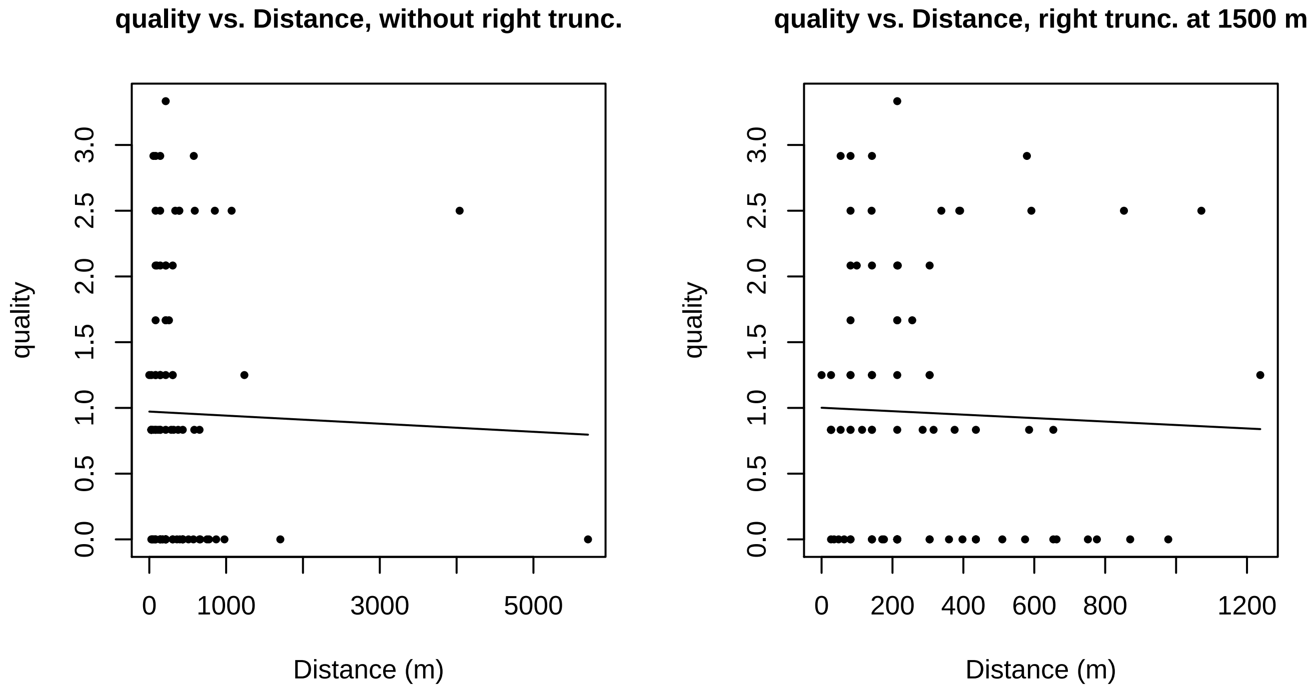

Figure 40: Scatterplots showing the relationship between the survey-specific index of the quality of observation conditions and perpendicular sighting distance, for all sightings (left) and only those not right truncated (right). Low values of the quality index correspond to better observation conditions. The line is a simple linear regression.

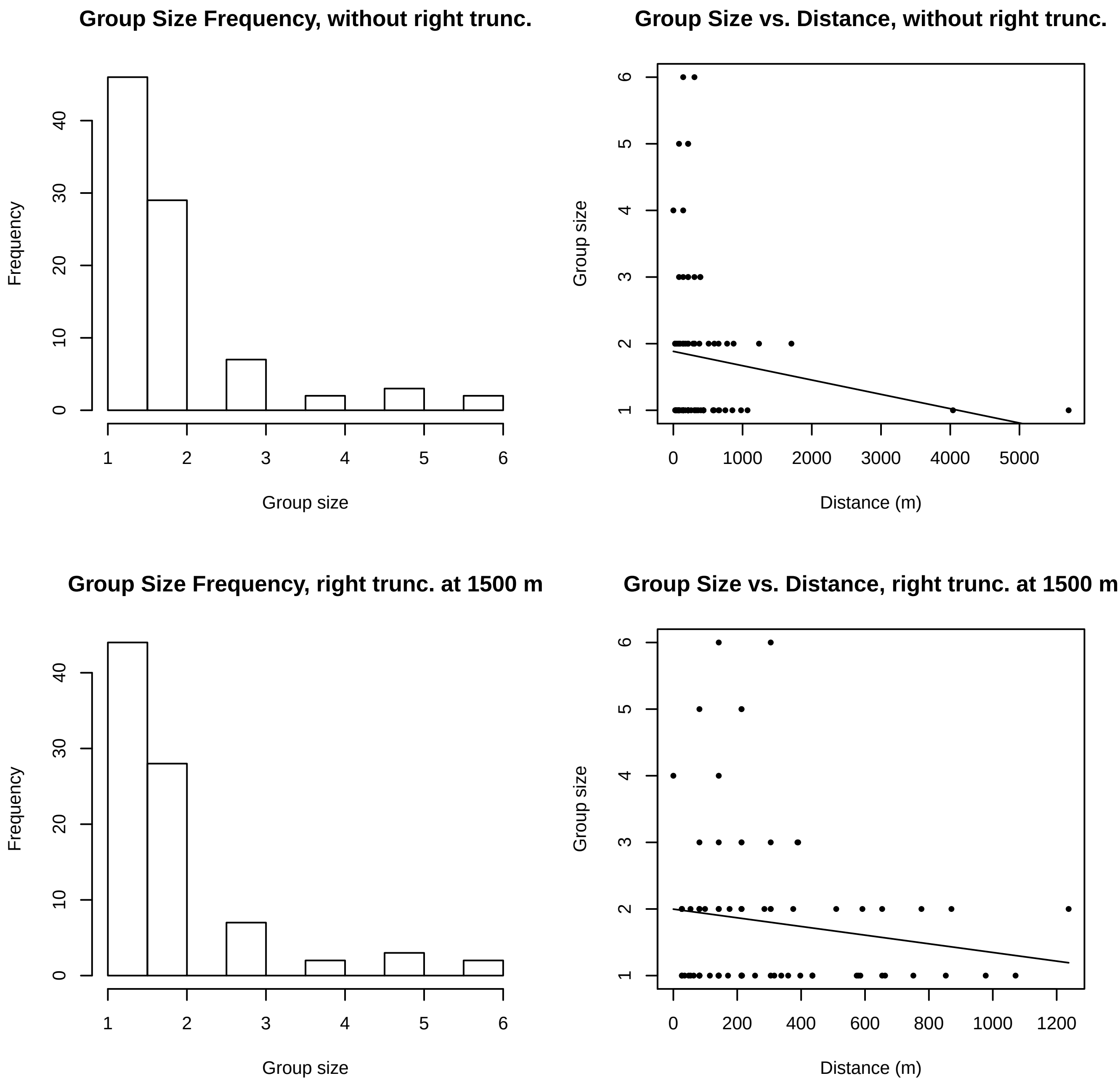

Figure 41: Histograms showing group size frequency and scatterplots showing the relationship between group size and perpendicular sighting distance, for all sightings (top row) and only those not right truncated (bottom row). In the scatterplot, the line is a simple linear regression.

NARWSS Grummans

The sightings were right truncated at 2000m.

Covariate	Description
beaufort	Beaufort sea state.
quality	Survey-specific index of the quality of observation conditions, utilizing relevant factors other than Beaufort sea state (see methods).
size	Estimated size (number of individuals) of the sighted group.

Table 29: Covariates tested in candidate "multi-covariate distance sampling" (MCDS) detection functions.

Key	Adjustment	Order	Covariates	Succeeded	Δ AIC	Mean ESHW (m)
hn	cos	3		Yes	0.00	924
hn				Yes	0.73	1138
hn			quality	Yes	1.83	1137
hn			beaufort	Yes	2.01	1145
hn	cos	2		Yes	2.31	1050
hr	poly	4		Yes	2.76	1024
hn			beaufort, quality	Yes	3.57	1142
hr	poly	2		Yes	4.02	1101
hr			quality	Yes	4.04	911
hr				Yes	4.39	953
hr			beaufort	Yes	4.93	870
hr			beaufort, quality	Yes	5.94	899
hn	herm	4		No		
hn			size	No		
hr			size	No		
hn			beaufort, size	No		
hr			beaufort, size	No		
hn			quality, size	No		
hr			quality, size	No		
hn			beaufort, quality, size	No		
hr			beaufort, quality, size	No		

Table 30: Candidate detection functions for NARWSS Grummans. The first one listed was selected for the density model.

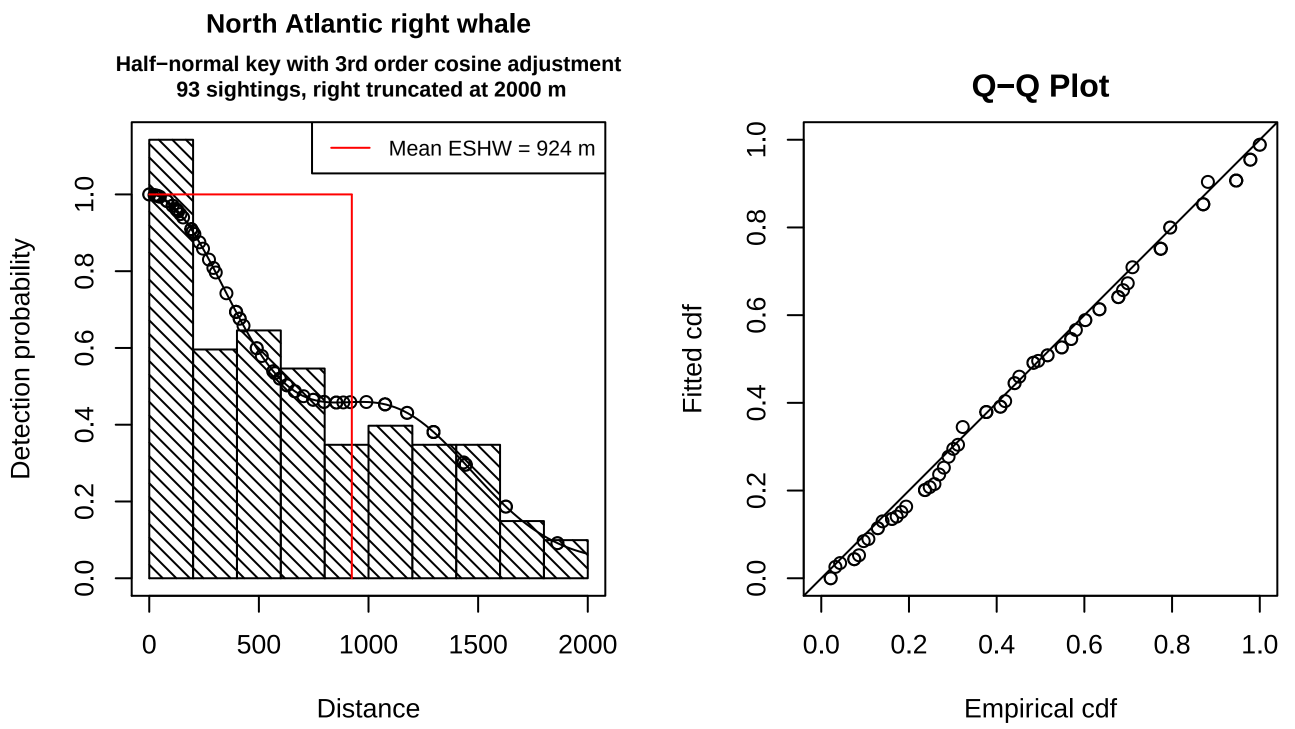

Figure 42: Detection function for NARWSS Grummans that was selected for the density model

Statistical output for this detection function:

```
Summary for ds object
Number of observations :  93
Distance range         :  0  -  2000
AIC                    :  1386.214

Detection function:
 Half-normal key function with cosine adjustment term of order 3

Detection function parameters
Scale Coefficients:
            estimate        se
(Intercept)  6.84024 0.1071695

Adjustment term parameter(s):
              estimate        se
cos, order 3 0.2293001 0.1371662


Monotonicity constraints were enforced.
                       Estimate          SE        CV
Average p             0.4619332  0.06821275 0.1476680
N in covered region 201.3278033 33.44193436 0.1661069

Monotonicity constraints were enforced.
```

Additional diagnostic plots:

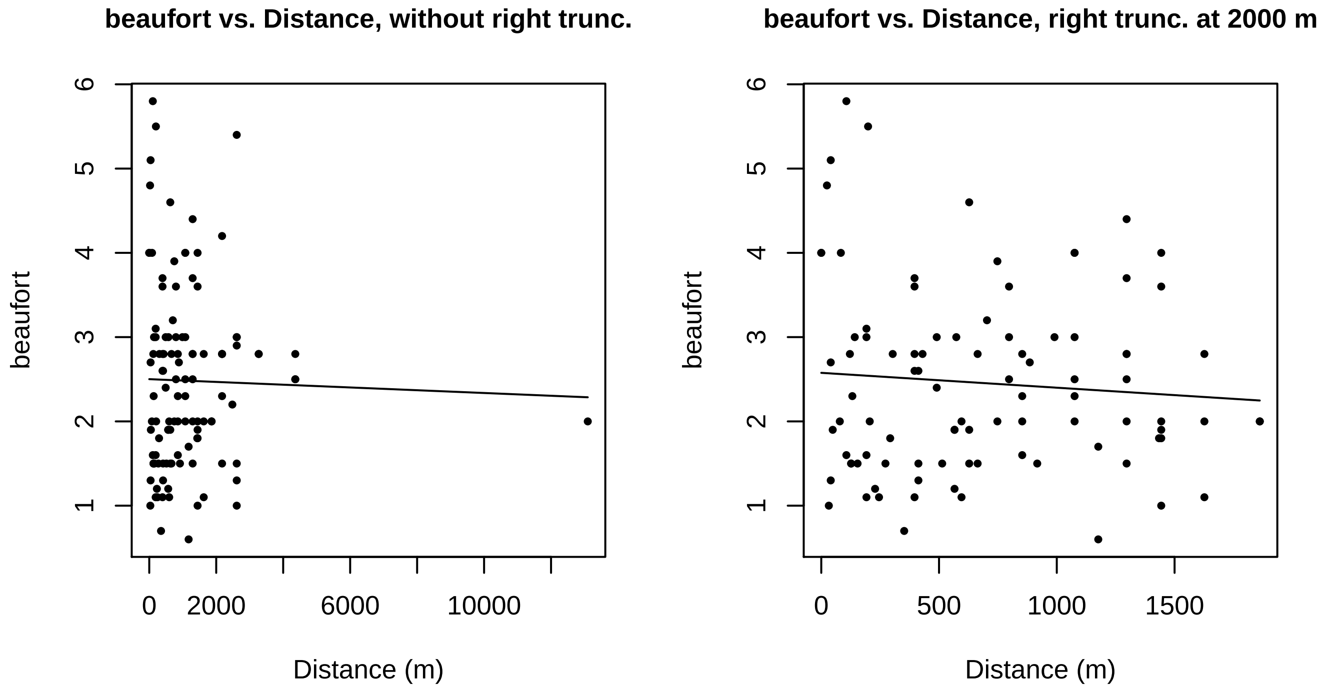

Figure 43: Scatterplots showing the relationship between Beaufort sea state and perpendicular sighting distance, for all sightings (left) and only those not right truncated (right). The line is a simple linear regression.

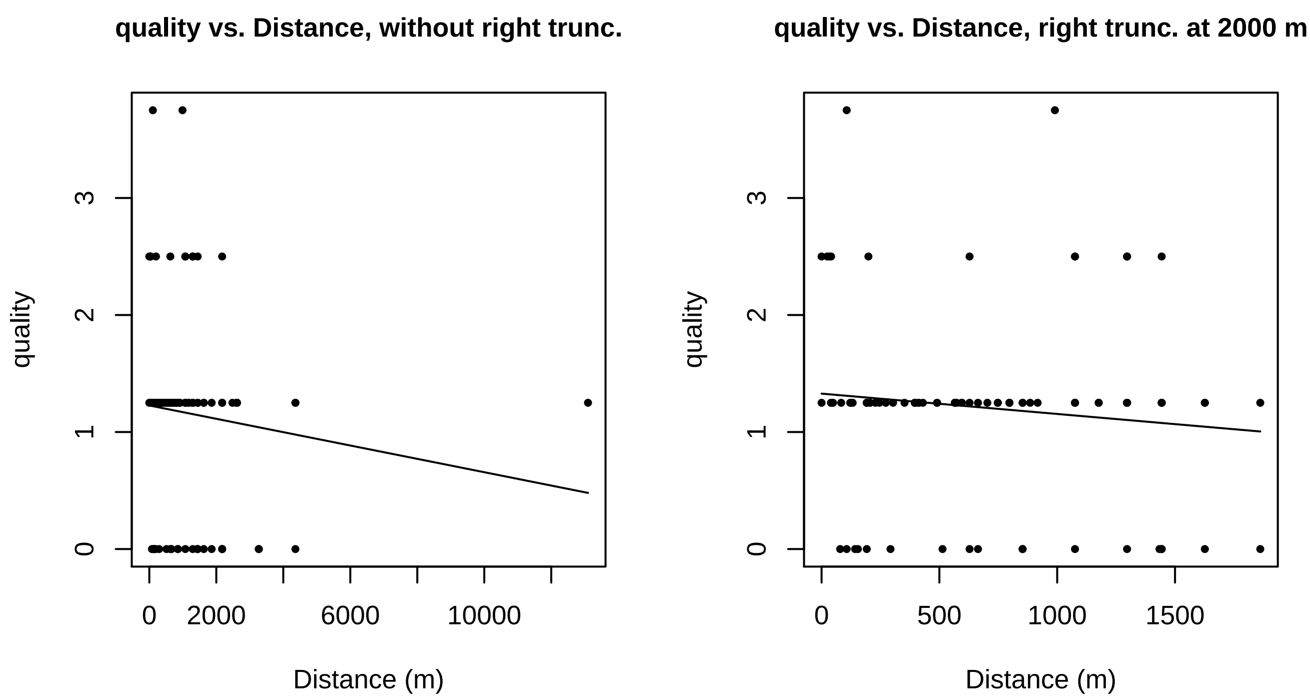

Figure 44: Scatterplots showing the relationship between the survey-specific index of the quality of observation conditions and perpendicular sighting distance, for all sightings (left) and only those not right truncated (right). Low values of the quality index correspond to better observation conditions. The line is a simple linear regression.

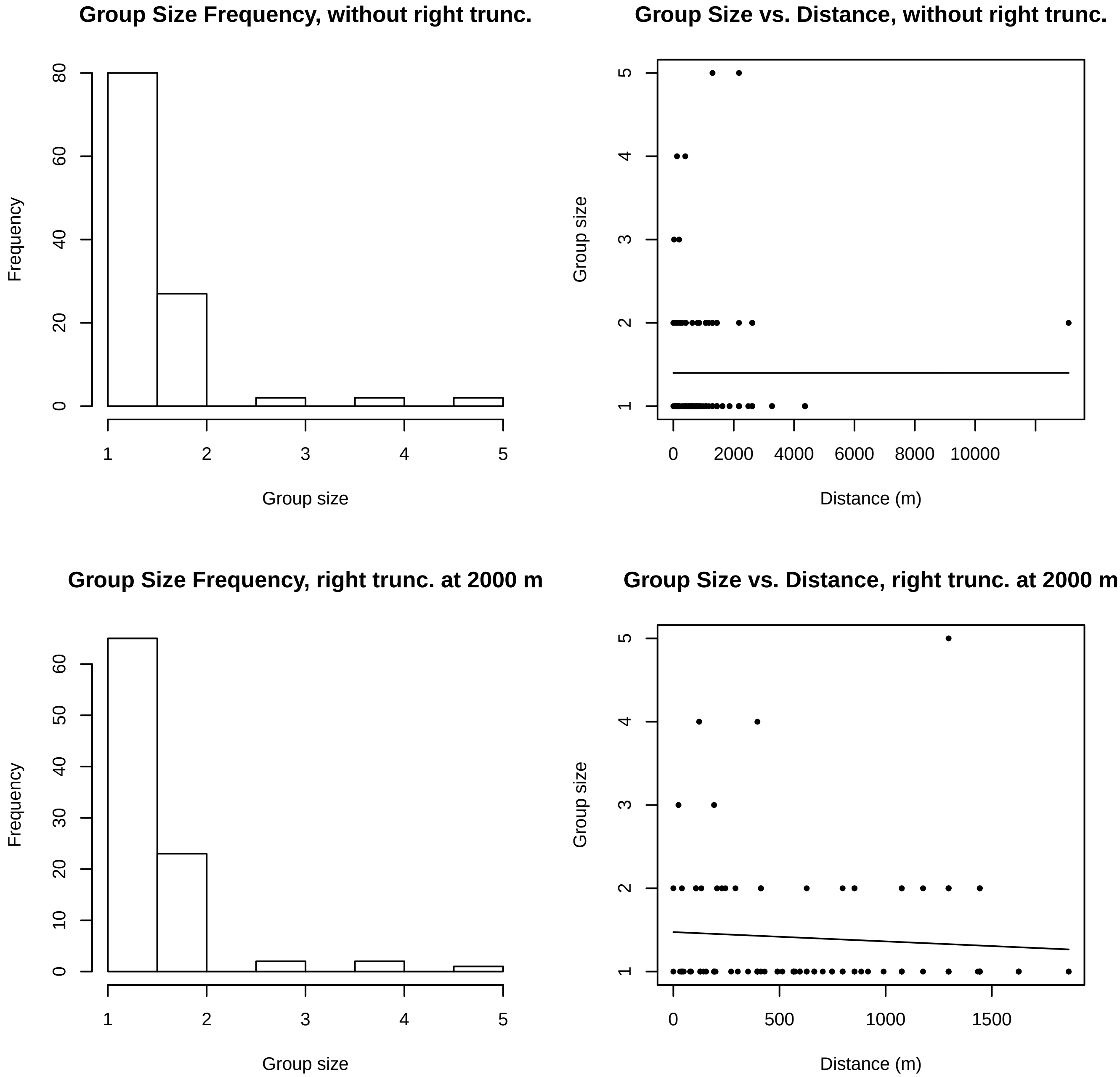

Figure 45: Histograms showing group size frequency and scatterplots showing the relationship between group size and perpendicular sighting distance, for all sightings (top row) and only those not right truncated (bottom row). In the scatterplot, the line is a simple linear regression.

NARWSS Twin Otters

The sightings were right truncated at 8730m. Due to a reduced frequency of sightings close to the trackline that plausibly resulted from the behavior of the observers and/or the configuration of the survey platform, the sightings were left truncted as well. Sightings closer than 107 m to the trackline were omitted from the analysis, and it was assumed that the the area closer to the trackline than this was not surveyed. This distance was estimated by inspecting histograms of perpendicular sighting distances. The vertical sighting angles were heaped at 10 degree increments up to 80 degrees and 1 degree increments thereafter, so the candidate detection functions were fitted using linear bins scaled accordingly.

Covariate	Description

beaufort	Beaufort sea state.
quality	Survey-specific index of the quality of observation conditions, utilizing relevant factors other than Beaufort sea state (see methods).
size	Estimated size (number of individuals) of the sighted group.

Table 31: Covariates tested in candidate “multi-covariate distance sampling” (MCDS) detection functions.

Key	Adjustment	Order	Covariates	Succeeded	Δ AIC	Mean ESHW (m)
hn	cos	2		Yes	0.00	2790
hn	cos	3		Yes	11.28	2829
hn				Yes	16.26	3100
hn	herm	4		Yes	17.68	3096
hn			quality	Yes	18.23	3100
hn			beaufort	No		
hn			size	No		
hn			beaufort, quality	No		
hn			beaufort, size	No		
hn			quality, size	No		
hn			beaufort, quality, size	No		

Table 32: Candidate detection functions for NARWSS Twin Otters. The first one listed was selected for the density model.

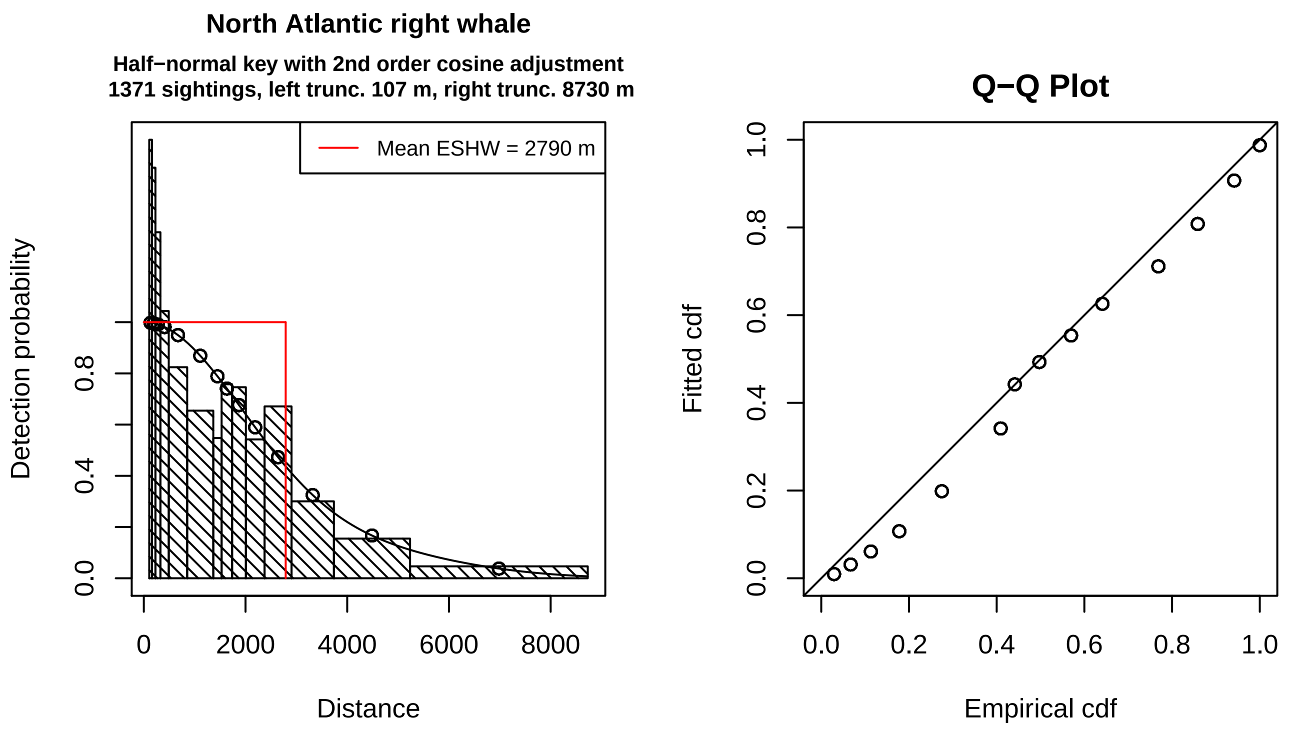

Figure 46: Detection function for NARWSS Twin Otters that was selected for the density model

Statistical output for this detection function:

```
Summary for ds object
Number of observations :  1371
Distance range         :  106.5979  -  8729.882
AIC                    :  7044.881

Detection function:
 Half-normal key function with cosine adjustment term of order 2

Detection function parameters
Scale Coefficients:
            estimate         se
(Intercept) 7.934921 0.02695208

Adjustment term parameter(s):
              estimate        se
cos, order 2 0.2455253 0.0530155


Monotonicity constraints were enforced.
                        Estimate           SE         CV
Average p              0.3195465 9.249111e-03 0.02894449
N in covered region 4290.4549720 1.567104e+02 0.03652537

Monotonicity constraints were enforced.
```

Additional diagnostic plots:

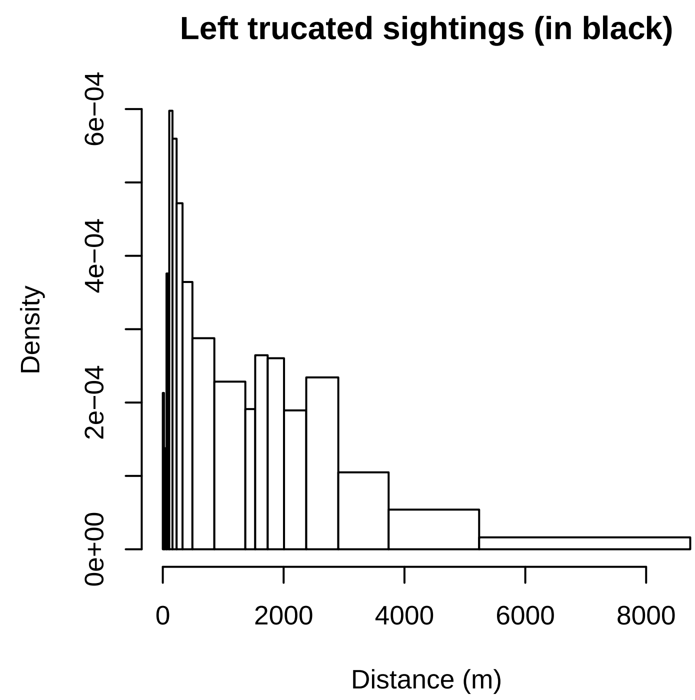

Figure 47: Density of sightings by perpendicular distance for NARWSS Twin Otters. Black bars on the left show sightings that were left truncated.

Figure 48: Scatterplots showing the relationship between Beaufort sea state and perpendicular sighting distance, for all sightings (left) and only those not right truncated (right). The line is a simple linear regression.

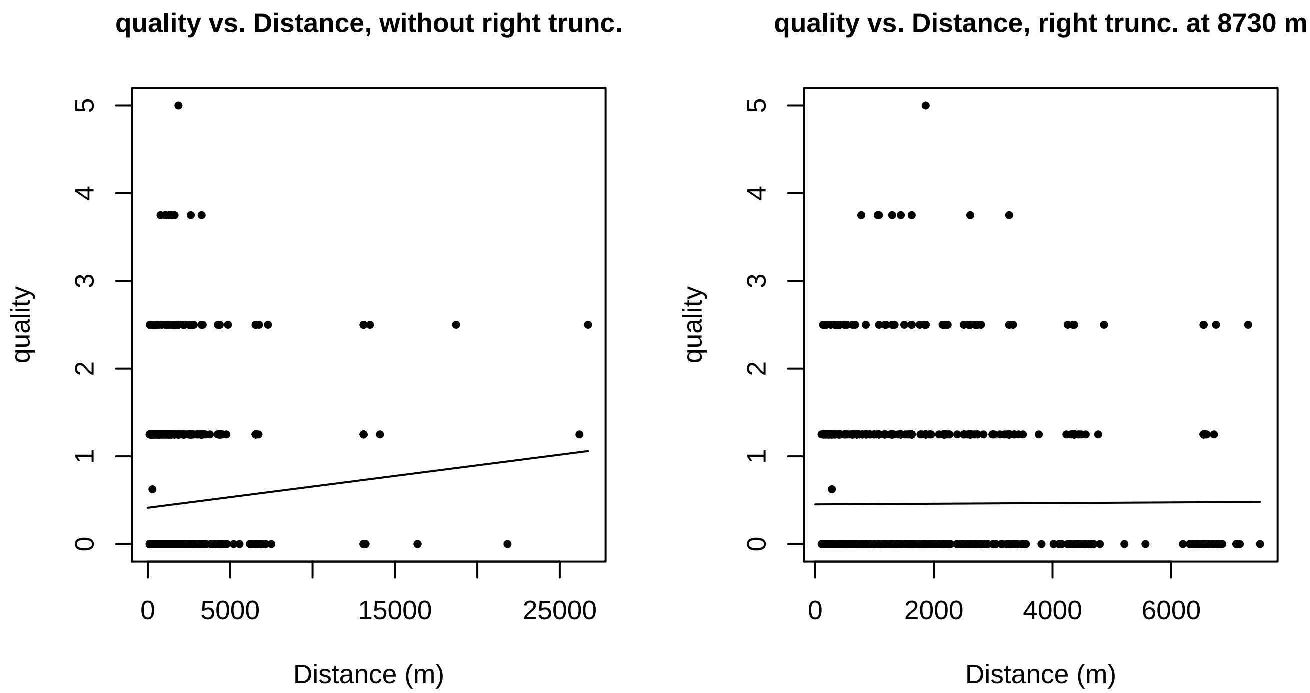

Figure 49: Scatterplots showing the relationship between the survey-specific index of the quality of observation conditions and perpendicular sighting distance, for all sightings (left) and only those not right truncated (right). Low values of the quality index correspond to better observation conditions. The line is a simple linear regression.

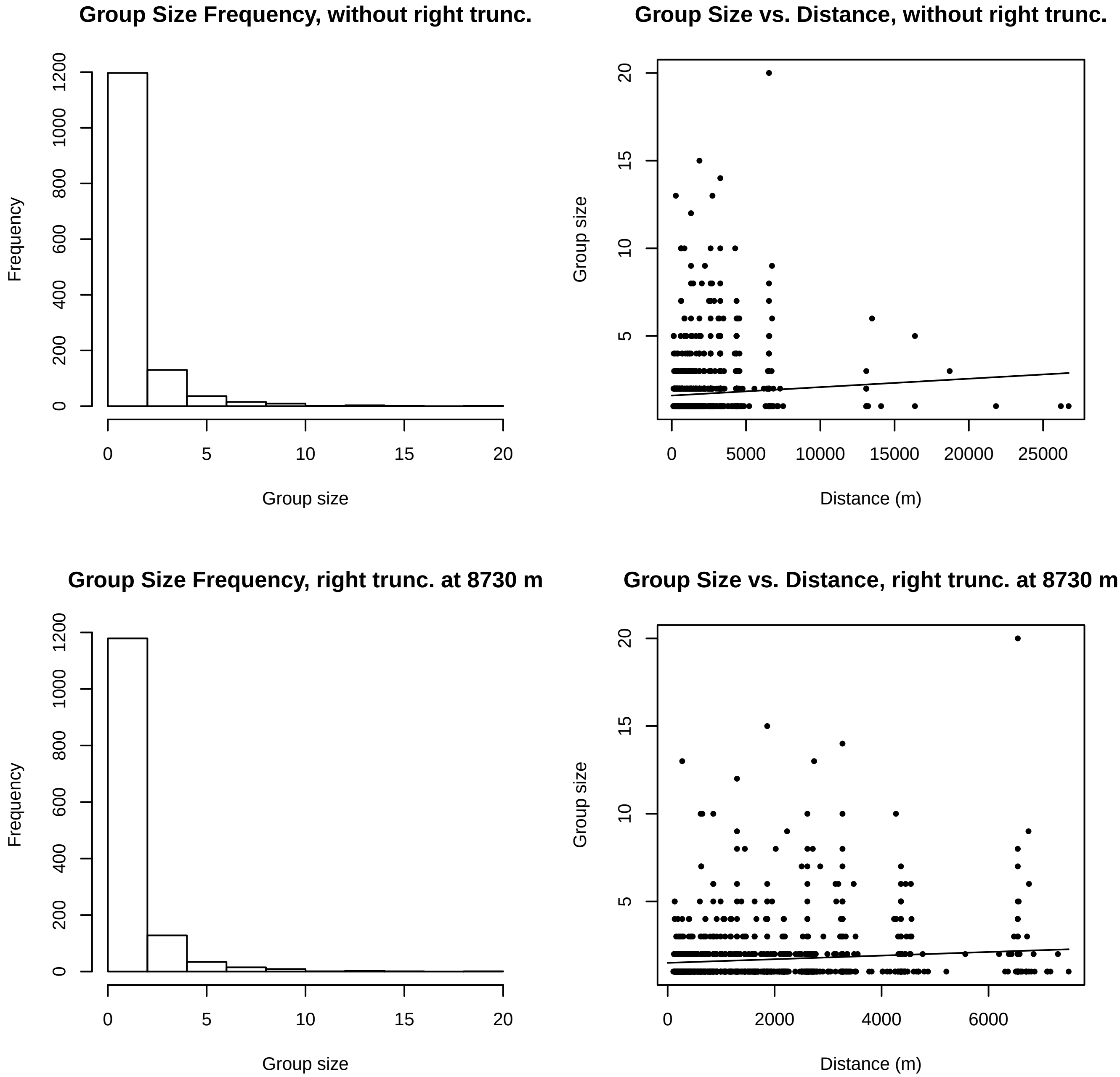

Figure 50: Histograms showing group size frequency and scatterplots showing the relationship between group size and perpendicular sighting distance, for all sightings (top row) and only those not right truncated (bottom row). In the scatterplot, the line is a simple linear regression.

g(0) Estimates

Platform	Surveys	Group Size	*g(0)*	Biases Addressed	Source
Shipboard	Binocular Surveys	Any	0.63	Perception	Palka (2006)
Shipboard	NEFSC Abel-J Binocular Surveys	Any	0.32	Perception	Palka (2006)
Shipboard	NEFSC Endeavor	Any	0.94	Perception	Palka (2006)
Shipboard	Naked Eye Surveys	Any	0.38	Perception	Palka (2006)
Aerial	NEFSC Surveys With Belly Observers	Any	0.334	Availability	CETAP (1982)
Aerial	SEFSC Surveys With Belly Observers	1	0.434	Availability	Hain et al. (1999)
		2	0.729	Availability	Hain et al. (1999)
		>2	0.861	Availability	Hain et al. (1999)
Aerial	Without Belly Observers	1	0.434	Availability	Hain et al. (1999)
		2	0.729	Availability	Hain et al. (1999)
		>2	0.861	Availability	Hain et al. (1999)
Aerial	Without Belly Observers - 600 ft	Any	0.334	Availability	CETAP (1982)
Aerial	NARWSS Aerial Surveys	Any	0.334	Availability	CETAP (1982)

Table 33: Estimates of *g(0)* used in this density model.

No species-specific estimate of g(0) was available in the literature for right whales observed from shipboard surveys with bigeye binoculars. Instead, we used Palka's (2006) survey-specific g(0) estimates for fin and sei whales for two NOAA NEFSC surveys that used bigeye binoculars: the Abel-J 1998 survey (0.32) and the Endeavor 2004 survey (0.94). We used the estimates for the lower teams, which were the primary teams and the teams for which we had sightings. We applied the survey-specific estimates to the two surveys that reported them; for all other binocular surveys, we used the simple mean of the two estimates (0.63).

Palka's (2006) estimates used a dual-team methodology that accounted for perception bias but not availability bias (Palka 2005b). This prompts the question of whether right whales undertake dives long enough to yield significant availability bias. Studies of right whale diving behavior reported a range of mean dive durations: 5.65 min (CETAP 1982, Special Topic D, Table 5), 4.76 min (Winn et al. 1995), and 12.17 min (Baumgartner and Mate 2003). Barlow (1999) used a simulation model to produce estimates of g(0) that incorporated both perception and availability bias for four long-diving whale taxa. For Kogia spp., Mesoplodon spp., and Ziphius cavirostris, all small whales with short surface intervals (Barlow assumed 1.2, 2.5, and 2.1 min, respectively), Barlow assumed dive times of 10.9, 20.4, and 28.6 min and estimated g(0)s of 0.35, 0.45, and 0.23. For Berardius bairdii, a large whale with a longer surface interval (Barlow assumed 3.5 min) that is much easier to perceive (see his Figure 3), he assumed a dive interval of 15.5 min and estimated g(0)=0.96. Right whales are much larger than B. bairdii and are likely to be easier to perceive at the surface; in Baumgartner and Mate's (2003) study, they exhibited a similar mean surface interval of 3.13 min. Even if right whales regularly undertake dives of the duration observed by Baumgartner and Mate, we believe they are more comparable to B. bairdii than the other species studied by Barlow. Our conclusion, therefore, is that availability bias is not likely to be a significant factor for observations of right whales made from shipboard surveys. In any case, because so few right whales were sighted on binocular surveys, the selection of g(0) does not greatly influence the final abundance estimate.

Palka (2006) provided a survey-specific estimate of g(0) for the NOAA NEFSC Abel-J 1999 naked eye shipboard survey. We used the estimate for the upper team, which was the primary team and the one for which we had sightings. This estimate used a dual-team methodology that accounted for perception bias but not availability bias (Palka 2005b), but as discussed above, we believe that availability bias is not likely to be a significant factor for observations of right whales made from shipboard surveys.

No species-specific estimates of g(0) were available in the literature for right whales observed from aircraft. Palka (2006) estimated g(0)=0.53 for groups of 1-5 large whales, estimated from two years of aerial surveys made in the northern half of the study area using the Hiby (1999) circle-back method. This estimate accounted for both availability and perception bias, but pooled sightings of all large whales together to provide a generic estimate, due to sample-size limitations. We were reluctant to use this estimate because it was not species-specific. Instead, following Carretta et al.'s (2000) assumption that availability bias would dominate perception bias for large whales observed from aircraft, we estimated availability bias by applying equation (3) of Carretta et al. (2000) to right whale dive data from the literature. We did not incorporate estimates of perception bias.

For aerial surveys conducted by NOAA NEFSC, which all occurred in and around the right whale feeding grounds, we estimated availability bias at 0.334 from mean durations of surface activity bouts and inter-bout dives (2.58 min and 5.65 min) reported for right whales observed at Stellwagen Bank, east of the elbow of Cape Cod, and the Great South Channel in May of 1980 and 1981 (CETAP (1982), Special Topic D, Table 5). These are areas where right whales regularly feed in spring. We applied this estimate to both the NEFSC aerial abundance surveys and the NARWSS program surveys.

Other diving studies conducted at different times and areas reported different diving behavior. Winn et al. (1995) reported shorter mean inter-bout dive durations of 4.76 min and 1.54 min for whales monitored with radio tags in the Great South Channel in 1989 and 1990, respectively. They did not provide surface activity bout durations, so we could not estimate availability bias from these data. Baumgartner and Mate (2003) reported longer mean surface and dive intervals (3.13 min and 12.17 min) for feeding right whales monitored with time- depth recorders in the lower Bay of Fundy and Roseway Basin; these intervals yield an availability bias of 0.216. Nieukirk (1992) reported a similar estimate of 21.65% time spent at the surface for 8 right whales tagged with satellite tags in the Bay of Fundy in 1989-1990. Together, these results suggest right whale diving behavior may vary substantially, and more data, or a comprehensive synthesis or existing data, may be needed to arrive at a more robust estimate of mean availability bias.

For aerial surveys south of New York, which occurred in right whale calving and migration areas, there were far fewer sightings than occurred in the northern feeding grounds. We assumed that these southern sightings were mainly of mothers, calves, and juveniles who had recently calved or were socializing or migrating. Rather than use dive data from the feeding grounds, we obtained it from Hain et al. (1999), who studied dive behavior at the calving grounds.

The majority of right whale sightings in the southern area were of pairs of animals. We assumed that these were mother and calf pairs and estimated availability bias at 0.729, based on mean surface and dive times for mother/calf pairs of 5.44 and 2.25 min respectively (Hain et al. 1999). Single animals were next most frequently sighted. We assumed these were single juveniles and estimated availability bias at 0.434, based on mean surface and dive times of 2.14 and 3.17 min respectively (Hain et al. 1999). Finally, there were several sightings of three or more animals. We assumed these were "surface active groups" (some were noted as such in the observer logs that we had access to) and estimated availability bias at 0.861, based on mean surface and dive times of 7.76 and 1.45 min respectively (Hain et al. 1999).

Density Models

Unlike all other baleen whales, most of the extant population of North Atlantic right whales is believed to remain within our study area throughout their annual feeding, migration, and reproductive cycle. In their classic description, Winn et al. (1986) posited that the cycle has six distinct phases. In winter (phase 1), pregnant cows give birth off the Florida-Georgia coast, while other whales overwinter in the central Gulf of Maine, possibly to mate (Cole et al. 2013), and Cape Cod Bay, to feed (Costa et al. 2006). In early spring (phase 2), whales at the southern calving grounds migrate north to the Gulf of Maine along the continental shelf. In late spring and throughout summer (phases 3, 4, and 5) whales migrate around the Gulf of Maine to feed, with large concentrations gathering initially in the Great South Channel, then moving north to the Bay of Fundy and the southeastern Scotian Shelf. In fall and early winter (phase 6), some whales migrate south to the calving grounds along the continental shelf while others remain in the Gulf of Maine.

Although our study integrated many surveys, the spatiotemporal distribution of the combined data was patchy enough that we could not confidently attempt something as complex as a six-phase model. For example, the northern feeding grounds were only completely surveyed in August and September. Instead, we modeled right whales with four seasonal models, with our winter model encompassing the end of Winn's phase 6 and all of phase 1, our spring model encompassing phase 2 and the start of phase 3, our summer model encompassing the end of phase 3 through the start of phase 5, and our fall model encompassing the end of phase 5 and most of phase 6.

We fixed our winter/spring transition at February/March based on the suggestion by Firestone et al. (2008) that whales typically depart the winter calving grounds in early to mid-March. We fixed the spring/summer transition at April/May based on those authors' suggestion of a 30-day departure range followed by a 21-24 day travel time to the tip of Long Island, which would mean that most whales complete their northern migration to the Gulf of Maine by the end of April. Our sightings data seemed to corroborate that pattern, with only two sightings southwest of Martha's Vineyard in May.

The summer/fall and fall/winter transitions were more difficult to determine. Survey effort was sparse in the traditional fall months (September-November) and less has been published in the literature about the fall migration than the spring migration. Winn et al. (1986) suggested that whales leave the Nova Scotian-Bay of Fundy region in October through January, migrating steadily southward. Mellinger et al. (2007) reported acoustic detections of right whales on the Scotian Shelf as late as December, with a peak in August-October, while Mitchell et al. (1986) reported sightings by whalers in this region from June-November, with substantially more sightings recorded in the last half this period (not corrected for effort). Baumgartner and Mate (2005) reported that one satellite-tagged right whale departed the northern feeding grounds in mid-November of 2000; Schick et al. (2009) reported this whale south of Charleston, South Carolina on December 15, 2000. Whitt et al. (2013) reported acoustic detections of right whales off New Jersey in August-December 2008 and August-November 2009, peaking in September both years. Hodge et al. (2015) reported acoustic detections of right whales south of Cape Lookout, North Carolina on 3-5% of the days of the months of June, July, and September 2012. Detections then elevated to 12-25% for December 2012 and February and March 2013, with a lull of 3% in January 2013. Near the Georgia-South Carolina border, they reported detections every month between June 2012 and March 2013, with detections less than 20% through October 2012, then rising to 44% in November, peaking at 93% in December, then falling to less than 30% in January 2013. Norris et al. (2014) reported acoustic detections of right whales at the shelf break off Jacksonville, Florida in all four months they monitored: September, November, and December of 2009, and January of 2010.

Together, these results indicate right whales throughout most of the latitudinal extent of the study area during June-March. Compounding the difficulty of modeling the second half of the year was a lack of survey data in Canada and much of the U.S. mid-Atlantic and southeast after September. We fixed the summer/fall transition at July/August as this was the point at which right whale sightings greatly diminished in the Great South Channel and northern edge of Georges Bank. We fixed the fall/winter transition at October/November based on the multiplicity of reports that suggest elevated right whale presence in the southeast starting in November, in particular the strong increase in acoustic detections at the Georgia-South Carolina border in November reported by Hodge et. al (2015).

Finally, we note that the months we designated as "summer" (May-July) and "fall" (August-October) do not correspond to traditional astronomical seasons or seasons that may have previously been defined for right whales. We are using the labels "summer" and "fall" for convenience and do not mean to imply consistency with other usages of those labels.

Winter

In this season, survey effort was moderate on the shelf north of Long Island to Canadian waters and south of Delaware to Florida, with almost no effort in Canadian waters, and very limited effort between Maryland and the middle of Long Island, or off the shelf. Many sightings were reported in the central Gulf of Maine and near Jeffreys Ledge, known wintertime aggregation areas (Cole et al. 2013, Weinrich et al. 2000). A smaller number were distributed between New Jersey and Florida, along the migration corridor and within the southern calving area.

With so few sightings in the calving grounds, this model would clearly benefit from incorporation of aerial surveys for right whales conducted in the southeast U.S., such as those utilized by Gowan and Ortega-Ortiz (2014). These data were collected by multiple organizations and not all of them collected distances to sightings; those that did not cannot be utilized by our modeling procedure. We have opened communications with these organizations and hope to establish a collaboration that would allow us to update this model in the future using the appropriate data from the southeast.

Proceeding with the data we had in hand, we split the study area at the Nantucket Shoals, under the hypothesis that whales overwintering on the feeding grounds to the north would express different environmental preferences than whales in the calving and migration habitat to the south. We selected Nantucket Shoals as the break between the regions because it was not near large concentrations of sightings and would allow each regional model to incorporate survey effort up to where the two models met.

In the Feeding Grounds region we fitted full models. In the Calving and Migration Area, data were very limited but as right whales are a species of the highest conservation concern, we sought to produce a density surface that plausibly reflected their non-uniform distribution along the eastern seaboard, if the data would allow it. First we fitted limited models that considered only distance to shore, SST, and wind speed, a proxy for sea surface roughness. Distance to shore, SST, and sea surface roughness were used successfully in prior published models of right whale calving and wintering habitats (Keller et al. 2012, Gowan and Ortega-Ortiz 2014, Good 2008). The model selection procedure discarded wind speed and fitted linear relationships to distance to shore and SST. This yielded models that failed to predict peak density at the core calving habitat between 29-32 N; instead the models predicted increasing density with increasing SST, peaking at the southernmost part of the modeled region, at 25 N. This was unrealistic, so we tried a series of chlorophyll and productivity predictors as proxies for that habitat, trying each variable one at a time. These results matched the known distribution much better.

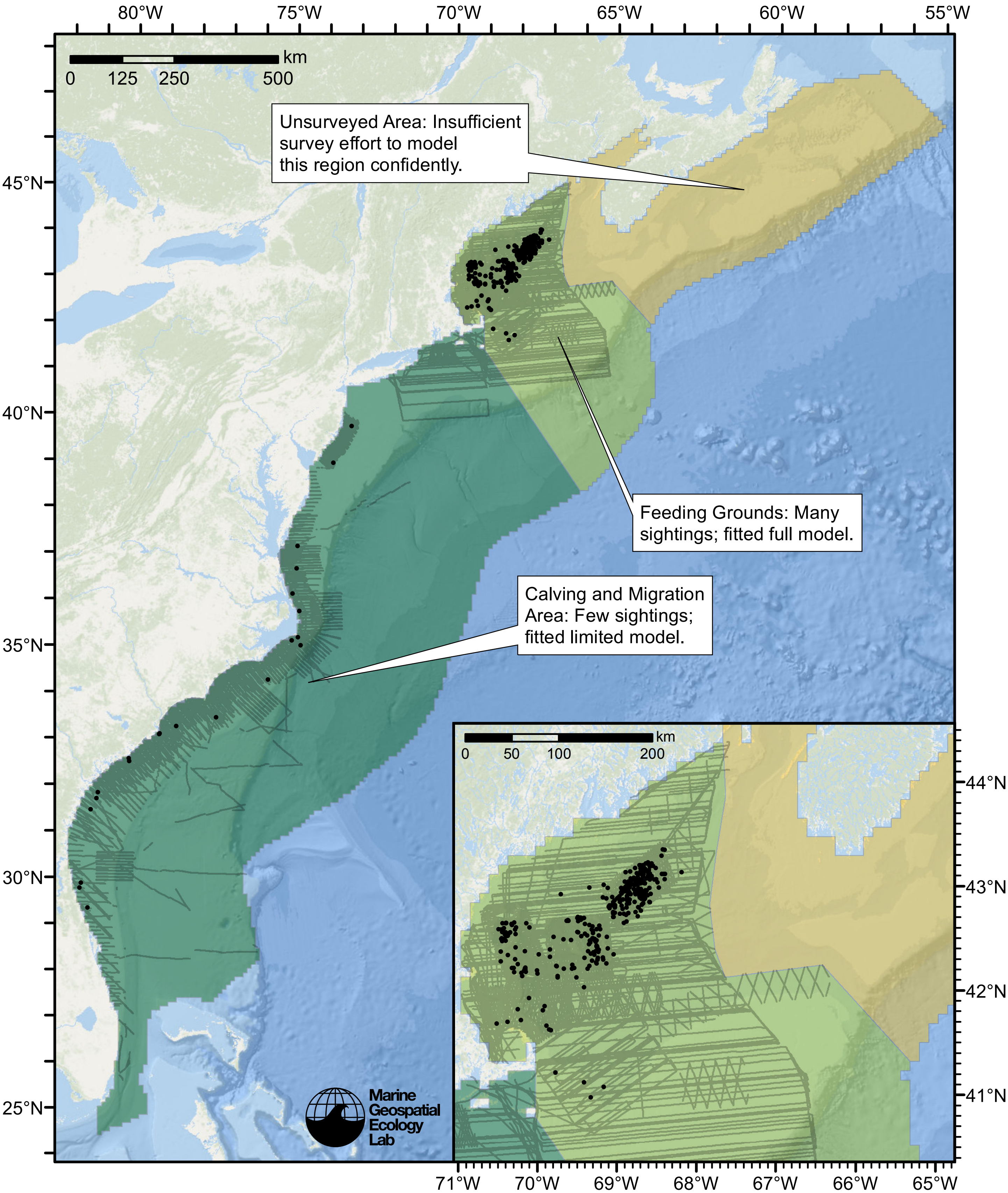

Figure 51: North Atlantic right whale density model schematic for Winter season. All on-effort sightings are shown, including those that were truncated when detection functions were fitted.

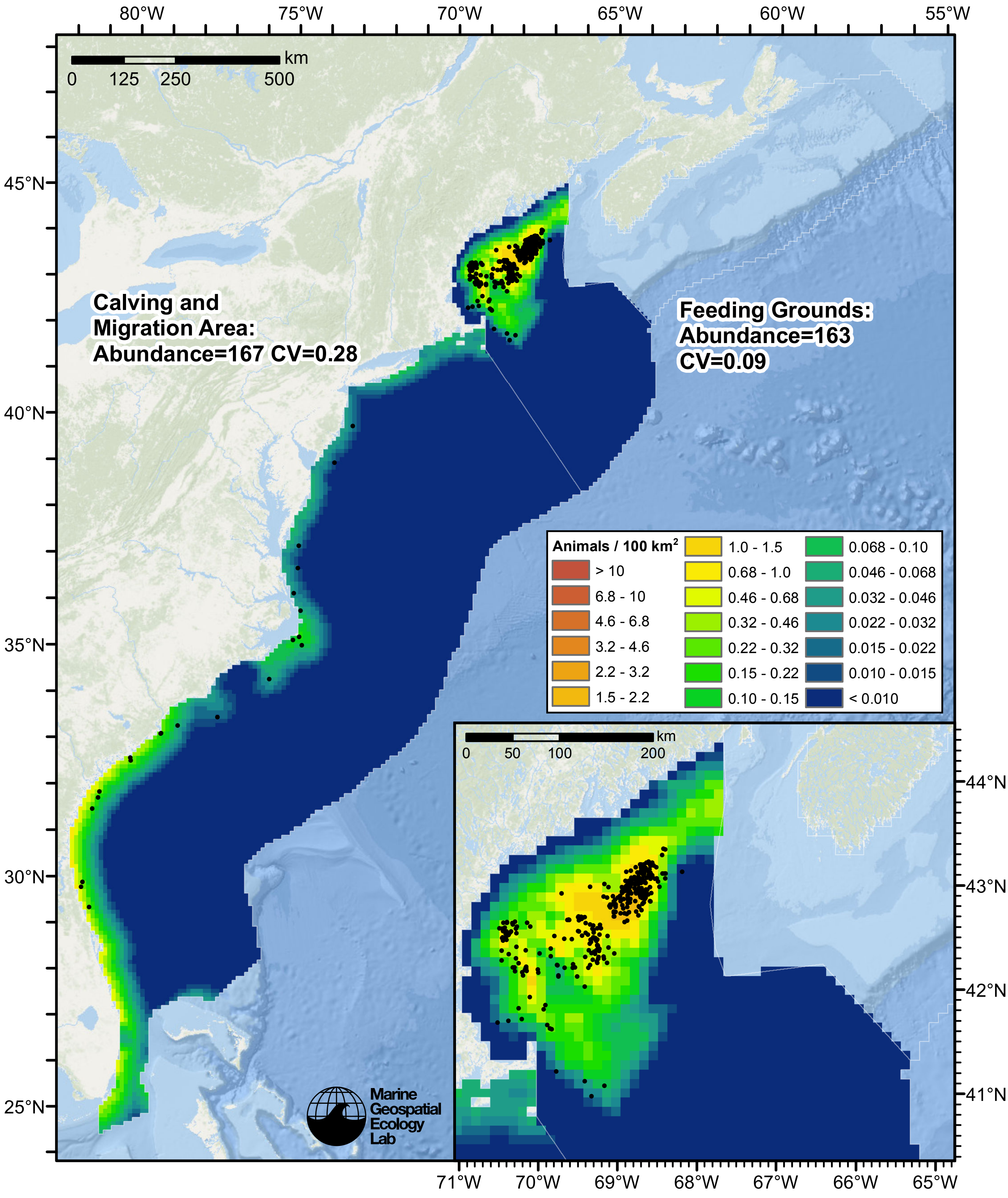

Figure 52: North Atlantic right whale density predicted by the Winter season climatological model that explained the most deviance. Pixels are 10x10 km. The legend gives the estimated individuals per pixel; breaks are logarithmic. The same scale is used for all seasons. Abundance for each region was computed by summing the density cells occuring in that region.

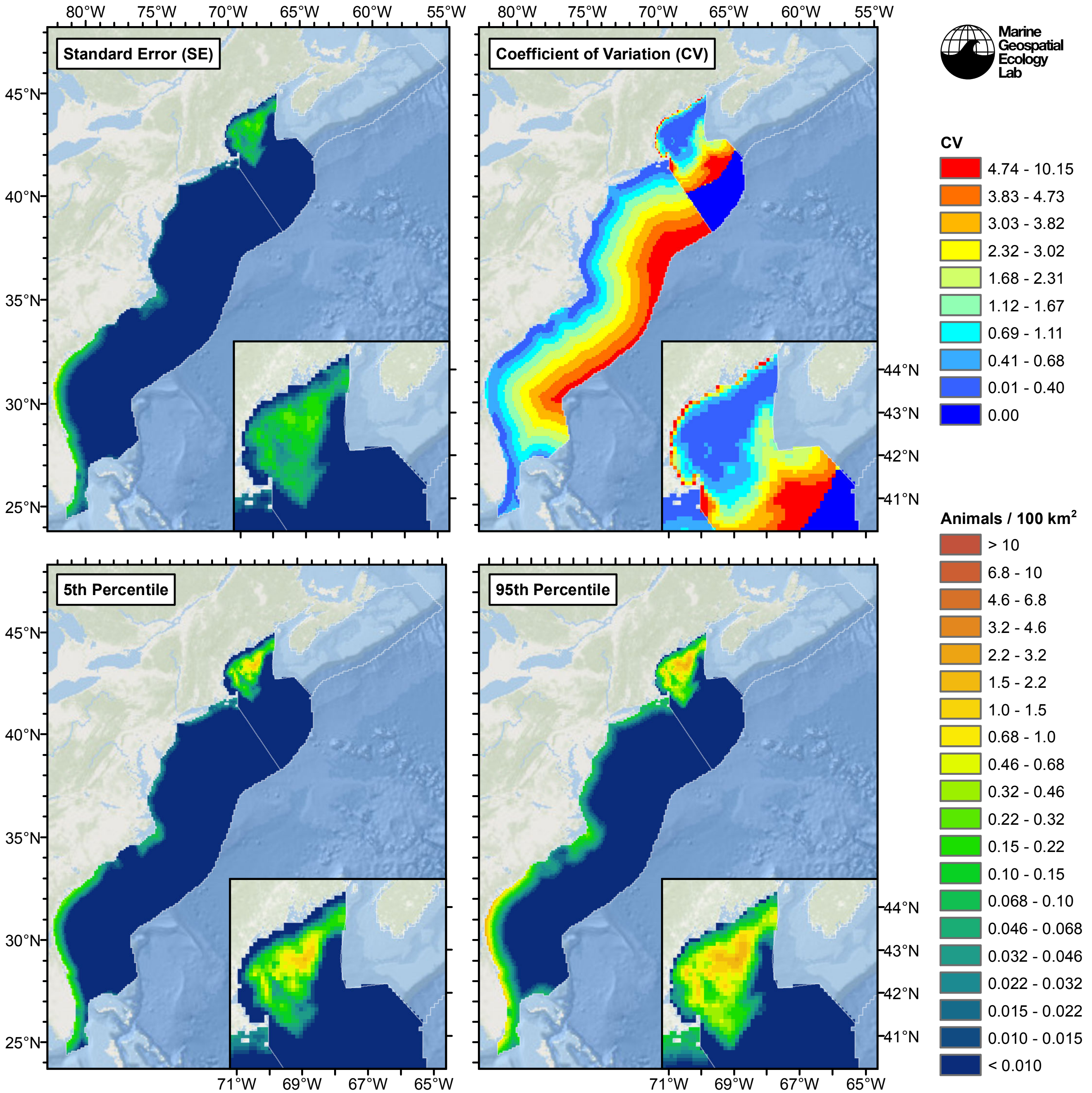

Figure 53: Estimated uncertainty for the Winter season climatological model that explained the most deviance. These estimates only incorporate the statistical uncertainty estimated for the spatial model (by the R mgcv package). They do not incorporate uncertainty in the detection functions, g(0) estimates, predictor variables, and so on.

Feeding Grounds

Statistical output

```
Rscript.exe: This is mgcv 1.8-2. For overview type 'help("mgcv-package")'.


Family: Tweedie(p=1.275)
```

```
Link function: log

Formula:
abundance ~ offset(log(area_km2)) + s(log10(Depth), bs = "ts",
    k = 5) + s(I(DistToShore/1000), bs = "ts", k = 5) + s(I(DistTo125m/1000),
    bs = "ts", k = 5) + s(I(DistTo300m/1000), bs = "ts", k = 5) +
    s(ClimSST, bs = "ts", k = 5) + s(log10(pmax(ClimEKE, 1e-04)),
    bs = "ts", k = 5) + s(log10(pmax(ClimEpiMnkPP, 1e-06)), bs = "ts",
    k = 5)

Parametric coefficients:
            Estimate Std. Error t value Pr(>|t|)
(Intercept)  -8.6735     0.5077  -17.08   <2e-16 ***
---
Signif. codes:  0 '***' 0.001 '**' 0.01 '*' 0.05 '.' 0.1 ' ' 1

Approximate significance of smooth terms:
                                  edf Ref.df      F  p-value
s(log10(Depth))                 3.646      4  9.336 1.99e-08 ***
s(I(DistToShore/1000))          2.426      4  4.558 4.27e-05 ***
s(I(DistTo125m/1000))           2.931      4  6.093 2.45e-06 ***
s(I(DistTo300m/1000))           2.433      4  7.093 2.25e-07 ***
s(ClimSST)                      2.644      4  7.060 4.10e-07 ***
s(log10(pmax(ClimEKE, 1e-04)))      1.638      4 10.211 2.21e-11 ***
s(log10(pmax(ClimEpiMnkPP, 1e-06))) 2.975      4  5.984 6.46e-06 ***
---
Signif. codes:  0 '***' 0.001 '**' 0.01 '*' 0.05 '.' 0.1 ' ' 1

R-sq.(adj) =  0.025   Deviance explained =   22%
-REML = 2039.9  Scale est. = 27.727    n = 8937

All predictors were significant. This is the final model.
Creating term plots.
Diagnostic output from gam.check():

Method: REML   Optimizer: outer newton
full convergence after 12 iterations.
Gradient range [-3.293372e-07,1.259479e-07]
(score 2039.894 & scale 27.72697).
Hessian positive definite, eigenvalue range [0.1756689,960.3972].
Model rank =  29 / 29

Basis dimension (k) checking results. Low p-value (k-index<1) may
indicate that k is too low, especially if edf is close to k'.

                                   k'   edf k-index p-value
s(log10(Depth))                 4.000 3.646   0.712    0.00
s(I(DistToShore/1000))          4.000 2.426   0.738    0.00
s(I(DistTo125m/1000))           4.000 2.931   0.778    0.12
s(I(DistTo300m/1000))           4.000 2.433   0.728    0.00
s(ClimSST)                      4.000 2.644   0.792    0.44
s(log10(pmax(ClimEKE, 1e-04)))      4.000 1.638   0.762    0.01
s(log10(pmax(ClimEpiMnkPP, 1e-06))) 4.000 2.975   0.779    0.14
```

Predictors retained during the model selection procedure: Depth, DistToShore, DistTo125m, DistTo300m, ClimSST, ClimEKE, ClimEpiMnkPP

Predictors dropped during the model selection procedure: Slope, ClimDistToFront2

Model term plots

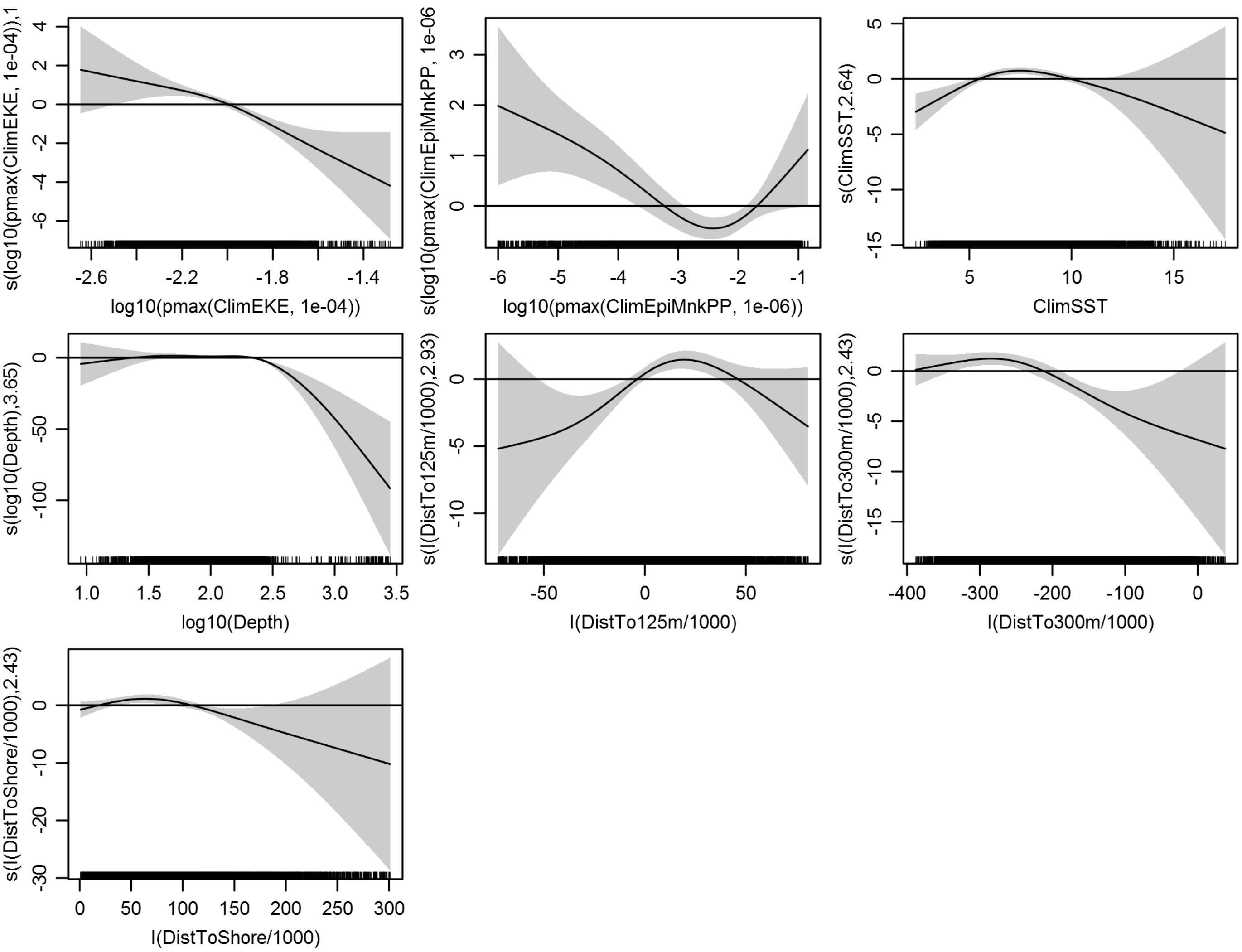

Diagnostic plots

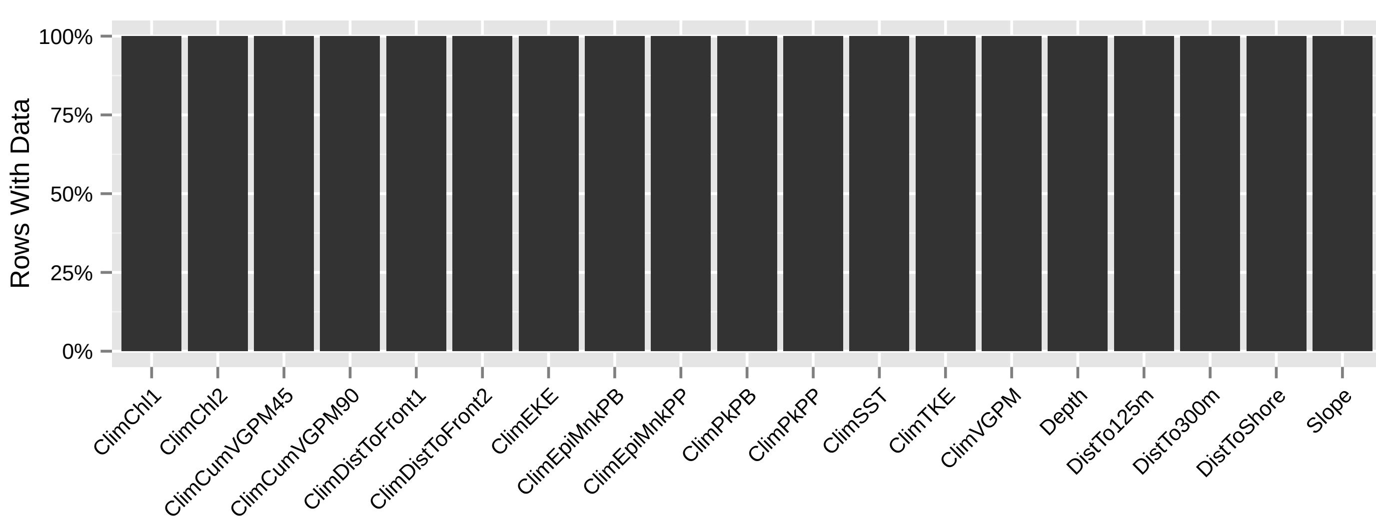

Figure 54: Segments with predictor values for the North Atlantic right whale Climatological model, Winter season, Feeding Grounds. This plot is used to assess how many segments would be lost by including a given predictor in a model.

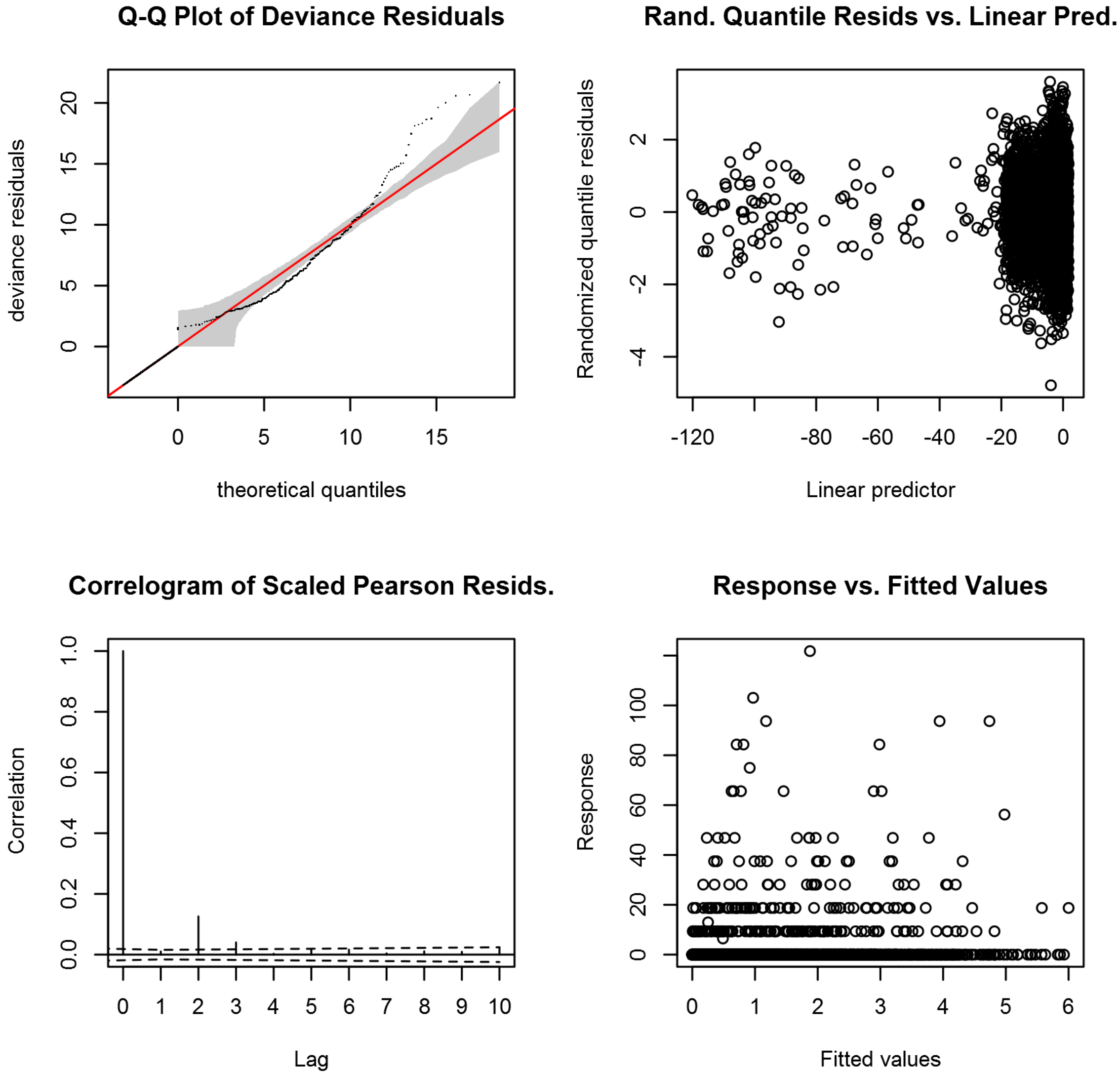

Figure 55: Statistical diagnostic plots for the North Atlantic right whale Climatological model, Winter season, Feeding Grounds.

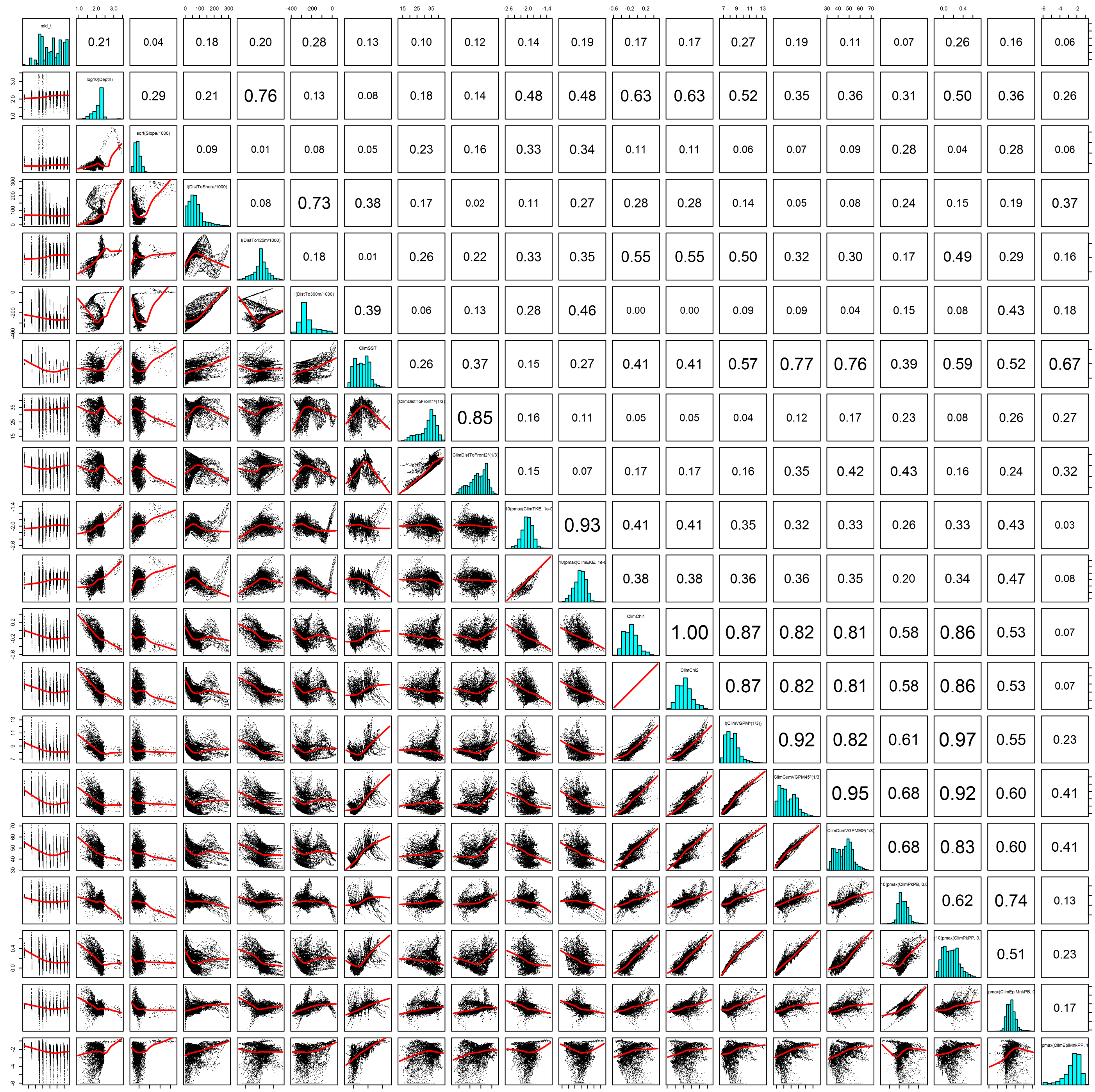

Figure 56: Scatterplot matrix for the North Atlantic right whale Climatological model, Winter season, Feeding Grounds. This plot is used to inspect the distribution of predictors (via histograms along the diagonal), simple correlation between predictors (via pairwise Pearson coefficients above the diagonal), and linearity of predictor correlations (via scatterplots below the diagonal). This plot is best viewed at high magnification.

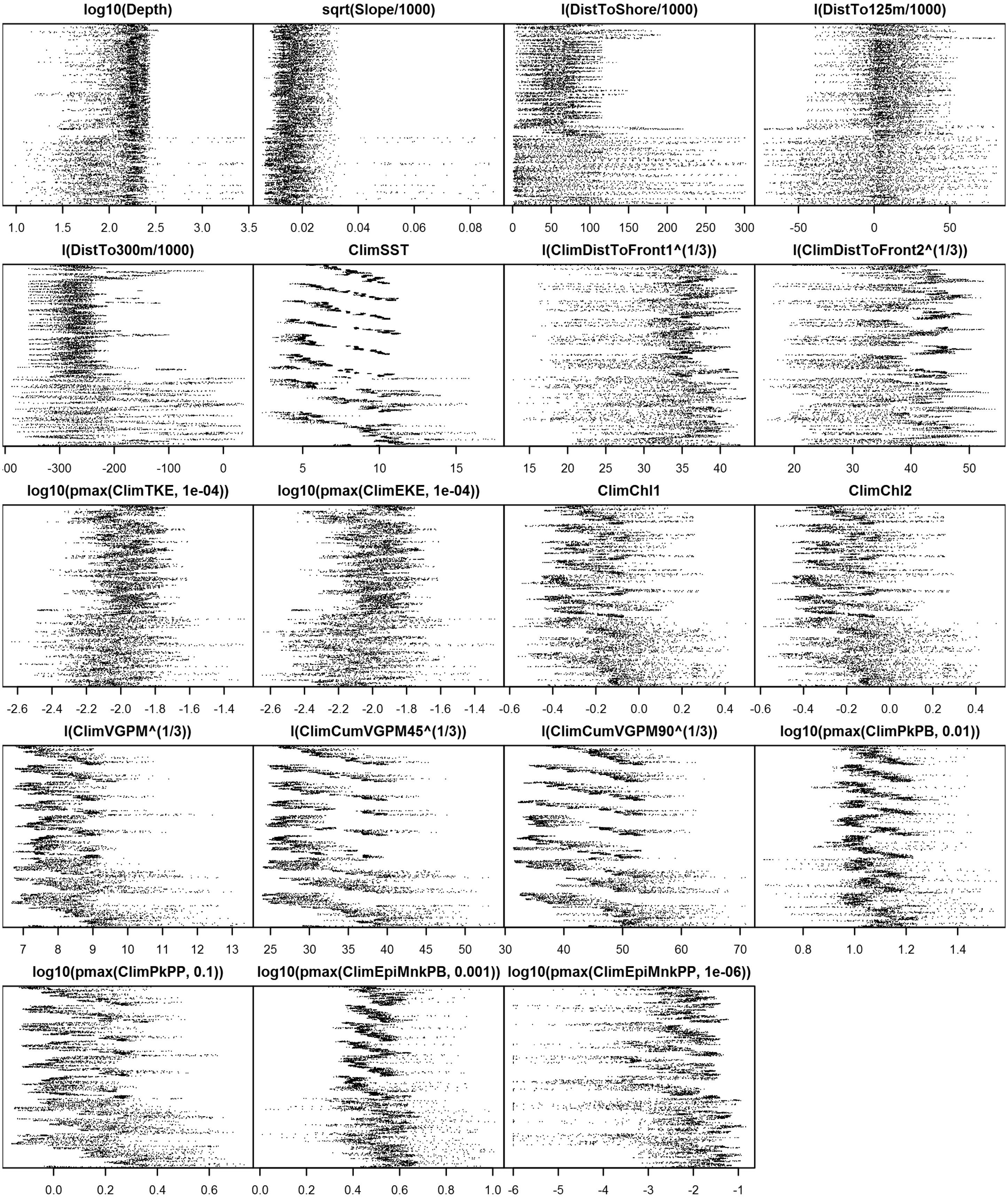

Figure 57: Dotplot for the North Atlantic right whale Climatological model, Winter season, Feeding Grounds. This plot is used to check for suspicious patterns and outliers in the data. Points are ordered vertically by transect ID, sequentially in time.

Calving and Migration Area

Statistical output

```
Rscript.exe: This is mgcv 1.8-2. For overview type 'help("mgcv-package")'.


Family: Tweedie(p=1.042)
Link function: log

Formula:
abundance ~ offset(log(area_km2)) + s(I(DistToShore/1000), bs = "ts",
    k = 5) + s(log10(pmax(ClimEpiMnkPB, 0.001)), bs = "ts", k = 5)

Parametric coefficients:
            Estimate Std. Error t value Pr(>|t|)
(Intercept)  -9.1955     0.5271  -17.45   <2e-16 ***
---
Signif. codes:  0 '***' 0.001 '**' 0.01 '*' 0.05 '.' 0.1 ' ' 1

Approximate significance of smooth terms:
                                       edf Ref.df     F  p-value
s(I(DistToShore/1000))              0.9652      4 4.264 1.86e-05 ***
s(log10(pmax(ClimEpiMnkPB, 0.001))) 1.8783      4 6.390 4.10e-07 ***
---
Signif. codes:  0 '***' 0.001 '**' 0.01 '*' 0.05 '.' 0.1 ' ' 1

R-sq.(adj) =  0.00205   Deviance explained = 12.4%
-REML = 207.38  Scale est. = 12.186    n = 18883

All predictors were significant. This is the final model.
Creating term plots.
Diagnostic output from gam.check():

Method: REML   Optimizer: outer newton
full convergence after 14 iterations.
Gradient range [-1.434477e-07,2.100847e-08]
(score 207.3764 & scale 12.18638).
Hessian positive definite, eigenvalue range [0.3637616,531.7949].
Model rank =  9 / 9

Basis dimension (k) checking results. Low p-value (k-index<1) may
indicate that k is too low, especially if edf is close to k'.

                                       k'   edf k-index p-value
s(I(DistToShore/1000))              4.000 0.965   0.849    0.02
s(log10(pmax(ClimEpiMnkPB, 0.001))) 4.000 1.878   0.870    0.00

Predictors retained during the model selection procedure: DistToShore, ClimEpiMnkPB

Predictors dropped during the model selection procedure: ClimSST, ClimWindSpeed
```

Model term plots

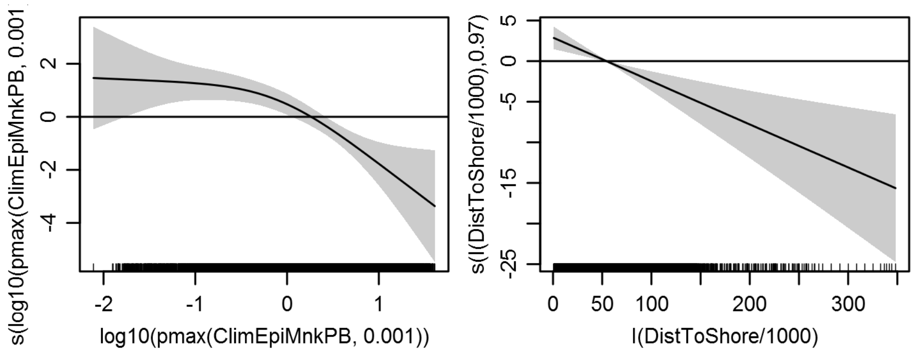

Diagnostic plots

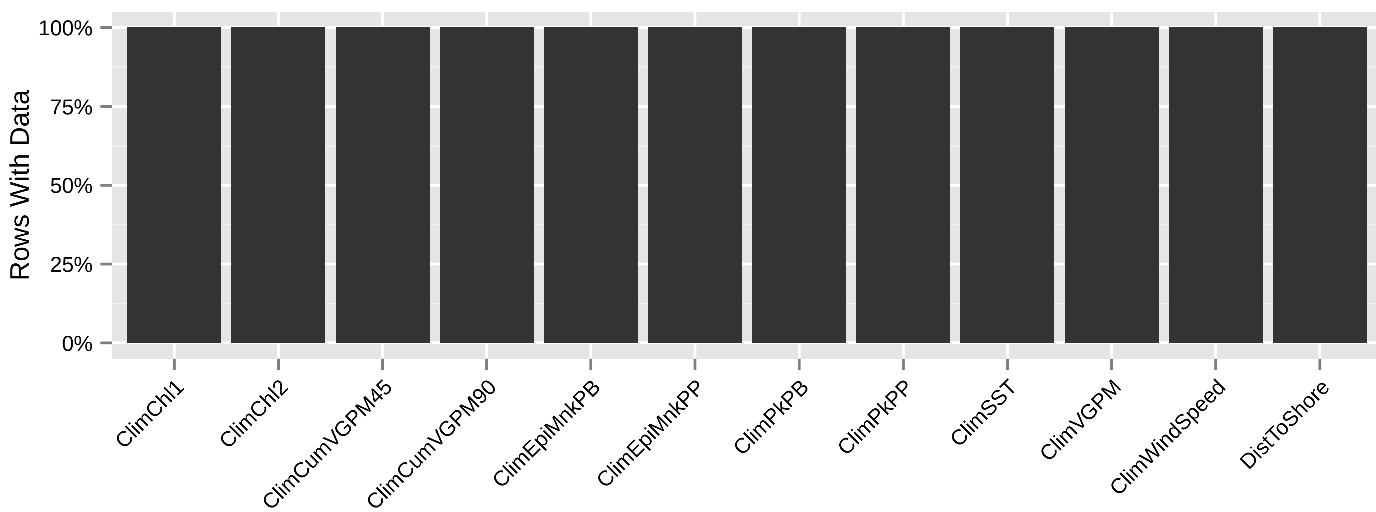

Figure 58: Segments with predictor values for the North Atlantic right whale Climatological model, Winter season, Calving and Migration Area. This plot is used to assess how many segments would be lost by including a given predictor in a model.

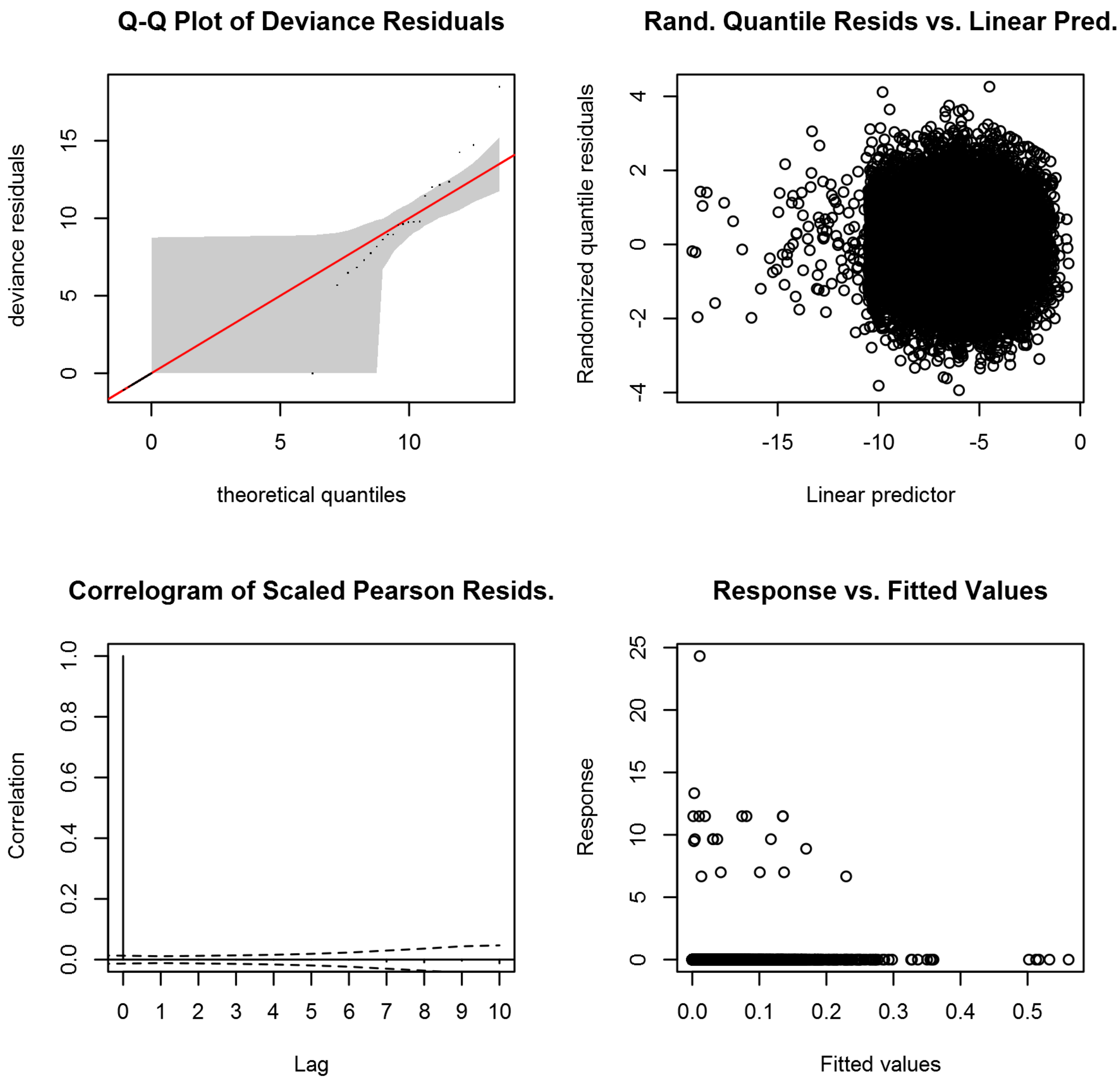

Figure 59: Statistical diagnostic plots for the North Atlantic right whale Climatological model, Winter season, Calving and Migration Area.

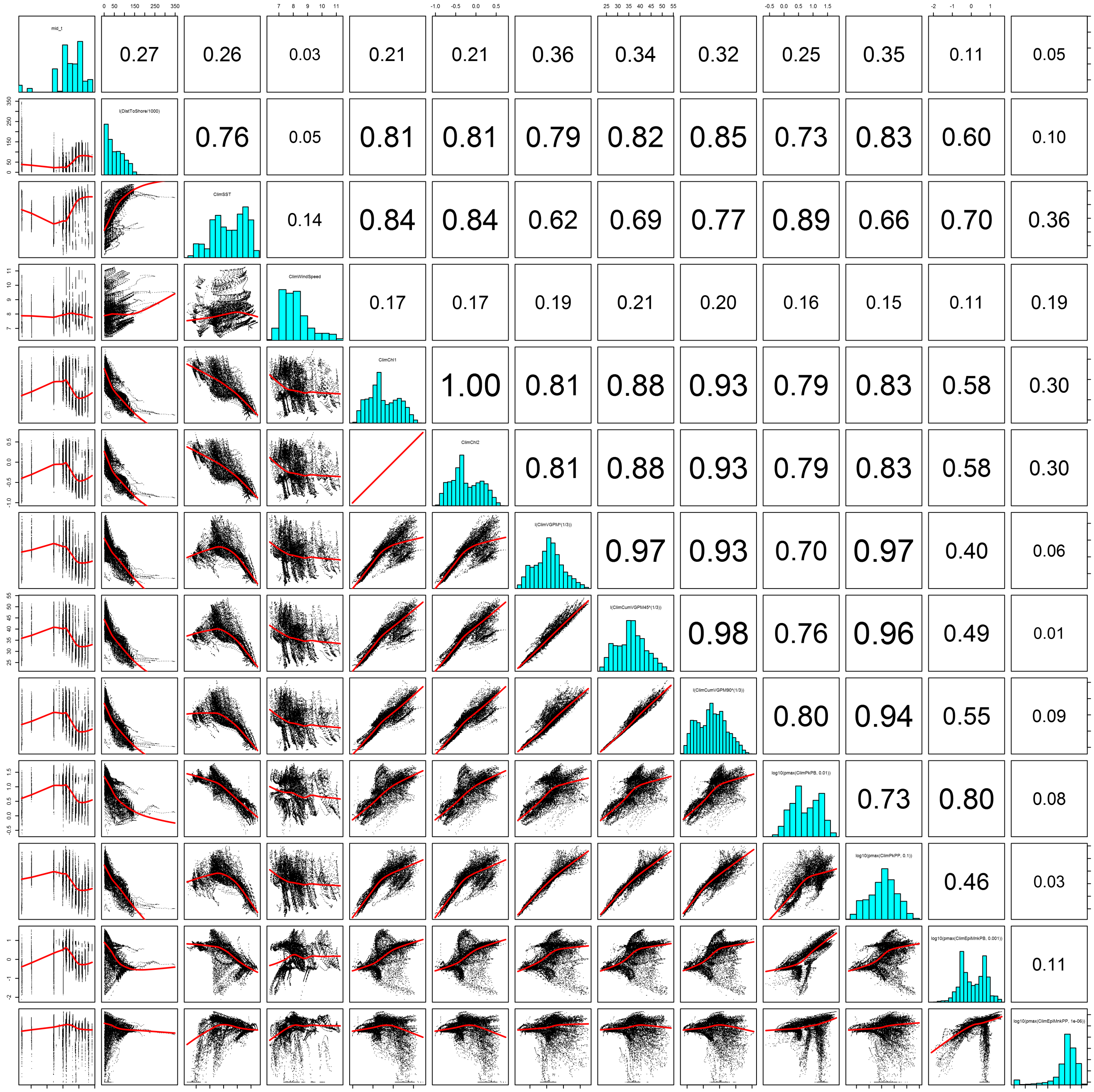

Figure 60: Scatterplot matrix for the North Atlantic right whale Climatological model, Winter season, Calving and Migration Area. This plot is used to inspect the distribution of predictors (via histograms along the diagonal), simple correlation between predictors (via pairwise Pearson coefficients above the diagonal), and linearity of predictor correlations (via scatterplots below the diagonal). This plot is best viewed at high magnification.

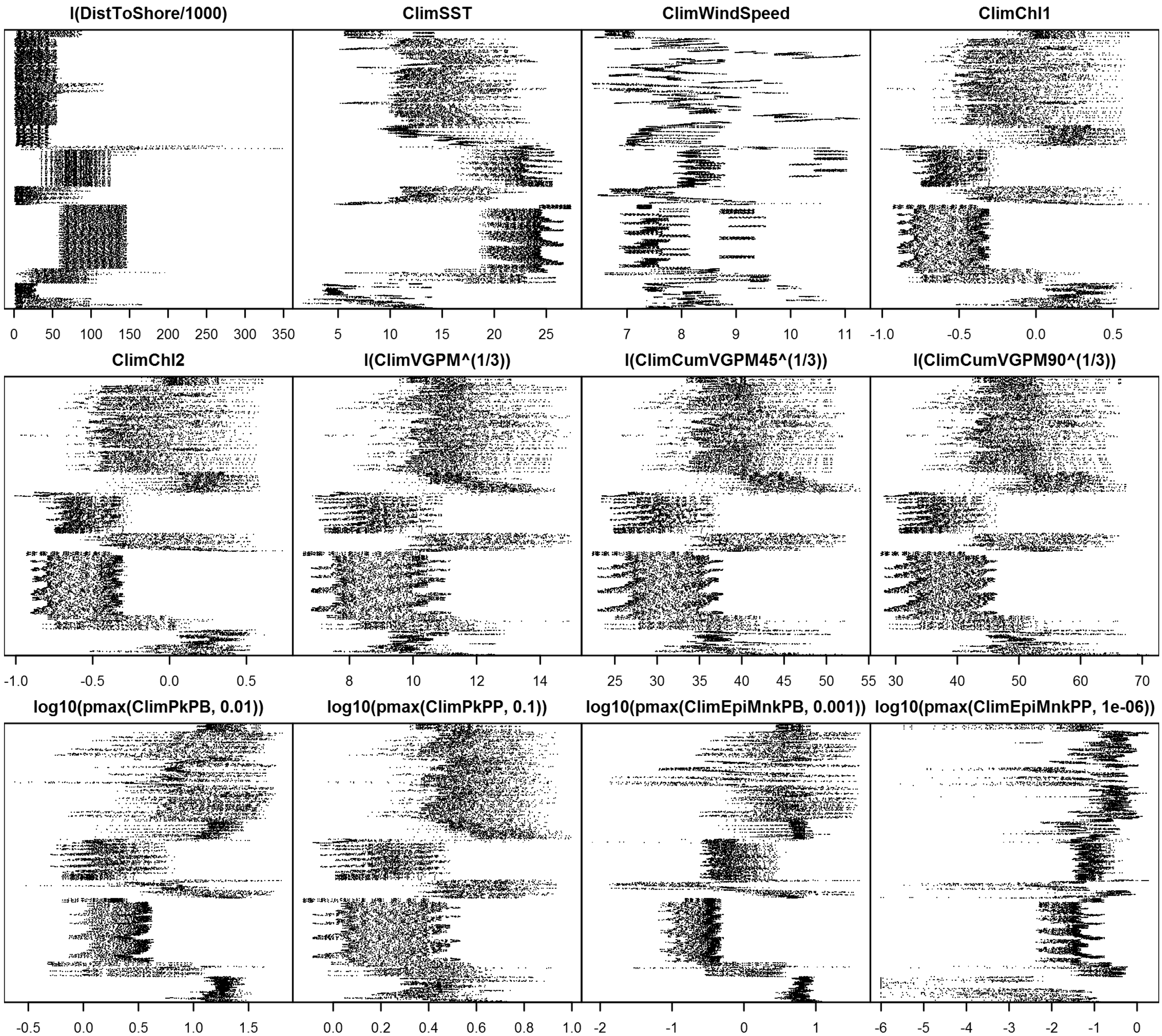

Figure 61: Dotplot for the North Atlantic right whale Climatological model, Winter season, Calving and Migration Area. This plot is used to check for suspicious patterns and outliers in the data. Points are ordered vertically by transect ID, sequentially in time.

Unsurveyed Area

Density was not modeled for this region.

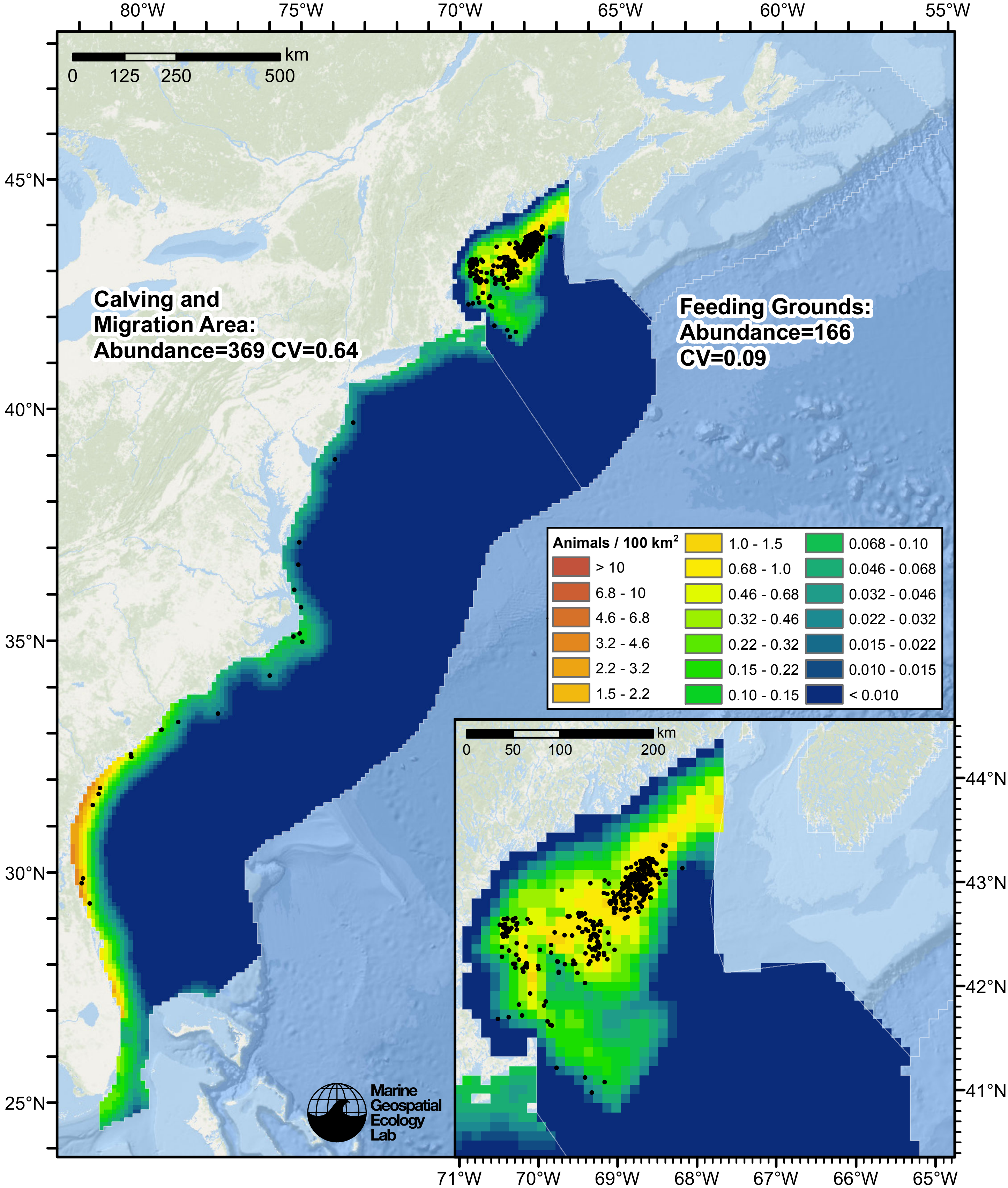

Figure 62: North Atlantic right whale density predicted by the Winter season contemporaneous model that explained the most deviance. Pixels are 10x10 km. The legend gives the estimated individuals per pixel; breaks are logarithmic. The same scale is used for all seasons. Abundance for each region was computed by summing the density cells occuring in that region.

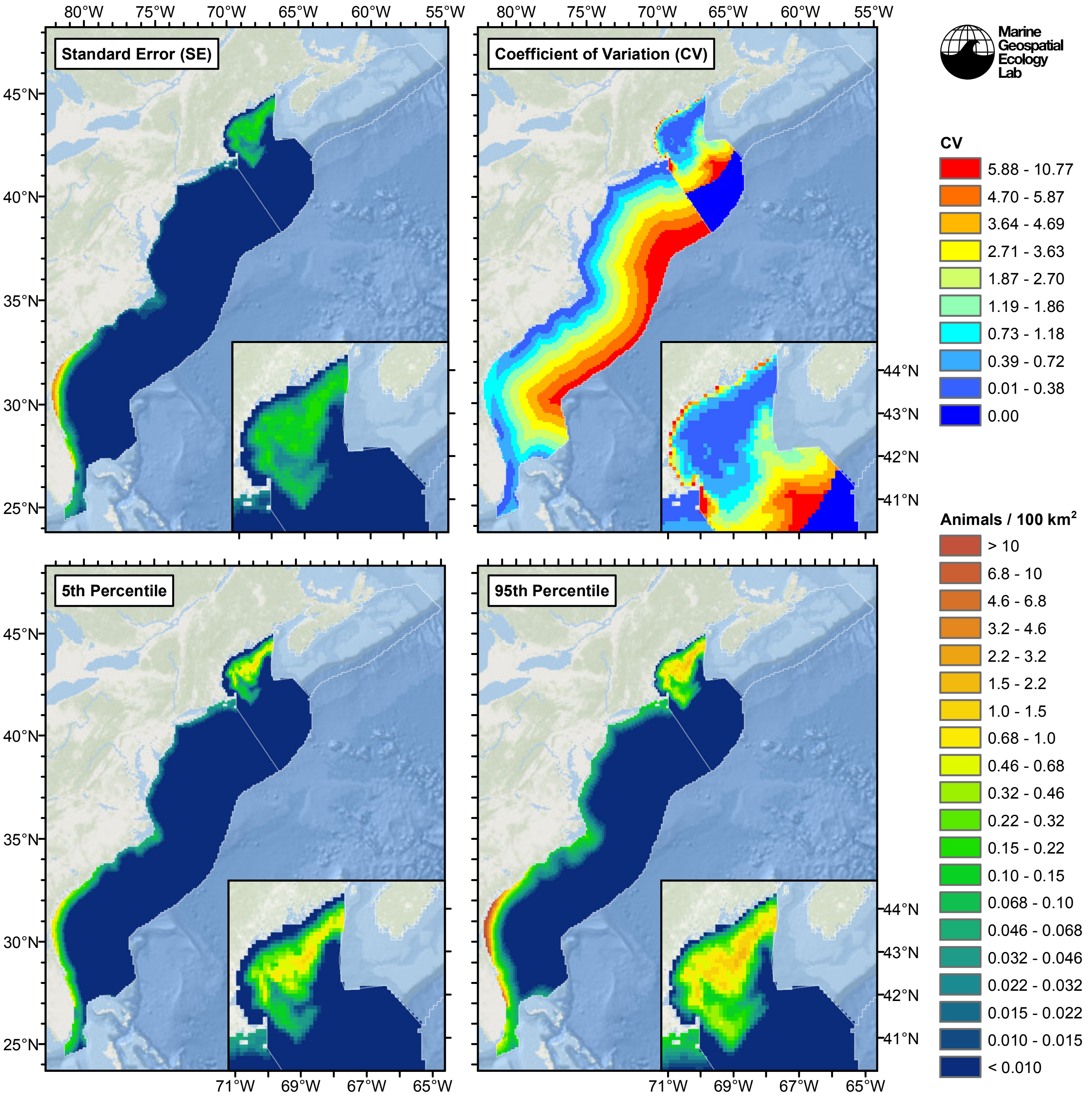

Figure 63: Estimated uncertainty for the Winter season contemporaneous model that explained the most deviance. These estimates only incorporate the statistical uncertainty estimated for the spatial model (by the R mgcv package). They do not incorporate uncertainty in the detection functions, g(0) estimates, predictor variables, and so on.

Feeding Grounds

Statistical output

```
Rscript.exe: This is mgcv 1.8-2. For overview type 'help("mgcv-package")'.


Family: Tweedie(p=1.277)
```

```
Link function: log

Formula:
abundance ~ offset(log(area_km2)) + s(log10(Depth), bs = "ts",
    k = 5) + s(I(DistToShore/1000), bs = "ts", k = 5) + s(I(DistTo125m/1000),
    bs = "ts", k = 5) + s(I(DistTo300m/1000), bs = "ts", k = 5) +
    s(SST, bs = "ts", k = 5) + s(I(DistToFront2^(1/3)), bs = "ts",
    k = 5) + s(I(CumVGPM90^(1/3)), bs = "ts", k = 5)

Parametric coefficients:
            Estimate Std. Error t value Pr(>|t|)
(Intercept)  -8.6668     0.5027  -17.24   <2e-16 ***
---
Signif. codes:  0 '***' 0.001 '**' 0.01 '*' 0.05 '.' 0.1 ' ' 1

Approximate significance of smooth terms:
                           edf Ref.df      F  p-value
s(log10(Depth))          3.622      4 10.302 2.62e-09 ***
s(I(DistToShore/1000))   2.464      4  4.290 8.93e-05 ***
s(I(DistTo125m/1000))    2.901      4  5.814 4.58e-06 ***
s(I(DistTo300m/1000))    2.468      4  5.753 5.66e-06 ***
s(SST)                   3.547      4  9.821 4.54e-09 ***
s(I(DistToFront2^(1/3))) 3.610      4  7.610 8.92e-07 ***
s(I(CumVGPM90^(1/3)))    1.114      4  3.161 0.000256 ***
---
Signif. codes:  0 '***' 0.001 '**' 0.01 '*' 0.05 '.' 0.1 ' ' 1

R-sq.(adj) =  0.0264   Deviance explained =   22%
-REML = 2043.7  Scale est. = 27.87     n = 8937

All predictors were significant. This is the final model.
Creating term plots.
Diagnostic output from gam.check():

Method: REML   Optimizer: outer newton
full convergence after 14 iterations.
Gradient range [-1.578726e-06,2.67818e-06]
(score 2043.744 & scale 27.86952).
Hessian positive definite, eigenvalue range [0.2465748,954.8064].
Model rank =  29 / 29

Basis dimension (k) checking results. Low p-value (k-index<1) may
indicate that k is too low, especially if edf is close to k'.

                            k'   edf k-index p-value
s(log10(Depth))          4.000 3.622   0.759    0.00
s(I(DistToShore/1000))   4.000 2.464   0.779    0.02
s(I(DistTo125m/1000))    4.000 2.901   0.745    0.00
s(I(DistTo300m/1000))    4.000 2.468   0.779    0.00
s(SST)                   4.000 3.547   0.800    0.32
s(I(DistToFront2^(1/3))) 4.000 3.610   0.791    0.11
s(I(CumVGPM90^(1/3)))    4.000 1.114   0.798    0.25
```

Predictors retained during the model selection procedure: Depth, DistToShore, DistTo125m, DistTo300m, SST, DistToFront2, CumVGPM90

Predictors dropped during the model selection procedure: Slope, TKE

Model term plots

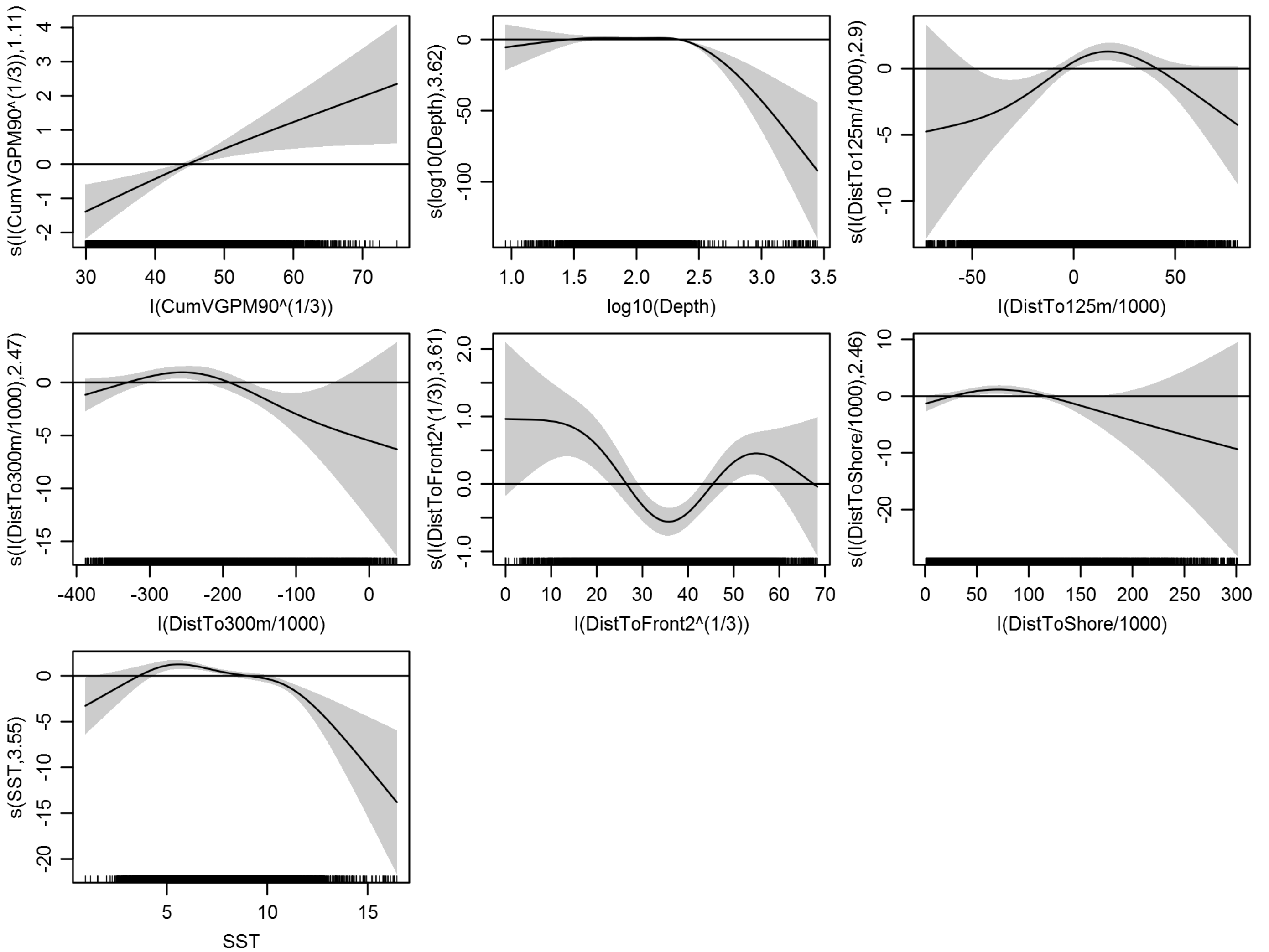

Diagnostic plots

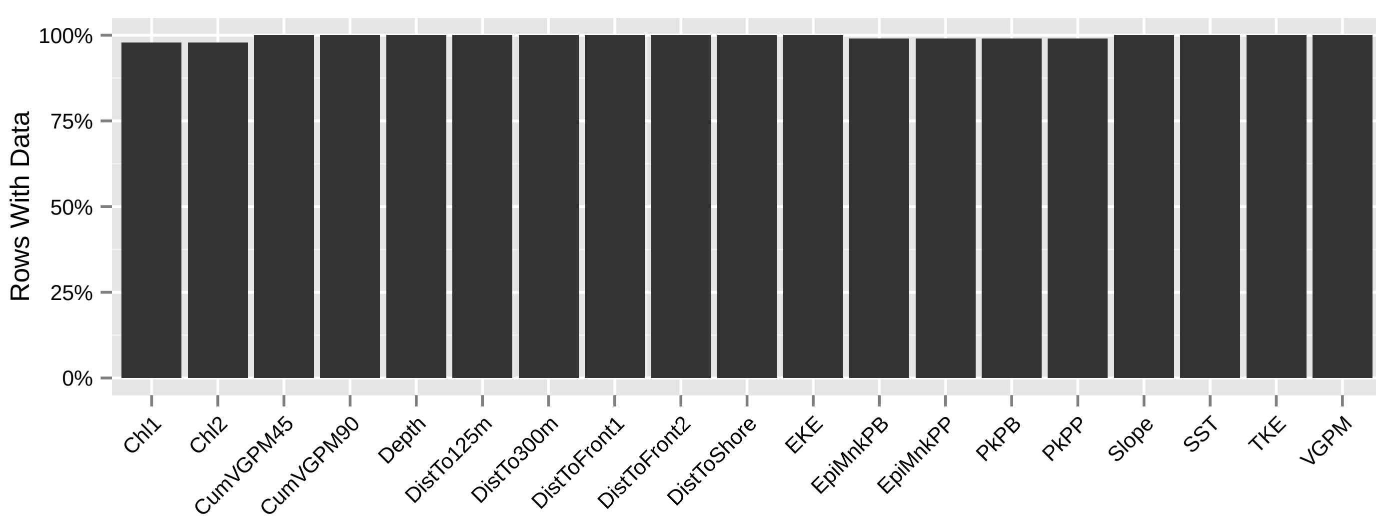

Figure 64: Segments with predictor values for the North Atlantic right whale Contemporaneous model, Winter season, Feeding Grounds. This plot is used to assess how many segments would be lost by including a given predictor in a model.

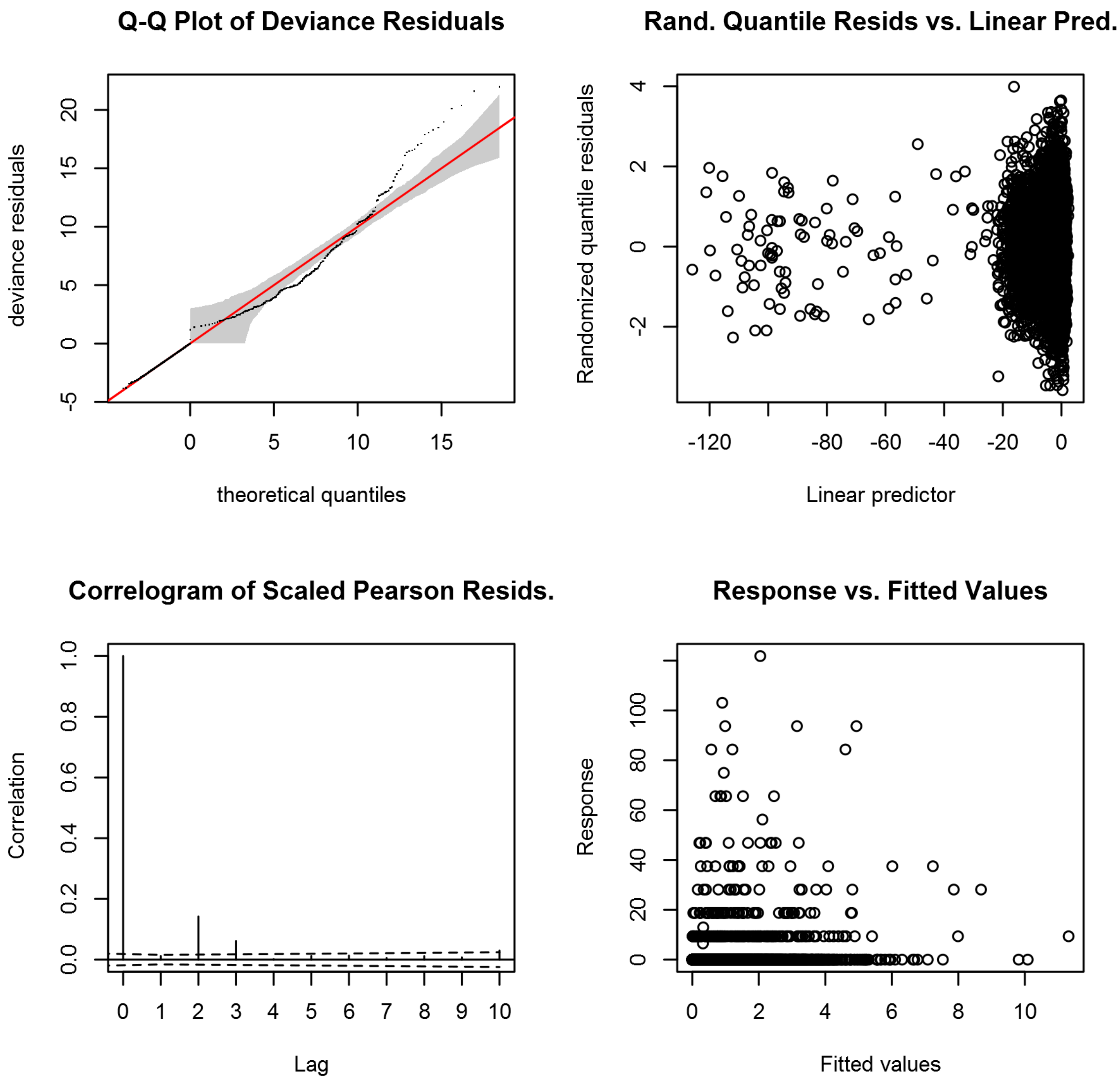

Figure 65: Statistical diagnostic plots for the North Atlantic right whale Contemporaneous model, Winter season, Feeding Grounds.

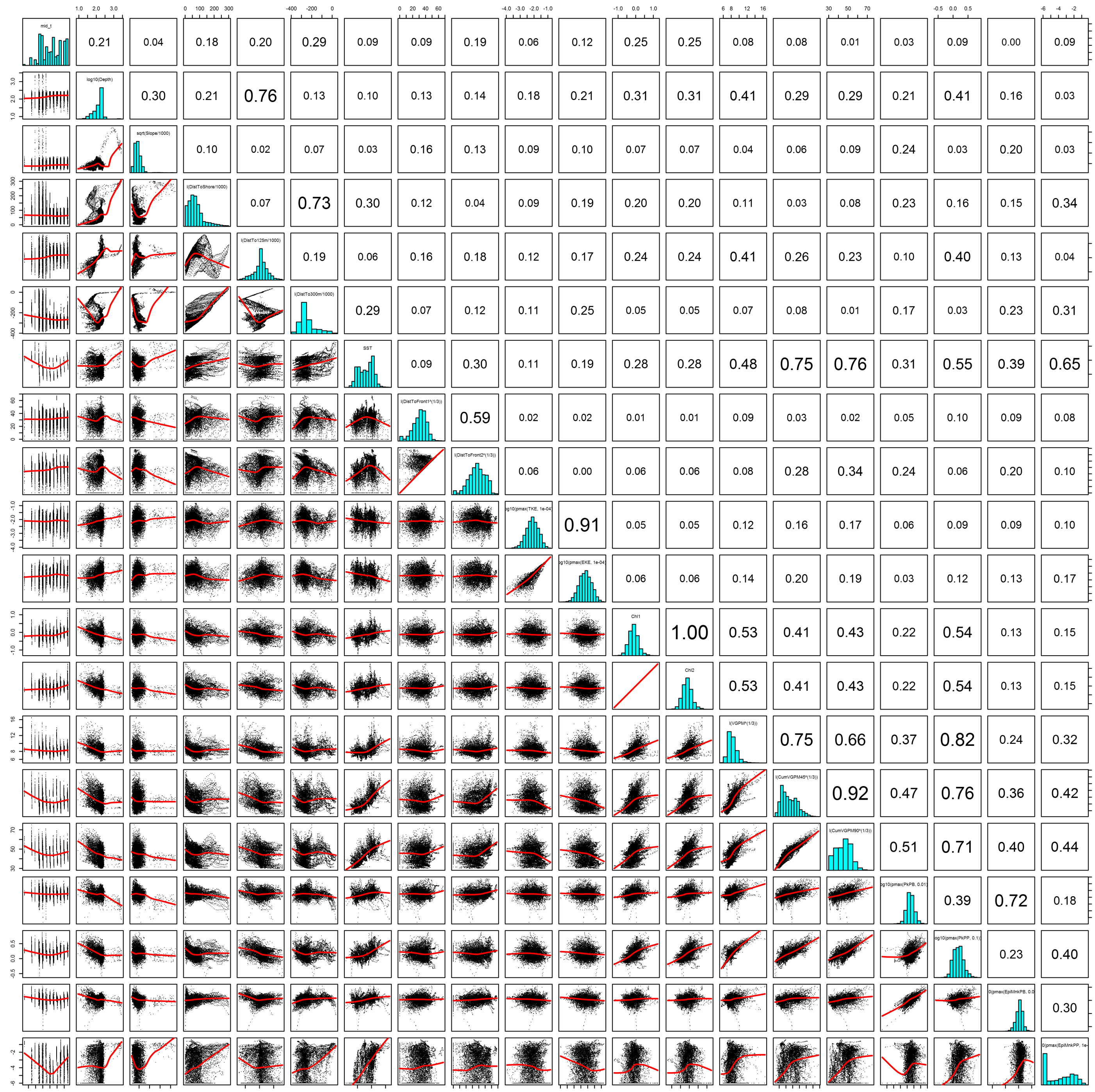

Figure 66: Scatterplot matrix for the North Atlantic right whale Contemporaneous model, Winter season, Feeding Grounds. This plot is used to inspect the distribution of predictors (via histograms along the diagonal), simple correlation between predictors (via pairwise Pearson coefficients above the diagonal), and linearity of predictor correlations (via scatterplots below the diagonal). This plot is best viewed at high magnification.

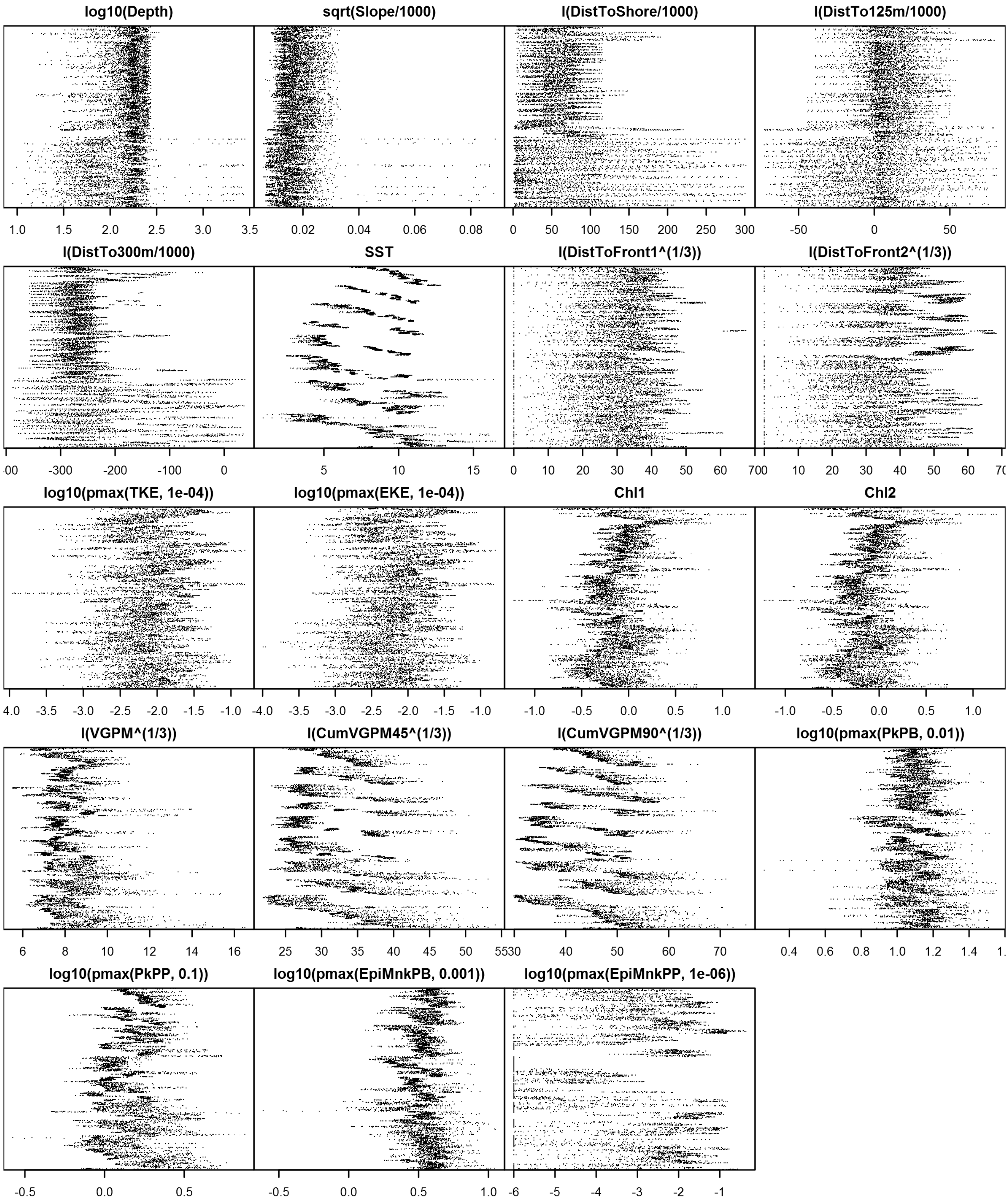

Figure 67: Dotplot for the North Atlantic right whale Contemporaneous model, Winter season, Feeding Grounds. This plot is used to check for suspicious patterns and outliers in the data. Points are ordered vertically by transect ID, sequentially in time.

Calving and Migration Area

Statistical output

```
Rscript.exe: This is mgcv 1.8-2. For overview type 'help("mgcv-package")'.


Family: Tweedie(p=1.045)
Link function: log

Formula:
abundance ~ offset(log(area_km2)) + s(I(DistToShore/1000), bs = "ts",
    k = 5) + s(log10(pmax(EpiMnkPB, 0.001)), bs = "ts", k = 5)

Parametric coefficients:
            Estimate Std. Error t value Pr(>|t|)
(Intercept)  -9.2145     0.5617  -16.41   <2e-16 ***
---
Signif. codes:  0 '***' 0.001 '**' 0.01 '*' 0.05 '.' 0.1 ' ' 1

Approximate significance of smooth terms:
                                  edf Ref.df     F  p-value
s(I(DistToShore/1000))          1.017      4 3.588 9.15e-05 ***
s(log10(pmax(EpiMnkPB, 0.001))) 1.154      4 6.791 1.17e-07 ***
---
Signif. codes:  0 '***' 0.001 '**' 0.01 '*' 0.05 '.' 0.1 ' ' 1

R-sq.(adj) =  -0.00231   Deviance explained = 12.3%
-REML = 196.46  Scale est. = 12.369    n = 17768

All predictors were significant. This is the final model.
Creating term plots.
Diagnostic output from gam.check():

Method: REML   Optimizer: outer newton
full convergence after 14 iterations.
Gradient range [-3.063412e-05,1.790586e-05]
(score 196.4574 & scale 12.36941).
Hessian positive definite, eigenvalue range [0.275411,475.6499].
Model rank =  9 / 9

Basis dimension (k) checking results. Low p-value (k-index<1) may
indicate that k is too low, especially if edf is close to k'.

                                   k'   edf k-index p-value
s(I(DistToShore/1000))          4.000 1.017   0.930    0.02
s(log10(pmax(EpiMnkPB, 0.001))) 4.000 1.154   0.939    0.13

Predictors retained during the model selection procedure: DistToShore, EpiMnkPB

Predictors dropped during the model selection procedure: SST, WindSpeed
```

Model term plots

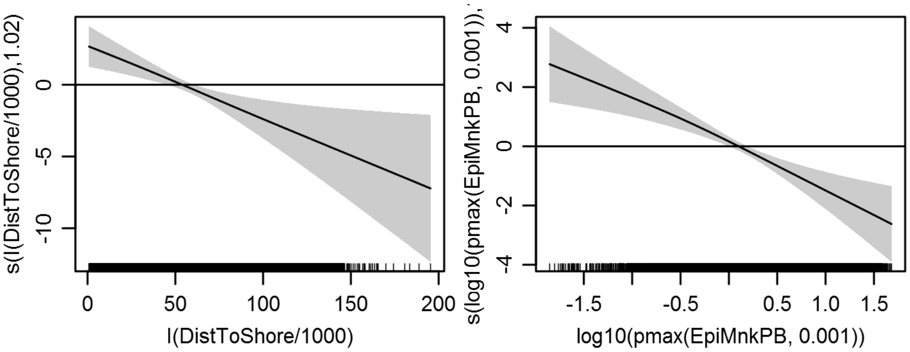

Diagnostic plots

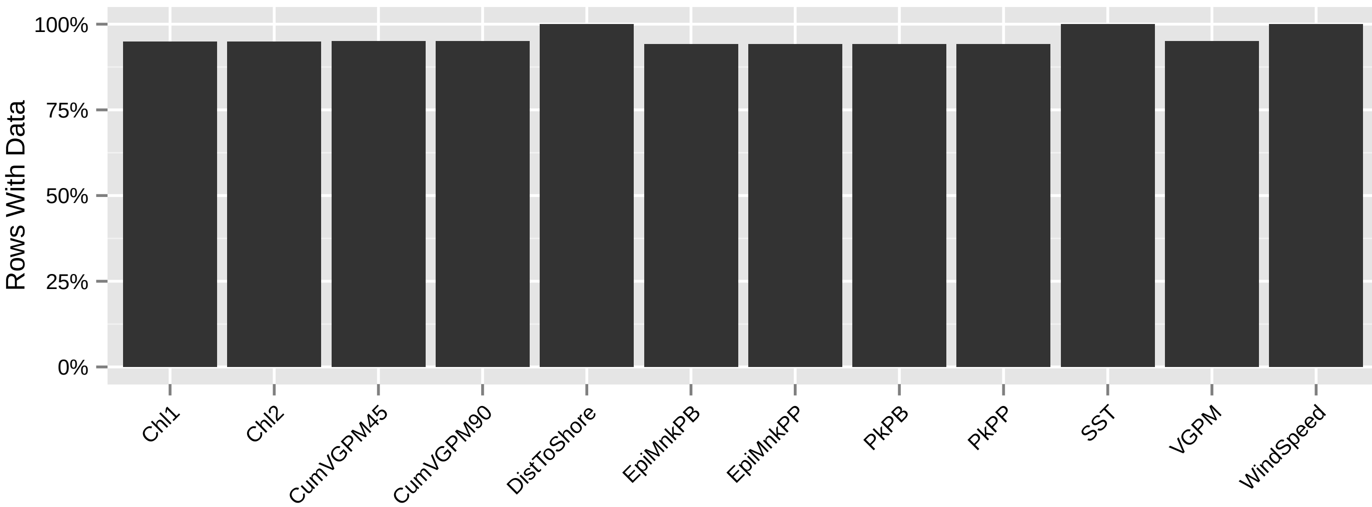

Figure 68: Segments with predictor values for the North Atlantic right whale Contemporaneous model, Winter season, Calving and Migration Area. This plot is used to assess how many segments would be lost by including a given predictor in a model.

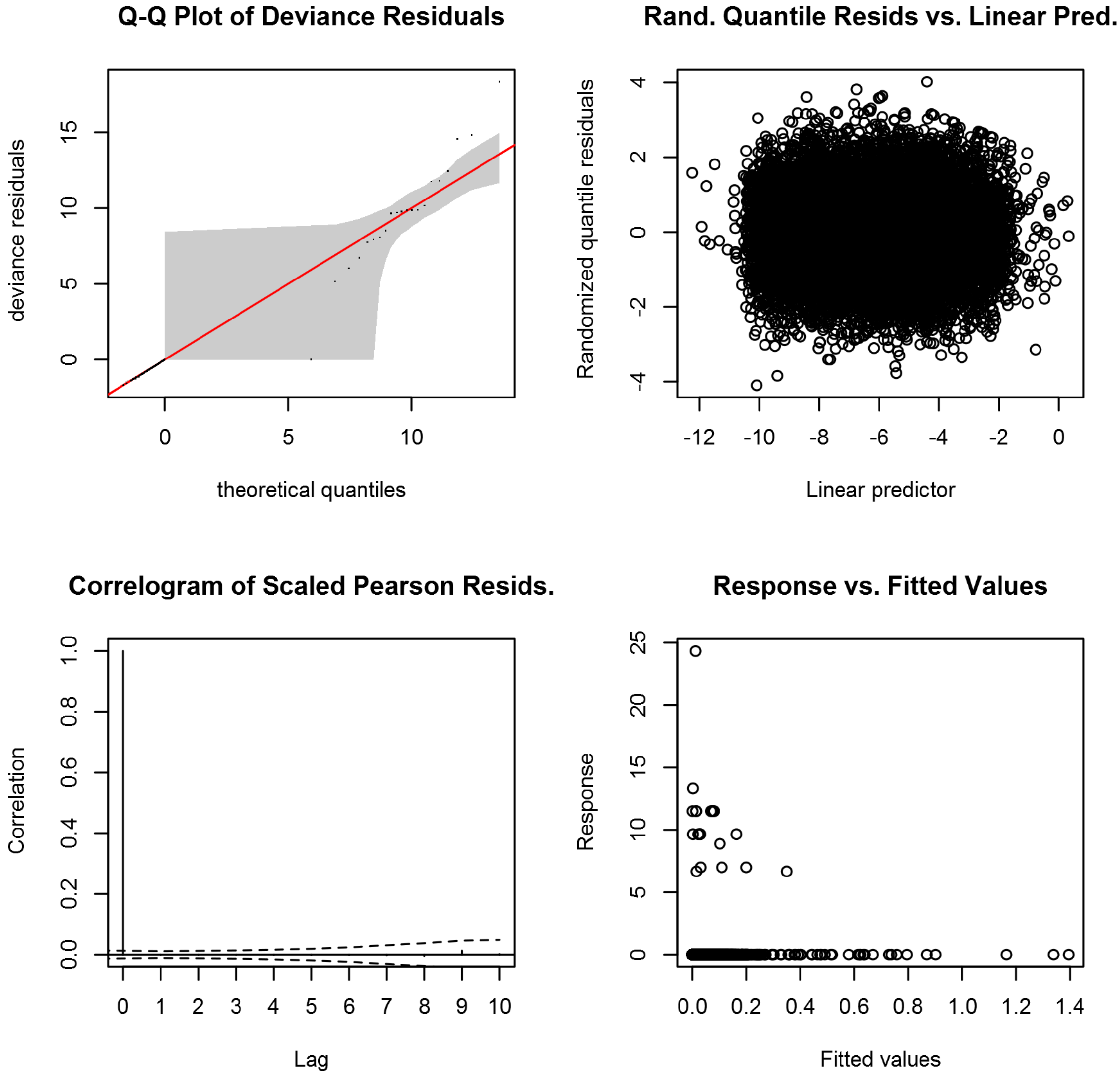

Figure 69: Statistical diagnostic plots for the North Atlantic right whale Contemporaneous model, Winter season, Calving and Migration Area.

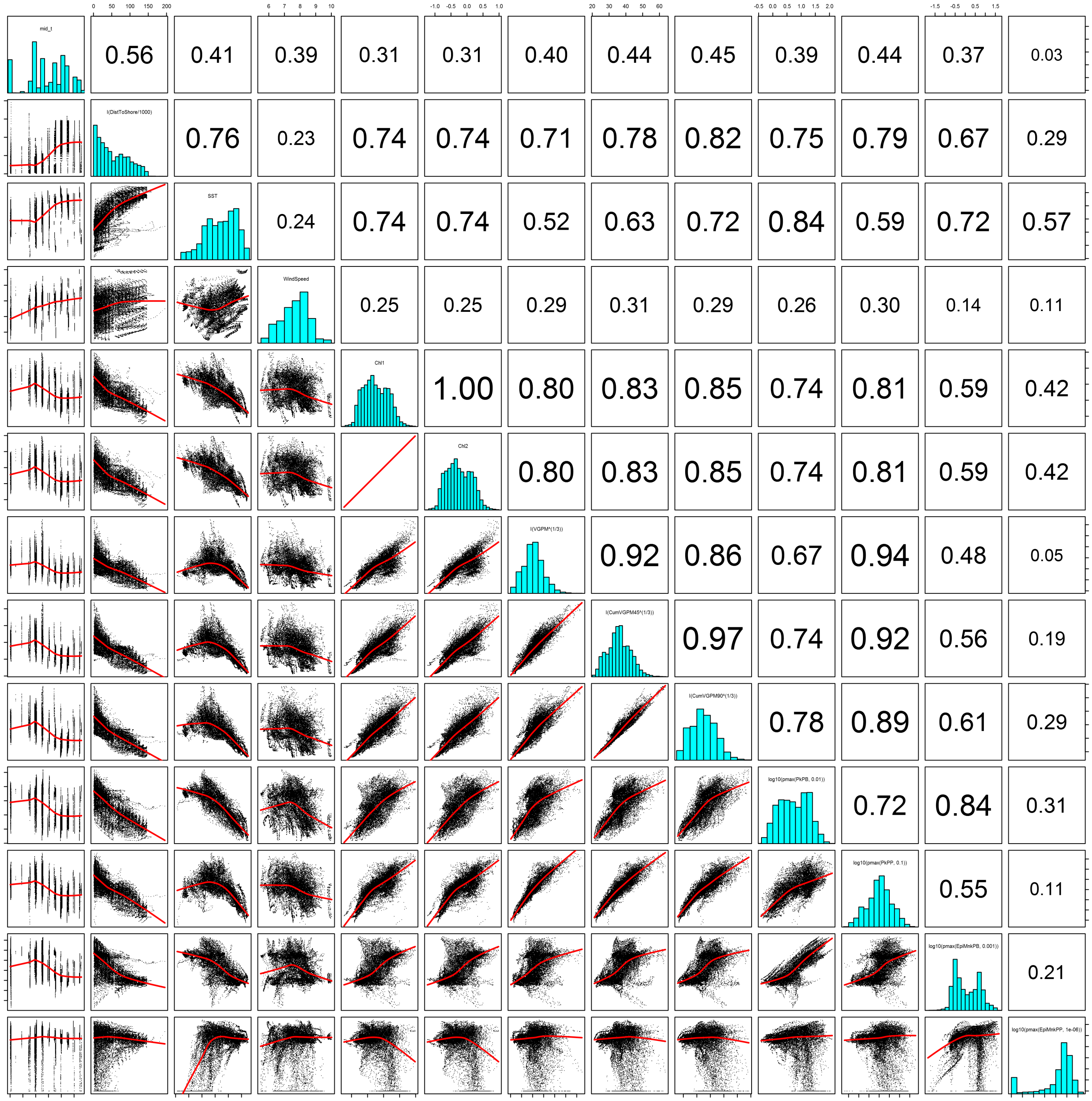

Figure 70: Scatterplot matrix for the North Atlantic right whale Contemporaneous model, Winter season, Calving and Migration Area. This plot is used to inspect the distribution of predictors (via histograms along the diagonal), simple correlation between predictors (via pairwise Pearson coefficients above the diagonal), and linearity of predictor correlations (via scatterplots below the diagonal). This plot is best viewed at high magnification.

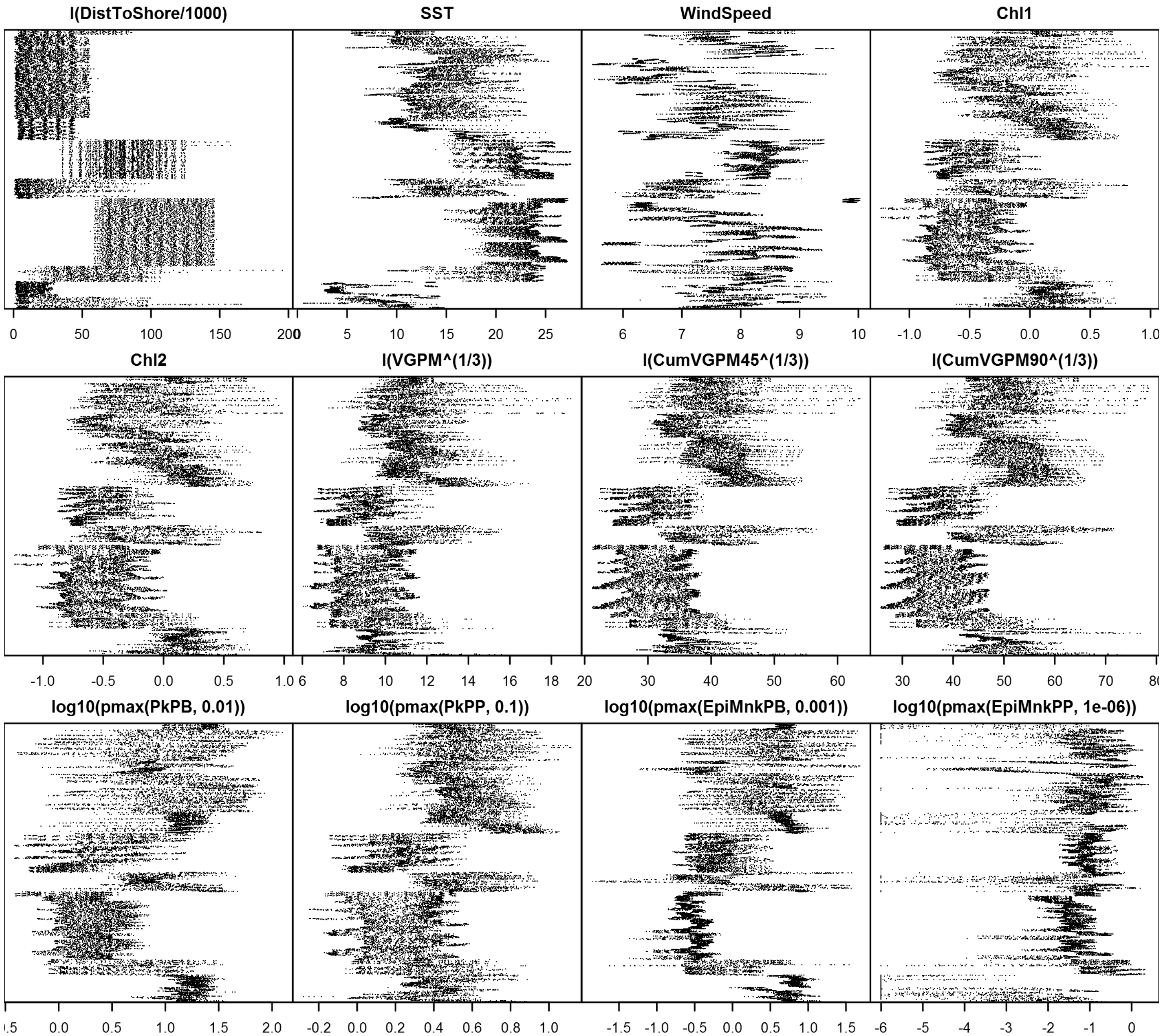

Figure 71: Dotplot for the North Atlantic right whale Contemporaneous model, Winter season, Calving and Migration Area. This plot is used to check for suspicious patterns and outliers in the data. Points are ordered vertically by transect ID, sequentially in time.

Unsurveyed Area

Density was not modeled for this region.

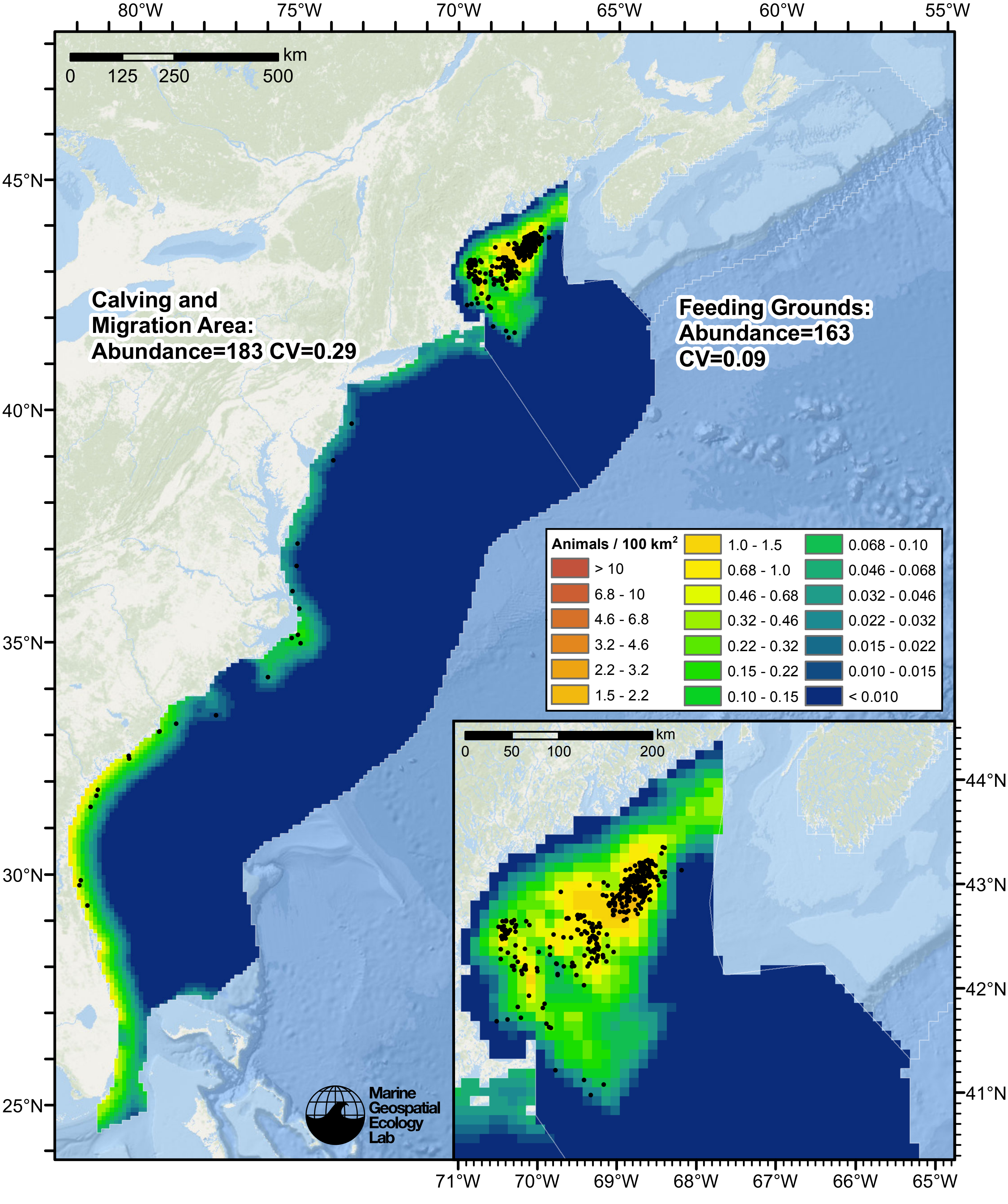

Figure 72: North Atlantic right whale density predicted by the Winter season climatological same segments model that explained the most deviance. Pixels are 10x10 km. The legend gives the estimated individuals per pixel; breaks are logarithmic. The same scale is used for all seasons. Abundance for each region was computed by summing the density cells occuring in that region.

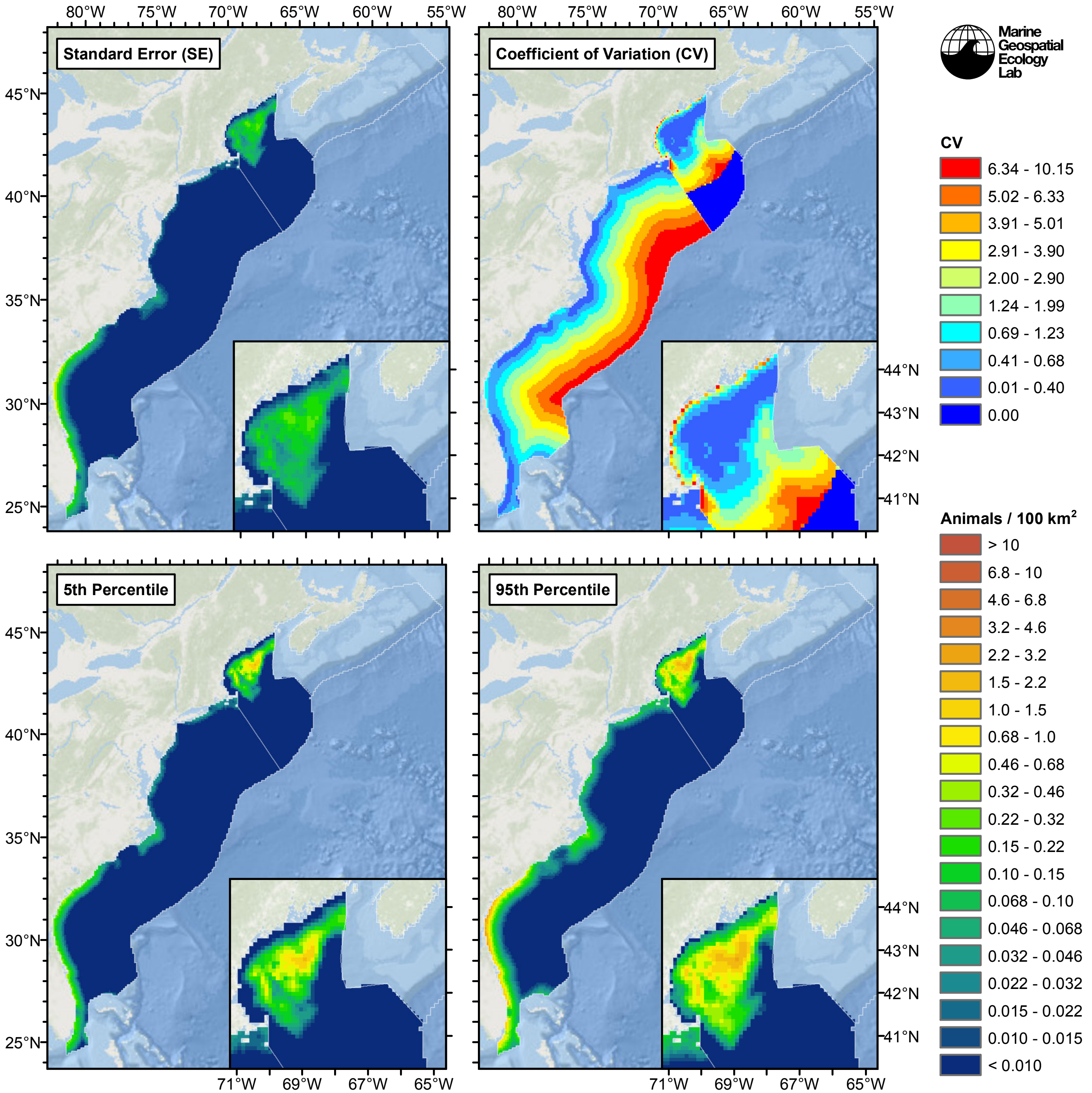

Figure 73: Estimated uncertainty for the Winter season climatological same segments model that explained the most deviance. These estimates only incorporate the statistical uncertainty estimated for the spatial model (by the R mgcv package). They do not incorporate uncertainty in the detection functions, g(0) estimates, predictor variables, and so on.

Feeding Grounds

Statistical output

```
Rscript.exe: This is mgcv 1.8-2. For overview type 'help("mgcv-package")'.


Family: Tweedie(p=1.275)
```

```
Link function: log

Formula:
abundance ~ offset(log(area_km2)) + s(log10(Depth), bs = "ts",
    k = 5) + s(I(DistToShore/1000), bs = "ts", k = 5) + s(I(DistTo125m/1000),
    bs = "ts", k = 5) + s(I(DistTo300m/1000), bs = "ts", k = 5) +
    s(ClimSST, bs = "ts", k = 5) + s(log10(pmax(ClimEKE, 1e-04)),
    bs = "ts", k = 5) + s(log10(pmax(ClimEpiMnkPP, 1e-06)), bs = "ts",
    k = 5)

Parametric coefficients:
            Estimate Std. Error t value Pr(>|t|)
(Intercept)  -8.6735     0.5077  -17.08   <2e-16 ***
---
Signif. codes:  0 '***' 0.001 '**' 0.01 '*' 0.05 '.' 0.1 ' ' 1

Approximate significance of smooth terms:
                                    edf Ref.df      F  p-value
s(log10(Depth))                   3.646      4  9.336 1.99e-08 ***
s(I(DistToShore/1000))            2.426      4  4.558 4.27e-05 ***
s(I(DistTo125m/1000))             2.931      4  6.093 2.45e-06 ***
s(I(DistTo300m/1000))             2.433      4  7.093 2.25e-07 ***
s(ClimSST)                        2.644      4  7.060 4.10e-07 ***
s(log10(pmax(ClimEKE, 1e-04)))    1.638      4 10.211 2.21e-11 ***
s(log10(pmax(ClimEpiMnkPP, 1e-06))) 2.975      4  5.984 6.46e-06 ***
---
Signif. codes:  0 '***' 0.001 '**' 0.01 '*' 0.05 '.' 0.1 ' ' 1

R-sq.(adj) =  0.025   Deviance explained =   22%
-REML = 2039.9  Scale est. = 27.727    n = 8937

All predictors were significant. This is the final model.
Creating term plots.
Diagnostic output from gam.check():

Method: REML   Optimizer: outer newton
full convergence after 12 iterations.
Gradient range [-3.293372e-07,1.259479e-07]
(score 2039.894 & scale 27.72697).
Hessian positive definite, eigenvalue range [0.1756689,960.3972].
Model rank =  29 / 29

Basis dimension (k) checking results. Low p-value (k-index<1) may
indicate that k is too low, especially if edf is close to k'.

                                     k'   edf k-index p-value
s(log10(Depth))                   4.000 3.646   0.767    0.00
s(I(DistToShore/1000))            4.000 2.426   0.772    0.00
s(I(DistTo125m/1000))             4.000 2.931   0.796    0.06
s(I(DistTo300m/1000))             4.000 2.433   0.761    0.00
s(ClimSST)                        4.000 2.644   0.807    0.18
s(log10(pmax(ClimEKE, 1e-04)))    4.000 1.638   0.779    0.00
s(log10(pmax(ClimEpiMnkPP, 1e-06))) 4.000 2.975   0.819    0.52
```

Predictors retained during the model selection procedure: Depth, DistToShore, DistTo125m, DistTo300m, ClimSST, ClimEKE, ClimEpiMnkPP

Predictors dropped during the model selection procedure: Slope, ClimDistToFront2

Model term plots

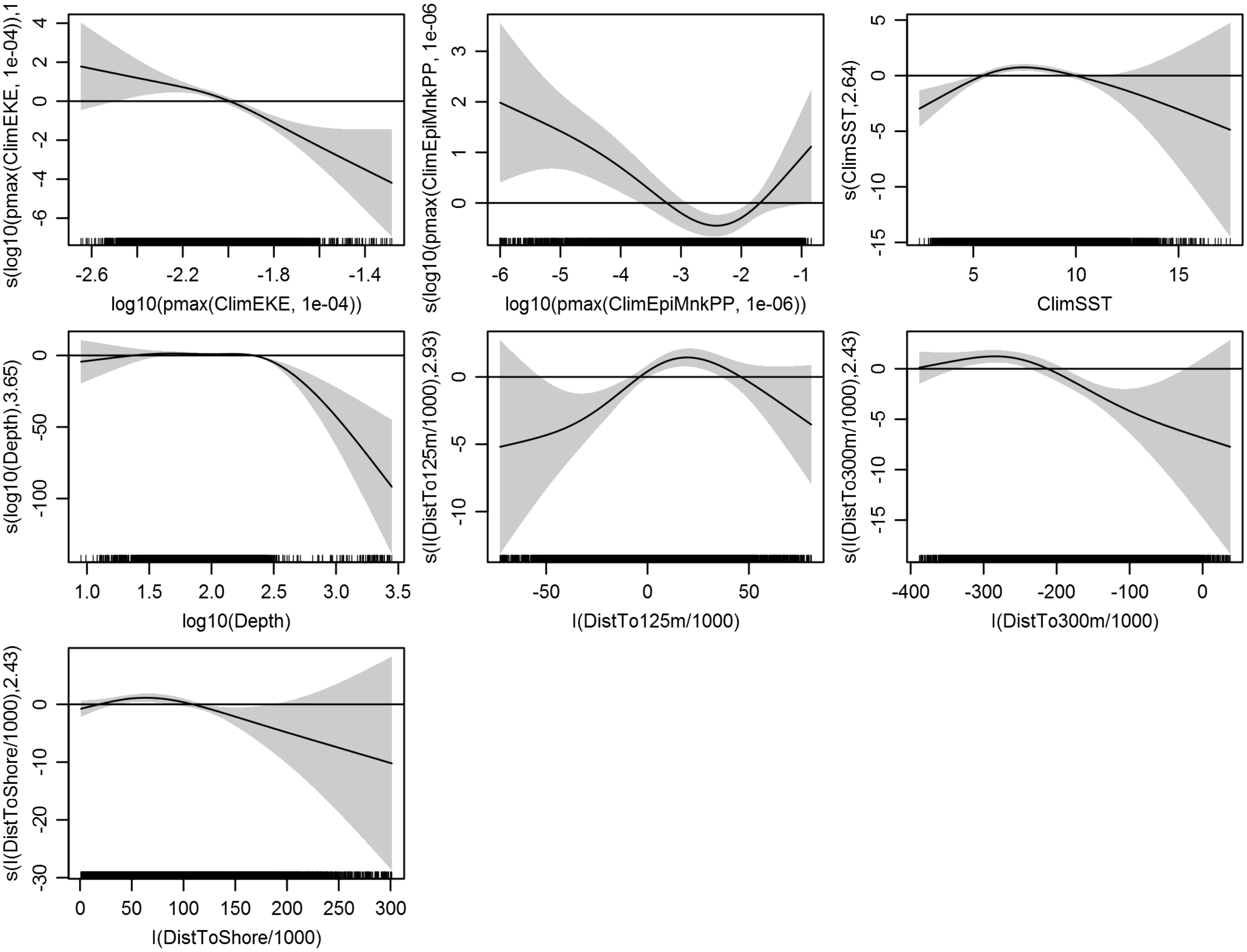

Diagnostic plots

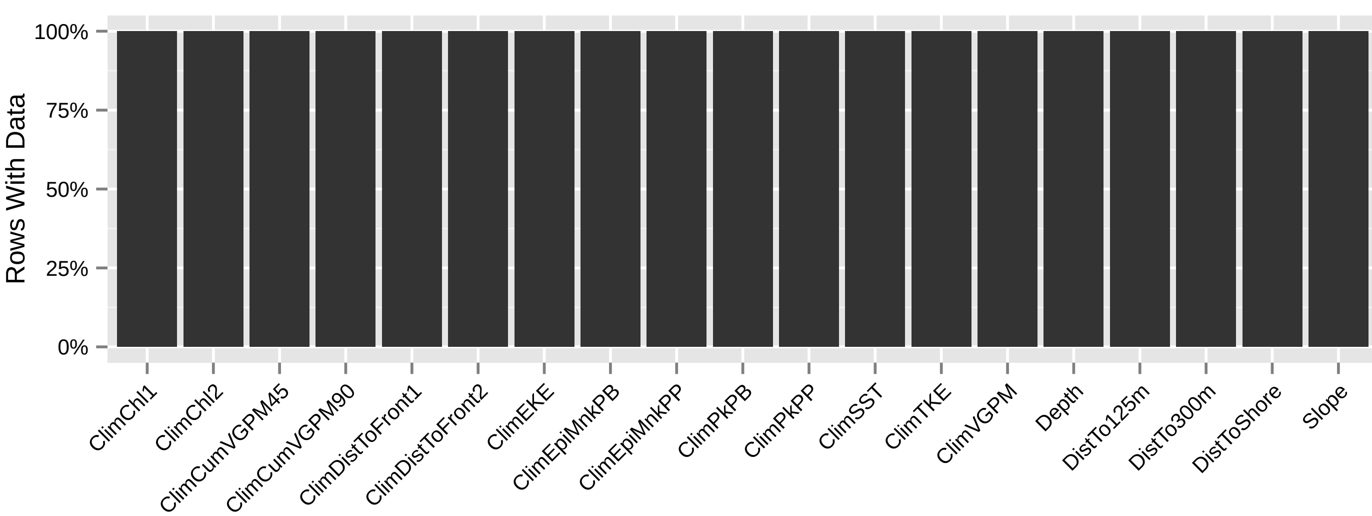

Figure 74: Segments with predictor values for the North Atlantic right whale Climatological model, Winter season, Feeding Grounds. This plot is used to assess how many segments would be lost by including a given predictor in a model.

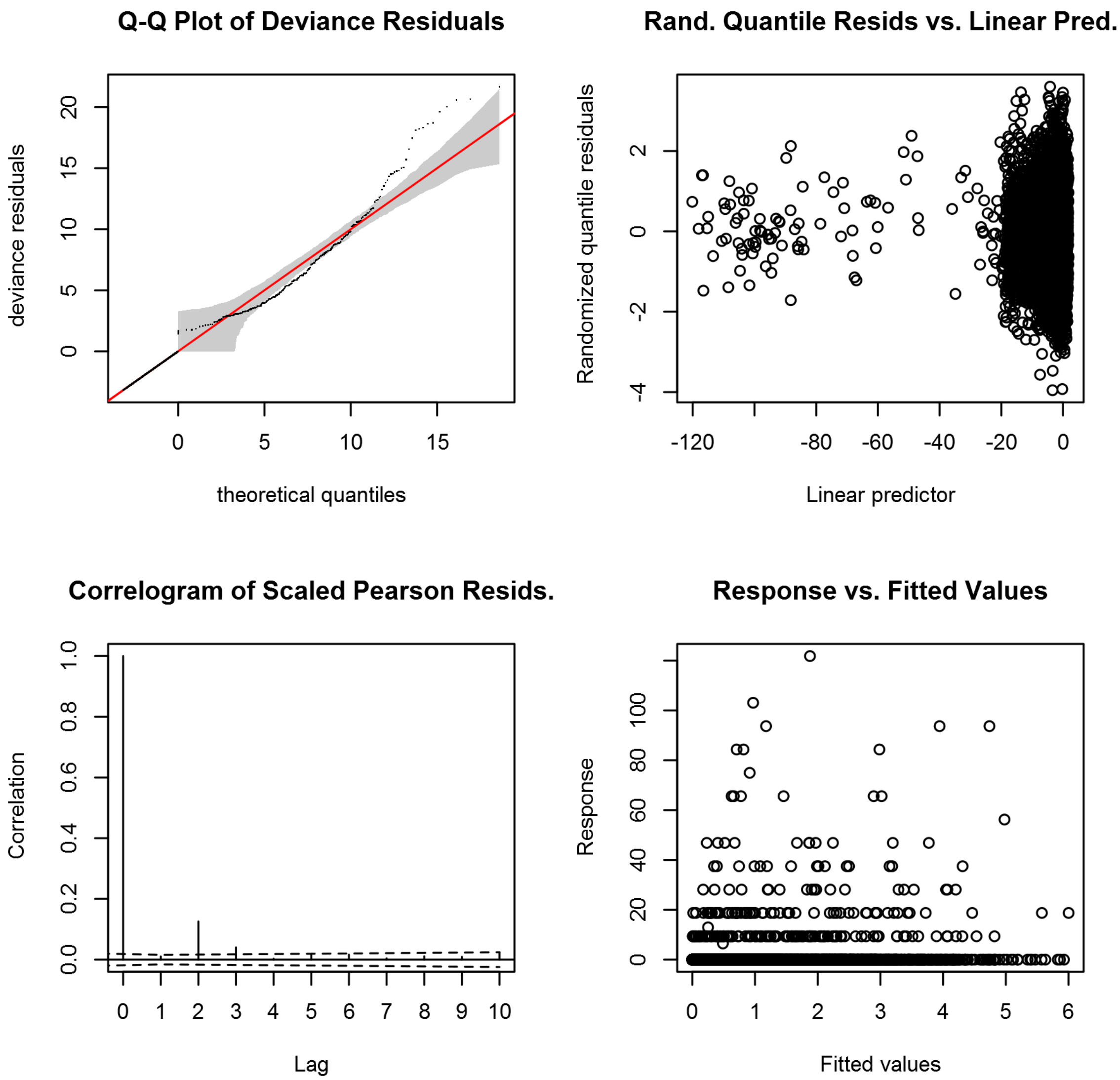

Figure 75: Statistical diagnostic plots for the North Atlantic right whale Climatological model, Winter season, Feeding Grounds.

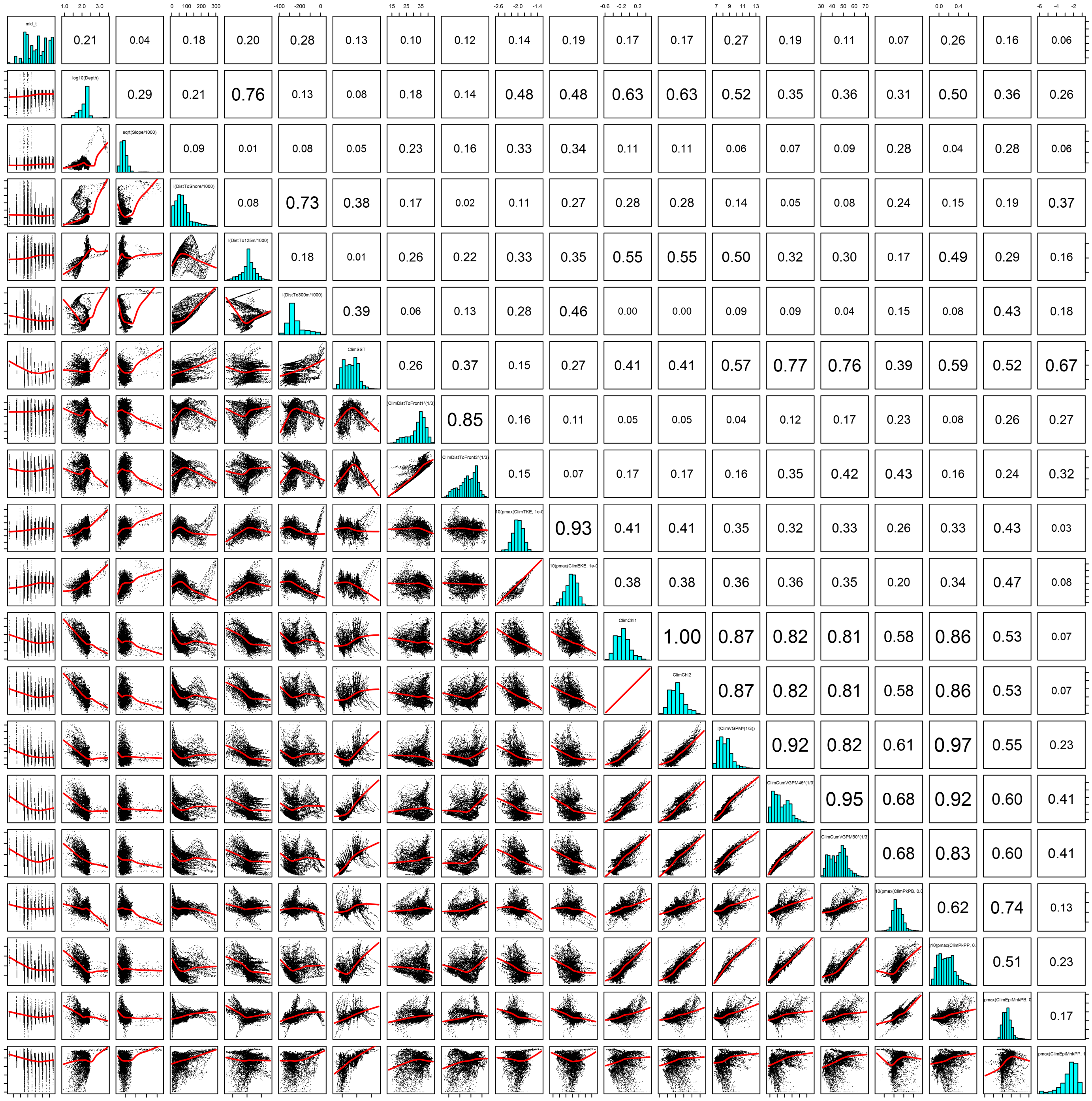

Figure 76: Scatterplot matrix for the North Atlantic right whale Climatological model, Winter season, Feeding Grounds. This plot is used to inspect the distribution of predictors (via histograms along the diagonal), simple correlation between predictors (via pairwise Pearson coefficients above the diagonal), and linearity of predictor correlations (via scatterplots below the diagonal). This plot is best viewed at high magnification.

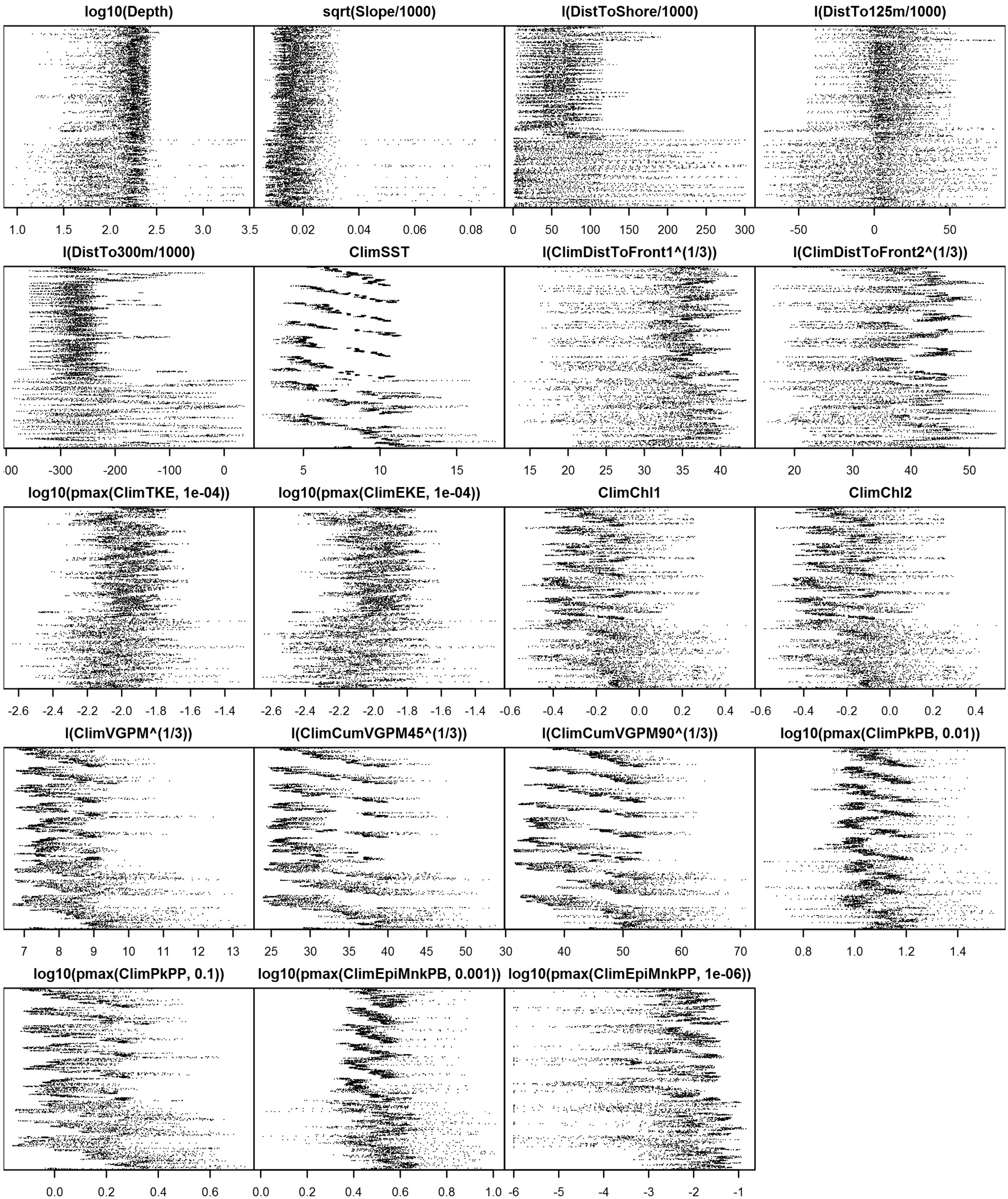

Figure 77: Dotplot for the North Atlantic right whale Climatological model, Winter season, Feeding Grounds. This plot is used to check for suspicious patterns and outliers in the data. Points are ordered vertically by transect ID, sequentially in time.

Calving and Migration Area

Statistical output

```
Rscript.exe: This is mgcv 1.8-2. For overview type 'help("mgcv-package")'.


Family: Tweedie(p=1.044)
Link function: log

Formula:
abundance ~ offset(log(area_km2)) + s(I(DistToShore/1000), bs = "ts",
    k = 5) + s(log10(pmax(ClimEpiMnkPB, 0.001)), bs = "ts", k = 5)

Parametric coefficients:
            Estimate Std. Error t value Pr(>|t|)
(Intercept)  -9.3309     0.5854  -15.94   <2e-16 ***
---
Signif. codes:  0 '***' 0.001 '**' 0.01 '*' 0.05 '.' 0.1 ' ' 1

Approximate significance of smooth terms:
                                       edf Ref.df     F  p-value
s(I(DistToShore/1000))               1.033      4 4.202 2.22e-05 ***
s(log10(pmax(ClimEpiMnkPB, 0.001))) 1.927      4 7.169 7.47e-08 ***
---
Signif. codes:  0 '***' 0.001 '**' 0.01 '*' 0.05 '.' 0.1 ' ' 1

R-sq.(adj) =  0.00258   Deviance explained = 14.7%
-REML = 195.79  Scale est. = 12.235    n = 17768

All predictors were significant. This is the final model.
Creating term plots.
Diagnostic output from gam.check():

Method: REML   Optimizer: outer newton
full convergence after 13 iterations.
Gradient range [-0.0002632373,9.032598e-06]
(score 195.7863 & scale 12.23531).
Hessian positive definite, eigenvalue range [0.382907,487.5828].
Model rank =  9 / 9

Basis dimension (k) checking results. Low p-value (k-index<1) may
indicate that k is too low, especially if edf is close to k'.

                                        k'   edf k-index p-value
s(I(DistToShore/1000))               4.000 1.033   0.953    0.03
s(log10(pmax(ClimEpiMnkPB, 0.001))) 4.000 1.927   0.952    0.00

Predictors retained during the model selection procedure: DistToShore, ClimEpiMnkPB

Predictors dropped during the model selection procedure: ClimSST, ClimWindSpeed
```

Model term plots

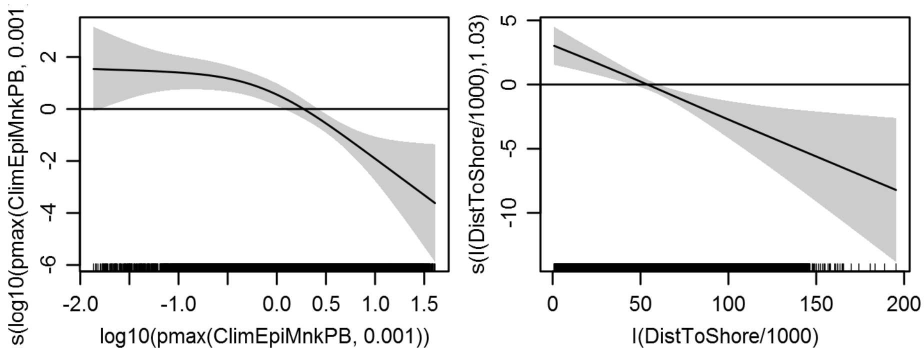

Diagnostic plots

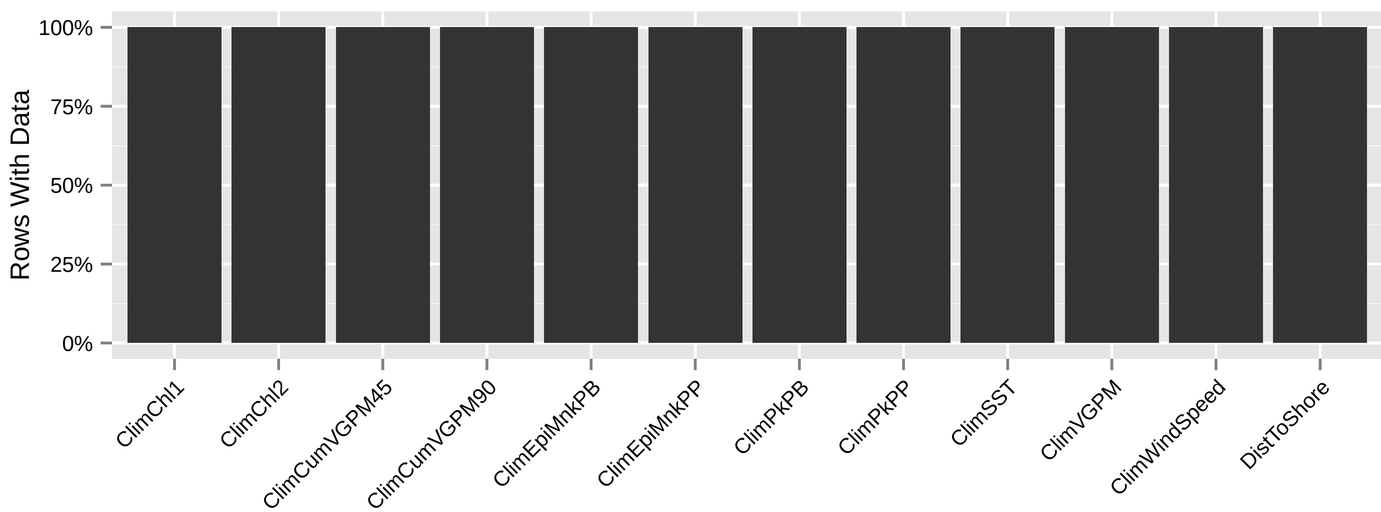

Figure 78: Segments with predictor values for the North Atlantic right whale Climatological model, Winter season, Calving and Migration Area. This plot is used to assess how many segments would be lost by including a given predictor in a model.

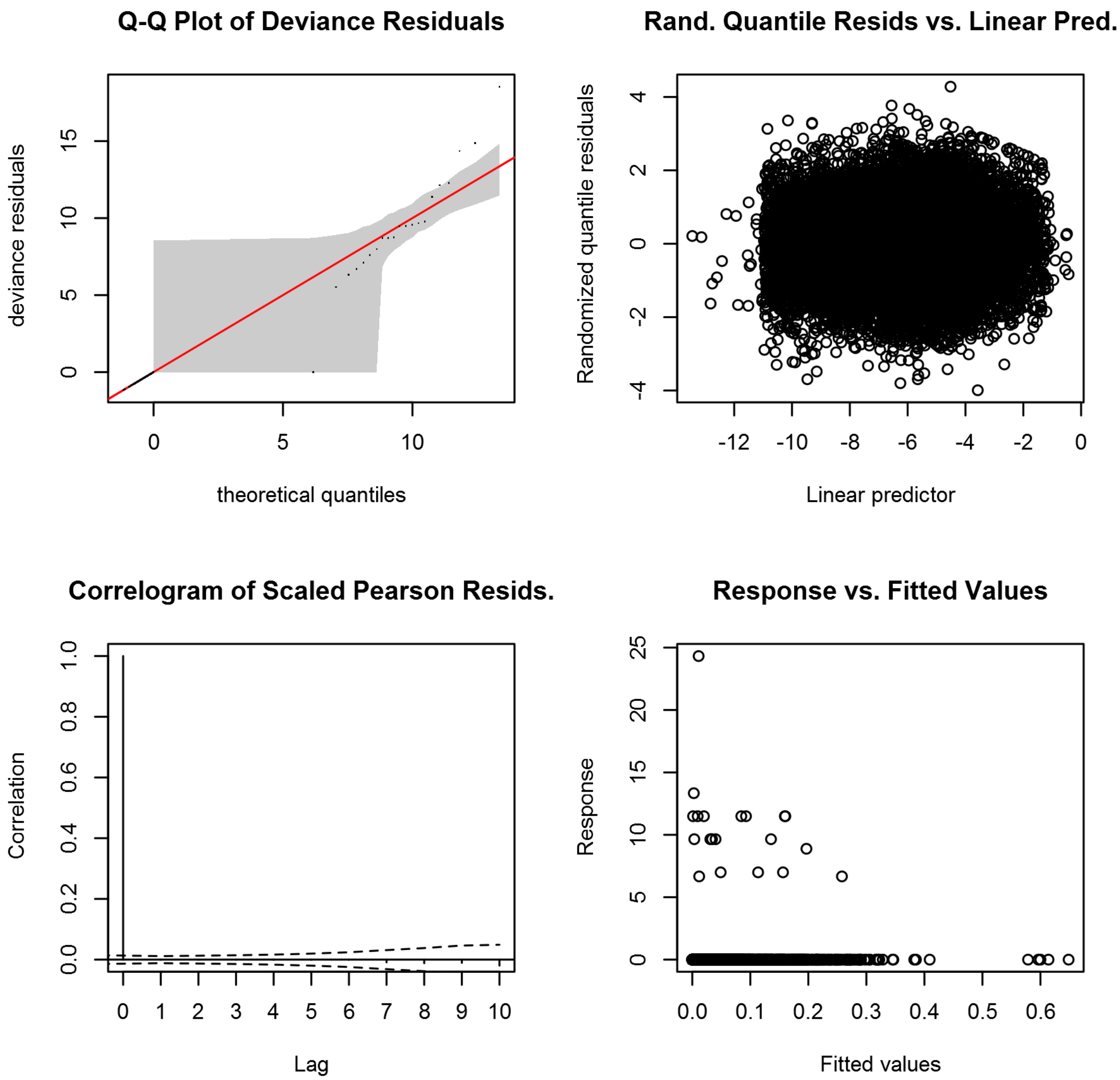

Figure 79: Statistical diagnostic plots for the North Atlantic right whale Climatological model, Winter season, Calving and Migration Area.

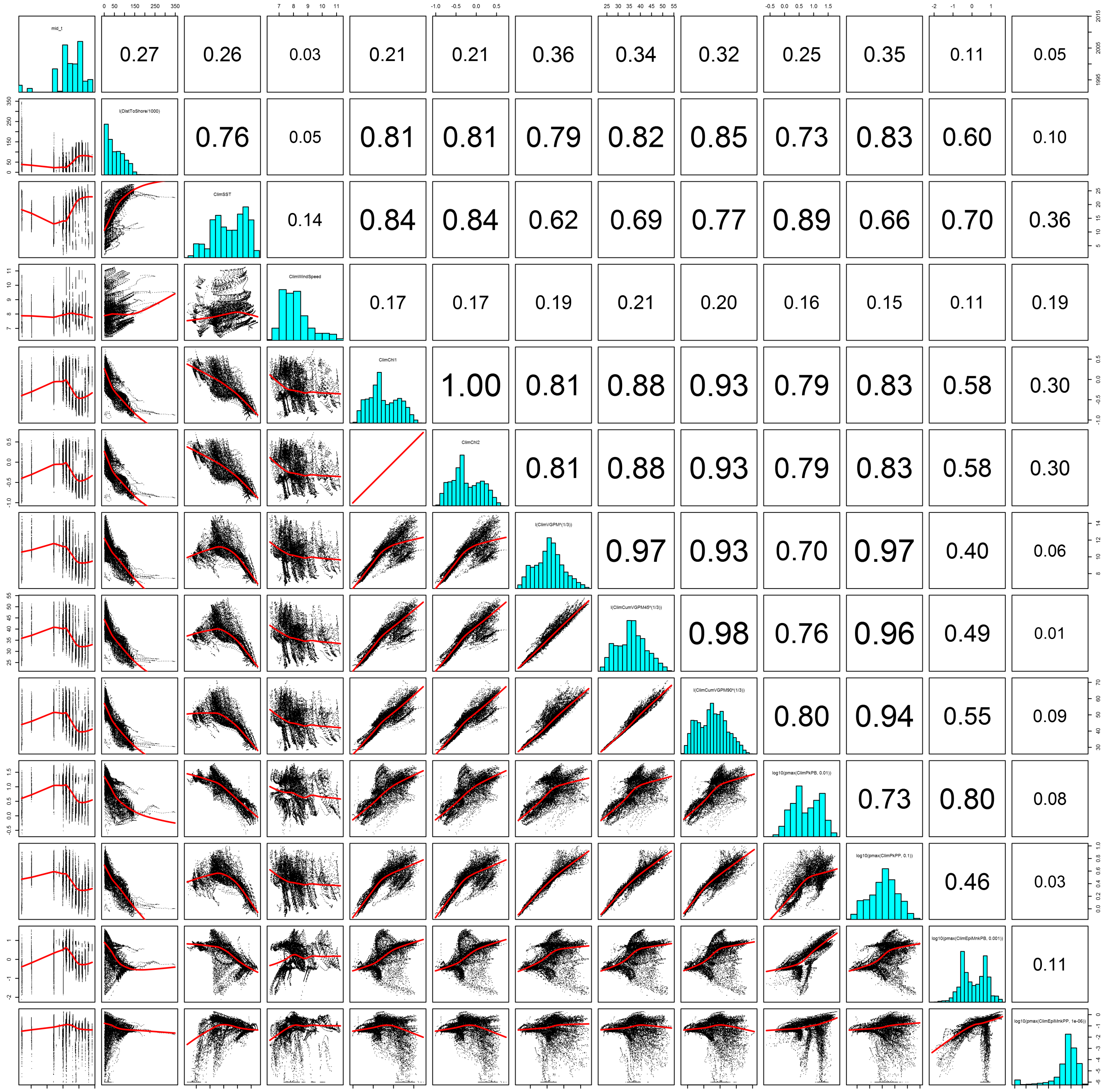

Figure 80: Scatterplot matrix for the North Atlantic right whale Climatological model, Winter season, Calving and Migration Area. This plot is used to inspect the distribution of predictors (via histograms along the diagonal), simple correlation between predictors (via pairwise Pearson coefficients above the diagonal), and linearity of predictor correlations (via scatterplots below the diagonal). This plot is best viewed at high magnification.

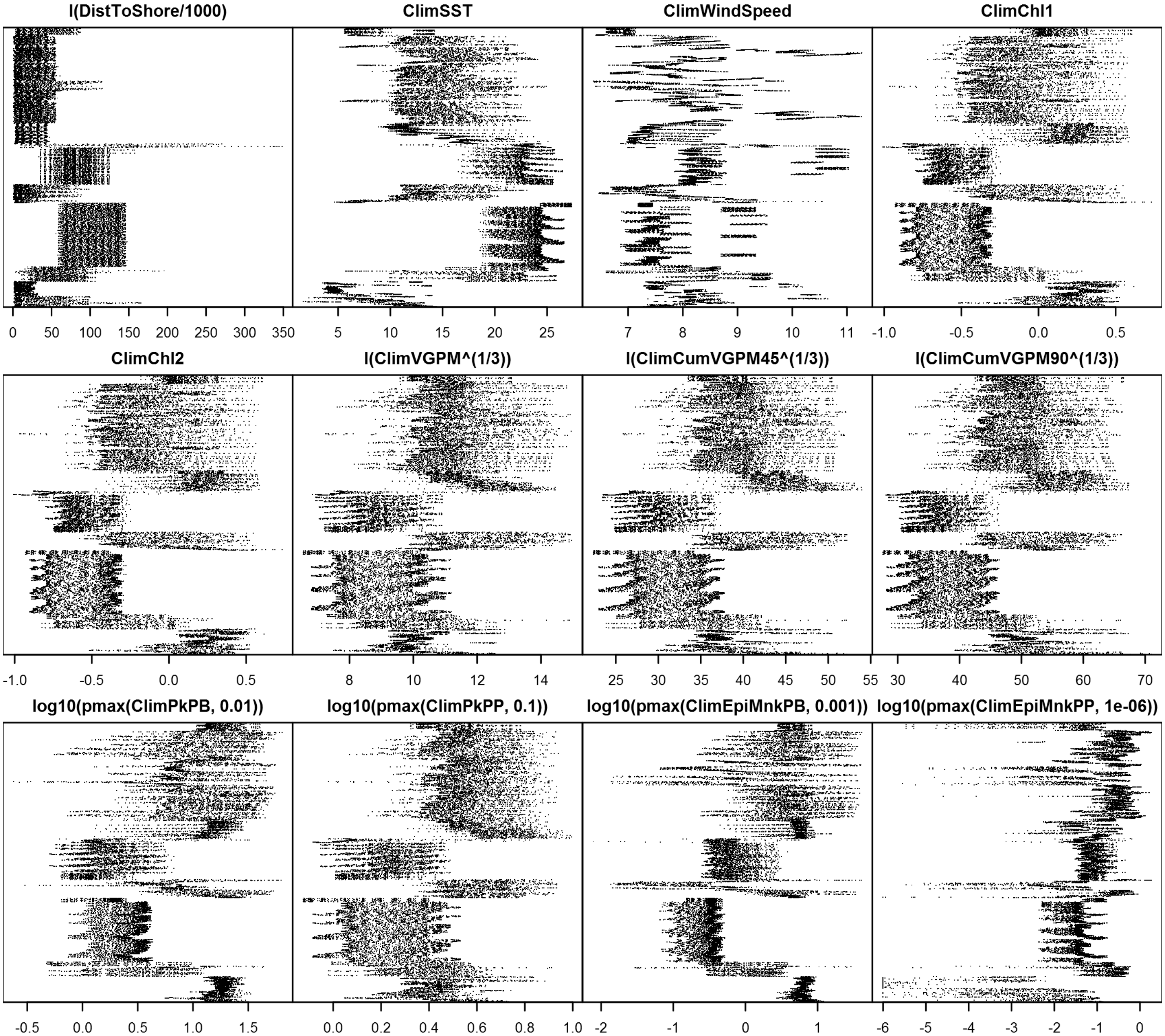

Figure 81: Dotplot for the North Atlantic right whale Climatological model, Winter season, Calving and Migration Area. This plot is used to check for suspicious patterns and outliers in the data. Points are ordered vertically by transect ID, sequentially in time.

Unsurveyed Area

Density was not modeled for this region.

Spring

In this season, similar to winter, survey effort was moderate on the shelf north of Long Island to Canadian waters and south of Delaware to Florida, with no effort in Canadian waters, and very limited effort between Maryland and the middle of Long Island, or off the shelf. Many sightings were reported close to Cape Cod and along the western side of the Great South Channel. Another aggregation was reported in Rhode Island Sound, where right whales are reported to feed during this time of year (Dawicki 2011). Finally, a much smaller number were distributed between New York and Florida, with the largest number reported off North Carolina, an area surveyed relatively heavily by the University of North Carolina at Wilmington.

Similar to the winter season, we split the study area into a northern Feeding Grounds region and a southern Calving and Migration Area and fitted separate models to each region, under the hypothesis that whales on the feeding grounds would express different environmental preferences than whales migrating from the south. We selected Block Island as the break between the regions because it allowed the Rhode Island Sound feeding aggregation to be modeled together with the Great South Channel feeding aggregation, while leaving the segments along Long Island to be considered with the migratory corridor.

In the Feeding Grounds region we fitted full models. In the Calving and Migration area, we had a very limited number of sightings to work with, but given the critically endangered status of the species, we wanted to provide a spatially-explicit density prediction, if possible. We assumed that right whales could be distributed at any latitude along the shelf, would be found in fewer numbers as the season progressed and the whales reached the northern feeding grounds, and would be found closer to shore, consistent with prior findings that migrating whales remain close to shore (Knowlton et al. 2002, Schick et al. 2009). We fitted a model that used distance to shore and day of year as covariates, in an attempt to capture the most basic spatial and temporal dynamics while remaining parsimonious (due to the low number of sightings).

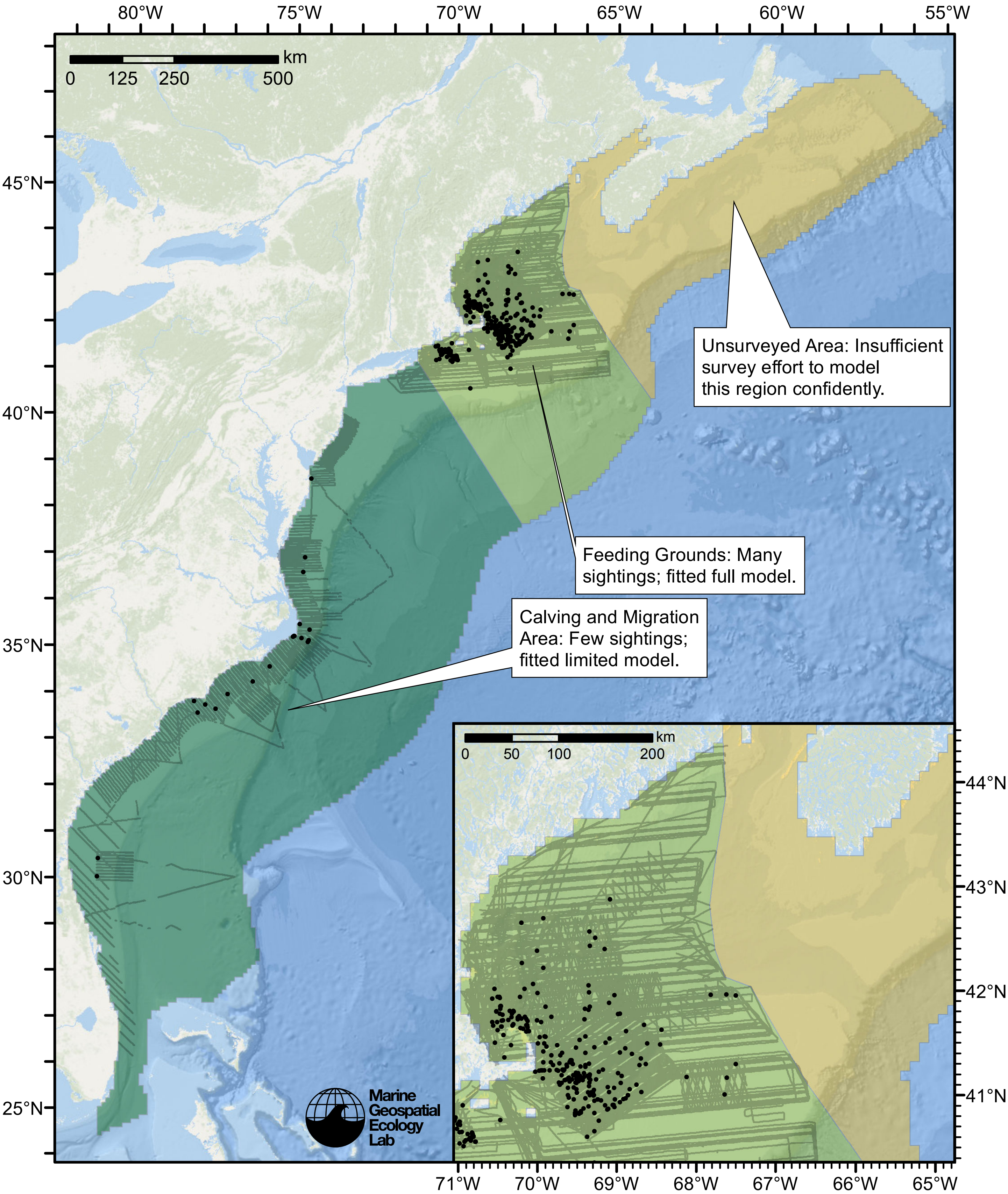

Figure 82: North Atlantic right whale density model schematic for Spring season. All on-effort sightings are shown, including those that were truncated when detection functions were fitted.

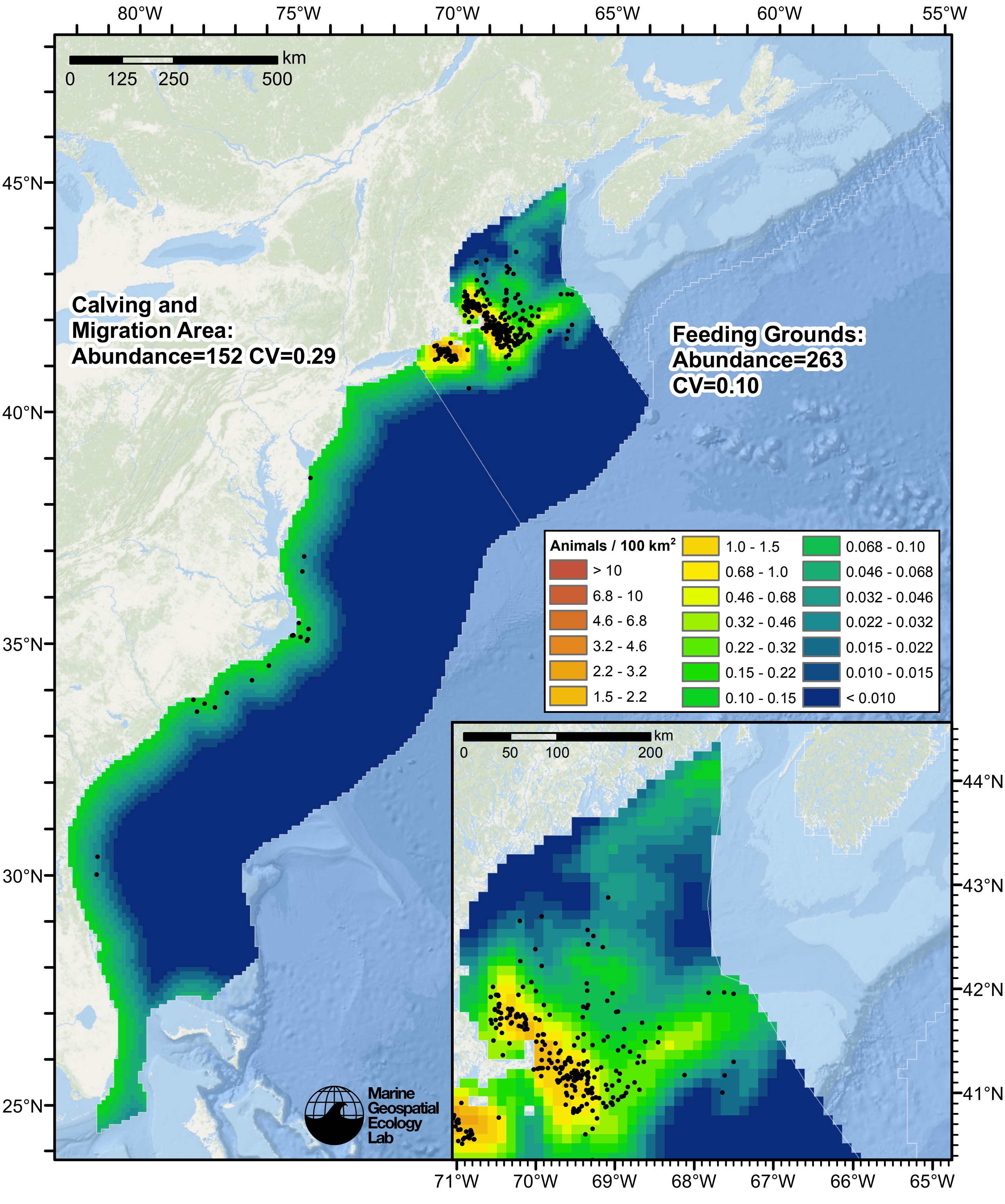

Figure 83: North Atlantic right whale density predicted by the Spring season climatological model that explained the most deviance. Pixels are 10x10 km. The legend gives the estimated individuals per pixel; breaks are logarithmic. The same scale is used for all seasons. Abundance for each region was computed by summing the density cells occuring in that region.

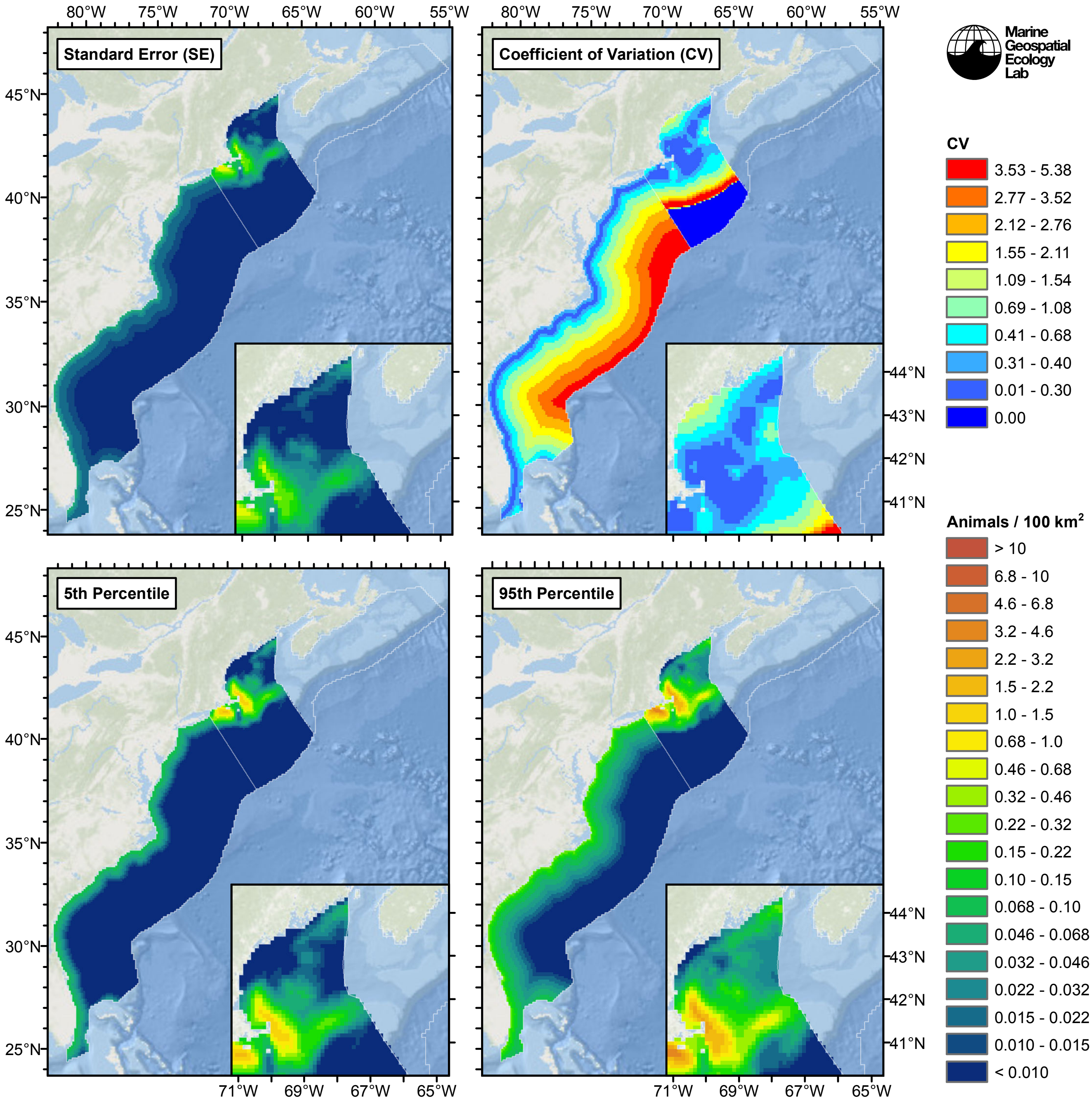

Figure 84: Estimated uncertainty for the Spring season climatological model that explained the most deviance. These estimates only incorporate the statistical uncertainty estimated for the spatial model (by the R mgcv package). They do not incorporate uncertainty in the detection functions, g(0) estimates, predictor variables, and so on.

Feeding Grounds

Statistical output

```
Rscript.exe: This is mgcv 1.8-2. For overview type 'help("mgcv-package")'.


Family: Tweedie(p=1.259)
```

```
Link function: log

Formula:
abundance ~ offset(log(area_km2)) + s(I(DistToShore/1000), bs = "ts",
    k = 5) + s(I(DistTo125m/1000), bs = "ts", k = 5) + s(I(DistTo300m/1000),
    bs = "ts", k = 5) + s(ClimSST, bs = "ts", k = 5) + s(I(ClimDistToFront1^(1/3)),
    bs = "ts", k = 5) + s(I(ClimCumVGPM90^(1/3)), bs = "ts",
    k = 5)

Parametric coefficients:
            Estimate Std. Error t value Pr(>|t|)
(Intercept)  -7.1467     0.1511  -47.29   <2e-16 ***
---
Signif. codes:  0 '***' 0.001 '**' 0.01 '*' 0.05 '.' 0.1 ' ' 1

Approximate significance of smooth terms:
                                edf Ref.df      F  p-value
s(I(DistToShore/1000))       0.9566      4  2.744 0.000471 ***
s(I(DistTo125m/1000))        3.0835      4 10.776 4.93e-11 ***
s(I(DistTo300m/1000))        3.3955      4 17.410  < 2e-16 ***
s(ClimSST)                   3.3731      4 10.289 4.35e-10 ***
s(I(ClimDistToFront1^(1/3))) 3.7282      4 12.878 1.42e-11 ***
s(I(ClimCumVGPM90^(1/3)))    3.2589      4 12.309 1.75e-12 ***
---
Signif. codes:  0 '***' 0.001 '**' 0.01 '*' 0.05 '.' 0.1 ' ' 1

R-sq.(adj) =  0.0694   Deviance explained = 32.3%
-REML = 1779.4  Scale est. = 26.51     n = 9594

All predictors were significant. This is the final model.
Creating term plots.
Diagnostic output from gam.check():

Method: REML   Optimizer: outer newton
full convergence after 13 iterations.
Gradient range [-2.313396e-05,1.696662e-06]
(score 1779.441 & scale 26.51034).
Hessian positive definite, eigenvalue range [0.3783521,883.8013].
Model rank =  25 / 25

Basis dimension (k) checking results. Low p-value (k-index<1) may
indicate that k is too low, especially if edf is close to k'.

                                k'   edf k-index p-value
s(I(DistToShore/1000))       4.000 0.957   0.818    0.53
s(I(DistTo125m/1000))        4.000 3.083   0.823    0.64
s(I(DistTo300m/1000))        4.000 3.395   0.798    0.10
s(ClimSST)                   4.000 3.373   0.827    0.83
s(I(ClimDistToFront1^(1/3))) 4.000 3.728   0.833    0.96
s(I(ClimCumVGPM90^(1/3)))    4.000 3.259   0.831    0.93

Predictors retained during the model selection procedure: DistToShore, DistTo125m, DistTo300m,
ClimSST, ClimDistToFront1, ClimCumVGPM90

Predictors dropped during the model selection procedure: Depth, ClimTKE, Slope
```

Model term plots

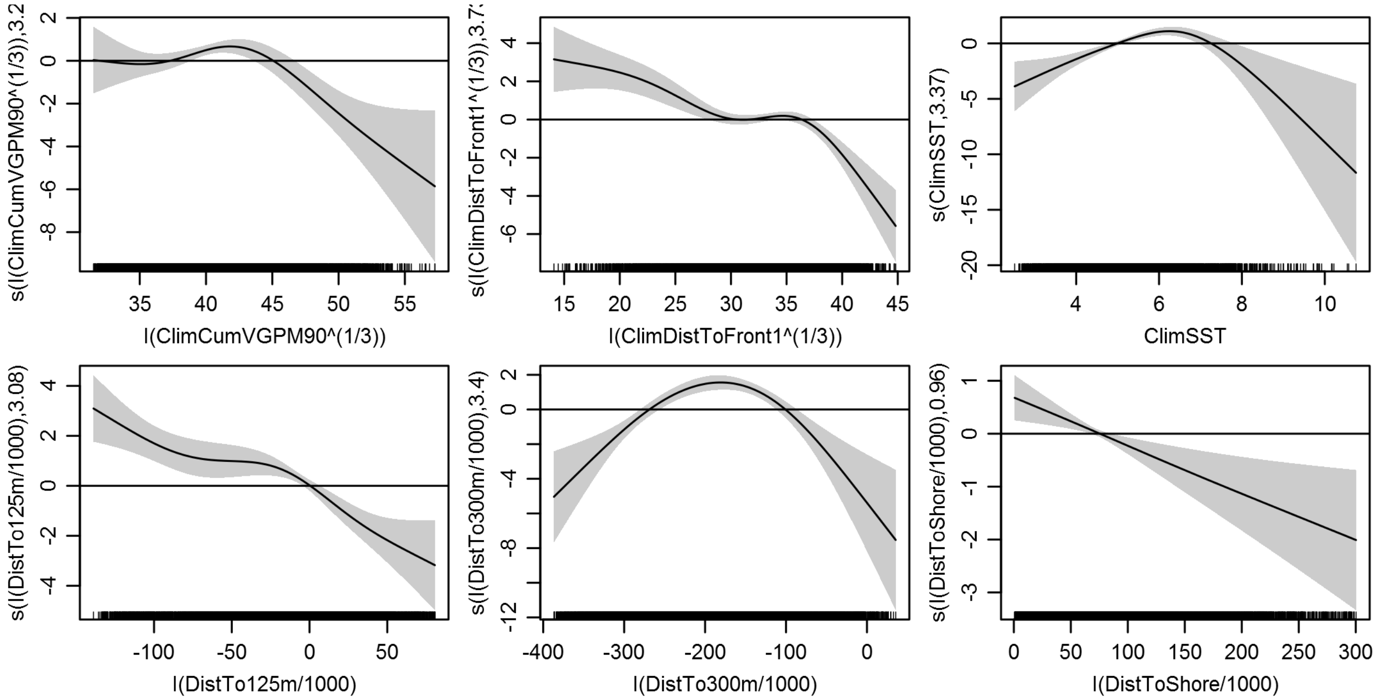

Diagnostic plots

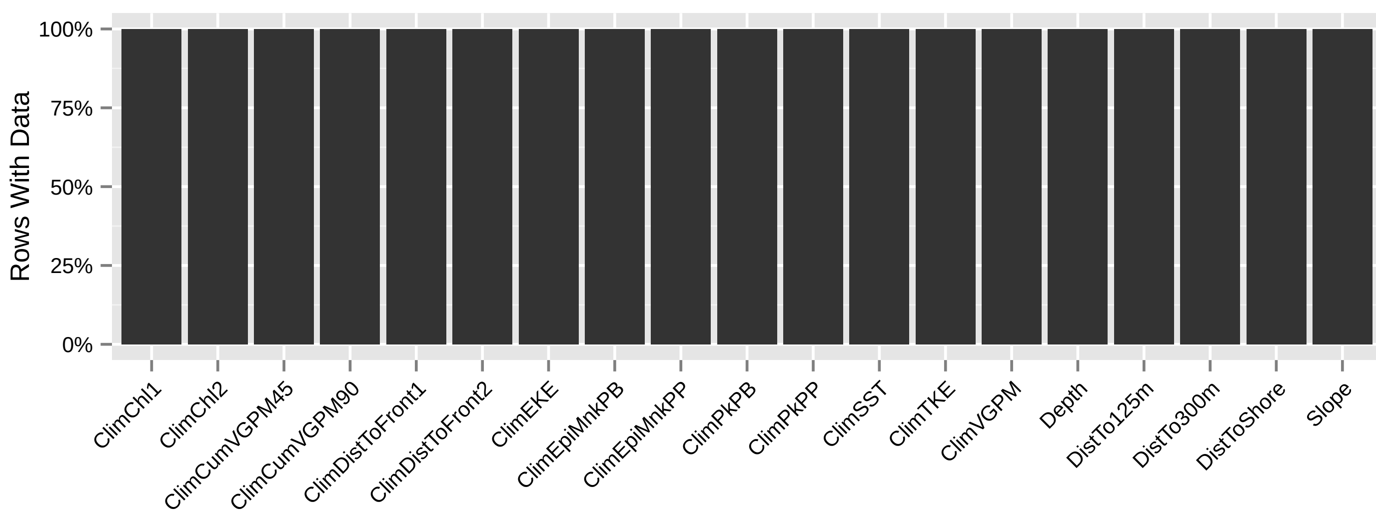

Figure 85: Segments with predictor values for the North Atlantic right whale Climatological model, Spring season, Feeding Grounds. This plot is used to assess how many segments would be lost by including a given predictor in a model.

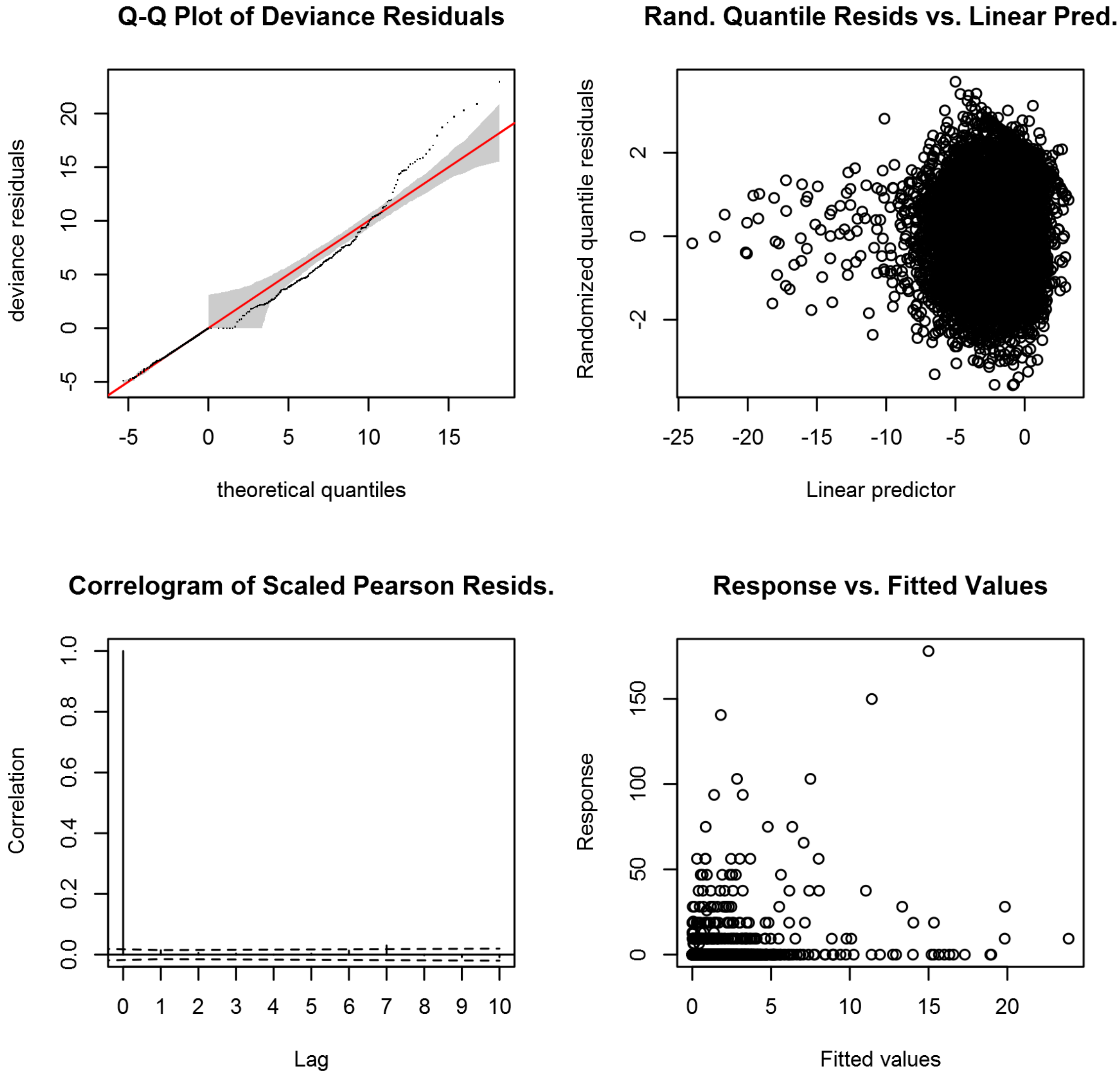

Figure 86: Statistical diagnostic plots for the North Atlantic right whale Climatological model, Spring season, Feeding Grounds.

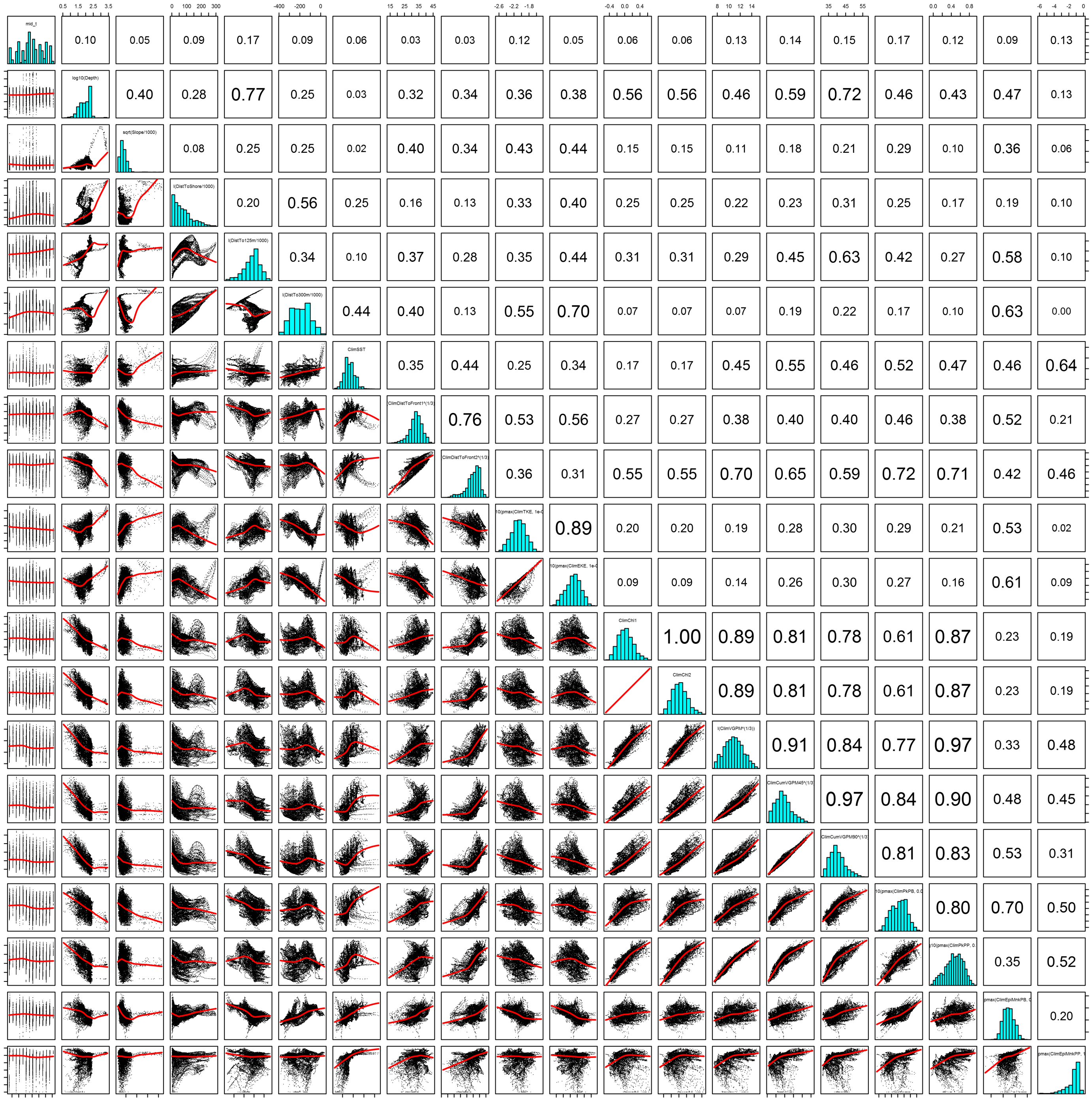

Figure 87: Scatterplot matrix for the North Atlantic right whale Climatological model, Spring season, Feeding Grounds. This plot is used to inspect the distribution of predictors (via histograms along the diagonal), simple correlation between predictors (via pairwise Pearson coefficients above the diagonal), and linearity of predictor correlations (via scatterplots below the diagonal). This plot is best viewed at high magnification.

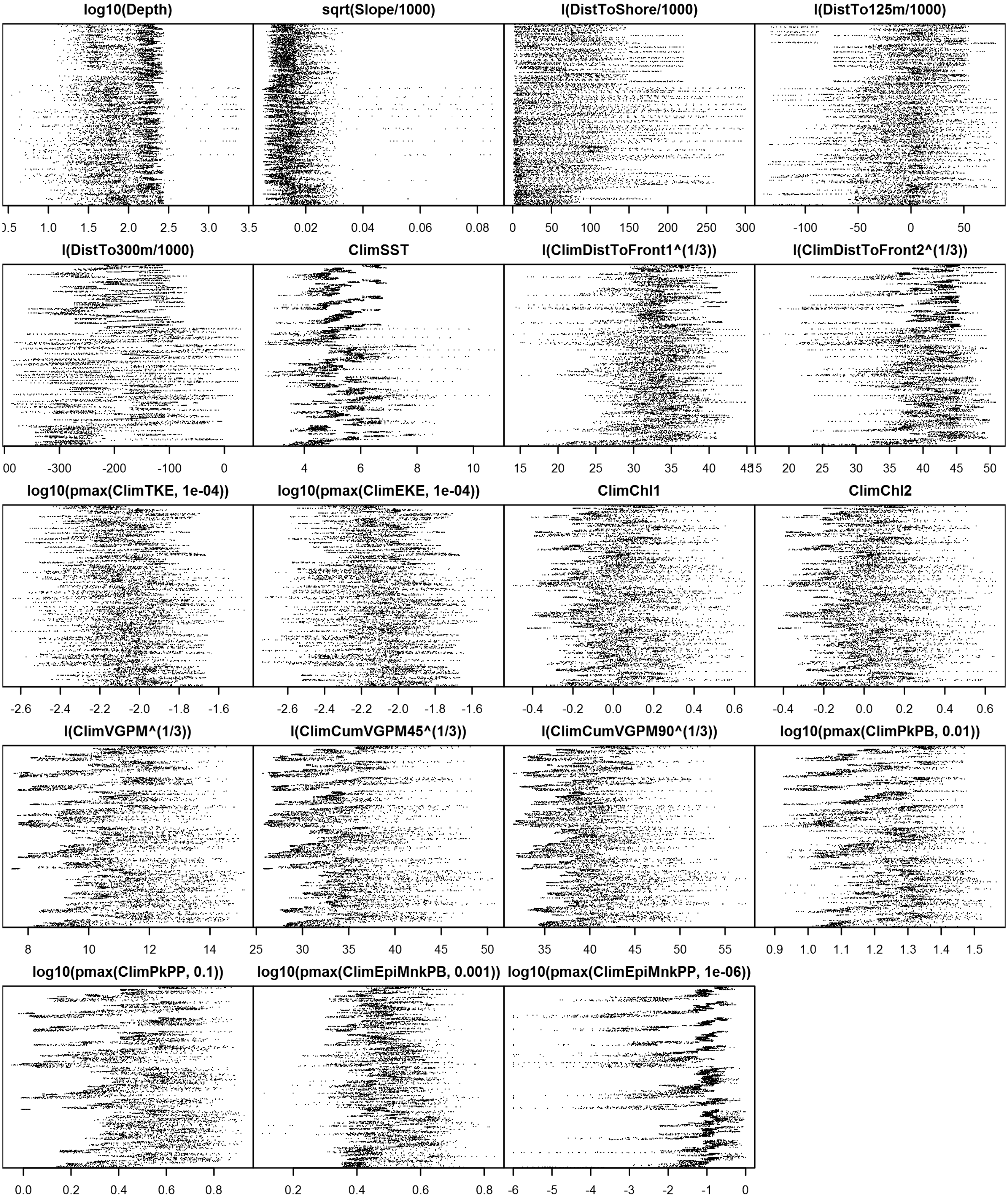

Figure 88: Dotplot for the North Atlantic right whale Climatological model, Spring season, Feeding Grounds. This plot is used to check for suspicious patterns and outliers in the data. Points are ordered vertically by transect ID, sequentially in time.

Calving and Migration Area

Statistical output

```
Rscript.exe: This is mgcv 1.8-2. For overview type 'help("mgcv-package")'.


Family: Tweedie(p=1.166)
Link function: log

Formula:
abundance ~ offset(log(area_km2)) + s(I(DistToShore/1000), bs = "ts",
    k = 4)

Parametric coefficients:
            Estimate Std. Error t value Pr(>|t|)
(Intercept)   -7.769      0.395  -19.66   <2e-16 ***
---
Signif. codes:  0 '***' 0.001 '**' 0.01 '*' 0.05 '.' 0.1 ' ' 1

Approximate significance of smooth terms:
                         edf Ref.df     F p-value
s(I(DistToShore/1000)) 0.863      3 1.735  0.0138 *
---
Signif. codes:  0 '***' 0.001 '**' 0.01 '*' 0.05 '.' 0.1 ' ' 1

R-sq.(adj) =  -0.00169   Deviance explained = -0.467%
-REML = 182.47  Scale est. = 30.603    n = 11605

All predictors were significant. This is the final model.
Creating term plots.
Diagnostic output from gam.check():

Method: REML   Optimizer: outer newton
full convergence after 11 iterations.
Gradient range [-0.0001816491,9.158778e-05]
(score 182.4662 & scale 30.60286).
Hessian positive definite, eigenvalue range [0.3445347,150.5255].
Model rank =  4 / 4

Basis dimension (k) checking results. Low p-value (k-index<1) may
indicate that k is too low, especially if edf is close to k'.

                          k'   edf k-index p-value
s(I(DistToShore/1000)) 3.000 0.863   0.807    0.04

Predictors retained during the model selection procedure: DistToShore

Predictors dropped during the model selection procedure: dayofyear
```

Model term plots

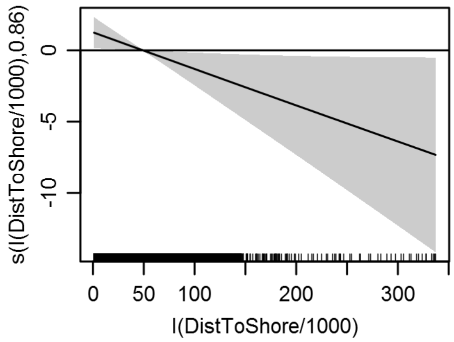

Diagnostic plots

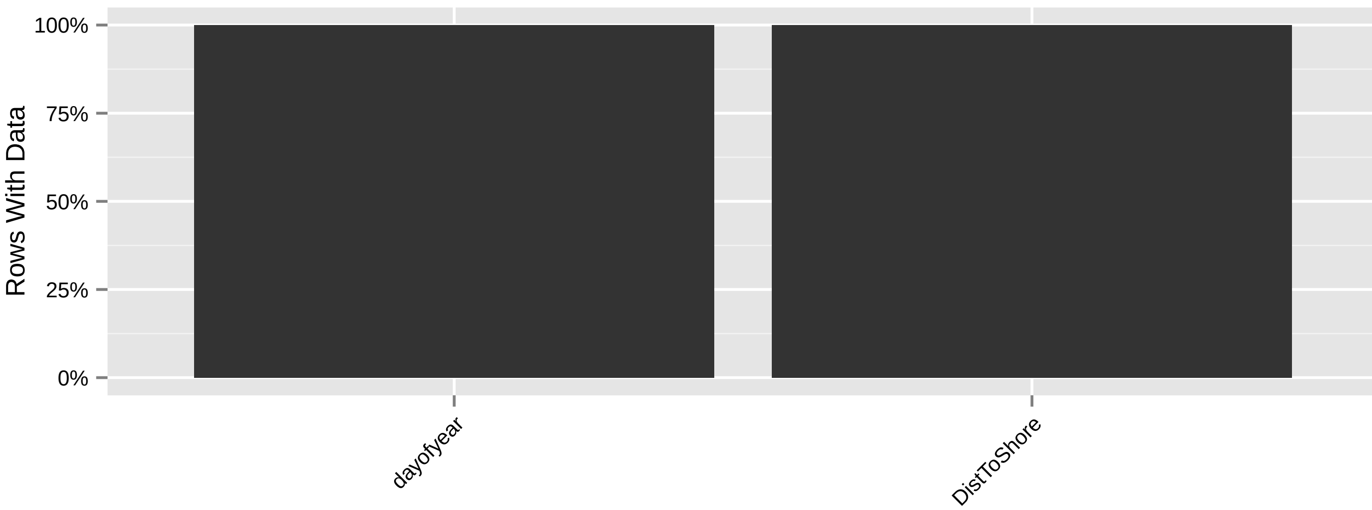

Figure 89: Segments with predictor values for the North Atlantic right whale Climatological model, Spring season, Calving and Migration Area. This plot is used to assess how many segments would be lost by including a given predictor in a model.

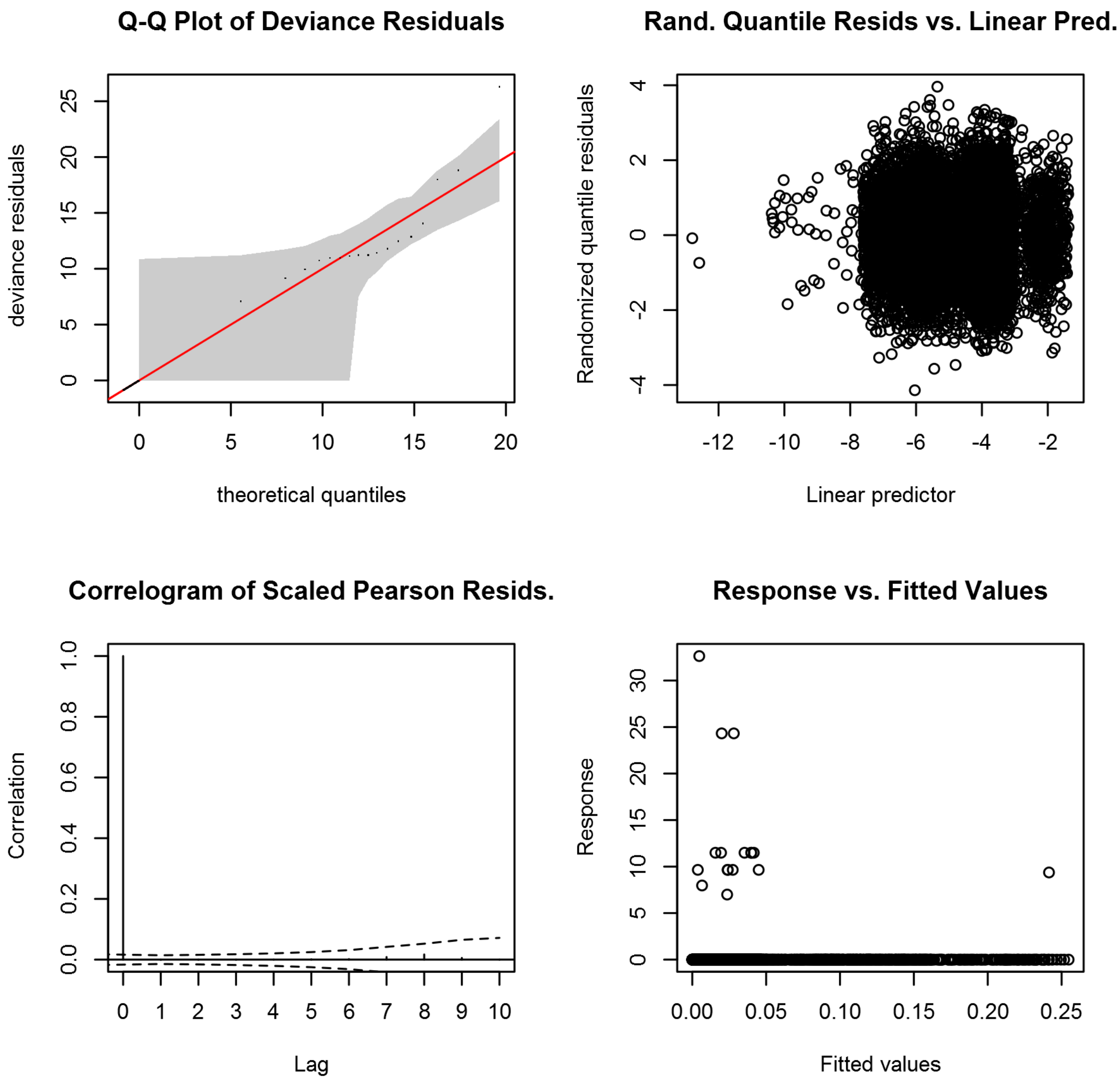

Figure 90: Statistical diagnostic plots for the North Atlantic right whale Climatological model, Spring season, Calving and Migration Area.

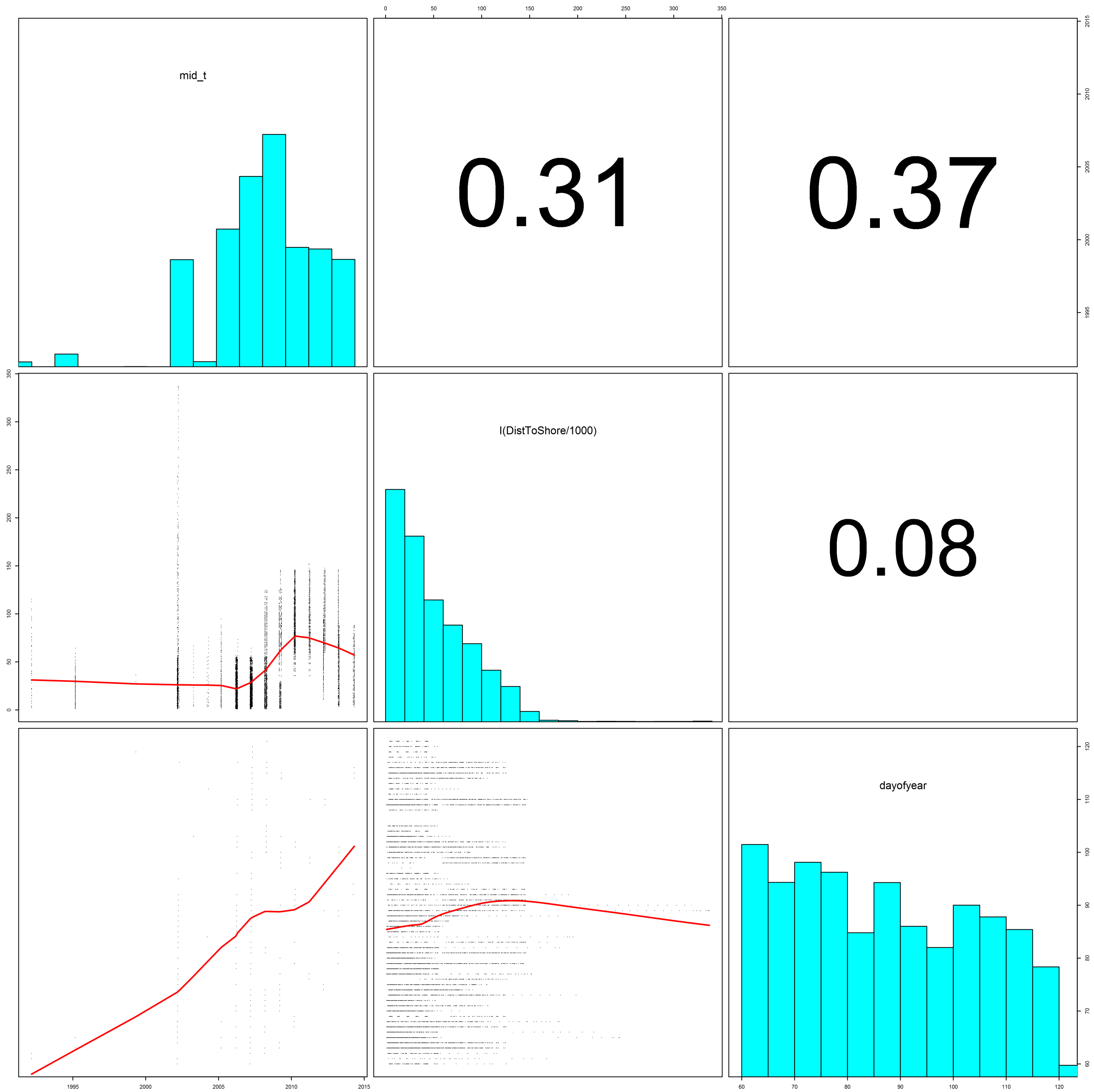

Figure 91: Scatterplot matrix for the North Atlantic right whale Climatological model, Spring season, Calving and Migration Area. This plot is used to inspect the distribution of predictors (via histograms along the diagonal), simple correlation between predictors (via pairwise Pearson coefficients above the diagonal), and linearity of predictor correlations (via scatterplots below the diagonal). This plot is best viewed at high magnification.

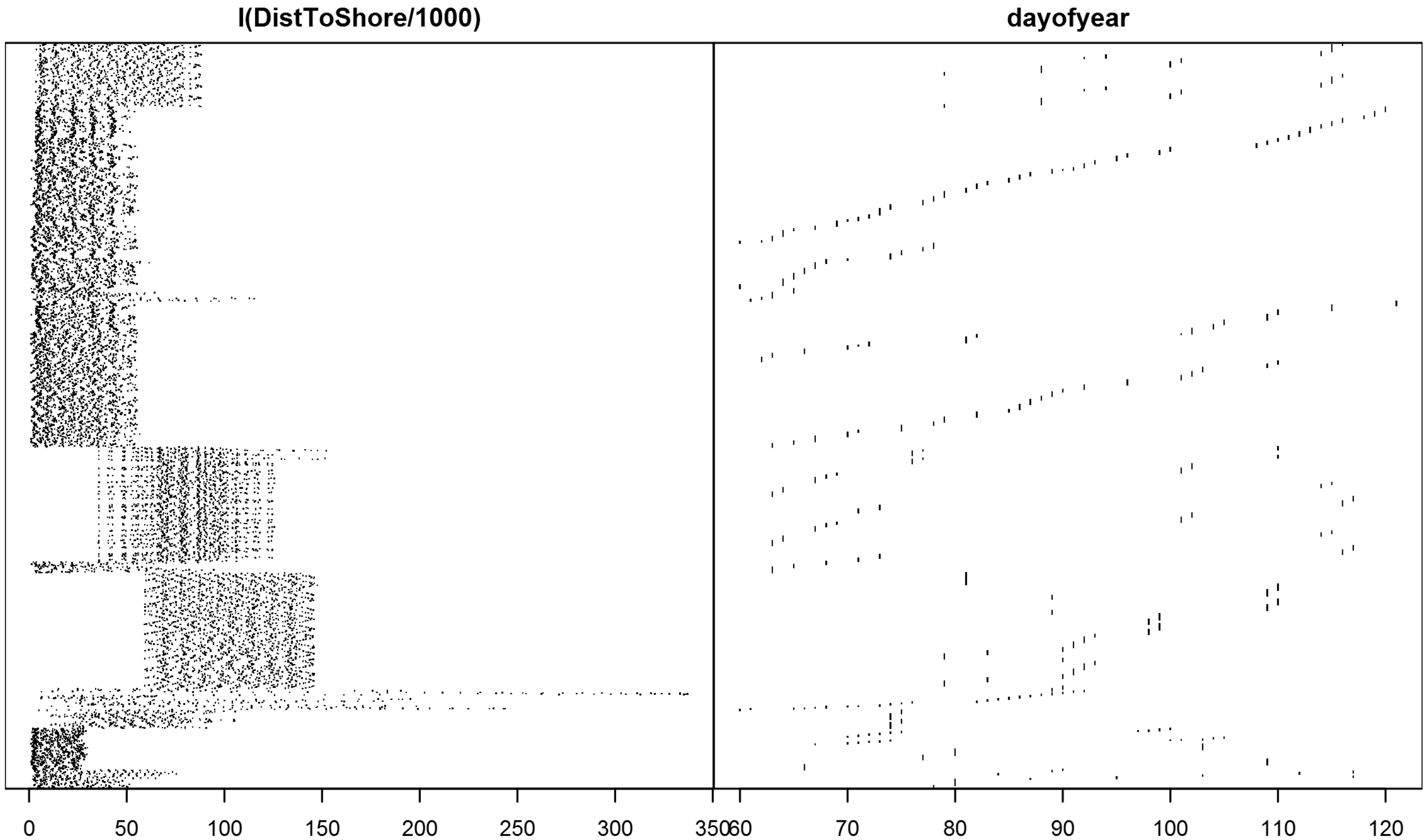

Figure 92: Dotplot for the North Atlantic right whale Climatological model, Spring season, Calving and Migration Area. This plot is used to check for suspicious patterns and outliers in the data. Points are ordered vertically by transect ID, sequentially in time.

Unsurveyed Area

Density was not modeled for this region.

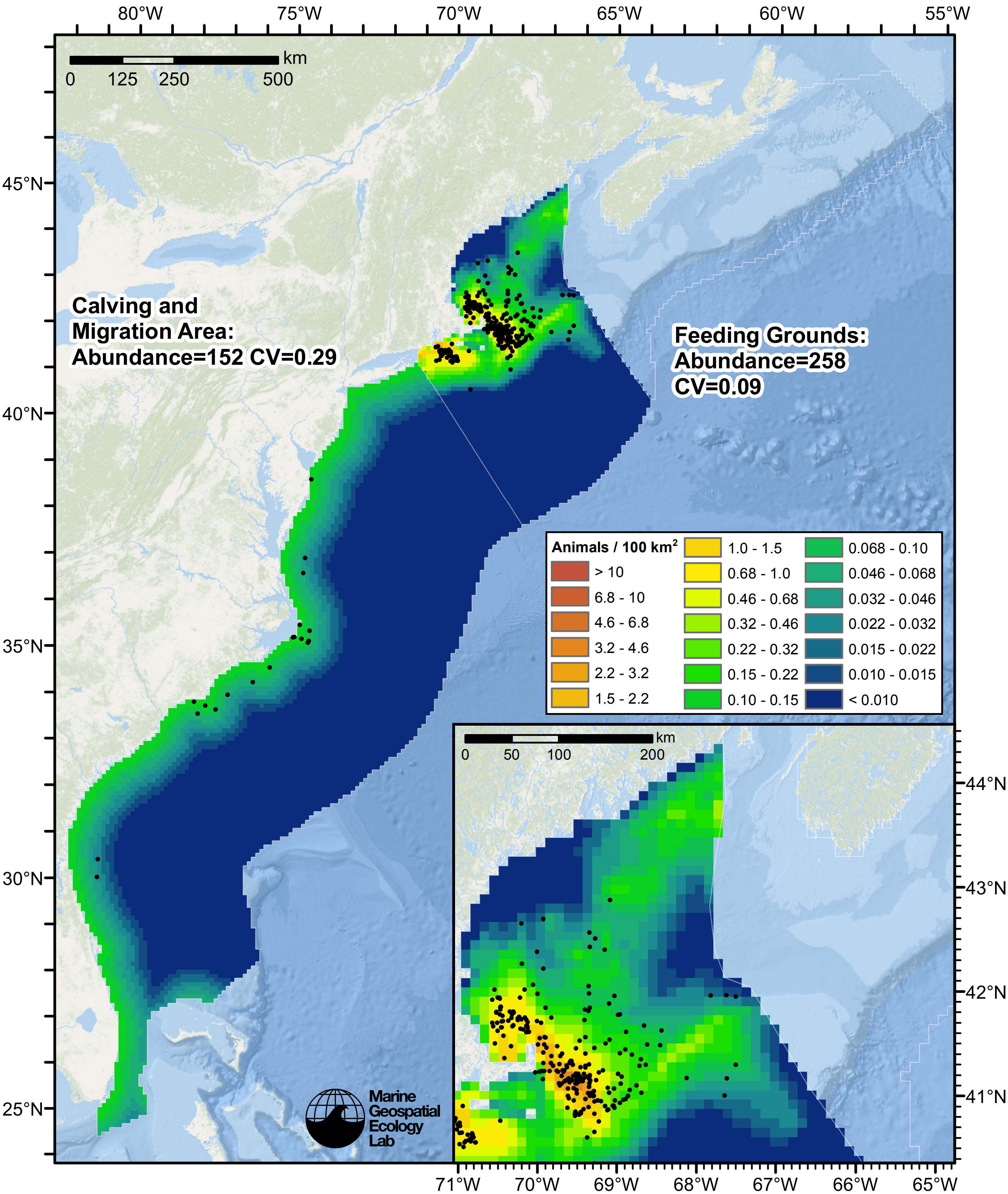

Figure 93: North Atlantic right whale density predicted by the Spring season contemporaneous model that explained the most deviance. Pixels are 10x10 km. The legend gives the estimated individuals per pixel; breaks are logarithmic. The same scale is used for all seasons. Abundance for each region was computed by summing the density cells occuring in that region.

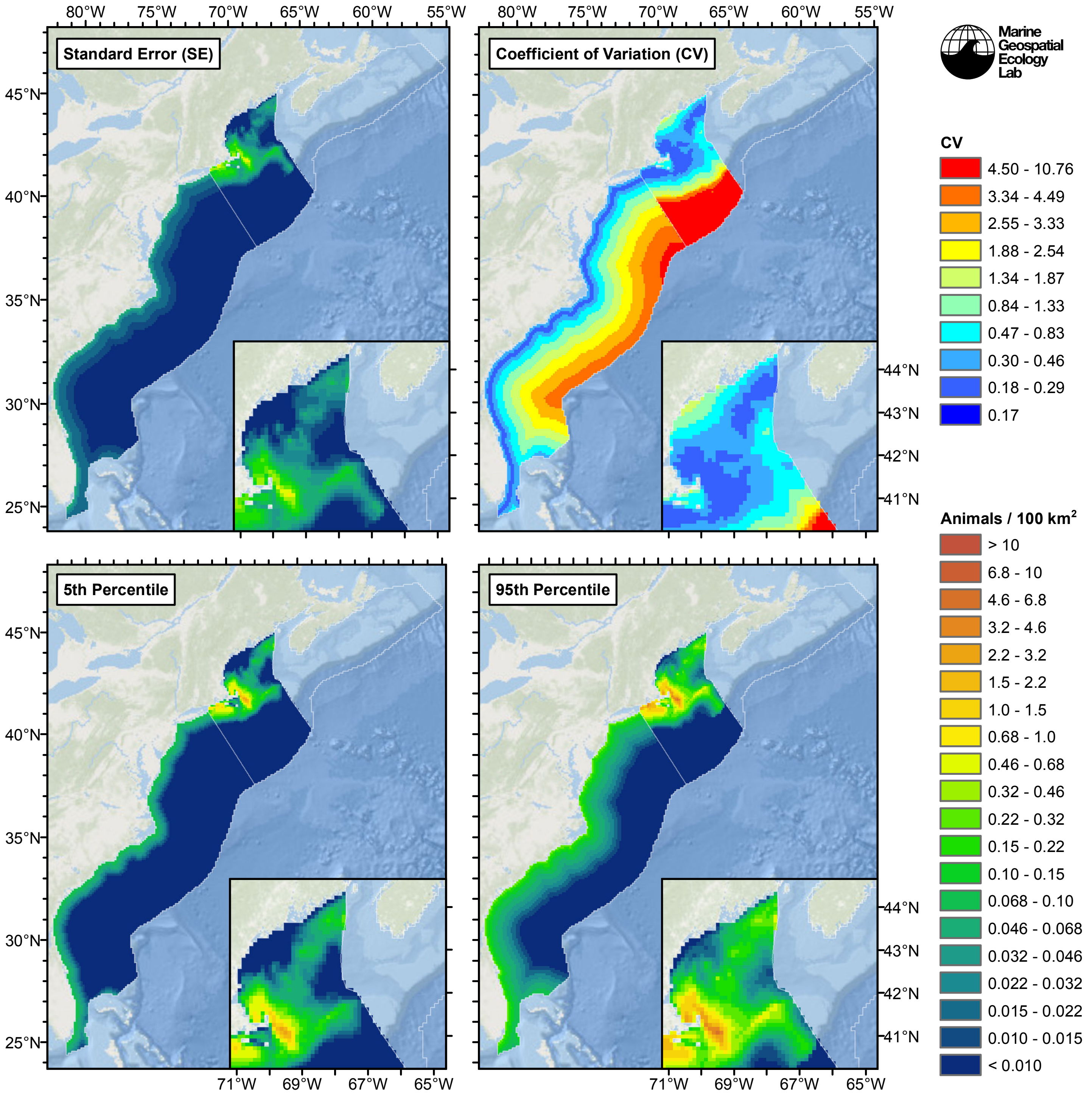

Figure 94: Estimated uncertainty for the Spring season contemporaneous model that explained the most deviance. These estimates only incorporate the statistical uncertainty estimated for the spatial model (by the R mgcv package). They do not incorporate uncertainty in the detection functions, g(0) estimates, predictor variables, and so on.

Feeding Grounds

Statistical output

```
Rscript.exe: This is mgcv 1.8-2. For overview type 'help("mgcv-package")'.


Family: Tweedie(p=1.278)
```

```
Link function: log

Formula:
abundance ~ offset(log(area_km2)) + s(log10(Depth), bs = "ts",
    k = 5) + s(I(DistToShore/1000), bs = "ts", k = 5) + s(I(DistTo125m/1000),
    bs = "ts", k = 5) + s(I(DistTo300m/1000), bs = "ts", k = 5) +
    s(SST, bs = "ts", k = 5) + s(log10(pmax(TKE, 1e-04)), bs = "ts",
    k = 5) + s(log10(pmax(EpiMnkPB, 0.001)), bs = "ts", k = 5)

Parametric coefficients:
            Estimate Std. Error t value Pr(>|t|)
(Intercept)  -7.0530     0.1556  -45.31   <2e-16 ***
---
Signif. codes:  0 '***' 0.001 '**' 0.01 '*' 0.05 '.' 0.1 ' ' 1

Approximate significance of smooth terms:
                                   edf Ref.df      F  p-value
s(log10(Depth))                 2.7120      4  7.623 1.99e-08 ***
s(I(DistToShore/1000))          3.2783      4  9.225 6.03e-09 ***
s(I(DistTo125m/1000))           2.8372      4  4.165 0.000119 ***
s(I(DistTo300m/1000))           3.3429      4 20.939  < 2e-16 ***
s(SST)                          1.0144      4  7.780 1.22e-08 ***
s(log10(pmax(TKE, 1e-04)))      0.8839      4  1.541 0.007390 **
s(log10(pmax(EpiMnkPB, 0.001))) 1.0882      4  8.773 1.27e-09 ***
---
Signif. codes:  0 '***' 0.001 '**' 0.01 '*' 0.05 '.' 0.1 ' ' 1

R-sq.(adj) =  0.0438   Deviance explained = 29.7%
-REML = 1790.4  Scale est. = 28.158    n = 9594

All predictors were significant. This is the final model.
Creating term plots.
Diagnostic output from gam.check():

Method: REML   Optimizer: outer newton
full convergence after 15 iterations.
Gradient range [-0.0001204382,3.786767e-05]
(score 1790.419 & scale 28.1579).
Hessian positive definite, eigenvalue range [0.3613505,848.172].
Model rank =  29 / 29

Basis dimension (k) checking results. Low p-value (k-index<1) may
indicate that k is too low, especially if edf is close to k'.

                                   k'   edf k-index p-value
s(log10(Depth))                 4.000 2.712   0.798    0.09
s(I(DistToShore/1000))          4.000 3.278   0.810    0.26
s(I(DistTo125m/1000))           4.000 2.837   0.806    0.19
s(I(DistTo300m/1000))           4.000 3.343   0.811    0.30
s(SST)                          4.000 1.014   0.823    0.70
s(log10(pmax(TKE, 1e-04)))      4.000 0.884   0.803    0.11
s(log10(pmax(EpiMnkPB, 0.001))) 4.000 1.088   0.814    0.44

Predictors retained during the model selection procedure: Depth, DistToShore, DistTo125m,
DistTo300m, SST, TKE, EpiMnkPB

Predictors dropped during the model selection procedure: Slope, DistToFront1
```

Model term plots

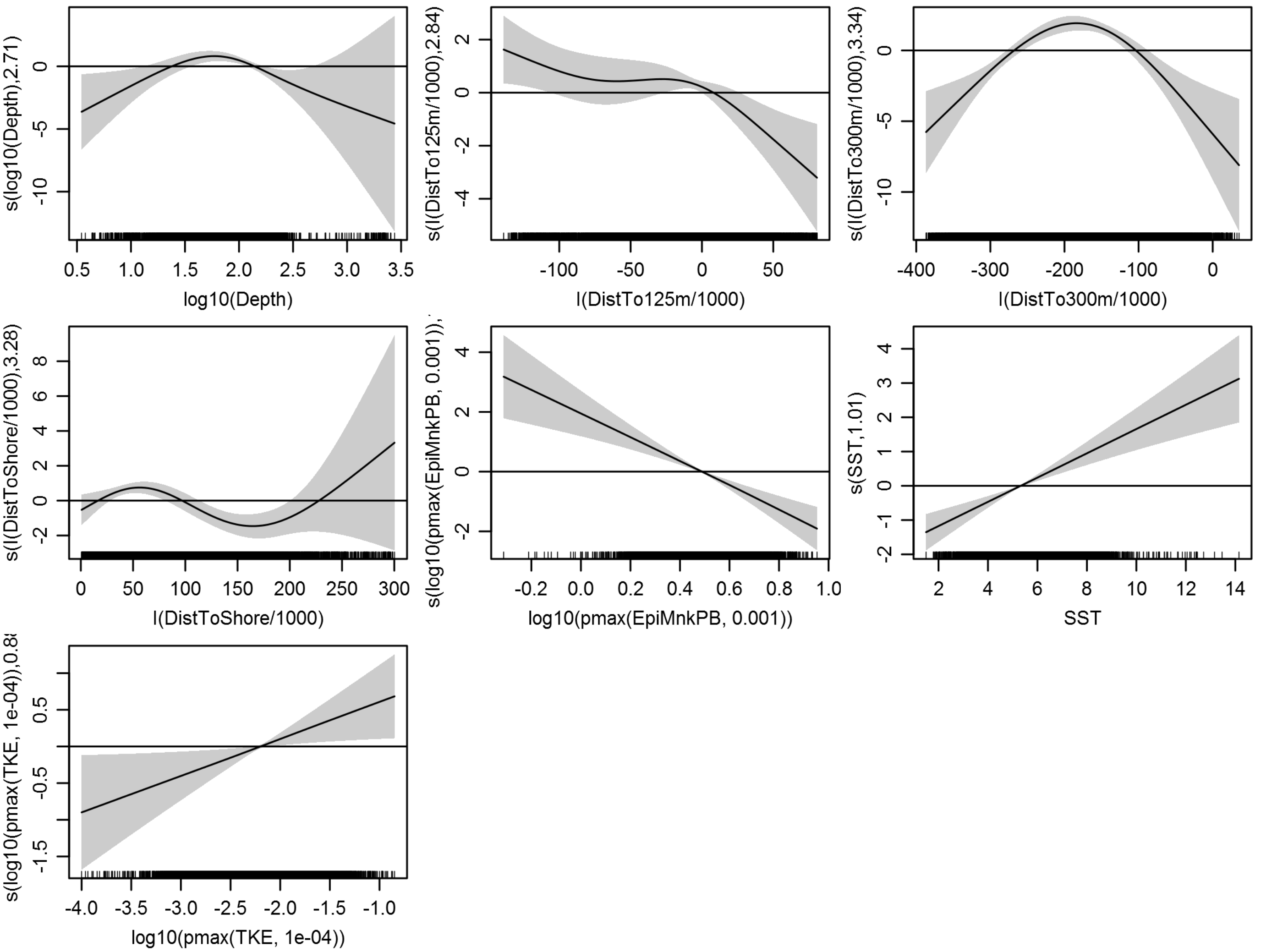

Diagnostic plots

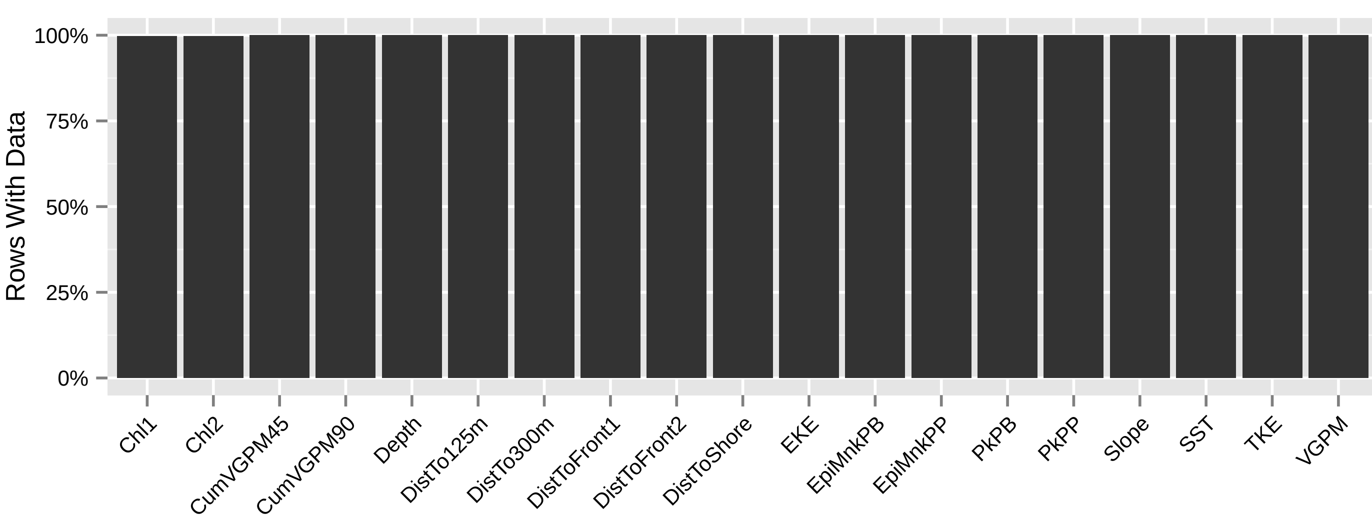

Figure 95: Segments with predictor values for the North Atlantic right whale Contemporaneous model, Spring season, Feeding Grounds. This plot is used to assess how many segments would be lost by including a given predictor in a model.

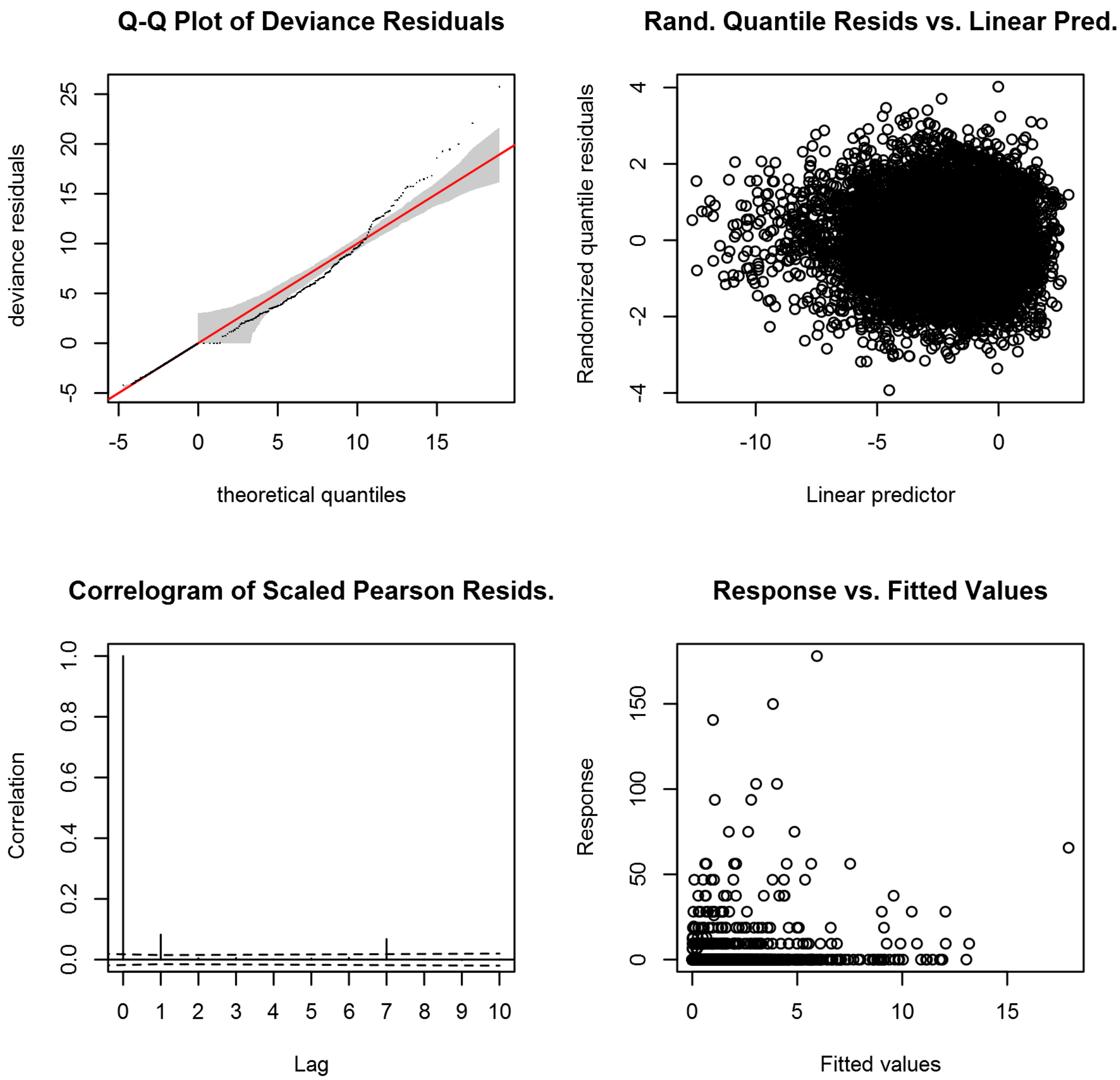

Figure 96: Statistical diagnostic plots for the North Atlantic right whale Contemporaneous model, Spring season, Feeding Grounds.

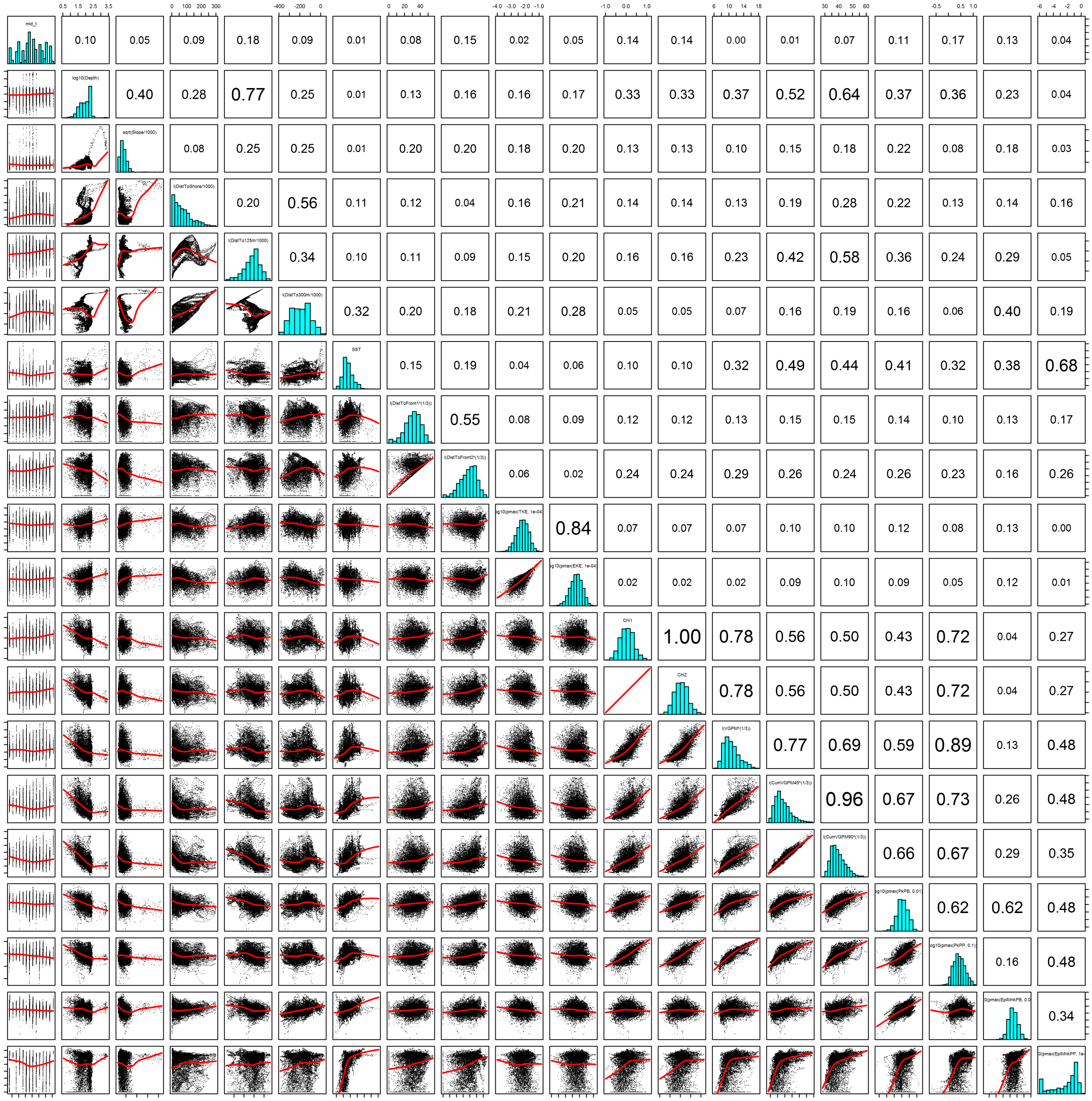

Figure 97: Scatterplot matrix for the North Atlantic right whale Contemporaneous model, Spring season, Feeding Grounds. This plot is used to inspect the distribution of predictors (via histograms along the diagonal), simple correlation between predictors (via pairwise Pearson coefficients above the diagonal), and linearity of predictor correlations (via scatterplots below the diagonal). This plot is best viewed at high magnification.

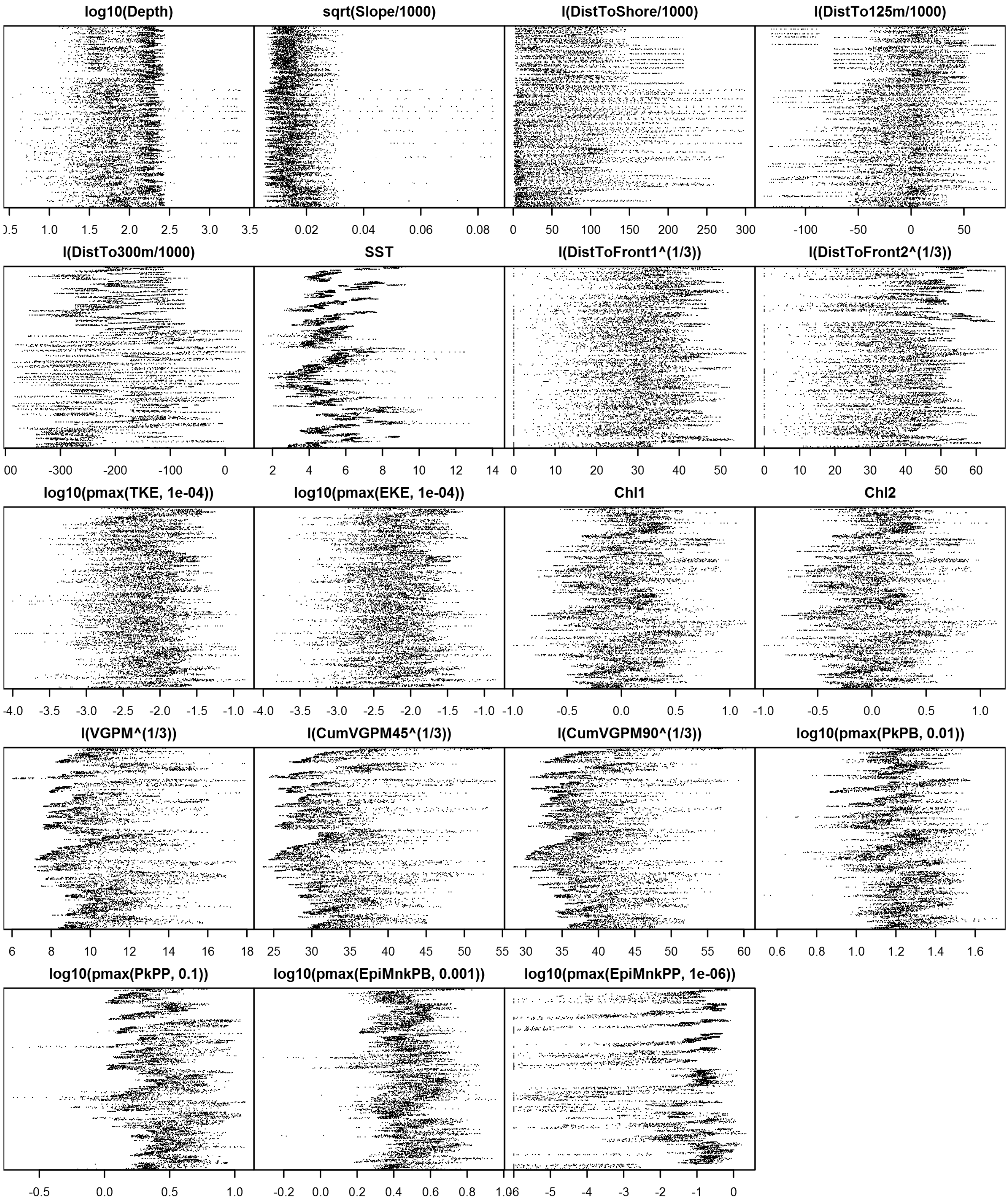

Figure 98: Dotplot for the North Atlantic right whale Contemporaneous model, Spring season, Feeding Grounds. This plot is used to check for suspicious patterns and outliers in the data. Points are ordered vertically by transect ID, sequentially in time.

Calving and Migration Area

Statistical output

```
Rscript.exe: This is mgcv 1.8-2. For overview type 'help("mgcv-package")'.


Family: Tweedie(p=1.166)
Link function: log

Formula:
abundance ~ offset(log(area_km2)) + s(I(DistToShore/1000), bs = "ts",
    k = 4)

Parametric coefficients:
            Estimate Std. Error t value Pr(>|t|)
(Intercept)   -7.769      0.395  -19.66   <2e-16 ***
---
Signif. codes:  0 '***' 0.001 '**' 0.01 '*' 0.05 '.' 0.1 ' ' 1

Approximate significance of smooth terms:
                         edf Ref.df     F p-value
s(I(DistToShore/1000)) 0.863      3 1.735  0.0138 *
---
Signif. codes:  0 '***' 0.001 '**' 0.01 '*' 0.05 '.' 0.1 ' ' 1

R-sq.(adj) =  -0.00169   Deviance explained = -0.467%
-REML = 182.47  Scale est. = 30.603    n = 11605

All predictors were significant. This is the final model.
Creating term plots.
Diagnostic output from gam.check():

Method: REML   Optimizer: outer newton
full convergence after 11 iterations.
Gradient range [-0.0001816491,9.158778e-05]
(score 182.4662 & scale 30.60286).
Hessian positive definite, eigenvalue range [0.3445347,150.5255].
Model rank =  4 / 4

Basis dimension (k) checking results. Low p-value (k-index<1) may
indicate that k is too low, especially if edf is close to k'.

                          k'   edf k-index p-value
s(I(DistToShore/1000)) 3.000 0.863   0.807    0.04

Predictors retained during the model selection procedure: DistToShore

Predictors dropped during the model selection procedure: dayofyear
```

Model term plots

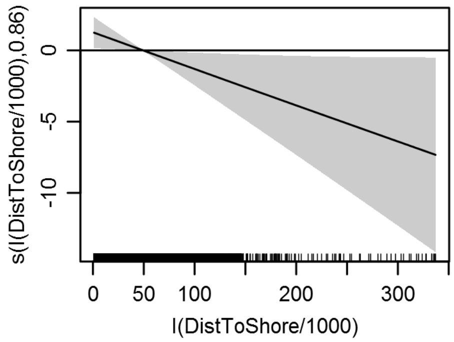

Diagnostic plots

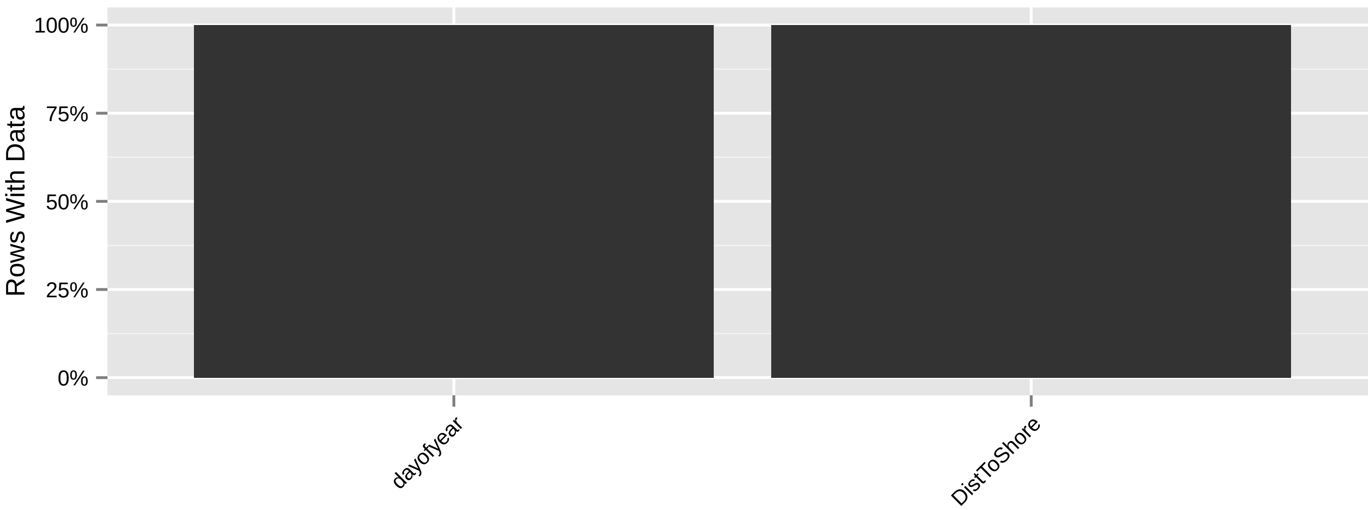

Figure 99: Segments with predictor values for the North Atlantic right whale Contemporaneous model, Spring season, Calving and Migration Area. This plot is used to assess how many segments would be lost by including a given predictor in a model.

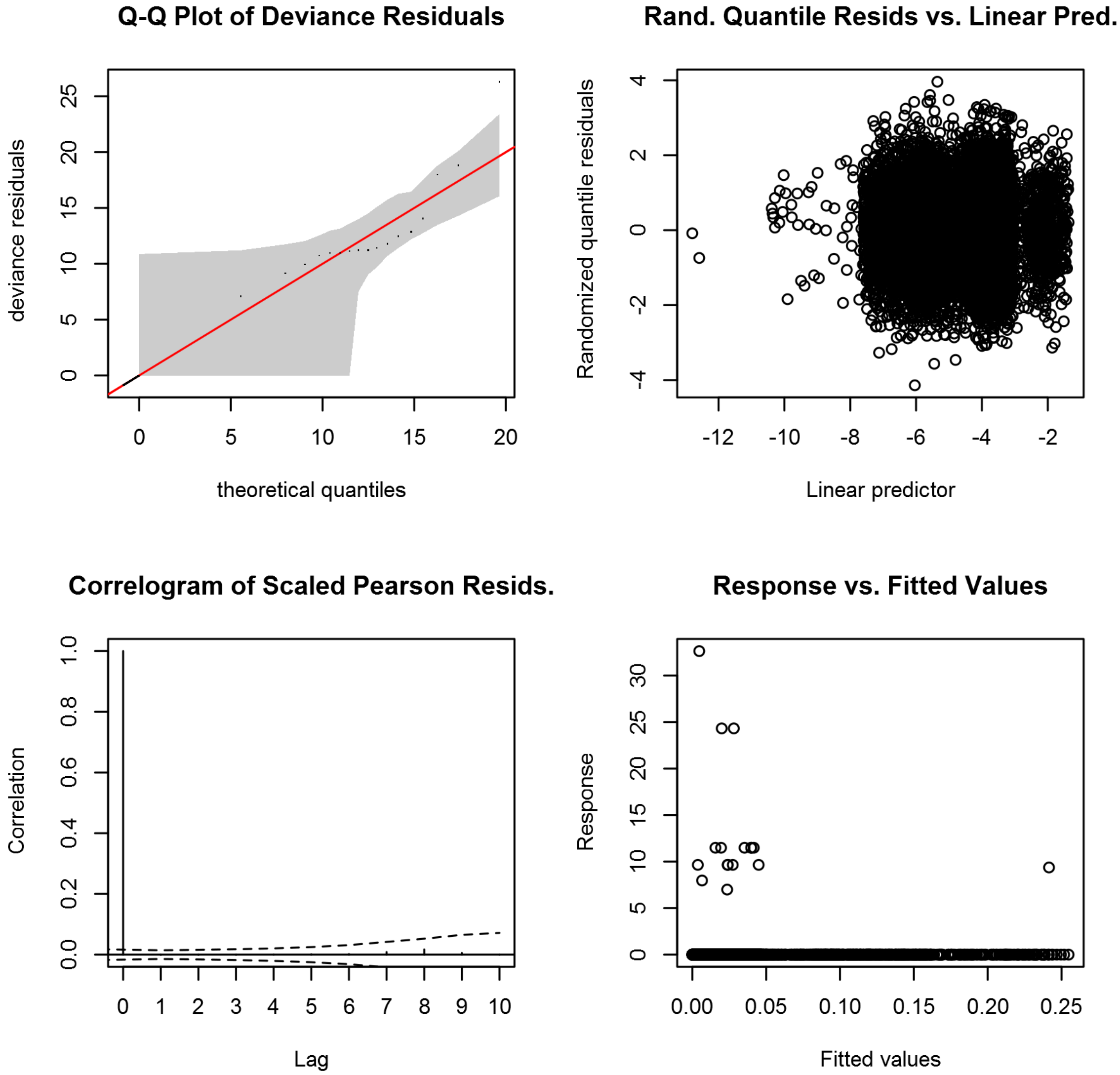

Figure 100: Statistical diagnostic plots for the North Atlantic right whale Contemporaneous model, Spring season, Calving and Migration Area.

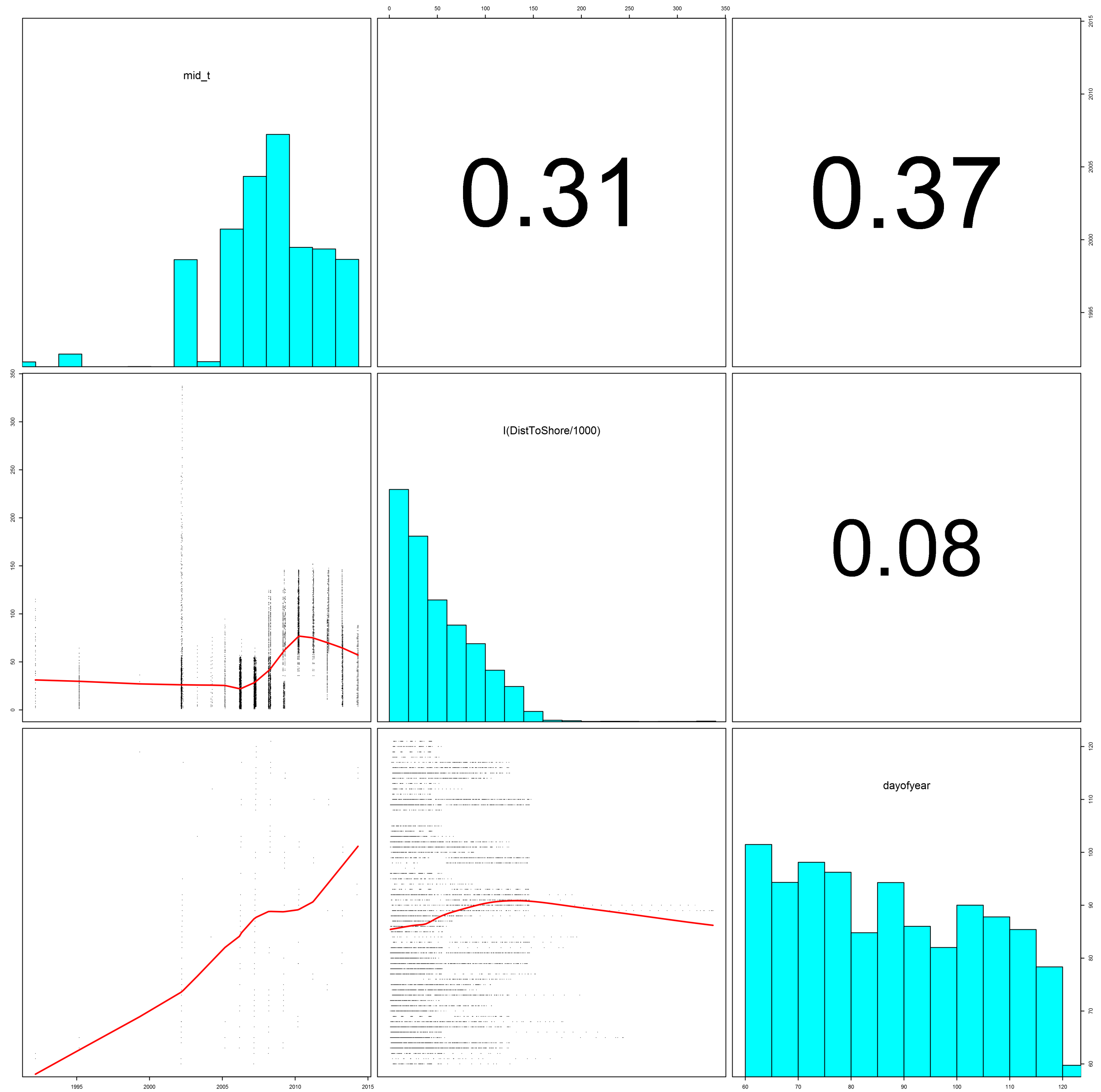

Figure 101: Scatterplot matrix for the North Atlantic right whale Contemporaneous model, Spring season, Calving and Migration Area. This plot is used to inspect the distribution of predictors (via histograms along the diagonal), simple correlation between predictors (via pairwise Pearson coefficients above the diagonal), and linearity of predictor correlations (via scatterplots below the diagonal). This plot is best viewed at high magnification.

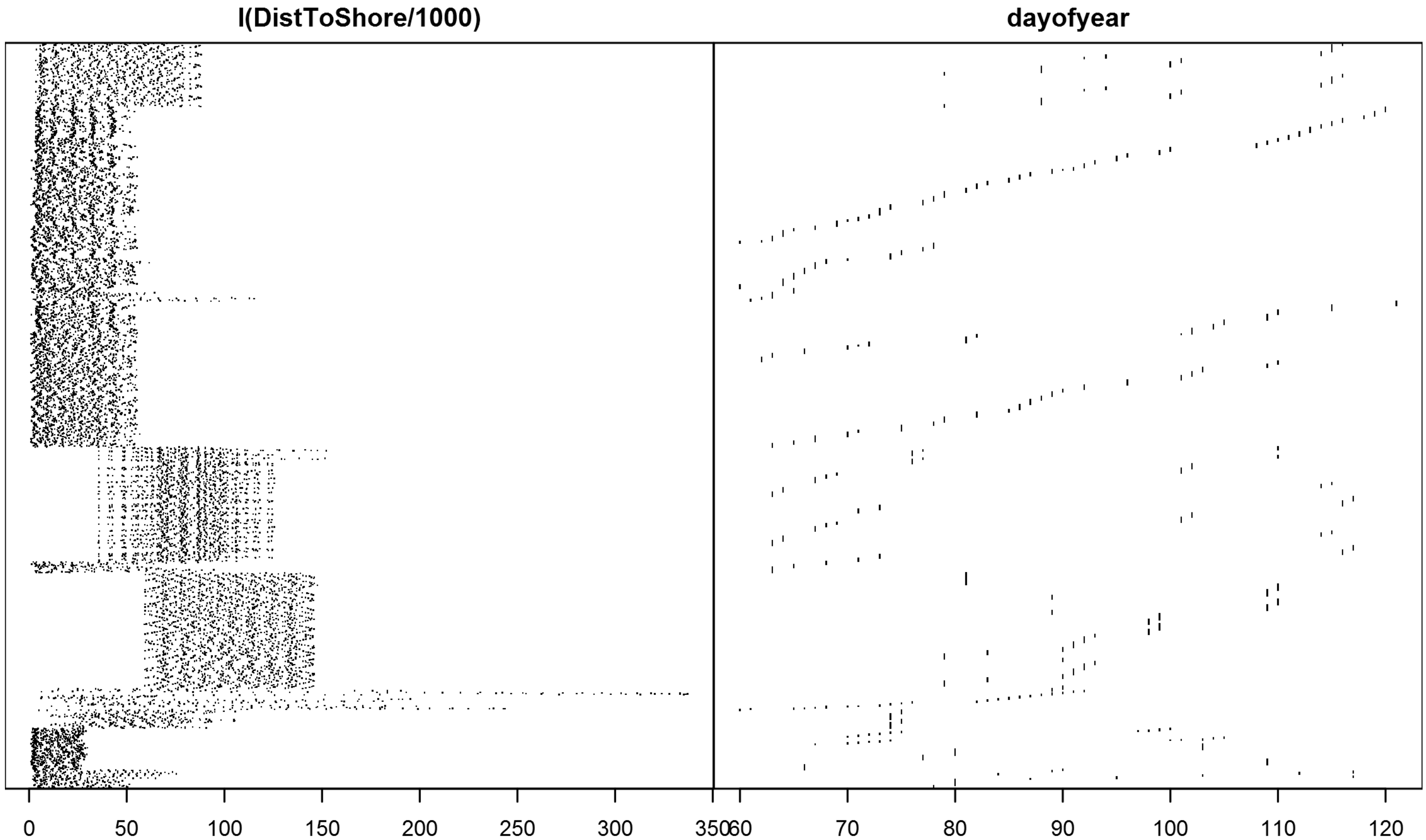

Figure 102: Dotplot for the North Atlantic right whale Contemporaneous model, Spring season, Calving and Migration Area. This plot is used to check for suspicious patterns and outliers in the data. Points are ordered vertically by transect ID, sequentially in time.

Unsurveyed Area

Density was not modeled for this region.

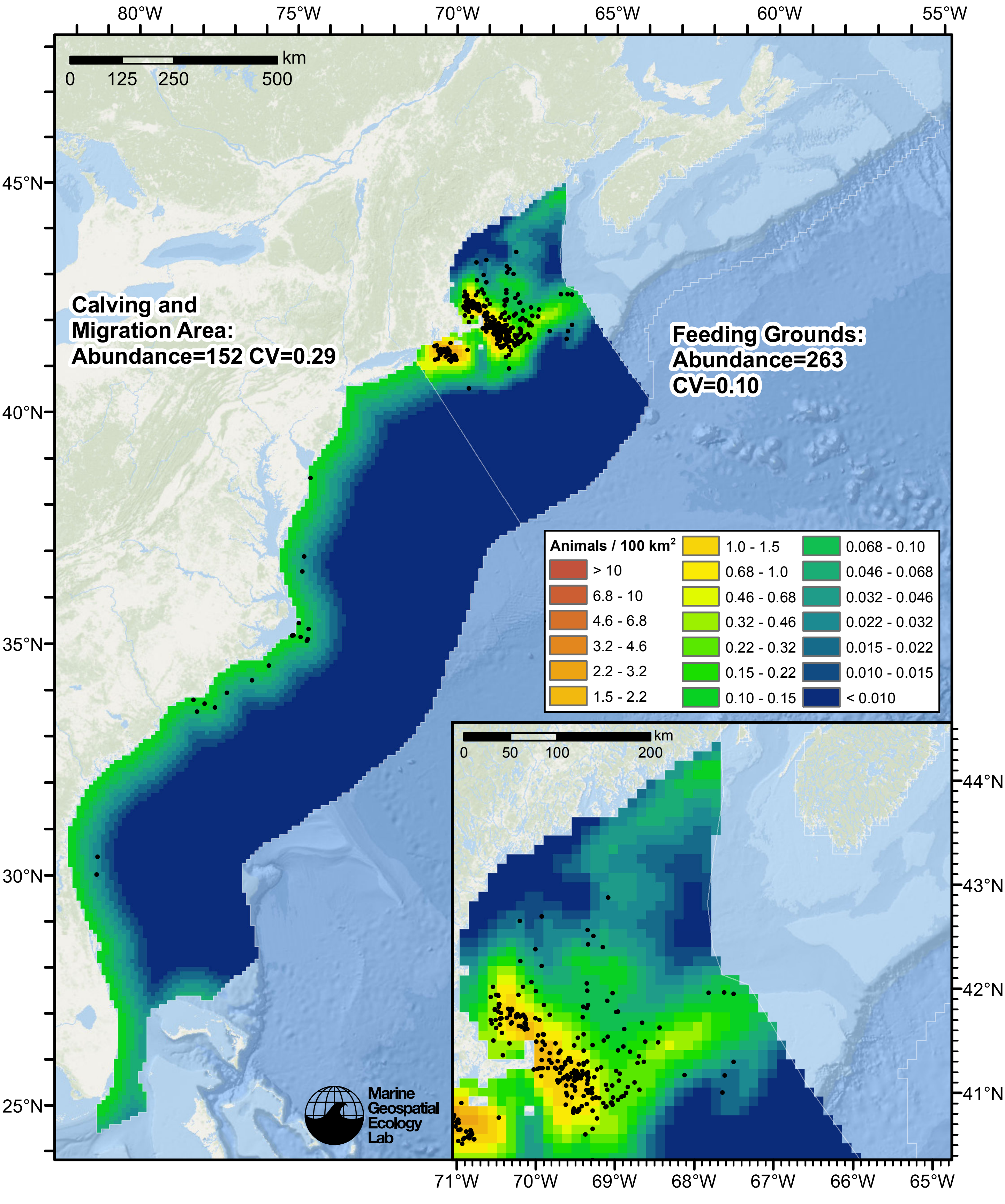

Figure 103: North Atlantic right whale density predicted by the Spring season climatological same segments model that explained the most deviance. Pixels are 10x10 km. The legend gives the estimated individuals per pixel; breaks are logarithmic. The same scale is used for all seasons. Abundance for each region was computed by summing the density cells occuring in that region.

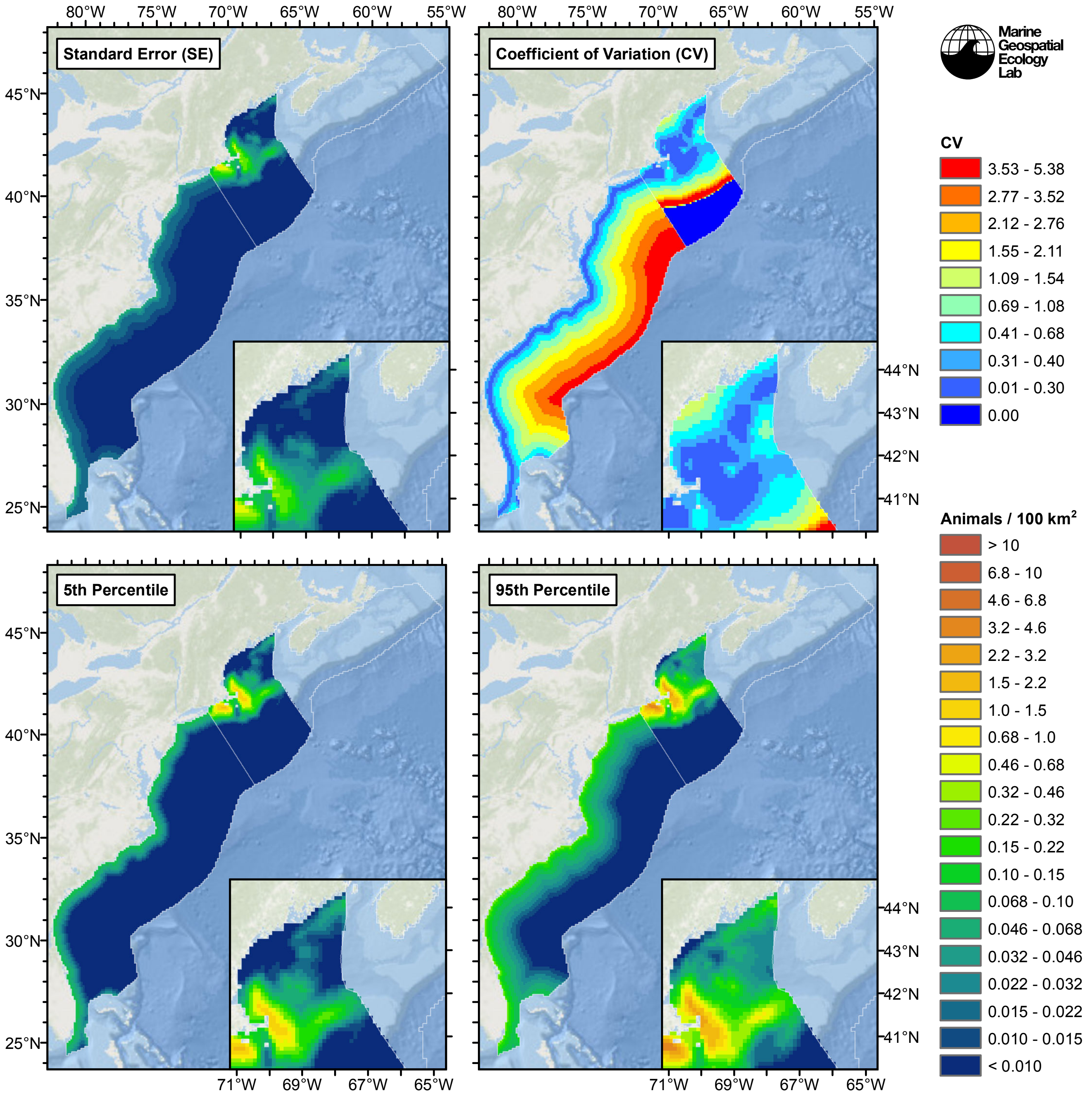

Figure 104: Estimated uncertainty for the Spring season climatological same segments model that explained the most deviance. These estimates only incorporate the statistical uncertainty estimated for the spatial model (by the R mgcv package). They do not incorporate uncertainty in the detection functions, g(0) estimates, predictor variables, and so on.

Feeding Grounds

Statistical output

```
Rscript.exe: This is mgcv 1.8-2. For overview type 'help("mgcv-package")'.


Family: Tweedie(p=1.259)
```

```
Link function: log

Formula:
abundance ~ offset(log(area_km2)) + s(I(DistToShore/1000), bs = "ts",
    k = 5) + s(I(DistTo125m/1000), bs = "ts", k = 5) + s(I(DistTo300m/1000),
    bs = "ts", k = 5) + s(ClimSST, bs = "ts", k = 5) + s(I(ClimDistToFront1^(1/3)),
    bs = "ts", k = 5) + s(I(ClimCumVGPM90^(1/3)), bs = "ts",
    k = 5)

Parametric coefficients:
            Estimate Std. Error t value Pr(>|t|)
(Intercept)  -7.1467     0.1511  -47.29   <2e-16 ***
---
Signif. codes:  0 '***' 0.001 '**' 0.01 '*' 0.05 '.' 0.1 ' ' 1

Approximate significance of smooth terms:
                                edf Ref.df      F  p-value
s(I(DistToShore/1000))       0.9566      4  2.744 0.000471 ***
s(I(DistTo125m/1000))        3.0835      4 10.776 4.93e-11 ***
s(I(DistTo300m/1000))        3.3955      4 17.410  < 2e-16 ***
s(ClimSST)                   3.3731      4 10.289 4.35e-10 ***
s(I(ClimDistToFront1^(1/3))) 3.7282      4 12.878 1.42e-11 ***
s(I(ClimCumVGPM90^(1/3)))    3.2589      4 12.309 1.75e-12 ***
---
Signif. codes:  0 '***' 0.001 '**' 0.01 '*' 0.05 '.' 0.1 ' ' 1

R-sq.(adj) =  0.0694   Deviance explained = 32.3%
-REML = 1779.4  Scale est. = 26.51     n = 9594

All predictors were significant. This is the final model.
Creating term plots.
Diagnostic output from gam.check():

Method: REML   Optimizer: outer newton
full convergence after 13 iterations.
Gradient range [-2.313396e-05,1.696662e-06]
(score 1779.441 & scale 26.51034).
Hessian positive definite, eigenvalue range [0.3783521,883.8013].
Model rank =  25 / 25

Basis dimension (k) checking results. Low p-value (k-index<1) may
indicate that k is too low, especially if edf is close to k'.

                                k'   edf k-index p-value
s(I(DistToShore/1000))       4.000 0.957   0.752    0.04
s(I(DistTo125m/1000))        4.000 3.083   0.772    0.32
s(I(DistTo300m/1000))        4.000 3.395   0.764    0.14
s(ClimSST)                   4.000 3.373   0.766    0.20
s(I(ClimDistToFront1^(1/3))) 4.000 3.728   0.760    0.12
s(I(ClimCumVGPM90^(1/3)))    4.000 3.259   0.777    0.52

Predictors retained during the model selection procedure: DistToShore, DistTo125m, DistTo300m,
ClimSST, ClimDistToFront1, ClimCumVGPM90

Predictors dropped during the model selection procedure: Depth, ClimTKE, Slope
```

Model term plots

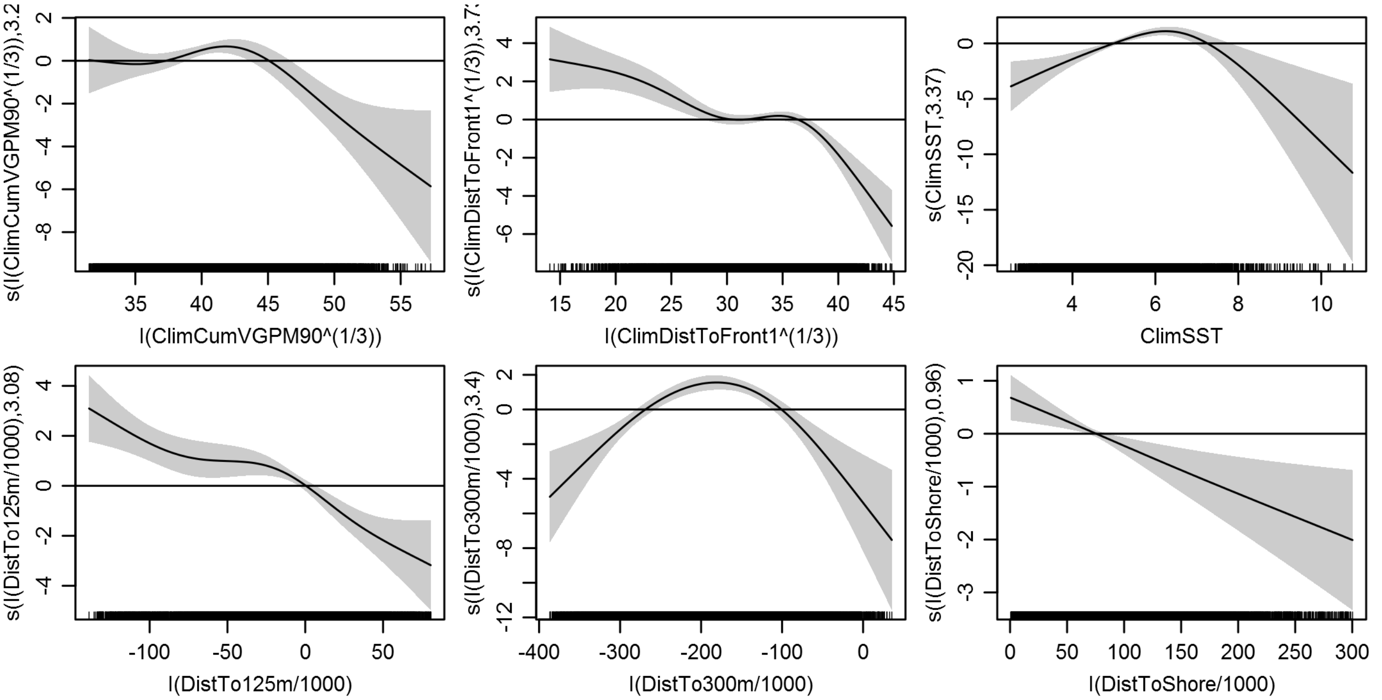

Diagnostic plots

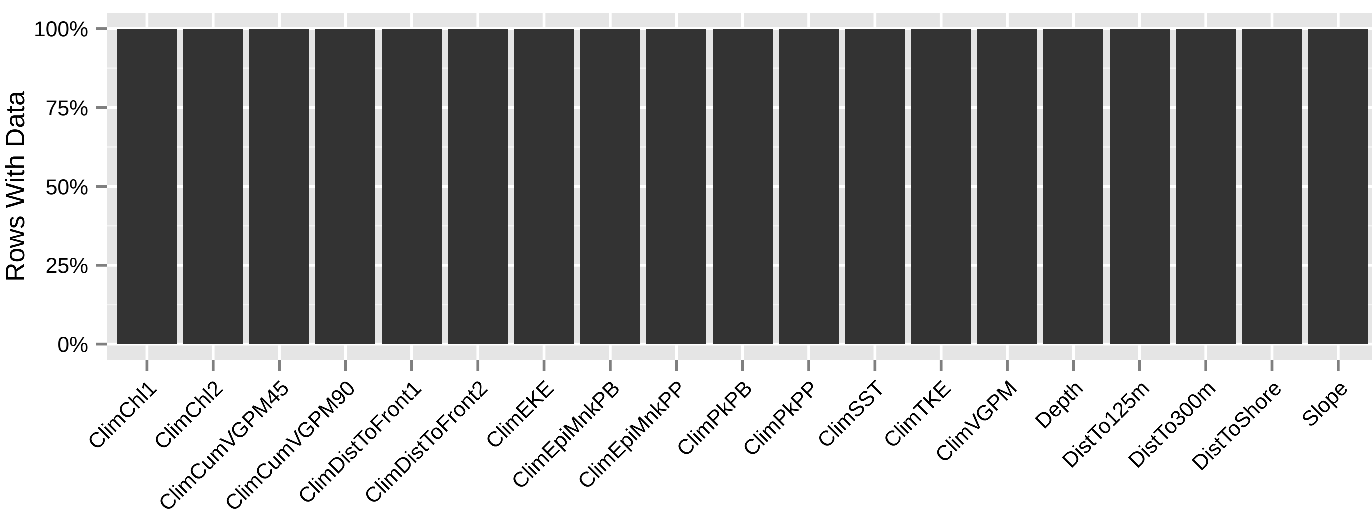

Figure 105: Segments with predictor values for the North Atlantic right whale Climatological model, Spring season, Feeding Grounds. This plot is used to assess how many segments would be lost by including a given predictor in a model.

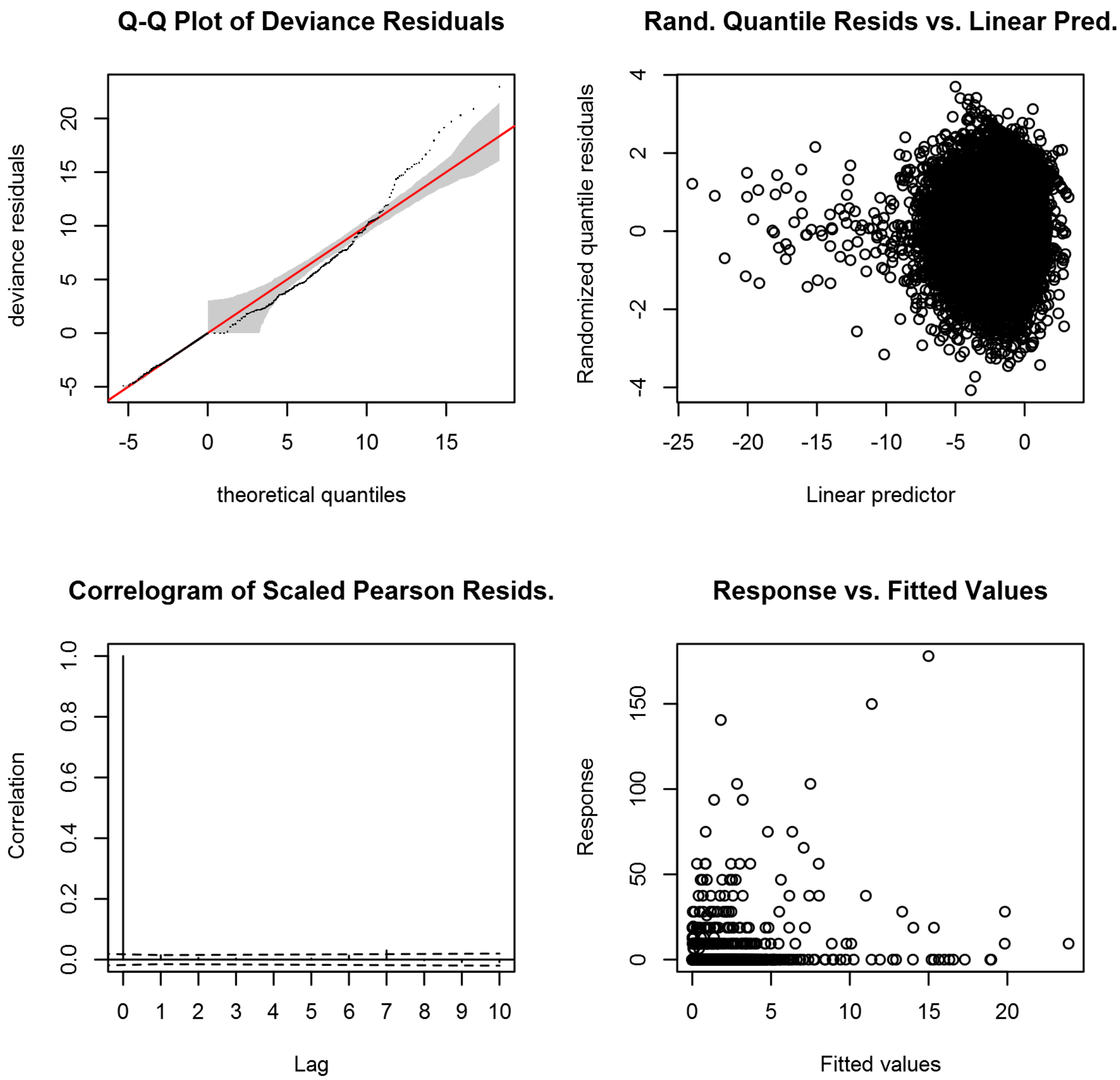

Figure 106: Statistical diagnostic plots for the North Atlantic right whale Climatological model, Spring season, Feeding Grounds.

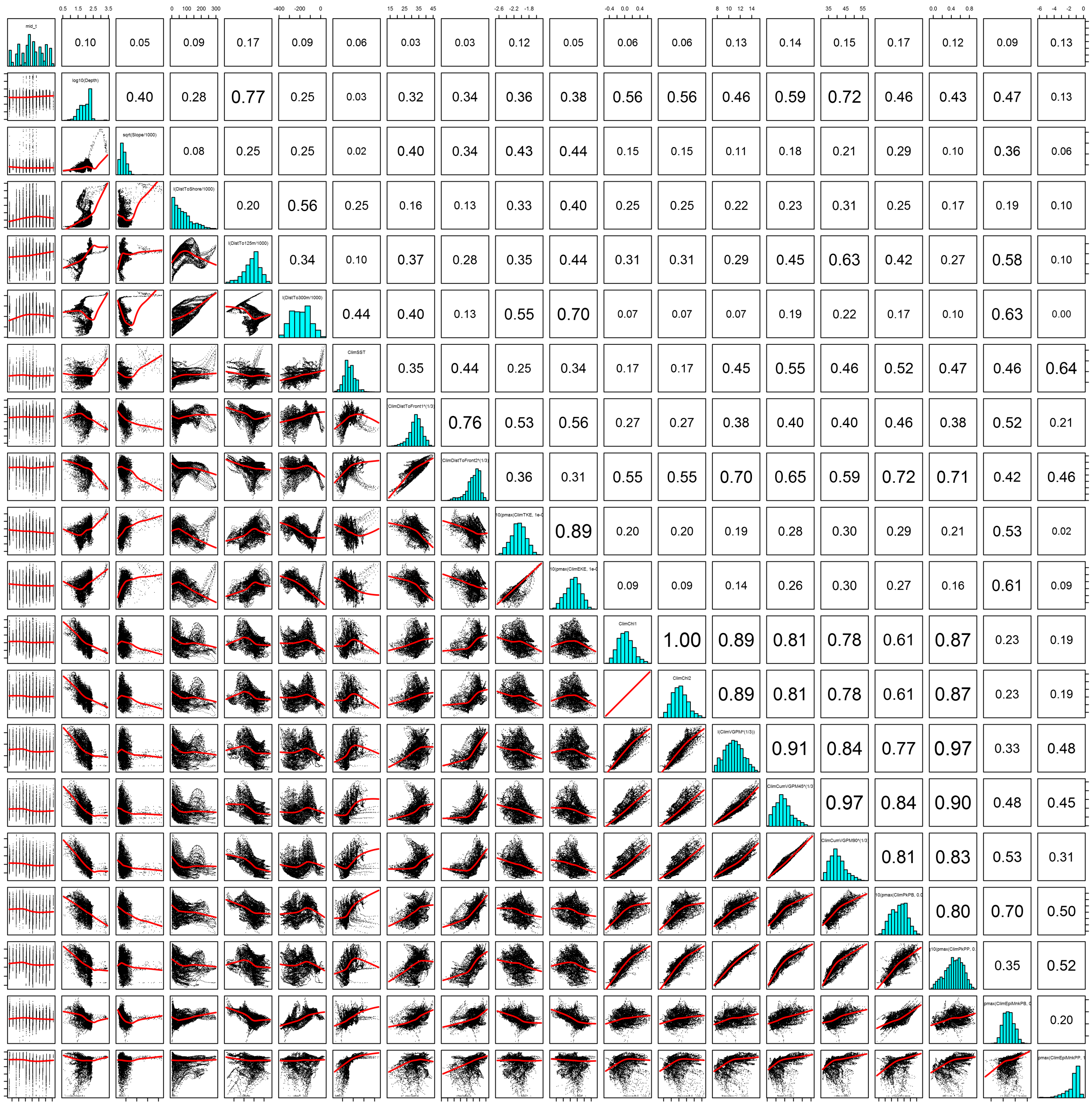

Figure 107: Scatterplot matrix for the North Atlantic right whale Climatological model, Spring season, Feeding Grounds. This plot is used to inspect the distribution of predictors (via histograms along the diagonal), simple correlation between predictors (via pairwise Pearson coefficients above the diagonal), and linearity of predictor correlations (via scatterplots below the diagonal). This plot is best viewed at high magnification.

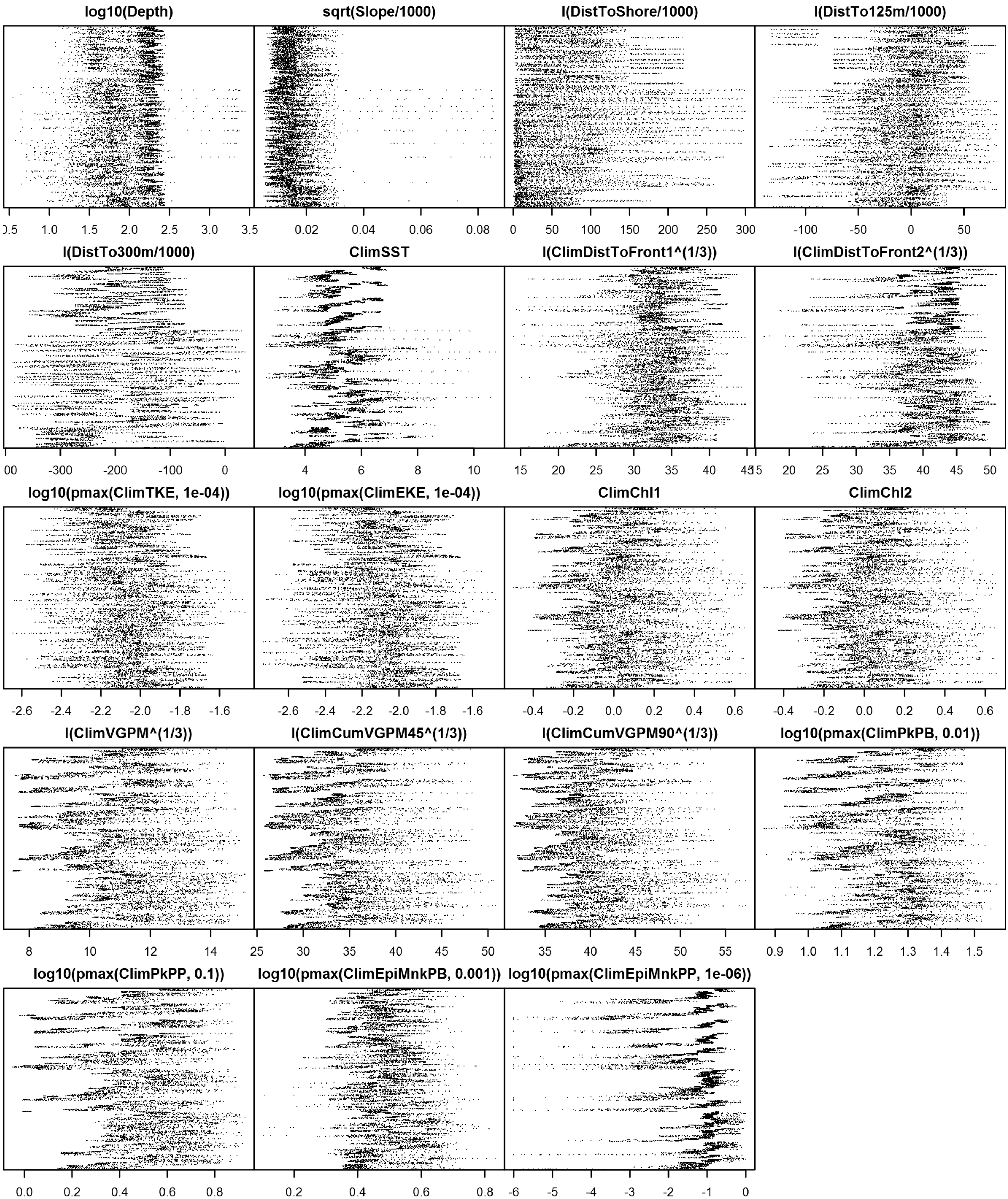

Figure 108: Dotplot for the North Atlantic right whale Climatological model, Spring season, Feeding Grounds. This plot is used to check for suspicious patterns and outliers in the data. Points are ordered vertically by transect ID, sequentially in time.

Calving and Migration Area

Statistical output

```
Rscript.exe: This is mgcv 1.8-2. For overview type 'help("mgcv-package")'.


Family: Tweedie(p=1.166)
Link function: log

Formula:
abundance ~ offset(log(area_km2)) + s(I(DistToShore/1000), bs = "ts",
    k = 4)

Parametric coefficients:
            Estimate Std. Error t value Pr(>|t|)
(Intercept)   -7.769      0.395  -19.66   <2e-16 ***
---
Signif. codes:  0 '***' 0.001 '**' 0.01 '*' 0.05 '.' 0.1 ' ' 1

Approximate significance of smooth terms:
                         edf Ref.df     F p-value
s(I(DistToShore/1000)) 0.863      3 1.735  0.0138 *
---
Signif. codes:  0 '***' 0.001 '**' 0.01 '*' 0.05 '.' 0.1 ' ' 1

R-sq.(adj) =  -0.00169   Deviance explained = -0.467%
-REML = 182.47  Scale est. = 30.603    n = 11605

All predictors were significant. This is the final model.
Creating term plots.
Diagnostic output from gam.check():

Method: REML   Optimizer: outer newton
full convergence after 11 iterations.
Gradient range [-0.0001816491,9.158778e-05]
(score 182.4662 & scale 30.60286).
Hessian positive definite, eigenvalue range [0.3445347,150.5255].
Model rank =  4 / 4

Basis dimension (k) checking results. Low p-value (k-index<1) may
indicate that k is too low, especially if edf is close to k'.

                          k'   edf k-index p-value
s(I(DistToShore/1000)) 3.000 0.863   0.807    0.04

Predictors retained during the model selection procedure: DistToShore

Predictors dropped during the model selection procedure: dayofyear
```

Model term plots

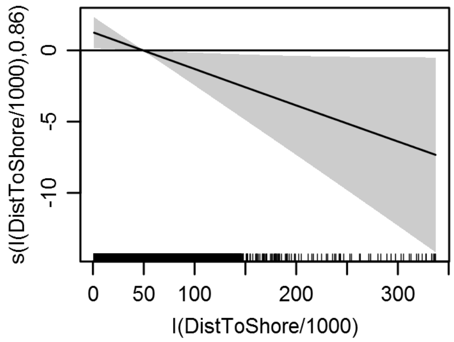

Diagnostic plots

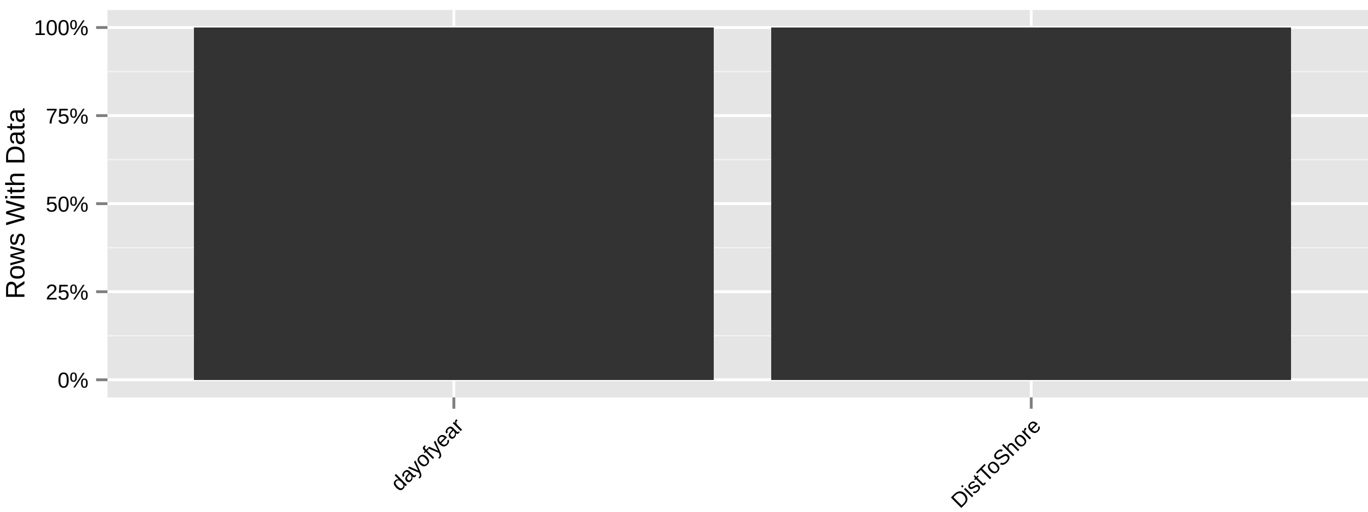

Figure 109: Segments with predictor values for the North Atlantic right whale Climatological model, Spring season, Calving and Migration Area. This plot is used to assess how many segments would be lost by including a given predictor in a model.

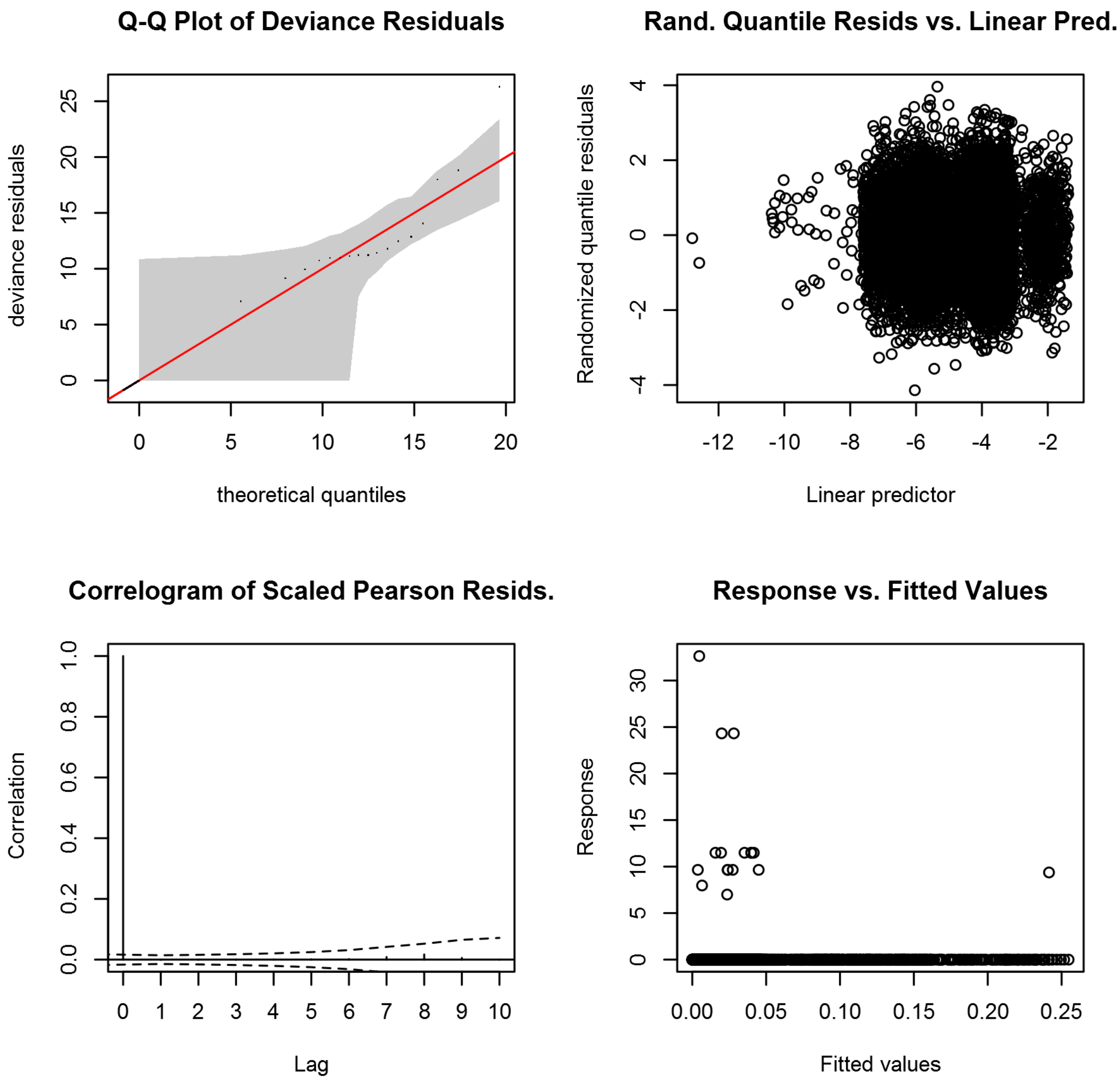

Figure 110: Statistical diagnostic plots for the North Atlantic right whale Climatological model, Spring season, Calving and Migration Area.

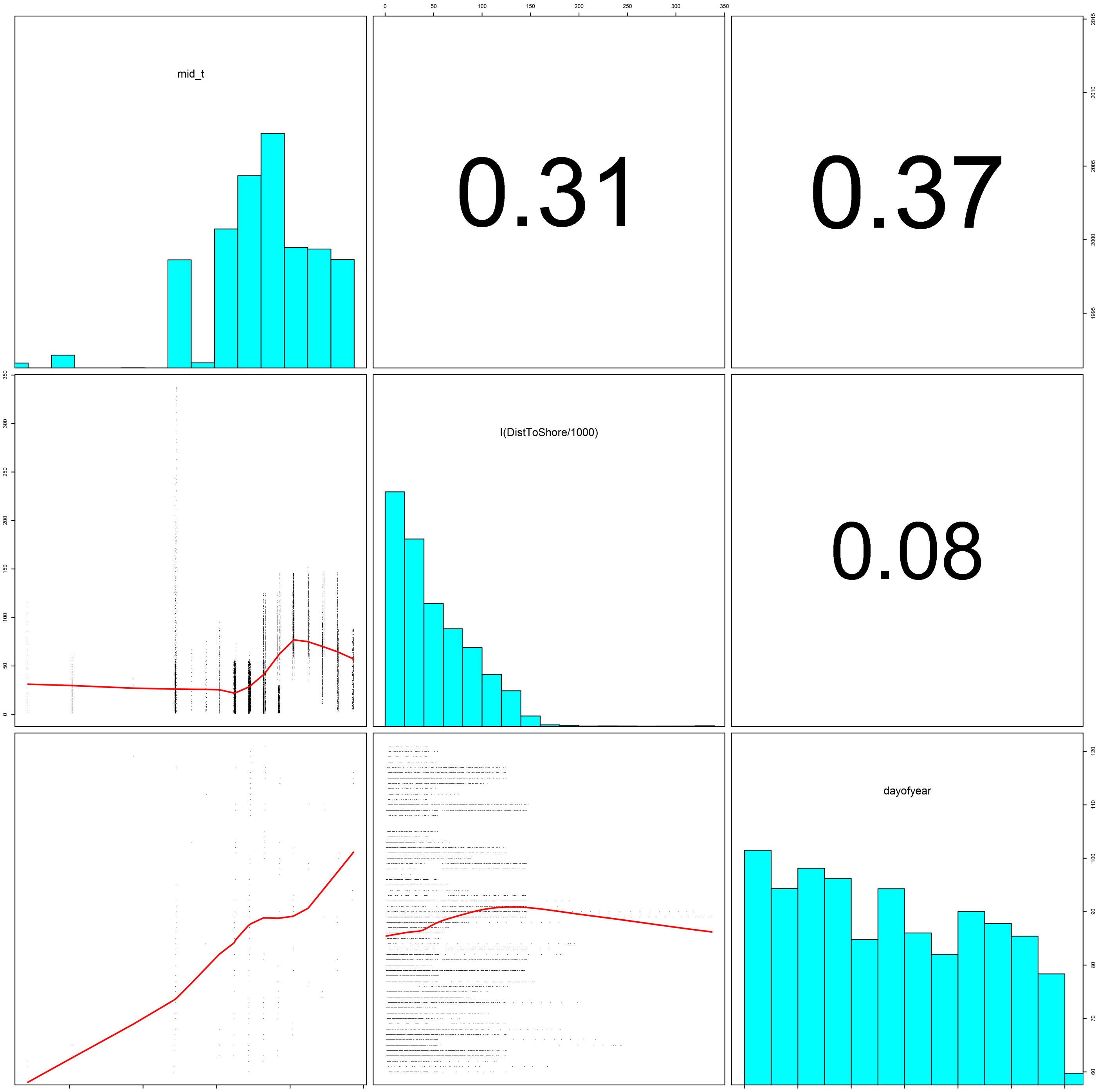

Figure 111: Scatterplot matrix for the North Atlantic right whale Climatological model, Spring season, Calving and Migration Area. This plot is used to inspect the distribution of predictors (via histograms along the diagonal), simple correlation between predictors (via pairwise Pearson coefficients above the diagonal), and linearity of predictor correlations (via scatterplots below the diagonal). This plot is best viewed at high magnification.

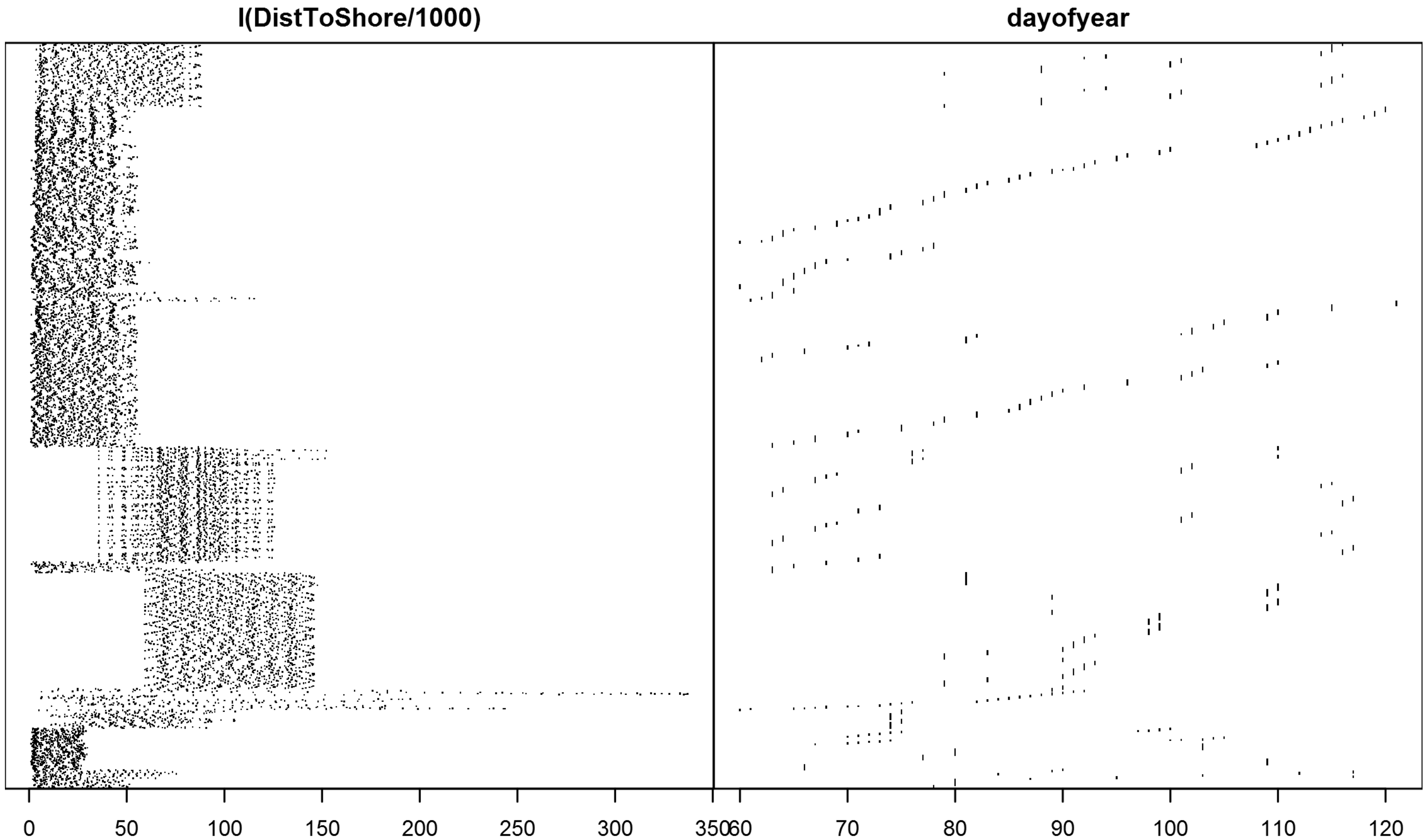

Figure 112: Dotplot for the North Atlantic right whale Climatological model, Spring season, Calving and Migration Area. This plot is used to check for suspicious patterns and outliers in the data. Points are ordered vertically by transect ID, sequentially in time.

Unsurveyed Area

Density was not modeled for this region.

Summer

In this season, the area between Cape Hatteras and Canada was well surveyed, with less effort to the south, and very little in Canada except along the northern edge of Georges Bank. In these months, right whales typically aggregate in the Great South Channel (Kenney et al. 1995), then move north to the Bay of Fundy and the southeastern Scotian Shelf as the summer progresses (Winn et al. 1986).

We split the study area at the Gulf Stream. Only one right whale sighting was reported south of here, near Cape Lookout, North Carolina. The presence of right whales in the southeast during these months was corroborated by acoustic monitoring. Hodge et al. (2015) reported acoustic detections of right whales in June and July 2012 Cape Lookout and near the Georgia-South Carolina border. However, with just one sighting we could not model density from environmental predictors and estimated the mean density across the this southeast on-shelf area instead.

North of the Gulf Stream, many right whales were sighted. Most were in the Gulf of Maine, but one was reported as far south as Long Island. Their presence south of the Gulf of Maine is corroborated by Knowlton et al. (2002) who reported a sighting near Delaware Bay in July (year unspecified), and by Whitt et al. (2013), who reported acoustic detections off New Jersey for all months March-December of 2008, and all months January-November 2009 except August.

We lacked sufficient survey effort to include Canadian waters in this season's models, except for the Canadian portion of Georges Bank.

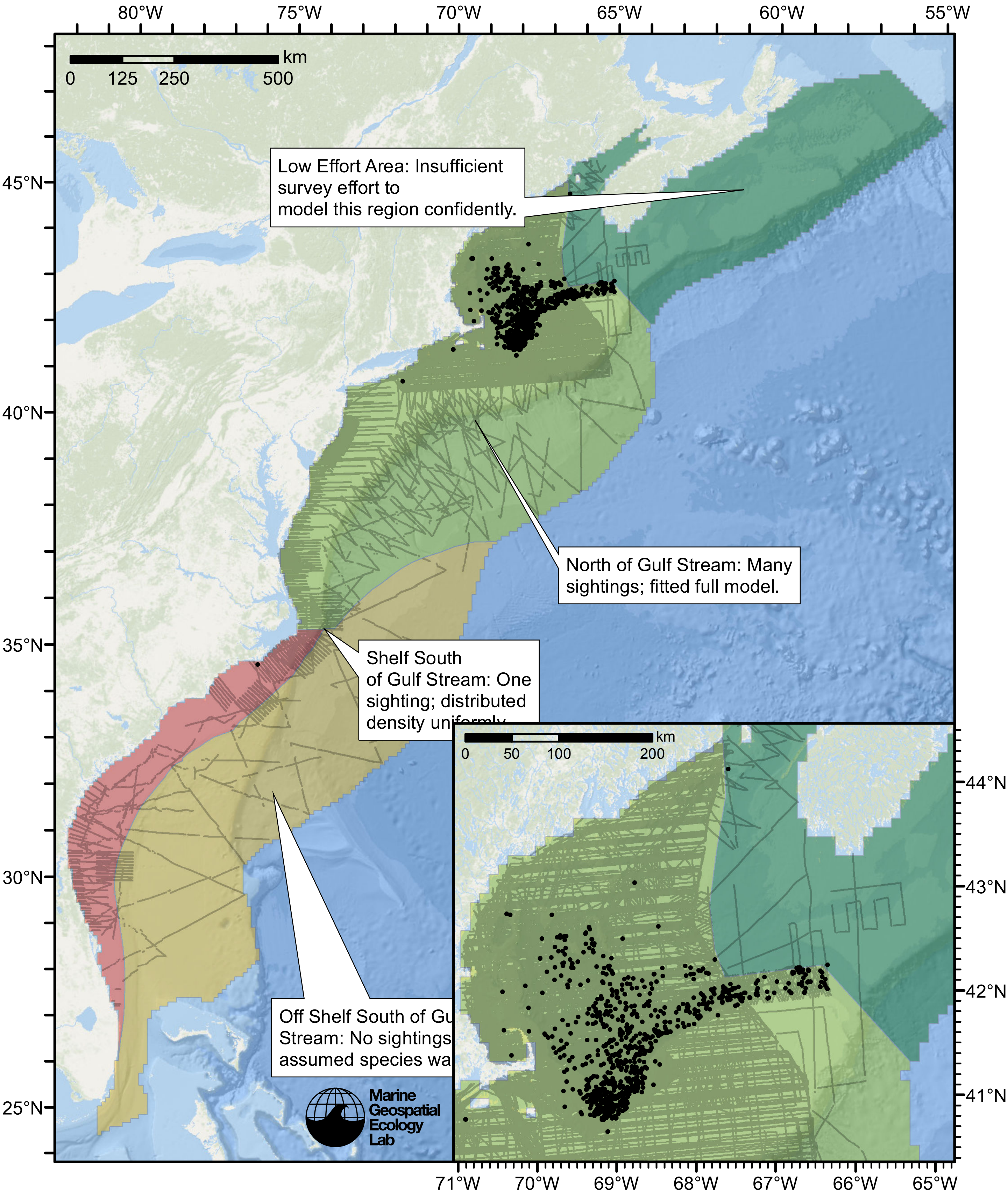

Figure 113: North Atlantic right whale density model schematic for Summer season. All on-effort sightings are shown, including those that were truncated when detection functions were fitted.

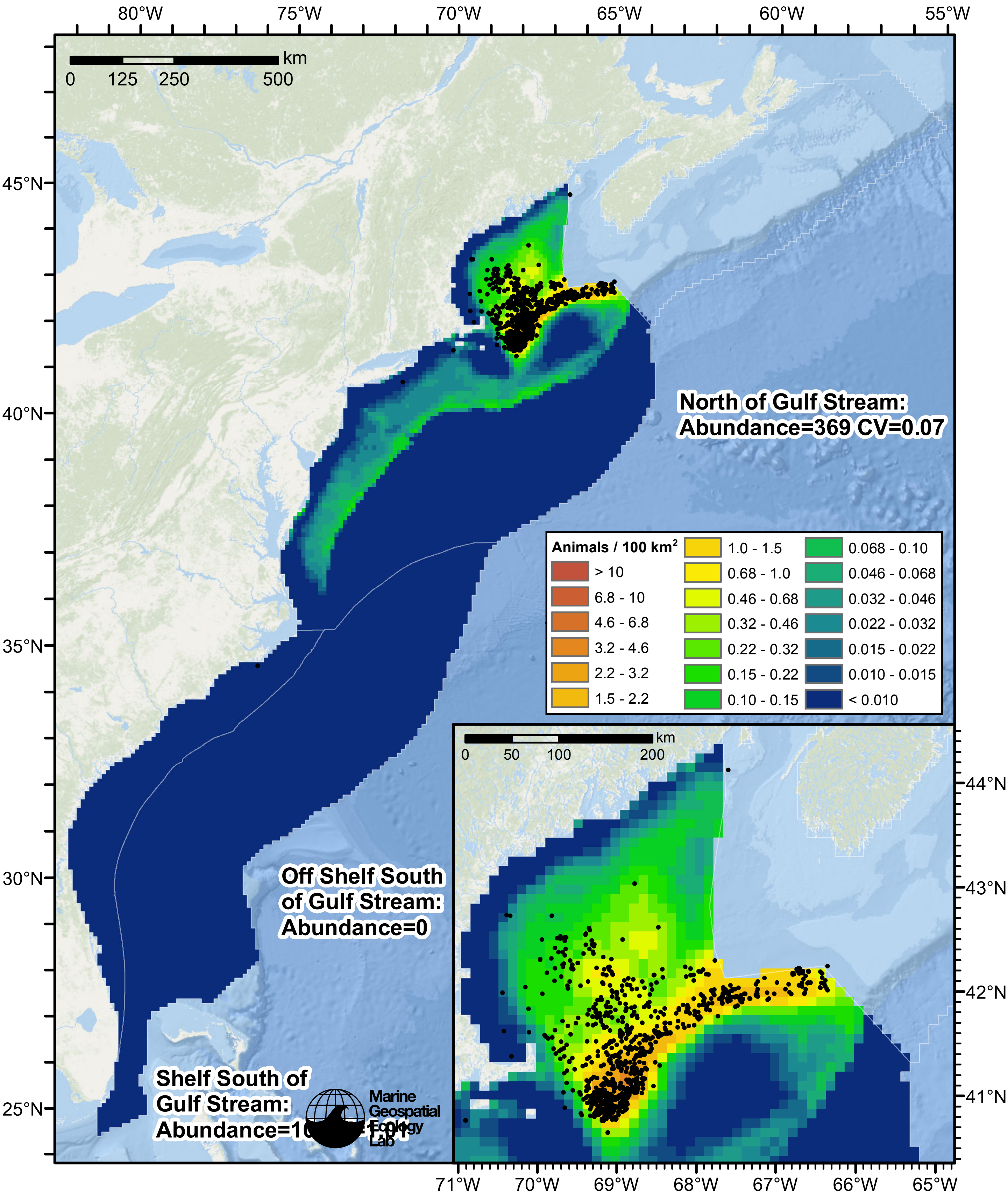

Figure 114: North Atlantic right whale density predicted by the Summer season climatological model that explained the most deviance. Pixels are 10x10 km. The legend gives the estimated individuals per pixel; breaks are logarithmic. The same scale is used for all seasons. Abundance for each region was computed by summing the density cells occuring in that region.

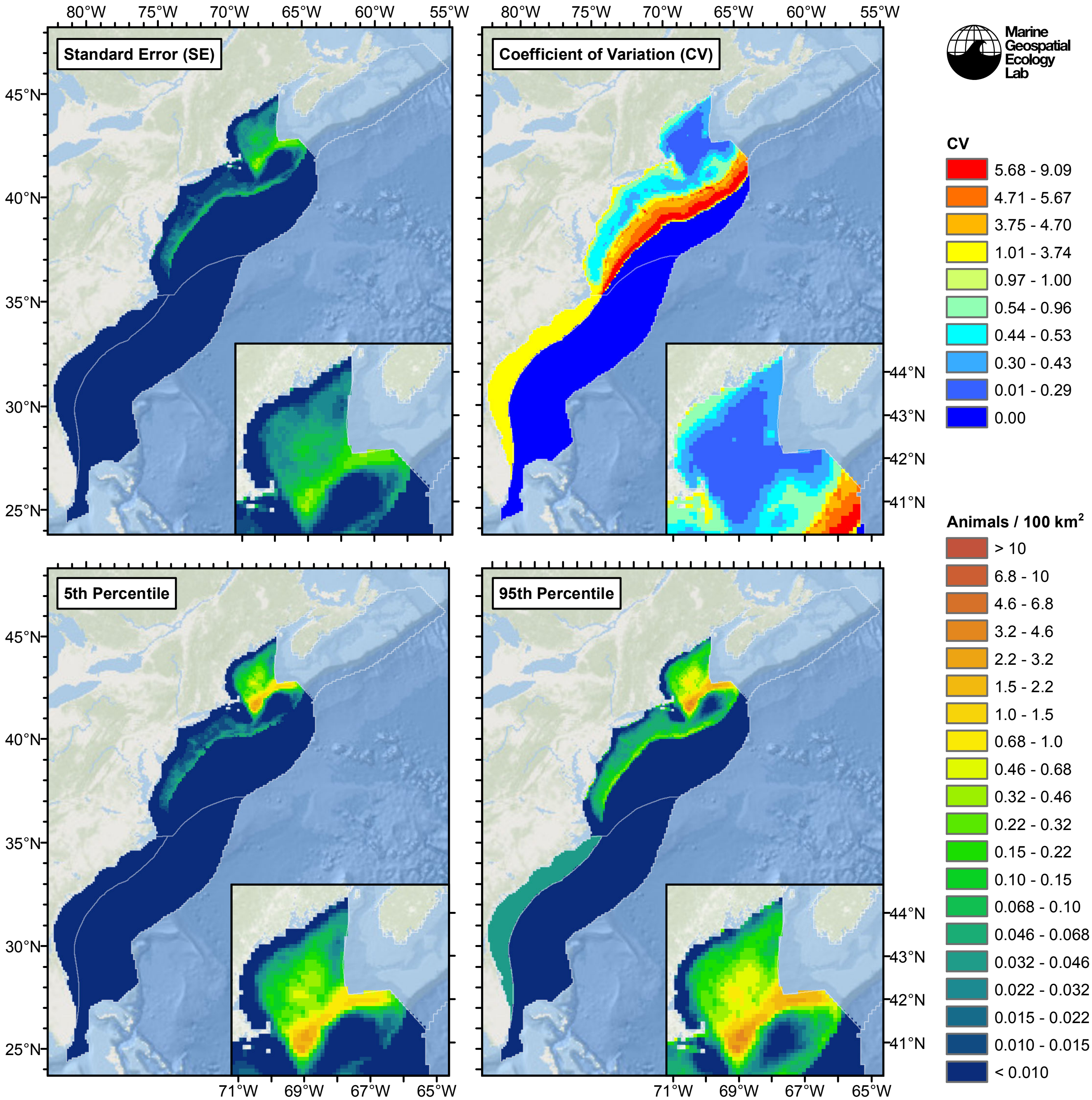

Figure 115: Estimated uncertainty for the Summer season climatological model that explained the most deviance. These estimates only incorporate the statistical uncertainty estimated for the spatial model (by the R mgcv package). They do not incorporate uncertainty in the detection functions, g(0) estimates, predictor variables, and so on.

North of Gulf Stream

Statistical output

```
Rscript.exe: This is mgcv 1.8-2. For overview type 'help("mgcv-package")'.


Family: Tweedie(p=1.287)
```

```
Link function: log

Formula:
abundance ~ offset(log(area_km2)) + s(log10(Depth), bs = "ts",
    k = 5) + s(sqrt(Slope/1000), bs = "ts", k = 5) + s(I(DistToShore/1000),
    bs = "ts", k = 5) + s(I(DistTo125m/1000), bs = "ts", k = 5) +
    s(I(DistTo300m/1000), bs = "ts", k = 5) + s(ClimSST, bs = "ts",
    k = 5) + s(I(ClimDistToFront1^(1/3)), bs = "ts", k = 5) +
    s(log10(pmax(ClimEKE, 1e-04)), bs = "ts", k = 5) + s(I(ClimCumVGPM90^(1/3)),
    bs = "ts", k = 5)

Parametric coefficients:
            Estimate Std. Error t value Pr(>|t|)
(Intercept) -11.8988     0.7947  -14.97   <2e-16 ***
---
Signif. codes:  0 '***' 0.001 '**' 0.01 '*' 0.05 '.' 0.1 ' ' 1

Approximate significance of smooth terms:
                                 edf Ref.df      F  p-value
s(log10(Depth))               3.2971      4  5.073 6.60e-05 ***
s(sqrt(Slope/1000))           2.2441      4  4.460 4.53e-05 ***
s(I(DistToShore/1000))        2.4790      4  4.560 4.94e-05 ***
s(I(DistTo125m/1000))         2.8157      4 10.926 7.93e-11 ***
s(I(DistTo300m/1000))         3.0978      4 38.759  < 2e-16 ***
s(ClimSST)                    3.7973      4  7.527 1.14e-06 ***
s(I(ClimDistToFront1^(1/3)))  0.9015      4  1.520  0.00699 **
s(log10(pmax(ClimEKE, 1e-04))) 2.4000      4  6.584 6.97e-07 ***
s(I(ClimCumVGPM90^(1/3)))     2.7368      4 16.986  < 2e-16 ***
---
Signif. codes:  0 '***' 0.001 '**' 0.01 '*' 0.05 '.' 0.1 ' ' 1

R-sq.(adj) =  0.0224   Deviance explained = 33.8%
-REML = 4802.4  Scale est. = 24.955    n = 24619

All predictors were significant. This is the final model.
Creating term plots.
Diagnostic output from gam.check():

Method: REML   Optimizer: outer newton
full convergence after 13 iterations.
Gradient range [-0.00145845,0.0006890338]
(score 4802.421 & scale 24.95488).
Hessian positive definite, eigenvalue range [0.3502525,2239.943].
Model rank =  37 / 37

Basis dimension (k) checking results. Low p-value (k-index<1) may
indicate that k is too low, especially if edf is close to k'.

                                 k'   edf k-index p-value
s(log10(Depth))               4.000 3.297   0.791    0.00
s(sqrt(Slope/1000))           4.000 2.244   0.847    0.21
s(I(DistToShore/1000))        4.000 2.479   0.847    0.20
s(I(DistTo125m/1000))         4.000 2.816   0.751    0.00
s(I(DistTo300m/1000))         4.000 3.098   0.811    0.00
s(ClimSST)                    4.000 3.797   0.809    0.00
s(I(ClimDistToFront1^(1/3)))  4.000 0.901   0.859    0.62
s(log10(pmax(ClimEKE, 1e-04))) 4.000 2.400   0.855    0.45
s(I(ClimCumVGPM90^(1/3)))     4.000 2.737   0.829    0.02
```

Predictors retained during the model selection procedure: Depth, Slope, DistToShore, DistTo125m, DistTo300m, ClimSST, ClimDistToFront1, ClimEKE, ClimCumVGPM90

Predictors dropped during the model selection procedure:

Model term plots

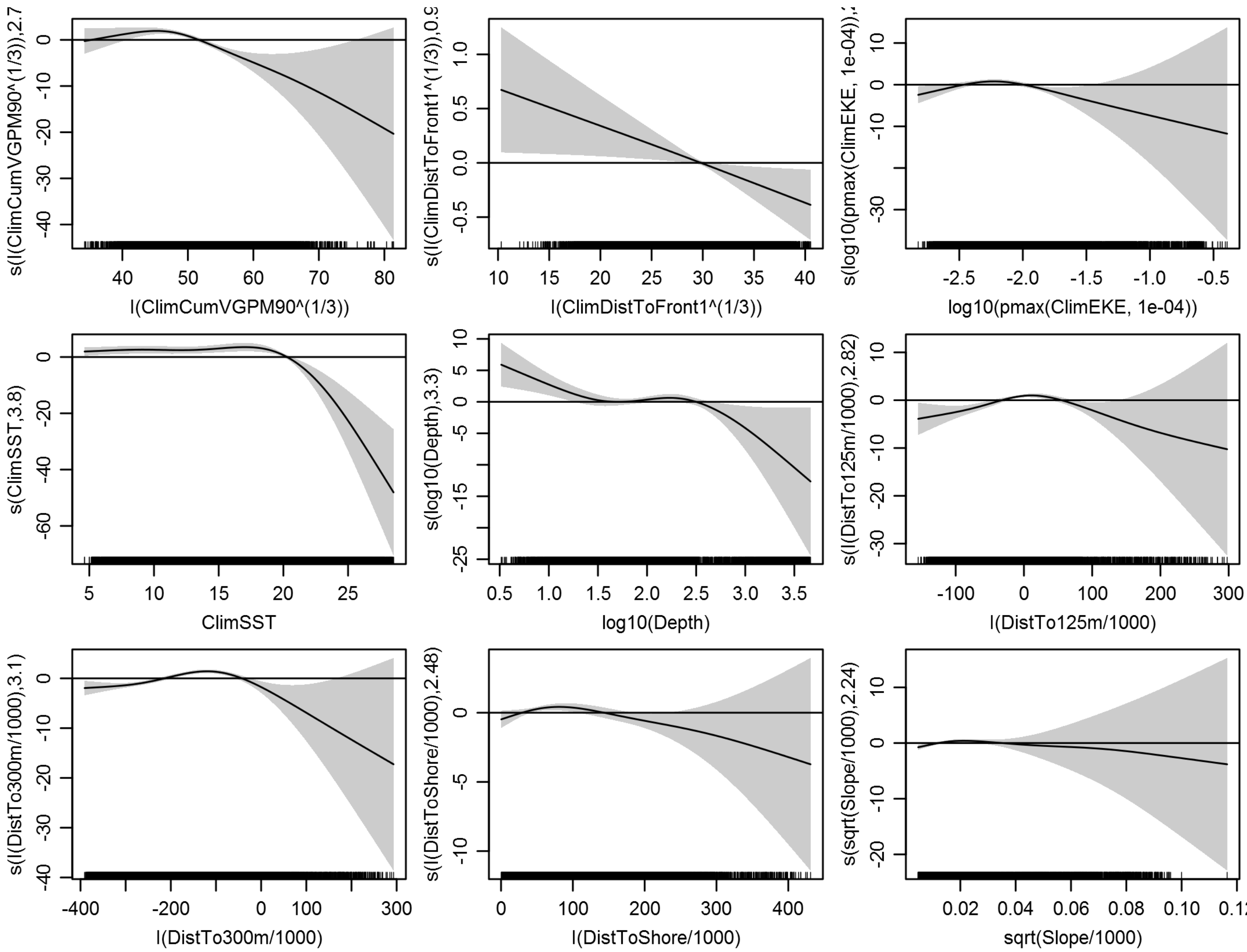

Diagnostic plots

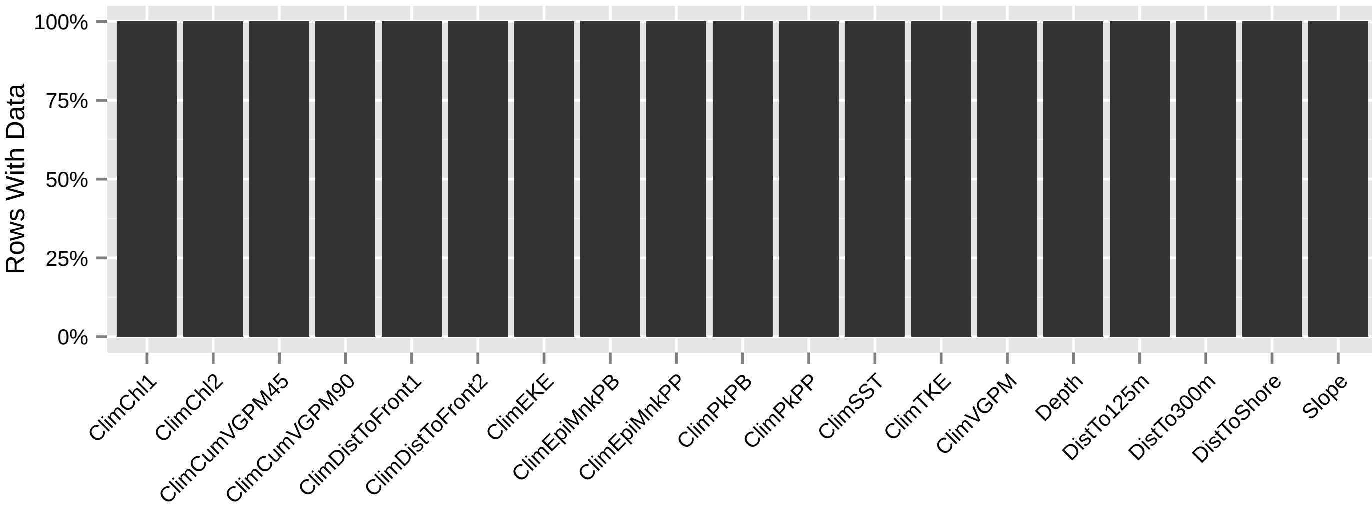

Figure 116: Segments with predictor values for the North Atlantic right whale Climatological model, Summer season, North of Gulf Stream. This plot is used to assess how many segments would be lost by including a given predictor in a model.

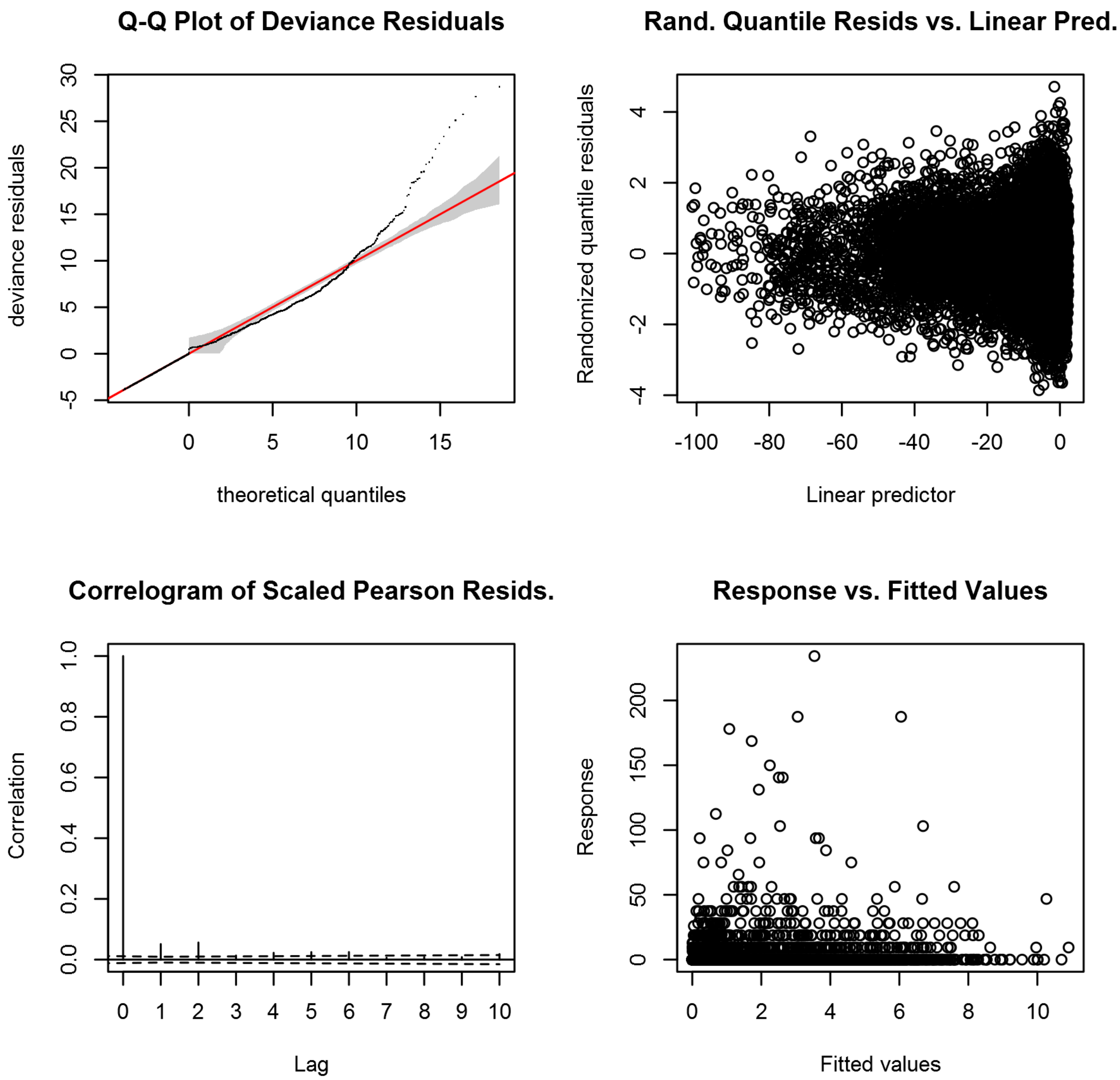

Figure 117: Statistical diagnostic plots for the North Atlantic right whale Climatological model, Summer season, North of Gulf Stream.

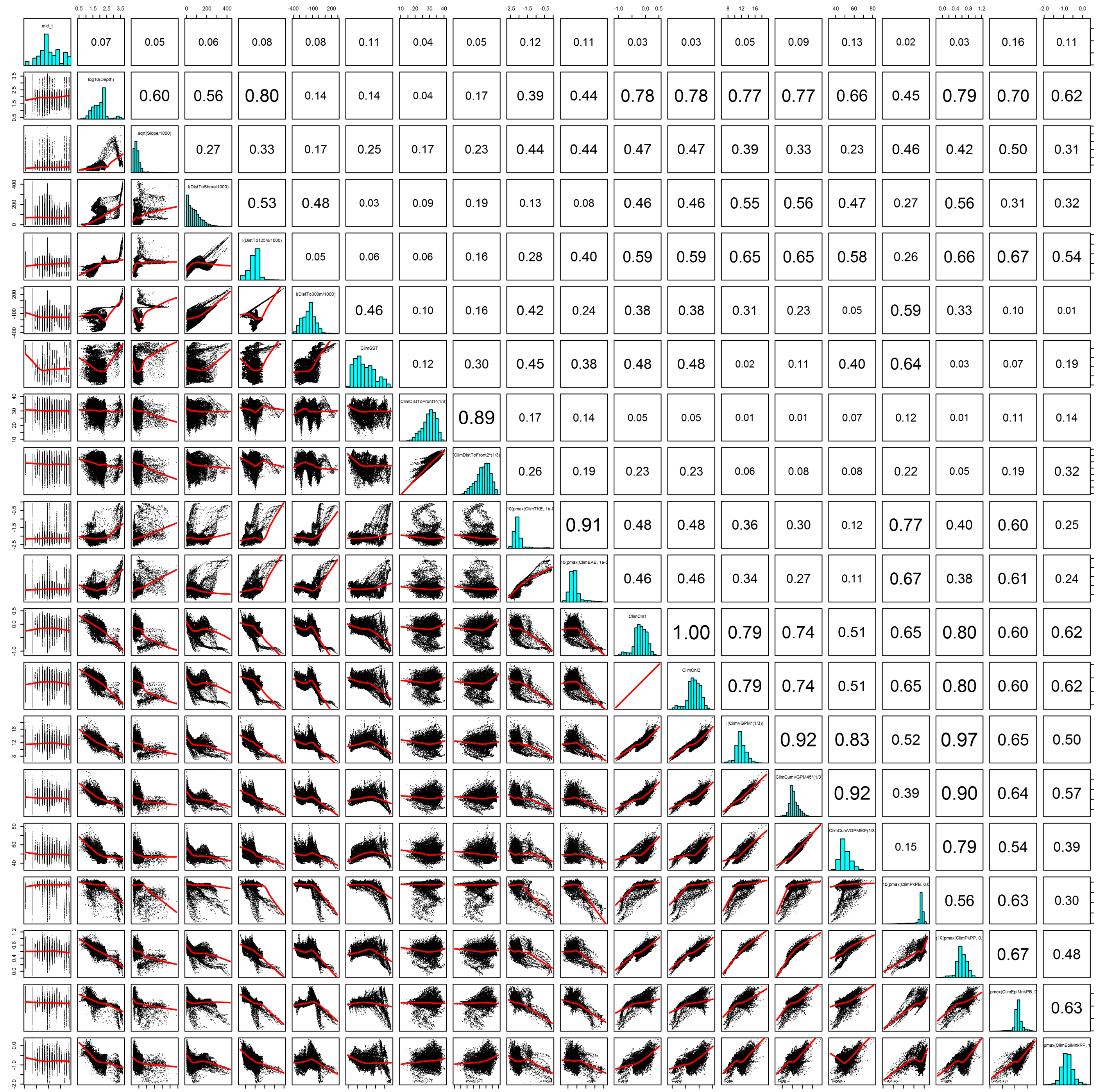

Figure 118: Scatterplot matrix for the North Atlantic right whale Climatological model, Summer season, North of Gulf Stream. This plot is used to inspect the distribution of predictors (via histograms along the diagonal), simple correlation between predictors (via pairwise Pearson coefficients above the diagonal), and linearity of predictor correlations (via scatterplots below the diagonal). This plot is best viewed at high magnification.

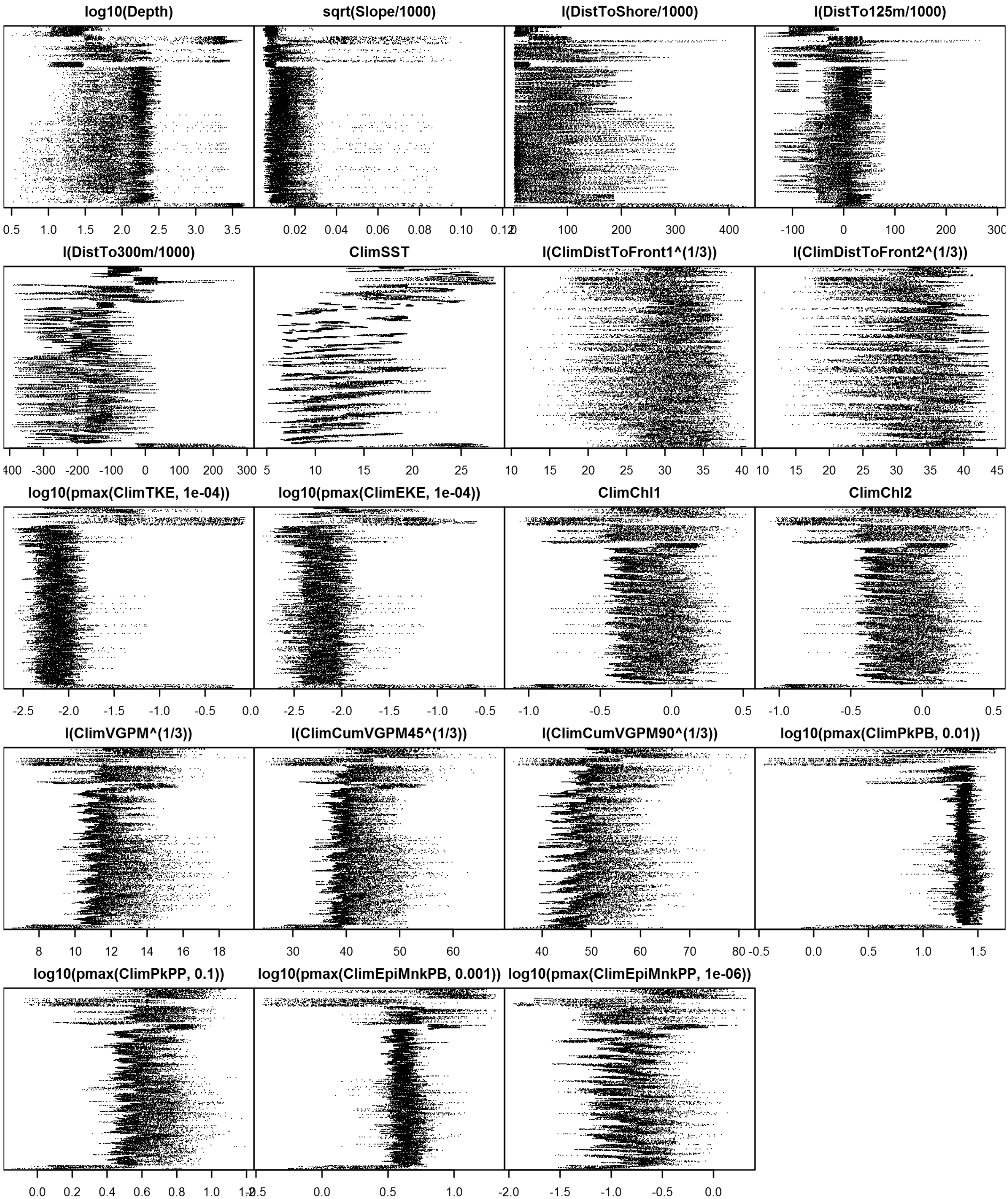

Figure 119: Dotplot for the North Atlantic right whale Climatological model, Summer season, North of Gulf Stream. This plot is used to check for suspicious patterns and outliers in the data. Points are ordered vertically by transect ID, sequentially in time.

Shelf South of Gulf Stream

A mean density estimate was made for this region. First, density (individuals per square kilometer) was calculated as the number of animals encountered divided by the area effectively surveyed, corrected by the detection functions and g(0) estimates. Then, density was multiplied by the size of each grid cell, in square kilometers, to obtain abundance (number of individuals) per grid cell. Finally, all grid cells in the region were assigned this abundance value.

Off Shelf South of Gulf Stream

Density assumed to be 0 in this region.

Low Effort Area

Density was not modeled for this region.

Contemporaneous Model

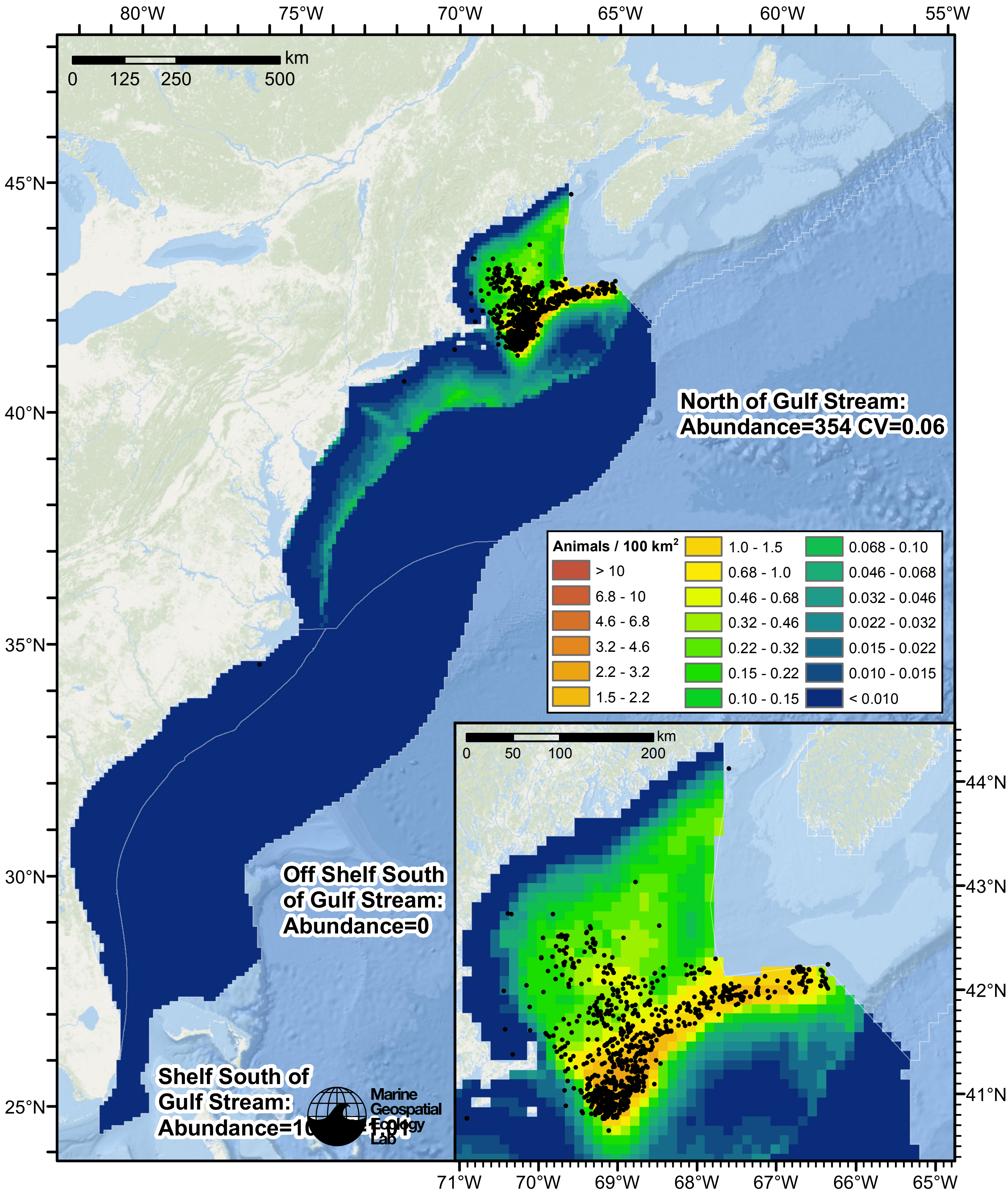

Figure 120: North Atlantic right whale density predicted by the Summer season contemporaneous model that explained the most deviance. Pixels are 10x10 km. The legend gives the estimated individuals per pixel; breaks are logarithmic. The same scale is used for all seasons. Abundance for each region was computed by summing the density cells occuring in that region.

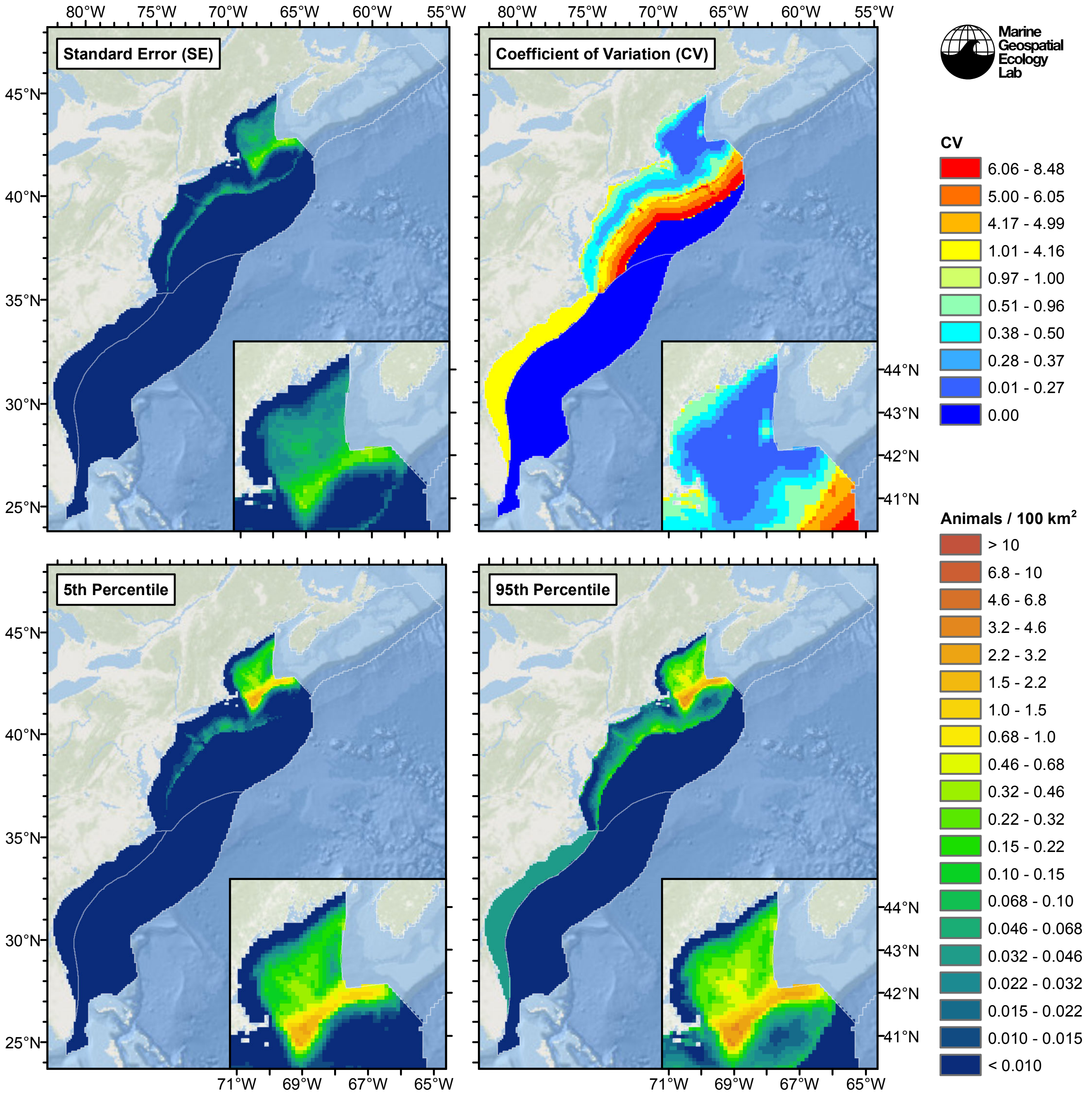

Figure 121: Estimated uncertainty for the Summer season contemporaneous model that explained the most deviance. These estimates only incorporate the statistical uncertainty estimated for the spatial model (by the R mgcv package). They do not incorporate uncertainty in the detection functions, g(0) estimates, predictor variables, and so on.

North of Gulf Stream

Statistical output

```
Rscript.exe: This is mgcv 1.8-2. For overview type 'help("mgcv-package")'.


Family: Tweedie(p=1.286)
```

```
Link function: log

Formula:
abundance ~ offset(log(area_km2)) + s(log10(Depth), bs = "ts",
    k = 5) + s(sqrt(Slope/1000), bs = "ts", k = 5) + s(I(DistToShore/1000),
    bs = "ts", k = 5) + s(I(DistTo125m/1000), bs = "ts", k = 5) +
    s(I(DistTo300m/1000), bs = "ts", k = 5) + s(log10(pmax(EKE,
    1e-04)), bs = "ts", k = 5) + s(I(CumVGPM90^(1/3)), bs = "ts",
    k = 5)

Parametric coefficients:
            Estimate Std. Error t value Pr(>|t|)
(Intercept)  -8.2430     0.3091  -26.66   <2e-16 ***
---
Signif. codes:  0 '***' 0.001 '**' 0.01 '*' 0.05 '.' 0.1 ' ' 1

Approximate significance of smooth terms:
                            edf Ref.df      F  p-value
s(log10(Depth))           3.313      4  7.275 5.40e-07 ***
s(sqrt(Slope/1000))       2.390      4  3.770 0.000307 ***
s(I(DistToShore/1000))    2.844      4  7.963 7.96e-08 ***
s(I(DistTo125m/1000))     3.198      4 12.764 5.30e-12 ***
s(I(DistTo300m/1000))     3.406      4 53.836  < 2e-16 ***
s(log10(pmax(EKE, 1e-04))) 1.907      4  2.657 0.002241 **
s(I(CumVGPM90^(1/3)))     2.959      4 11.988 2.37e-11 ***
---
Signif. codes:  0 '***' 0.001 '**' 0.01 '*' 0.05 '.' 0.1 ' ' 1

R-sq.(adj) =  0.0187   Deviance explained = 30.8%
-REML = 4828.4  Scale est. = 25.381    n = 23886

All predictors were significant. This is the final model.
Creating term plots.
Diagnostic output from gam.check():

Method: REML   Optimizer: outer newton
full convergence after 11 iterations.
Gradient range [-0.002474828,0.002157146]
(score 4828.416 & scale 25.38116).
Hessian positive definite, eigenvalue range [0.07770208,2277.995].
Model rank =  29 / 29

Basis dimension (k) checking results. Low p-value (k-index<1) may
indicate that k is too low, especially if edf is close to k'.

                             k'   edf k-index p-value
s(log10(Depth))           4.000 3.313   0.858    0.18
s(sqrt(Slope/1000))       4.000 2.390   0.872    0.64
s(I(DistToShore/1000))    4.000 2.844   0.861    0.26
s(I(DistTo125m/1000))     4.000 3.198   0.829    0.01
s(I(DistTo300m/1000))     4.000 3.406   0.841    0.02
s(log10(pmax(EKE, 1e-04))) 4.000 1.907   0.860    0.21
s(I(CumVGPM90^(1/3)))     4.000 2.959   0.879    0.78

Predictors retained during the model selection procedure: Depth, Slope, DistToShore, DistTo125m,
DistTo300m, EKE, CumVGPM90

Predictors dropped during the model selection procedure: SST, DistToFront1
```

Model term plots

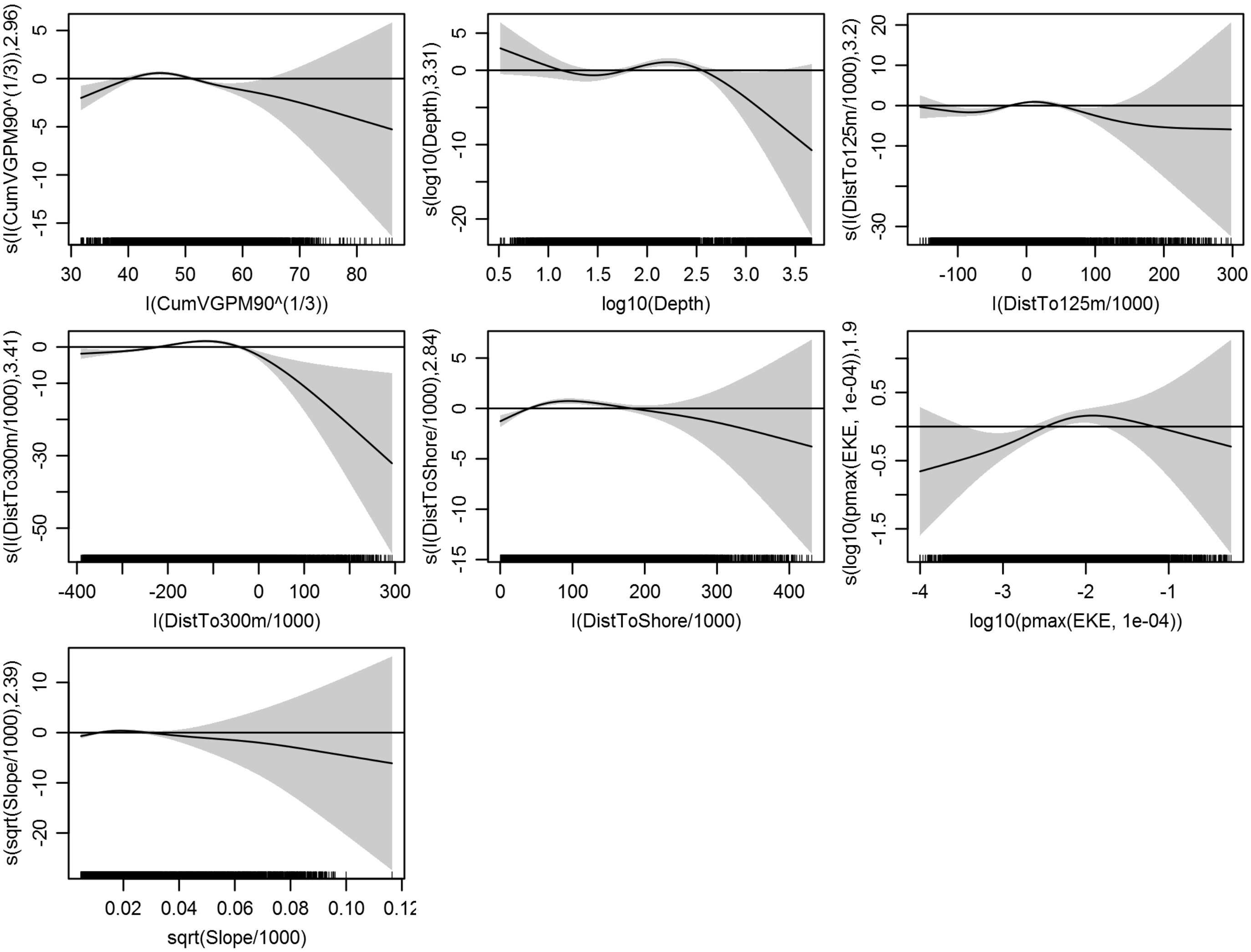

Diagnostic plots

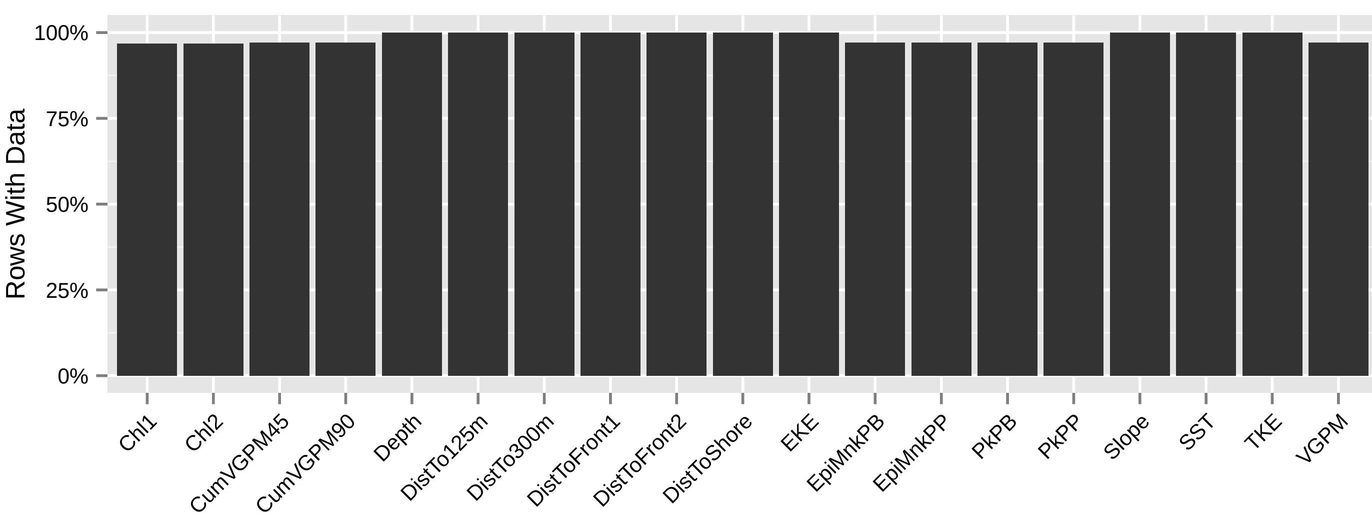

Figure 122: Segments with predictor values for the North Atlantic right whale Contemporaneous model, Summer season, North of Gulf Stream. This plot is used to assess how many segments would be lost by including a given predictor in a model.

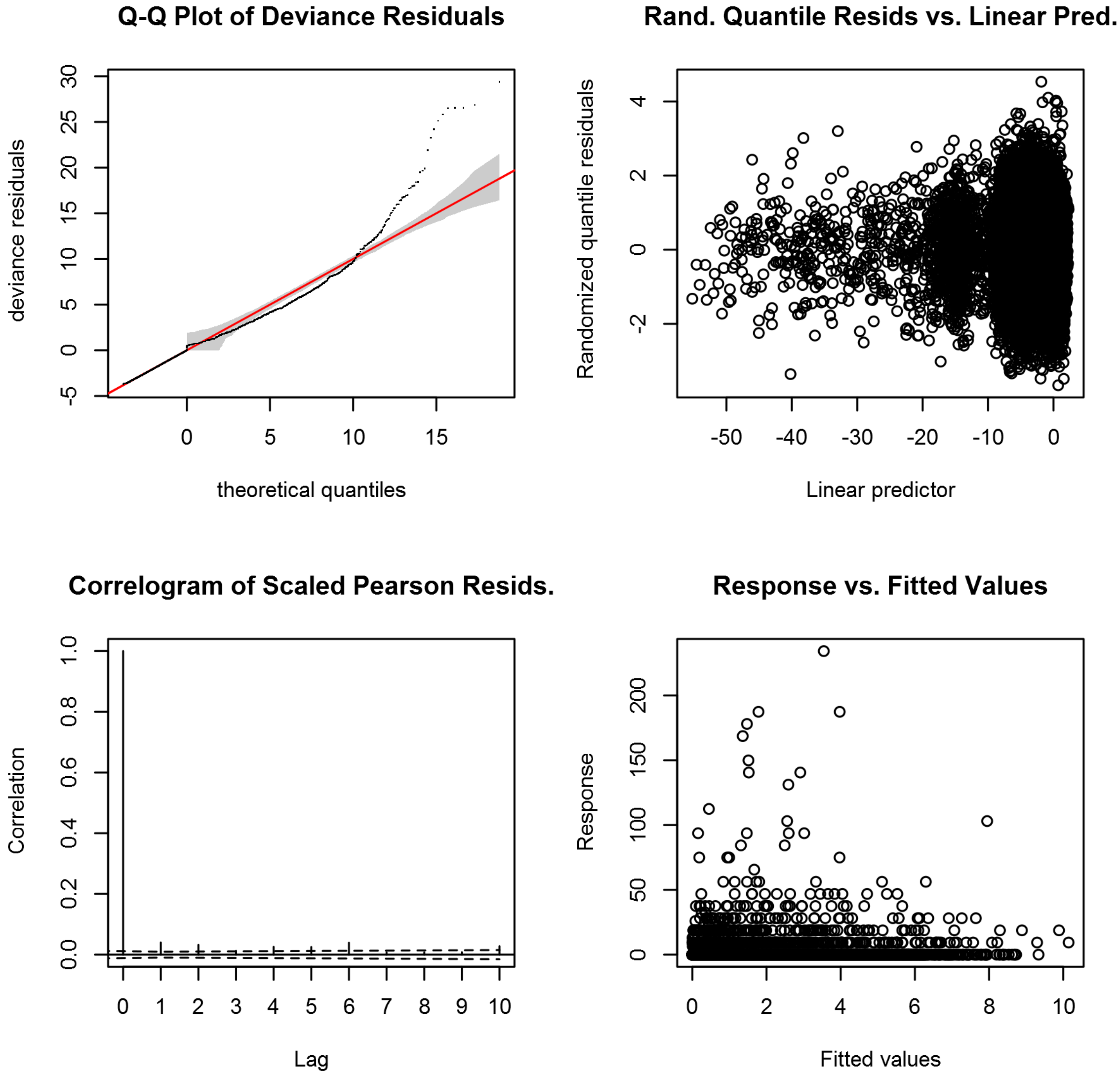

Figure 123: Statistical diagnostic plots for the North Atlantic right whale Contemporaneous model, Summer season, North of Gulf Stream.

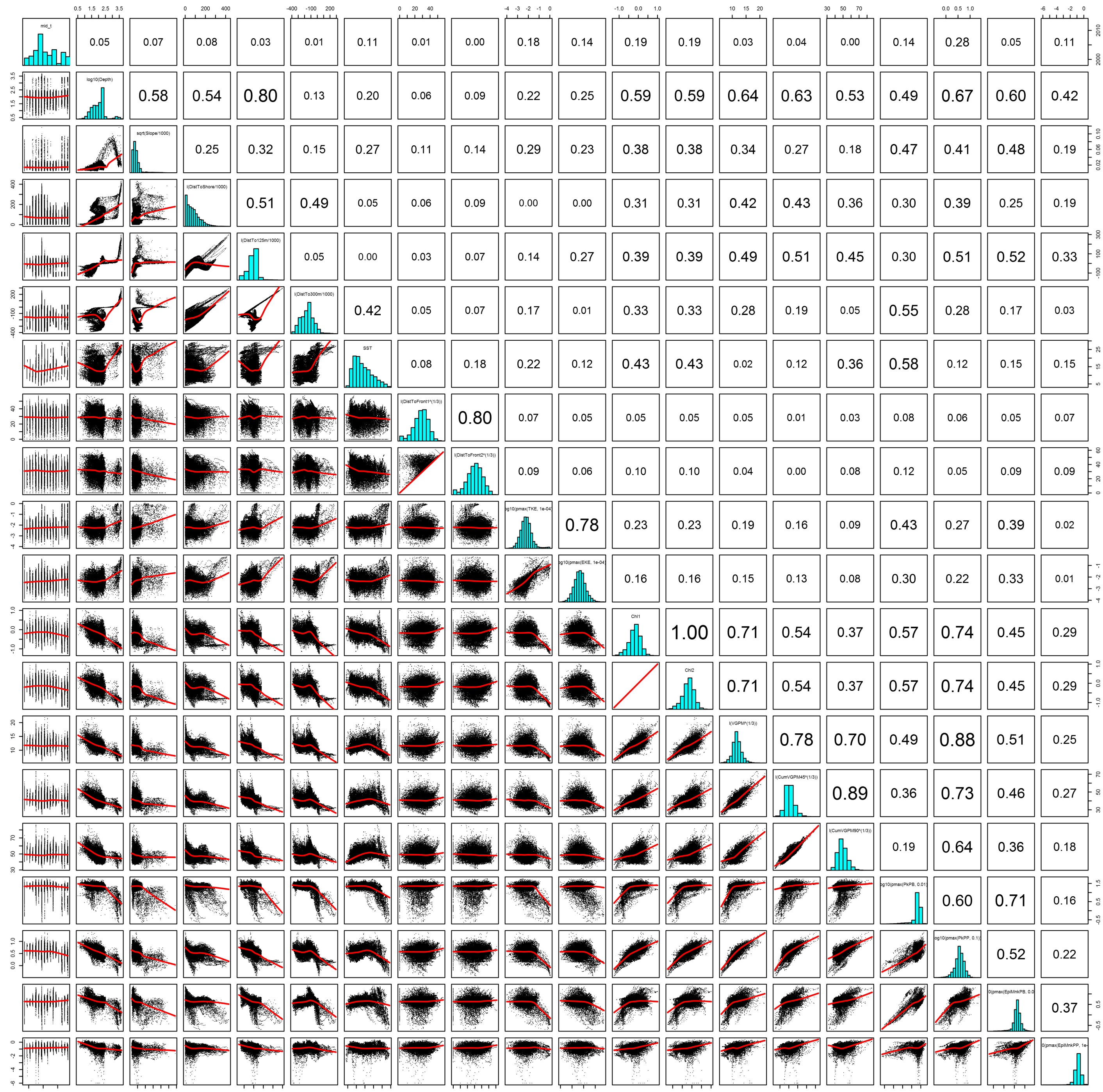

Figure 124: Scatterplot matrix for the North Atlantic right whale Contemporaneous model, Summer season, North of Gulf Stream. This plot is used to inspect the distribution of predictors (via histograms along the diagonal), simple correlation between predictors (via pairwise Pearson coefficients above the diagonal), and linearity of predictor correlations (via scatterplots below the diagonal). This plot is best viewed at high magnification.

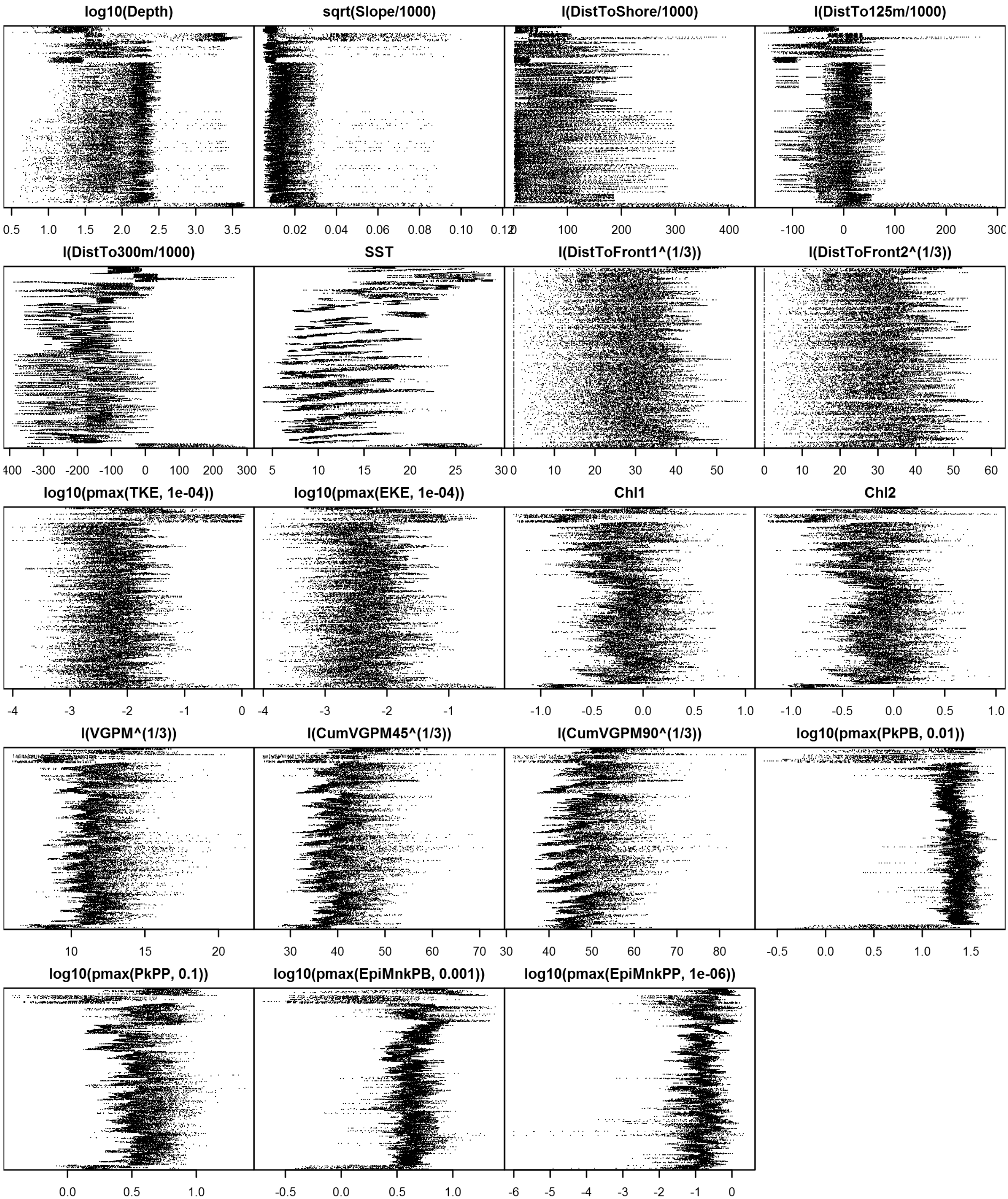

Figure 125: Dotplot for the North Atlantic right whale Contemporaneous model, Summer season, North of Gulf Stream. This plot is used to check for suspicious patterns and outliers in the data. Points are ordered vertically by transect ID, sequentially in time.

Shelf South of Gulf Stream

A mean density estimate was made for this region. First, density (individuals per square kilometer) was calculated as the number of animals encountered divided by the area effectively surveyed, corrected by the detection functions and g(0) estimates. Then, density was multiplied by the size of each grid cell, in square kilometers, to obtain abundance (number of individuals) per grid cell. Finally, all grid cells in the region were assigned this abundance value.

Off Shelf South of Gulf Stream

Density assumed to be 0 in this region.

Low Effort Area

Density was not modeled for this region.

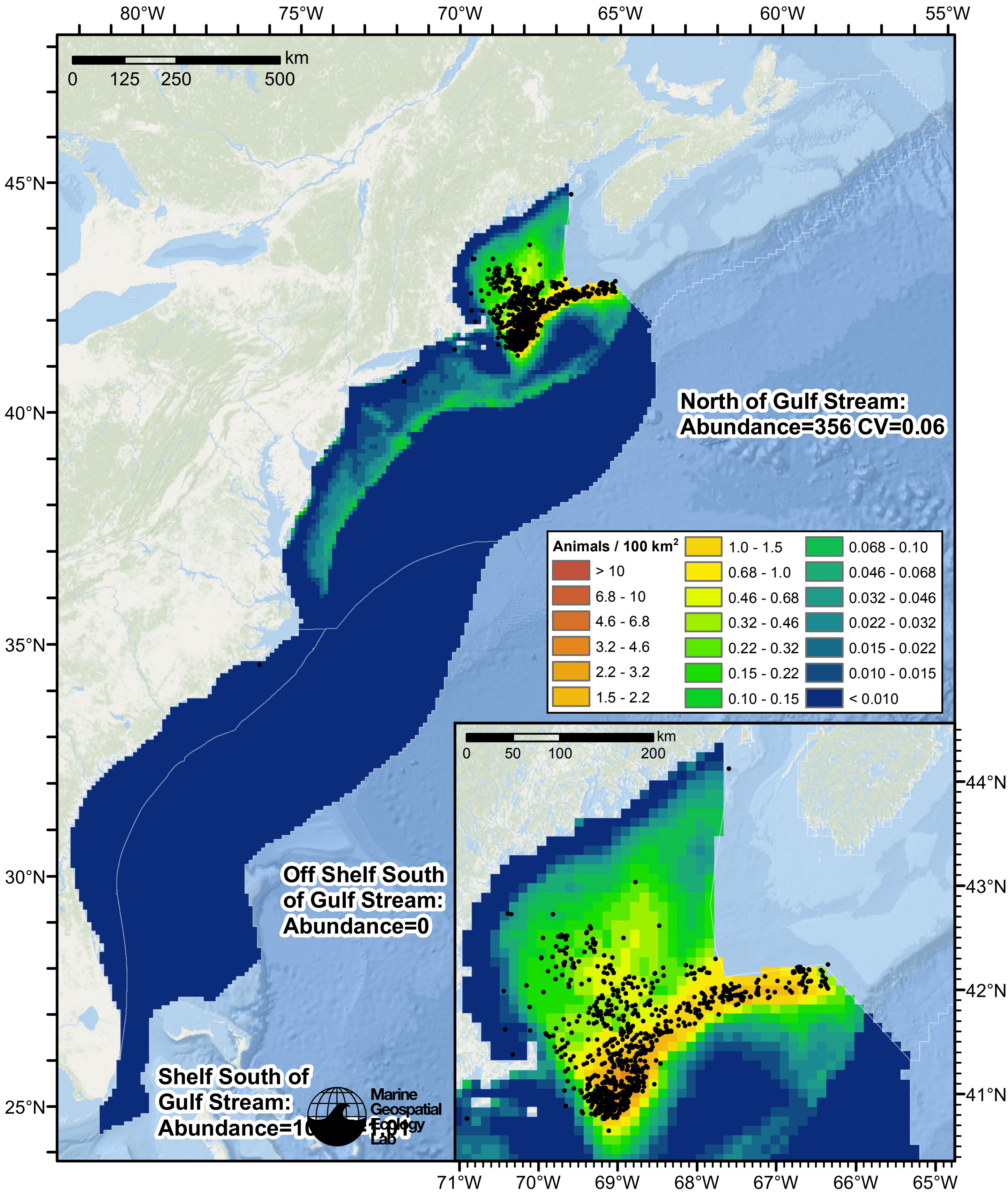

Figure 126: North Atlantic right whale density predicted by the Summer season climatological same segments model that explained the most deviance. Pixels are 10x10 km. The legend gives the estimated individuals per pixel; breaks are logarithmic. The same scale is used for all seasons. Abundance for each region was computed by summing the density cells occuring in that region.

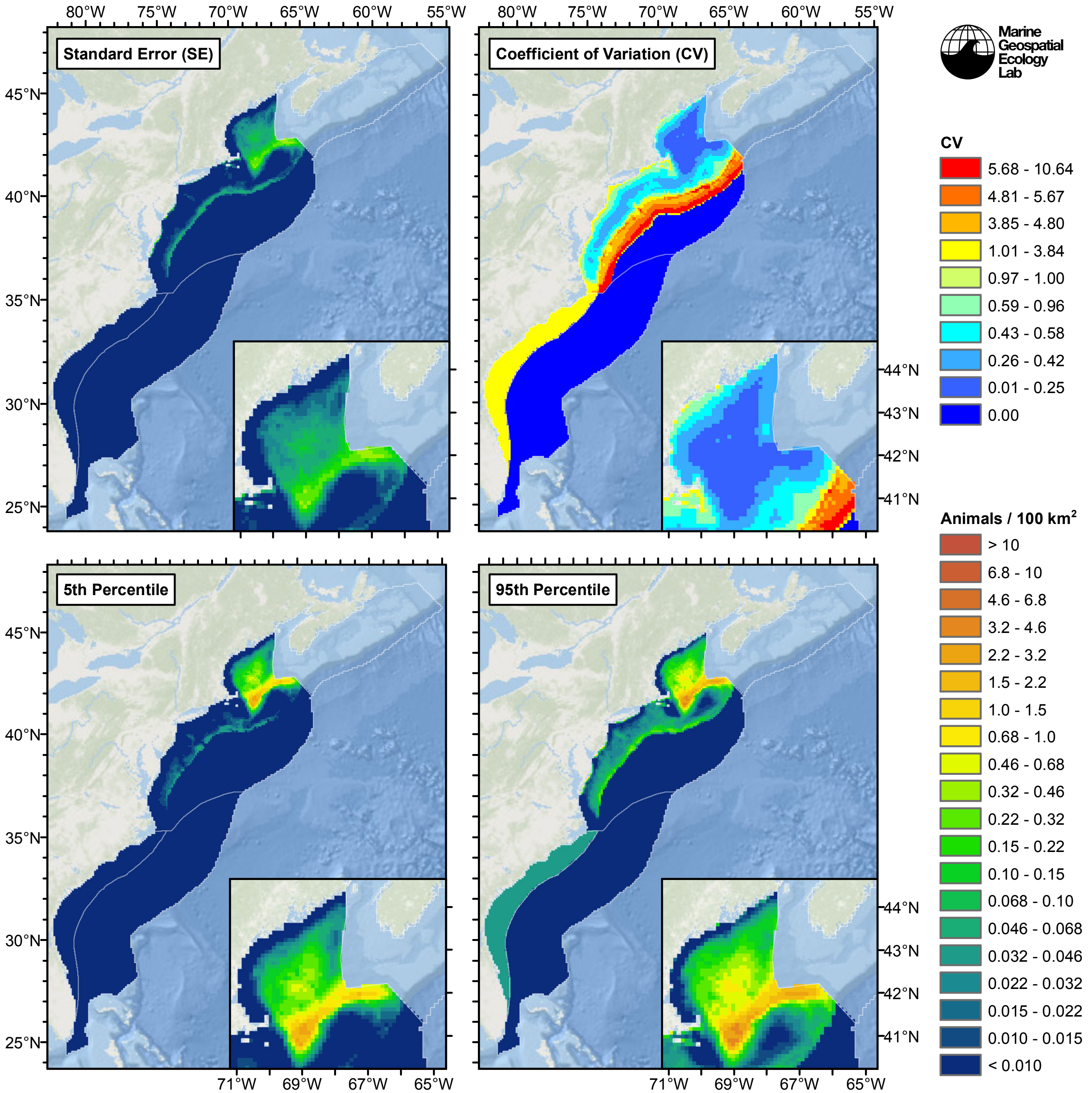

Figure 127: Estimated uncertainty for the Summer season climatological same segments model that explained the most deviance. These estimates only incorporate the statistical uncertainty estimated for the spatial model (by the R mgcv package). They do not incorporate uncertainty in the detection functions, g(0) estimates, predictor variables, and so on.

North of Gulf Stream

Statistical output

```
Rscript.exe: This is mgcv 1.8-2. For overview type 'help("mgcv-package")'.


Family: Tweedie(p=1.286)
```

```
Link function: log

Formula:
abundance ~ offset(log(area_km2)) + s(log10(Depth), bs = "ts",
    k = 5) + s(sqrt(Slope/1000), bs = "ts", k = 5) + s(I(DistToShore/1000),
    bs = "ts", k = 5) + s(I(DistTo125m/1000), bs = "ts", k = 5) +
    s(I(DistTo300m/1000), bs = "ts", k = 5) + s(log10(pmax(ClimEKE,
    1e-04)), bs = "ts", k = 5) + s(I(ClimCumVGPM90^(1/3)), bs = "ts",
    k = 5)

Parametric coefficients:
            Estimate Std. Error t value Pr(>|t|)
(Intercept)  -9.0842     0.4259  -21.33   <2e-16 ***
---
Signif. codes:  0 '***' 0.001 '**' 0.01 '*' 0.05 '.' 0.1 ' ' 1

Approximate significance of smooth terms:
                                 edf Ref.df      F  p-value
s(log10(Depth))                3.377      4  6.456 3.16e-06 ***
s(sqrt(Slope/1000))            2.384      4  4.669 3.77e-05 ***
s(I(DistToShore/1000))         2.572      4  4.194 0.000163 ***
s(I(DistTo125m/1000))          3.011      4 11.753 2.78e-11 ***
s(I(DistTo300m/1000))          3.473      4 47.322  < 2e-16 ***
s(log10(pmax(ClimEKE, 1e-04))) 2.442      4  7.302 1.65e-07 ***
s(I(ClimCumVGPM90^(1/3)))      2.893      4 19.035  < 2e-16 ***
---
Signif. codes:  0 '***' 0.001 '**' 0.01 '*' 0.05 '.' 0.1 ' ' 1

R-sq.(adj) =  0.0229   Deviance explained = 32.1%
-REML = 4805.8  Scale est. = 25.097    n = 23886

All predictors were significant. This is the final model.
Creating term plots.
Diagnostic output from gam.check():

Method: REML   Optimizer: outer newton
full convergence after 12 iterations.
Gradient range [-0.002528751,0.0005288297]
(score 4805.751 & scale 25.09702).
Hessian positive definite, eigenvalue range [0.409731,2257.722].
Model rank =  29 / 29

Basis dimension (k) checking results. Low p-value (k-index<1) may
indicate that k is too low, especially if edf is close to k'.

                                  k'   edf k-index p-value
s(log10(Depth))                4.000 3.377   0.756    0.00
s(sqrt(Slope/1000))            4.000 2.384   0.803    0.06
s(I(DistToShore/1000))         4.000 2.572   0.780    0.00
s(I(DistTo125m/1000))          4.000 3.011   0.771    0.00
s(I(DistTo300m/1000))          4.000 3.473   0.791    0.00
s(log10(pmax(ClimEKE, 1e-04))) 4.000 2.442   0.762    0.00
s(I(ClimCumVGPM90^(1/3)))      4.000 2.893   0.801    0.05
```

Predictors retained during the model selection procedure: Depth, Slope, DistToShore, DistTo125m, DistTo300m, ClimEKE, ClimCumVGPM90

Predictors dropped during the model selection procedure: ClimSST, ClimDistToFront1

Model term plots

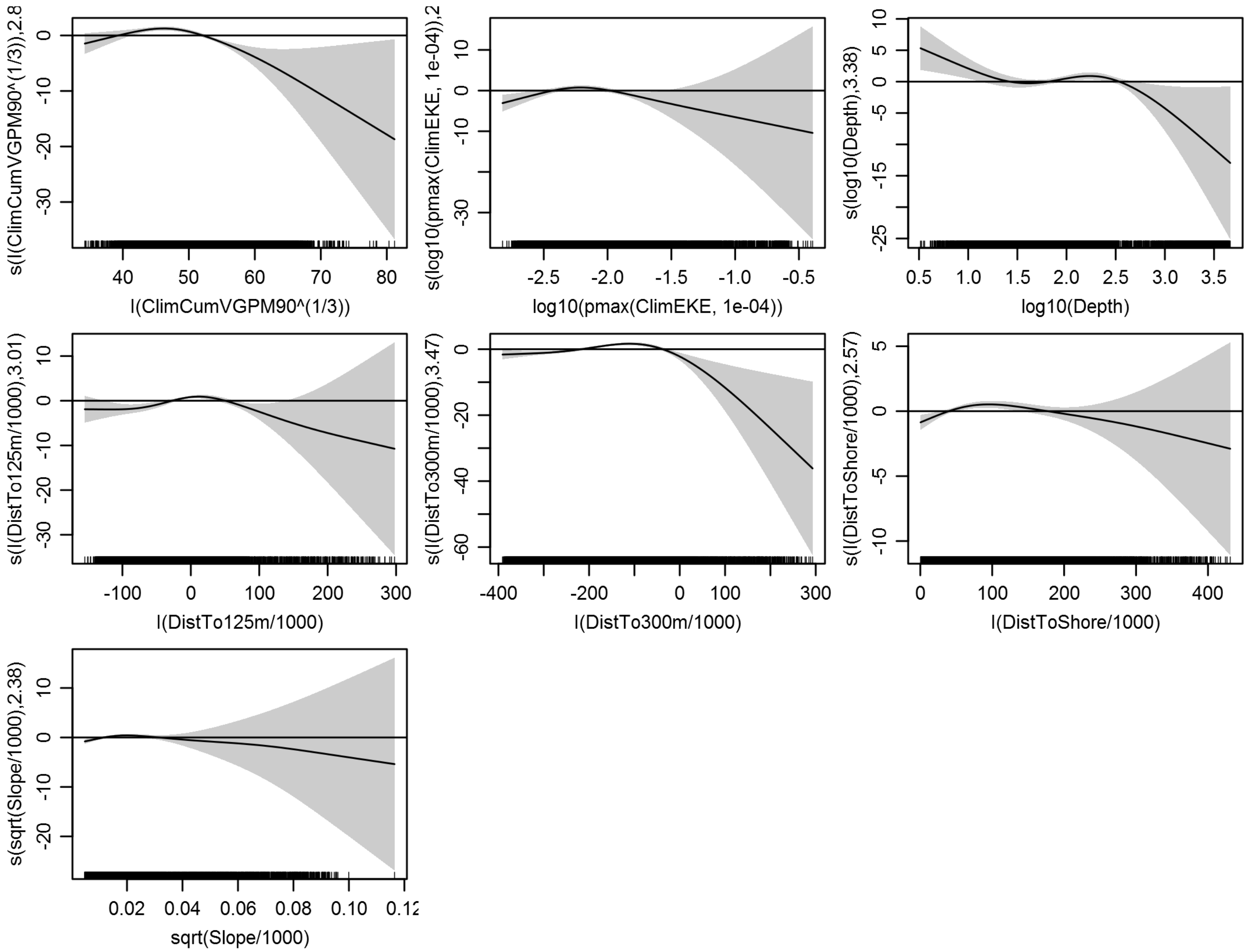

Diagnostic plots

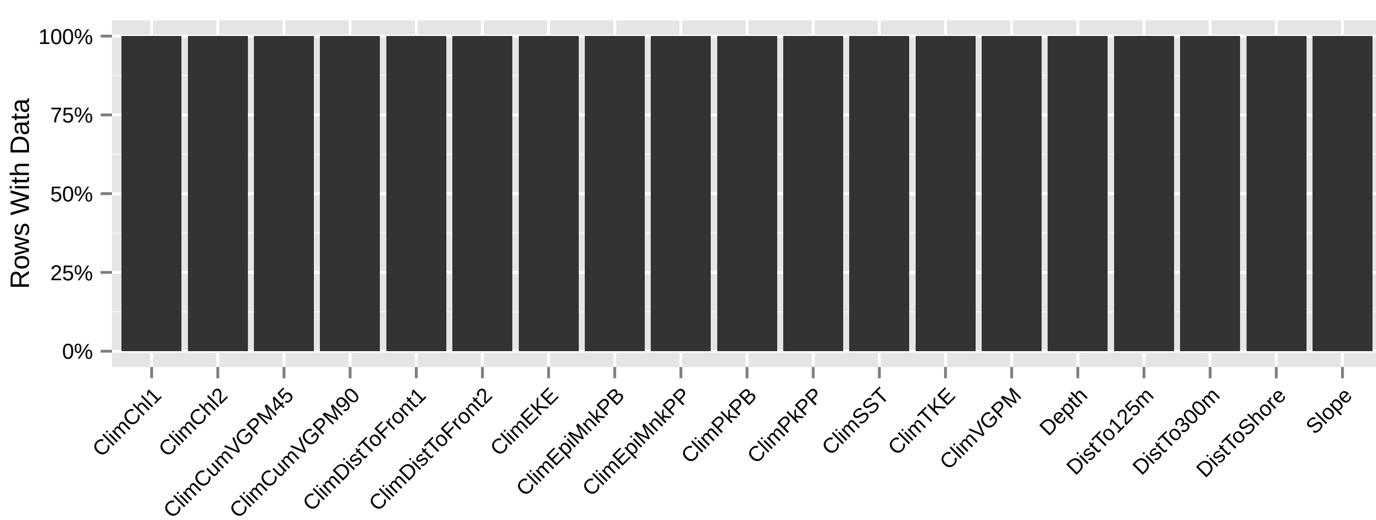

Figure 128: Segments with predictor values for the North Atlantic right whale Climatological model, Summer season, North of Gulf Stream. This plot is used to assess how many segments would be lost by including a given predictor in a model.

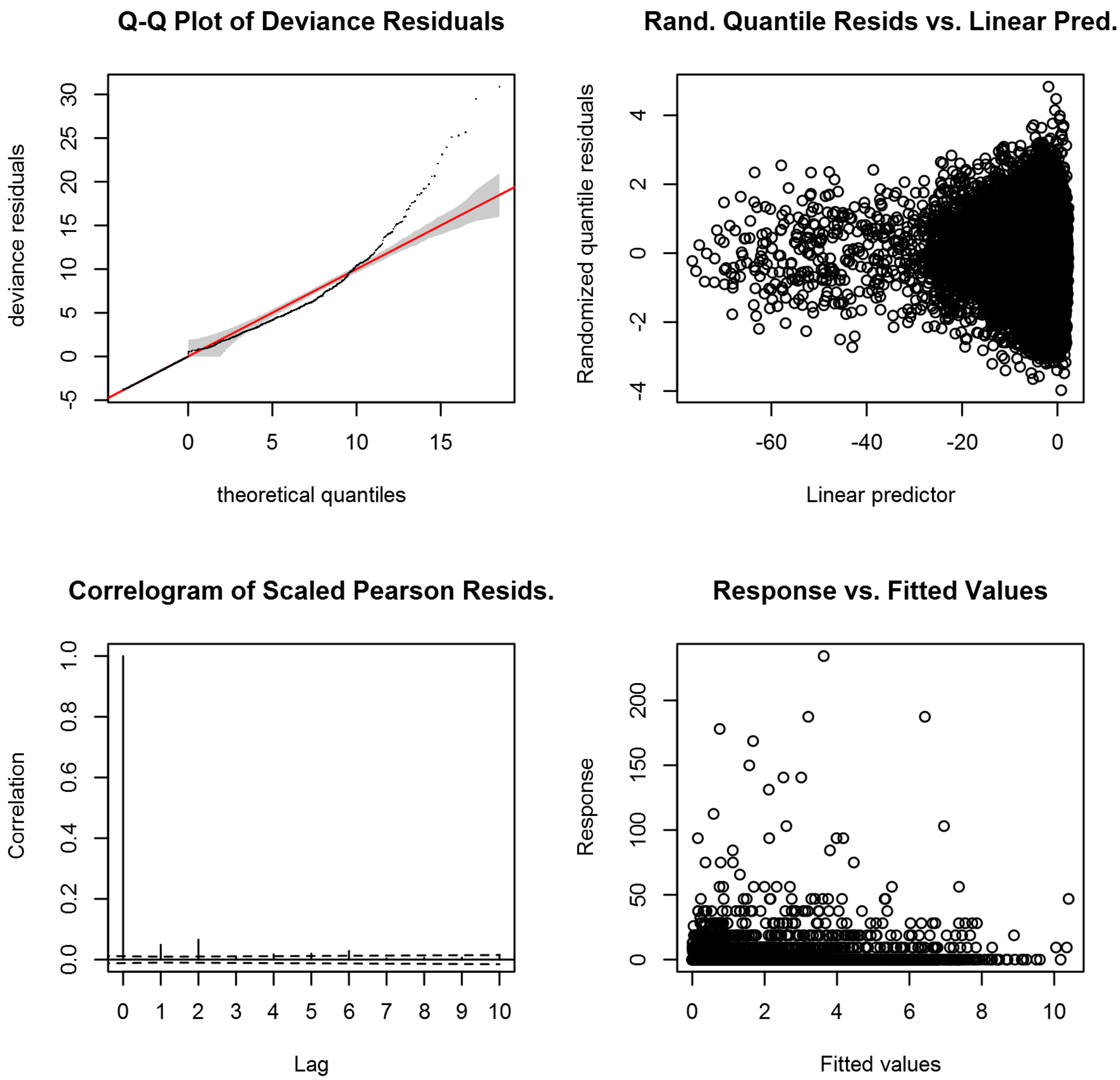

Figure 129: Statistical diagnostic plots for the North Atlantic right whale Climatological model, Summer season, North of Gulf Stream.

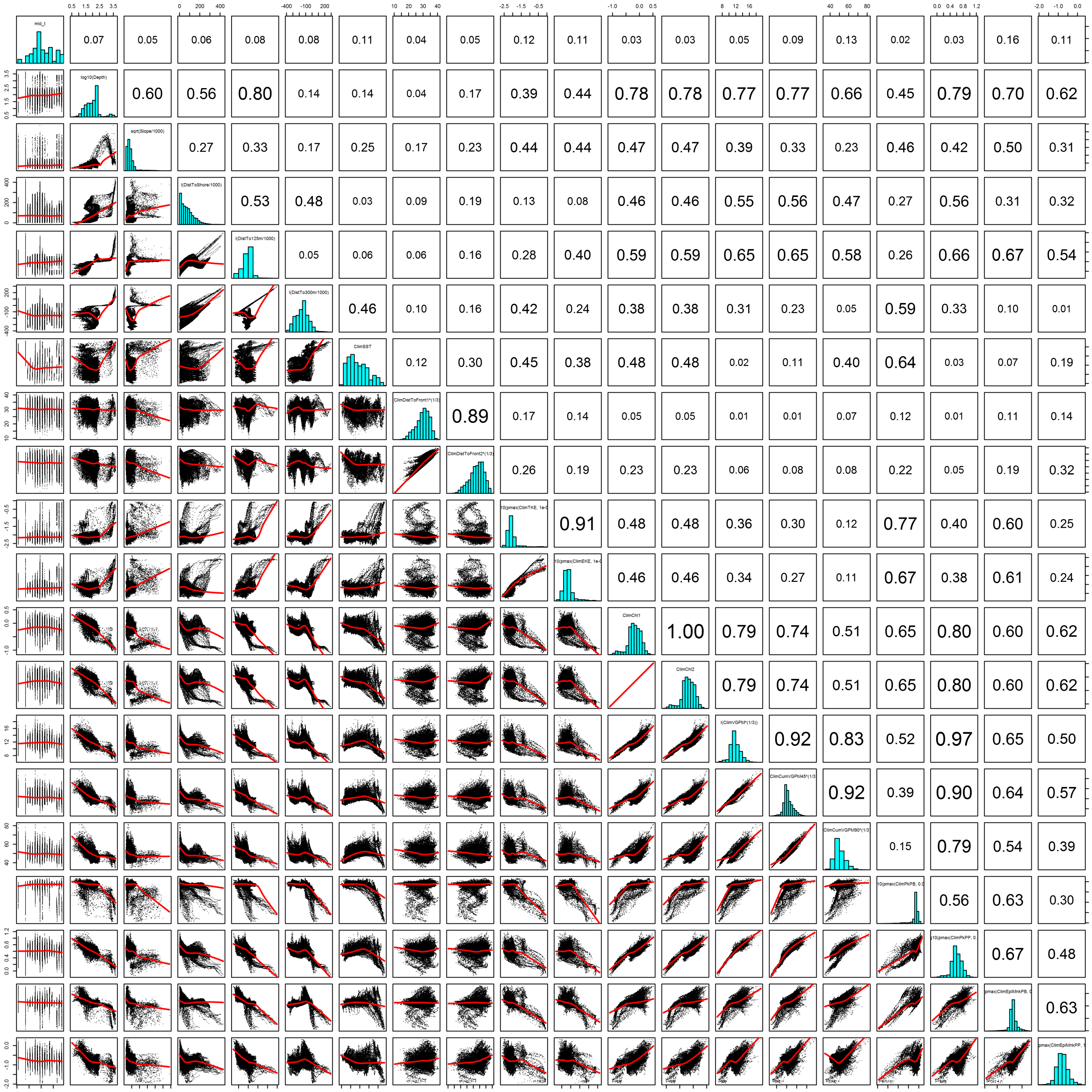

Figure 130: Scatterplot matrix for the North Atlantic right whale Climatological model, Summer season, North of Gulf Stream. This plot is used to inspect the distribution of predictors (via histograms along the diagonal), simple correlation between predictors (via pairwise Pearson coefficients above the diagonal), and linearity of predictor correlations (via scatterplots below the diagonal). This plot is best viewed at high magnification.

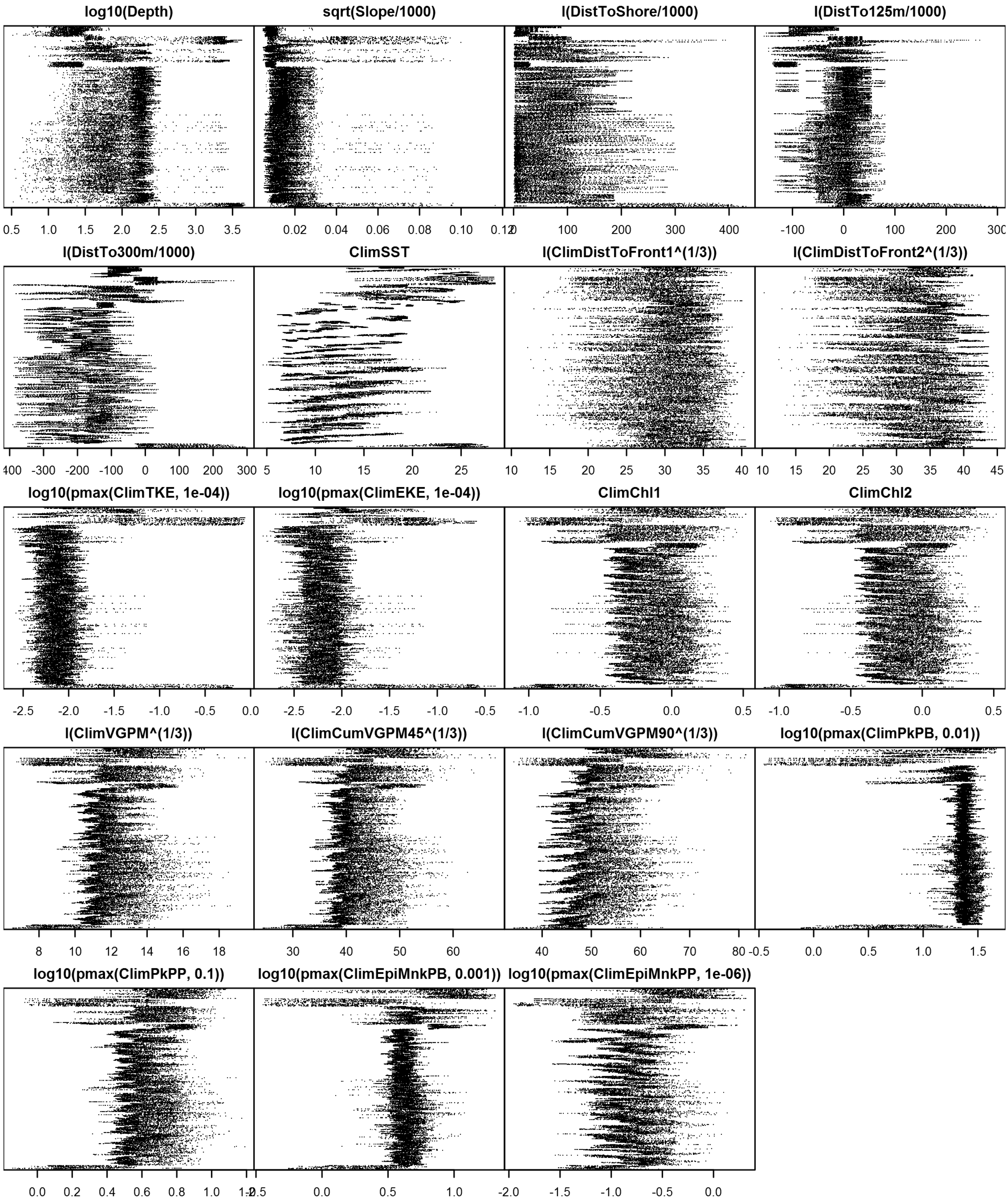

Figure 131: Dotplot for the North Atlantic right whale Climatological model, Summer season, North of Gulf Stream. This plot is used to check for suspicious patterns and outliers in the data. Points are ordered vertically by transect ID, sequentially in time.

Shelf South of Gulf Stream

A mean density estimate was made for this region. First, density (individuals per square kilometer) was calculated as the number of animals encountered divided by the area effectively surveyed, corrected by the detection functions and g(0) estimates. Then, density was multiplied by the size of each grid cell, in square kilometers, to obtain abundance (number of individuals) per grid cell. Finally, all grid cells in the region were assigned this abundance value.

Off Shelf South of Gulf Stream

Density assumed to be 0 in this region.

Low Effort Area

Density was not modeled for this region.

Fall

In mid to late summer, right whales typically move northeast from the Great South Channel to feed in the lower Bay of Fundy and on the southeastern Scotian Shelf, particularly in Roseway Basin (Winn et al. 1986). They have also been observed farther north on the Scotian Shelf, particularly in August-October, by acoustic monitoring (Mellinger et al. 2007) and by whalers (Mitchell et al. 1986). Their distribution in fall is less understood. As fall progresses, many are presumed to depart the Canadian feeding grounds and disperse to several different areas. Calving females migrate to feeding grounds in the southeast U.S. (Winn et al. 1986). Some juveniles and males also migrate to this area (Keller et al. 2012). Another segment of the population may move southwest in the Gulf of Maine to Jeffreys Ledge (Weinrich et al. 2000). Still others may move to the central Gulf of Maine, a possible mating ground (Cole et al. 2013).

In our fall season, defined as August-October (see reasoning under the Density Models heading above), the shelf and shelf-break were surveyed across the entire study area, with the most intense effort occurring in the Gulf of Maine feeding grounds. This was the only season in which Canada was surveyed, although the surveying was constrained to August. In August, nearly all of the sightings occurred in or near the lower Bay of Fundy and Roseway Basin. In September, only two sightings were reported, but surveying in Canada only occurred at the beginning of the month in the northern half of the Scotian Shelf, which is not believed to be primary habitat for right whales. In October, many sightings were reported in the central Gulf of Maine and somewhat less near Jeffreys Ledge. No sightings were reported south of Rhode Island during any of these months, but surveying was very sparse except in August.

As with summer, we split the study area at the Gulf Stream. North of here, where all sightings occurred, we fitted a full model, except for the northern Scotian Shelf, which is not believed to be primary habitat for right whales and where we judged survey effort to be insufficient to model spatial distribution confidently. South of the Gulf Stream, where oceanographic conditions differ substantially from the north, no sightings were reported. Accordingly, we assumed the species was absent, but other evidence may indicate otherwise (see Discussion section below).

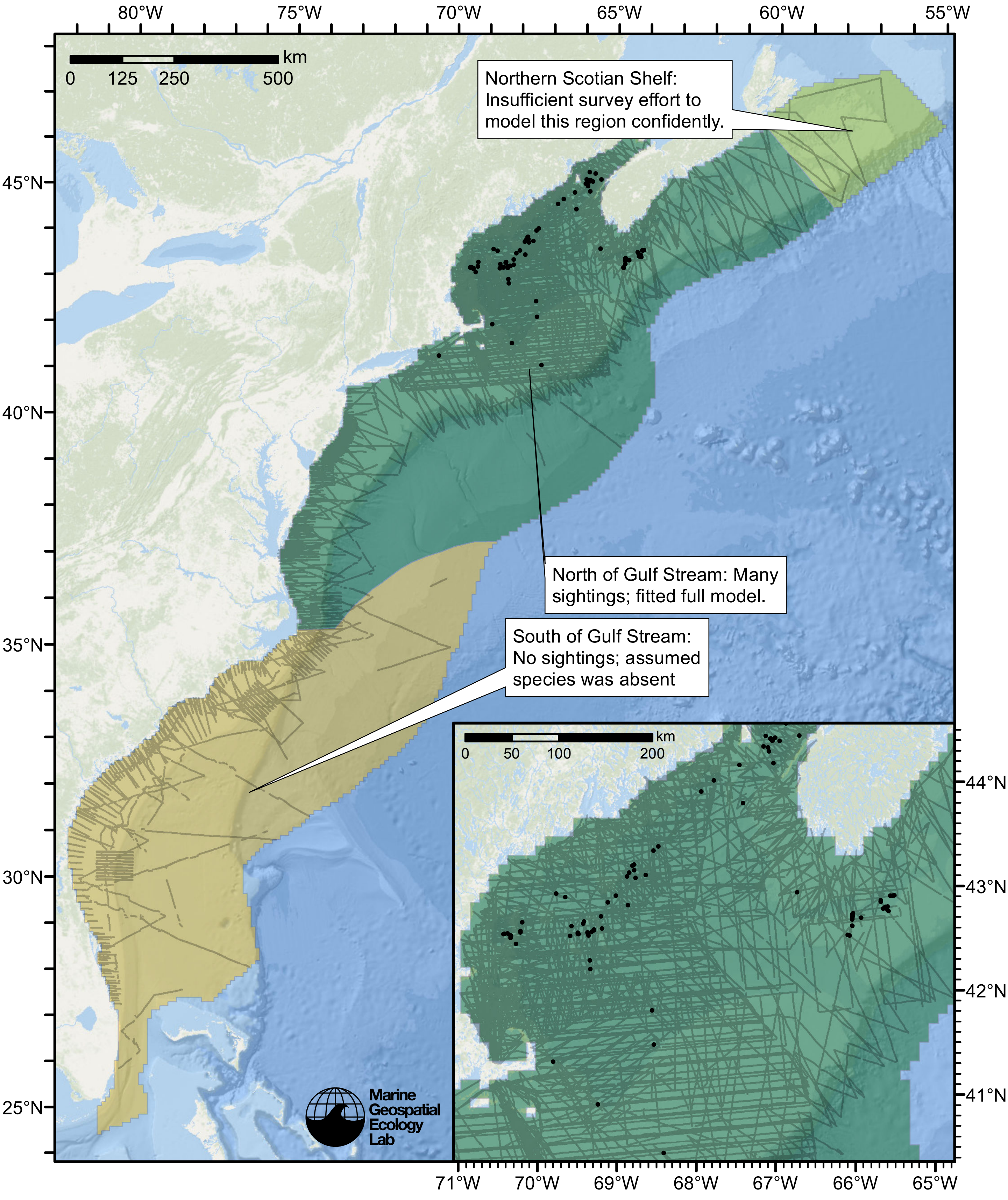

Figure 132: North Atlantic right whale density model schematic for Fall season. All on-effort sightings are shown, including those that were truncated when detection functions were fitted.

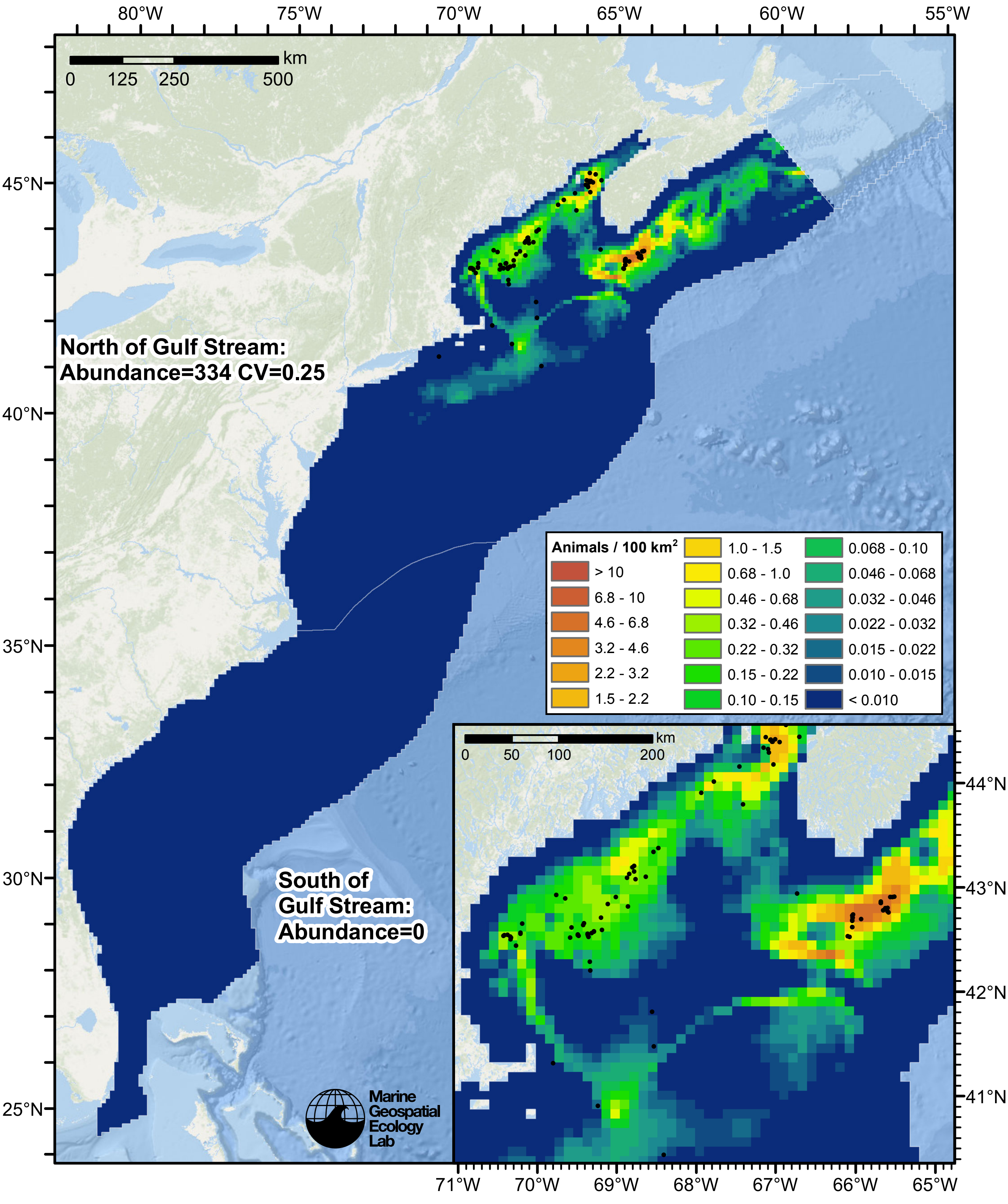

Figure 133: North Atlantic right whale density predicted by the Fall season climatological model that explained the most deviance. Pixels are 10x10 km. The legend gives the estimated individuals per pixel; breaks are logarithmic. The same scale is used for all seasons. Abundance for each region was computed by summing the density cells occuring in that region.

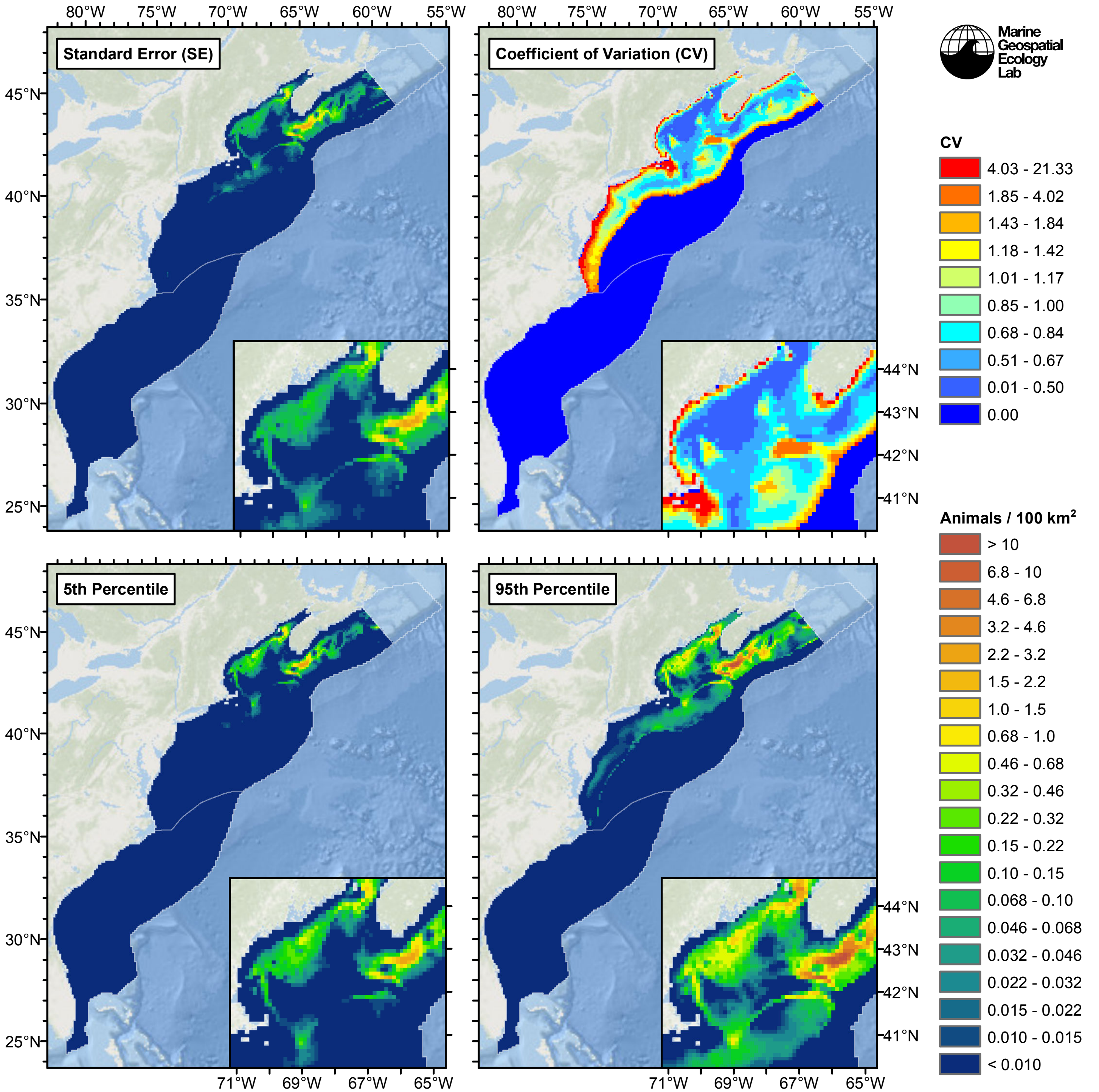

Figure 134: Estimated uncertainty for the Fall season climatological model that explained the most deviance. These estimates only incorporate the statistical uncertainty estimated for the spatial model (by the R mgcv package). They do not incorporate uncertainty in the detection functions, g(0) estimates, predictor variables, and so on.

North of Gulf Stream

Statistical output

```
Rscript.exe: This is mgcv 1.8-2. For overview type 'help("mgcv-package")'.


Family: Tweedie(p=1.22)
```

```
Link function: log

Formula:
abundance ~ offset(log(area_km2)) + s(log10(Depth), bs = "ts",
    k = 5) + s(I(DistToShore/1000), bs = "ts", k = 5) + s(I(DistTo300m/1000),
    bs = "ts", k = 5) + s(ClimSST, bs = "ts", k = 5) + s(I(ClimDistToFront1^(1/3)),
    bs = "ts", k = 5) + s(log10(pmax(ClimPkPP, 0.1)), bs = "ts",
    k = 5)

Parametric coefficients:
            Estimate Std. Error t value Pr(>|t|)
(Intercept)  -24.562      4.019  -6.112 1.01e-09 ***
---
Signif. codes:  0 '***' 0.001 '**' 0.01 '*' 0.05 '.' 0.1 ' ' 1

Approximate significance of smooth terms:
                                edf Ref.df      F  p-value
s(log10(Depth))              3.7178      4 17.455 2.44e-15 ***
s(I(DistToShore/1000))       0.8807      4  1.398 0.009689 **
s(I(DistTo300m/1000))        3.8273      4 14.440 1.35e-12 ***
s(ClimSST)                   0.9987      4  3.138 0.000199 ***
s(I(ClimDistToFront1^(1/3)))  2.4871      4  3.157 0.001625 **
s(log10(pmax(ClimPkPP, 0.1))) 0.9187      4  1.900 0.002561 **
---
Signif. codes:  0 '***' 0.001 '**' 0.01 '*' 0.05 '.' 0.1 ' ' 1

R-sq.(adj) =  0.0325   Deviance explained = 46.1%
-REML = 569.42  Scale est. = 27.343    n = 12828

All predictors were significant. This is the final model.
Creating term plots.
Diagnostic output from gam.check():

Method: REML   Optimizer: outer newton
full convergence after 13 iterations.
Gradient range [-1.897547e-08,1.202844e-08]
(score 569.4171 & scale 27.34285).
Hessian positive definite, eigenvalue range [0.270899,323.0364].
Model rank =  25 / 25

Basis dimension (k) checking results. Low p-value (k-index<1) may
indicate that k is too low, especially if edf is close to k'.

                                 k'   edf k-index p-value
s(log10(Depth))              4.000 3.718   0.800    0.00
s(I(DistToShore/1000))       4.000 0.881   0.864    0.03
s(I(DistTo300m/1000))        4.000 3.827   0.816    0.00
s(ClimSST)                   4.000 0.999   0.839    0.00
s(I(ClimDistToFront1^(1/3)))  4.000 2.487   0.880    0.06
s(log10(pmax(ClimPkPP, 0.1))) 4.000 0.919   0.857    0.01
```

Predictors retained during the model selection procedure: Depth, DistToShore, DistTo300m, ClimSST, ClimDistToFront1, ClimPkPP

Predictors dropped during the model selection procedure: Slope, DistTo125m, ClimTKE

Model term plots

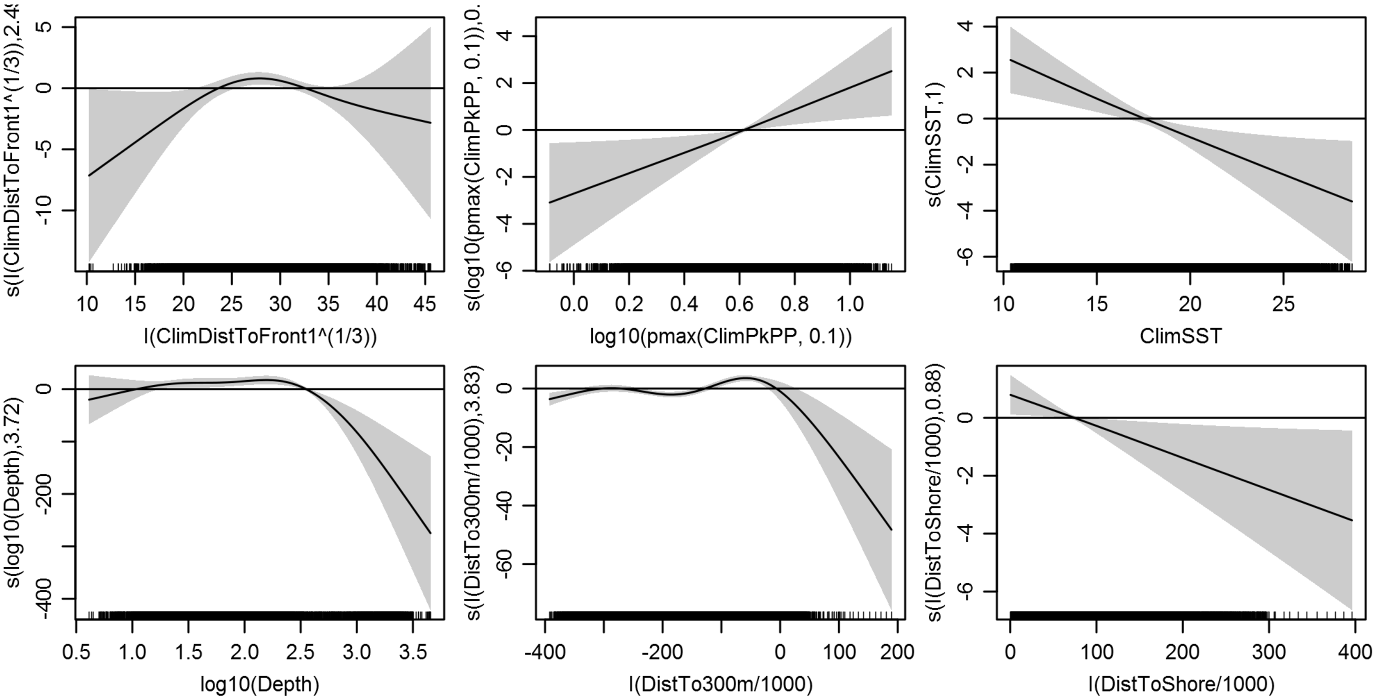

Diagnostic plots

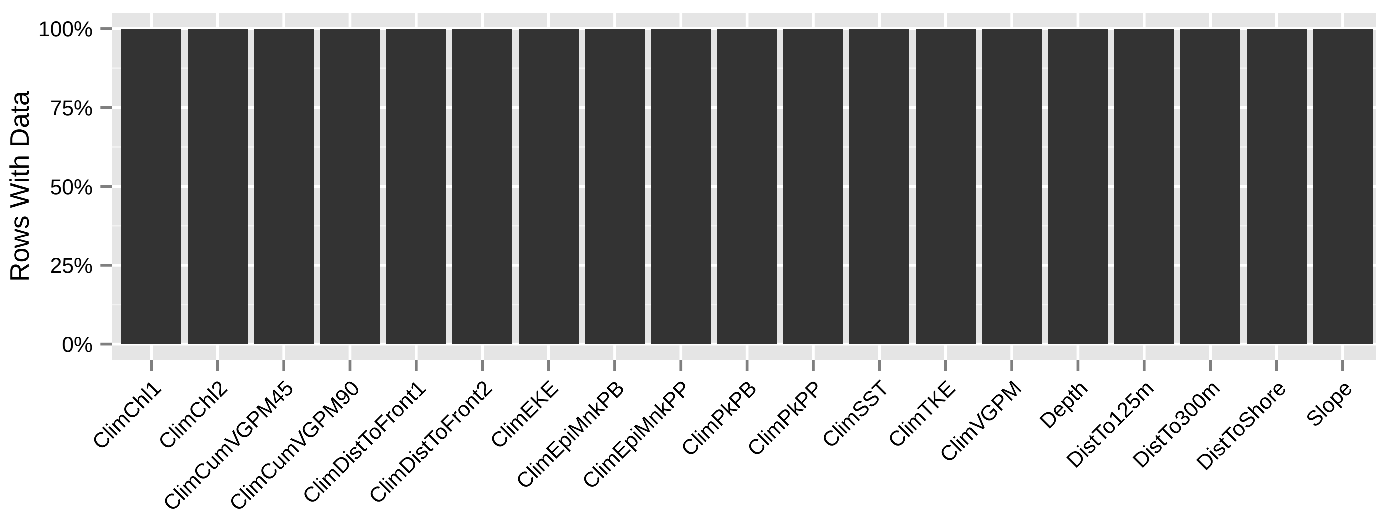

Figure 135: Segments with predictor values for the North Atlantic right whale Climatological model, Fall season, North of Gulf Stream. This plot is used to assess how many segments would be lost by including a given predictor in a model.

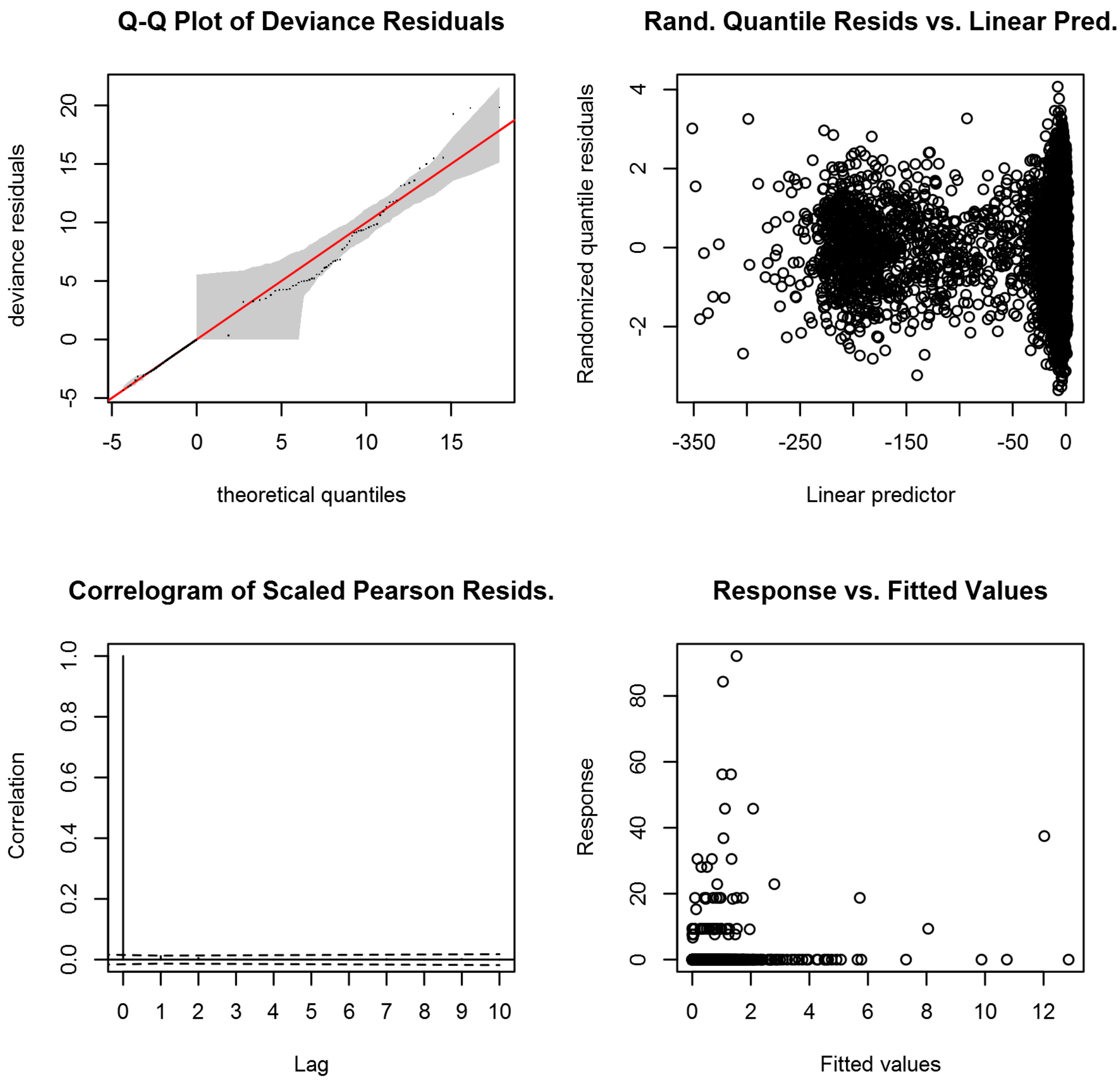

Figure 136: Statistical diagnostic plots for the North Atlantic right whale Climatological model, Fall season, North of Gulf Stream.

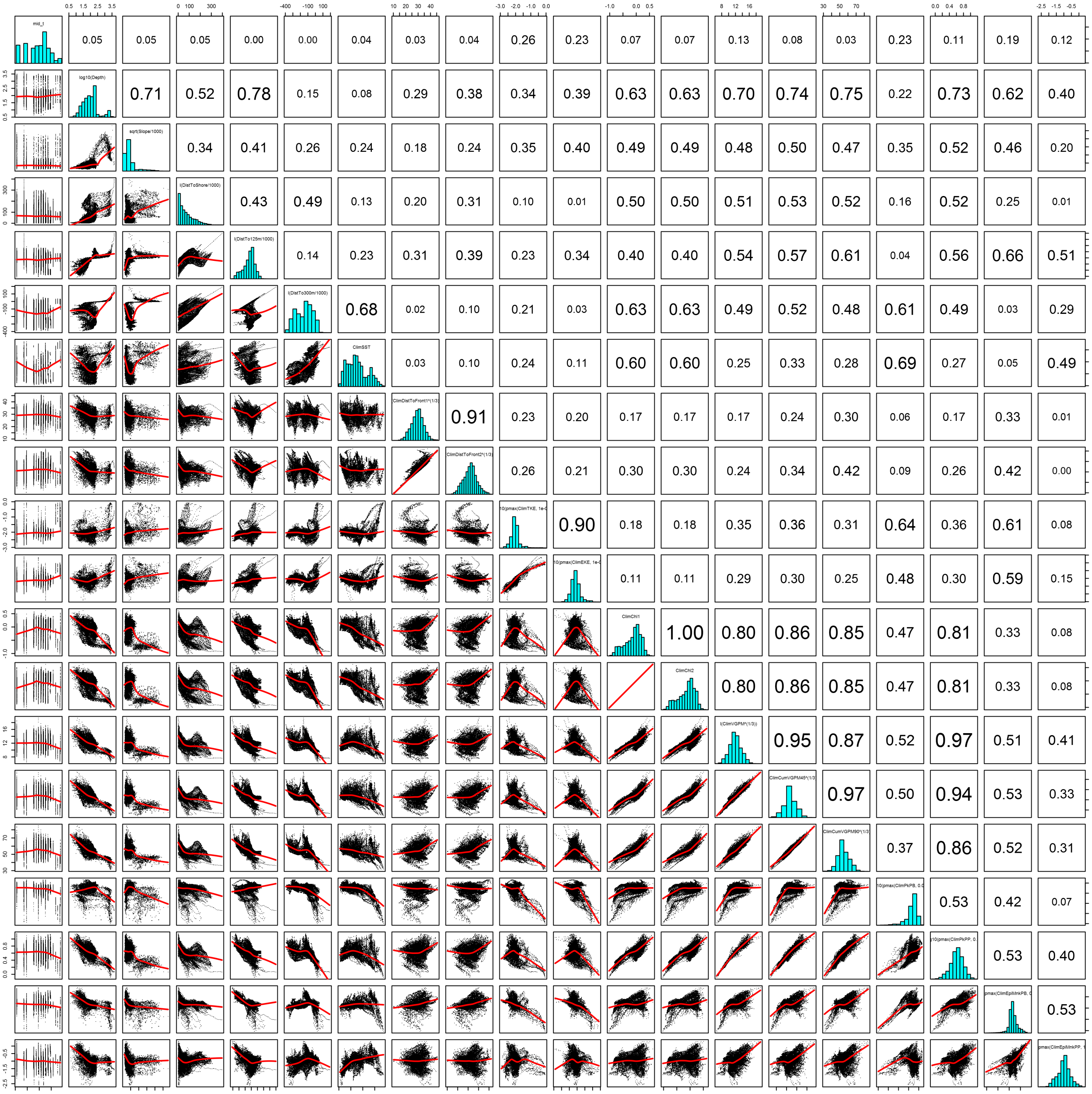

Figure 137: Scatterplot matrix for the North Atlantic right whale Climatological model, Fall season, North of Gulf Stream. This plot is used to inspect the distribution of predictors (via histograms along the diagonal), simple correlation between predictors (via pairwise Pearson coefficients above the diagonal), and linearity of predictor correlations (via scatterplots below the diagonal). This plot is best viewed at high magnification.

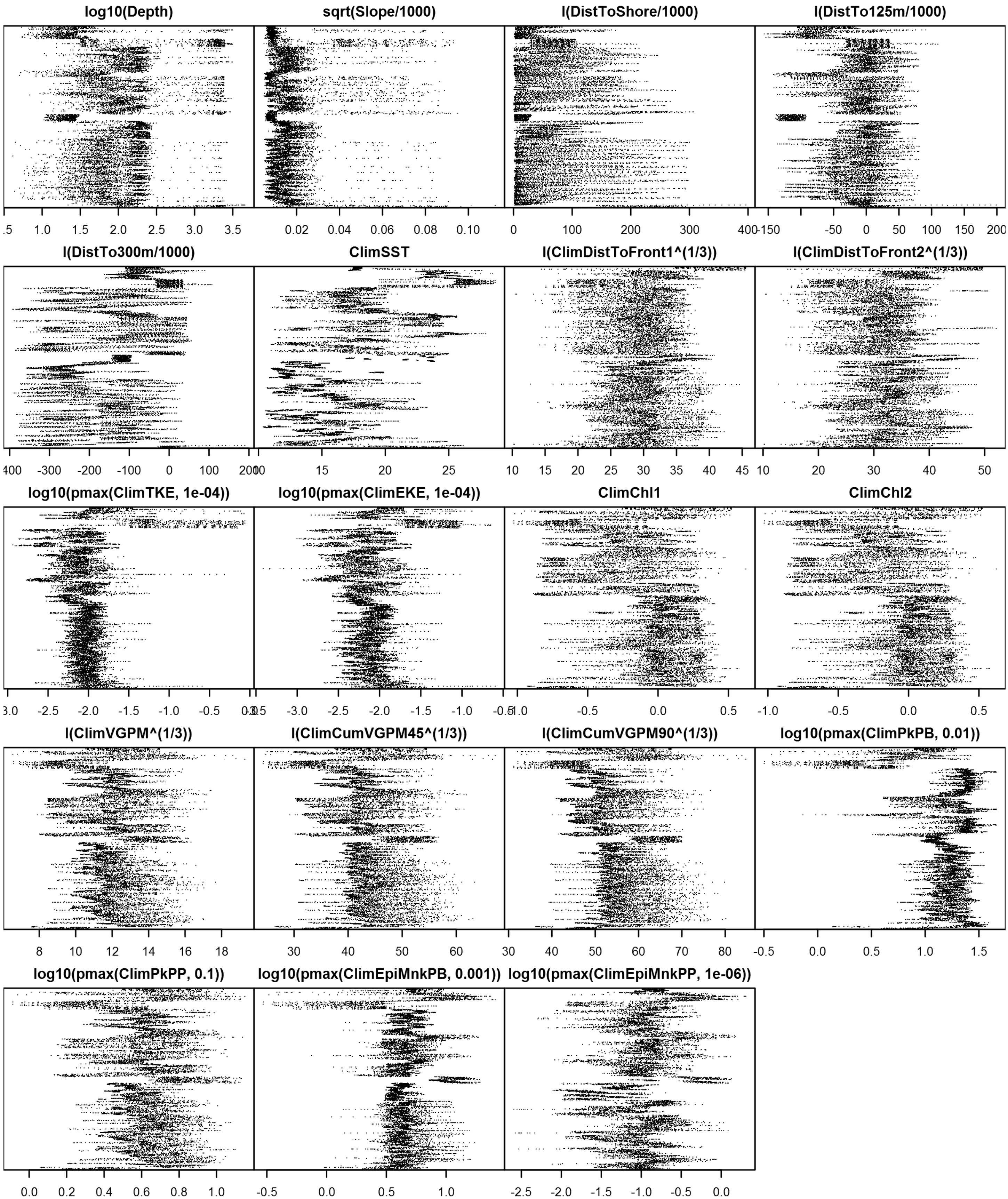

Figure 138: Dotplot for the North Atlantic right whale Climatological model, Fall season, North of Gulf Stream. This plot is used to check for suspicious patterns and outliers in the data. Points are ordered vertically by transect ID, sequentially in time.

South of Gulf Stream

Density assumed to be 0 in this region.

Northern Scotian Shelf

Density was not modeled for this region.

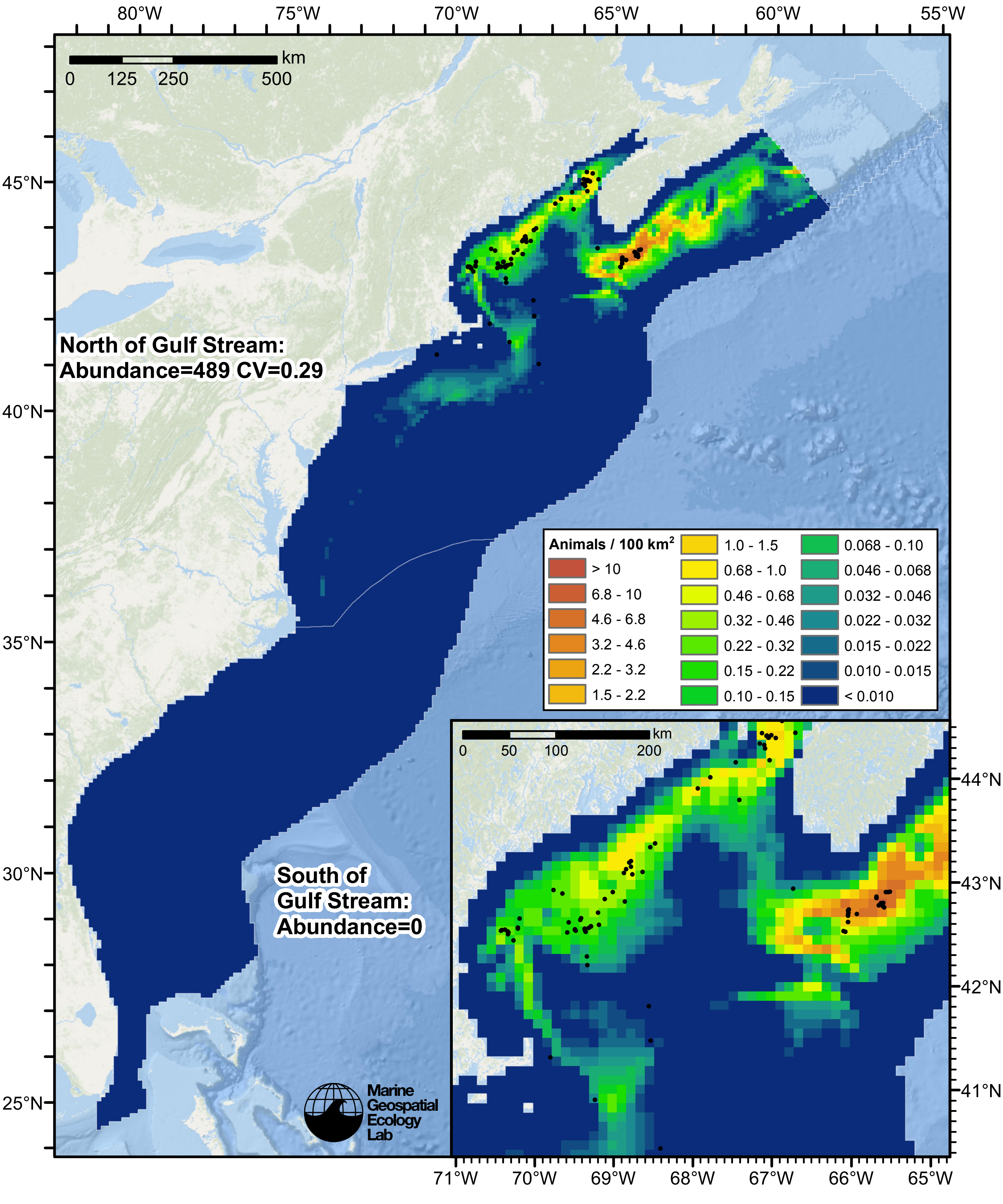

Figure 139: North Atlantic right whale density predicted by the Fall season contemporaneous model that explained the most deviance. Pixels are 10x10 km. The legend gives the estimated individuals per pixel; breaks are logarithmic. The same scale is used for all seasons. Abundance for each region was computed by summing the density cells occuring in that region.

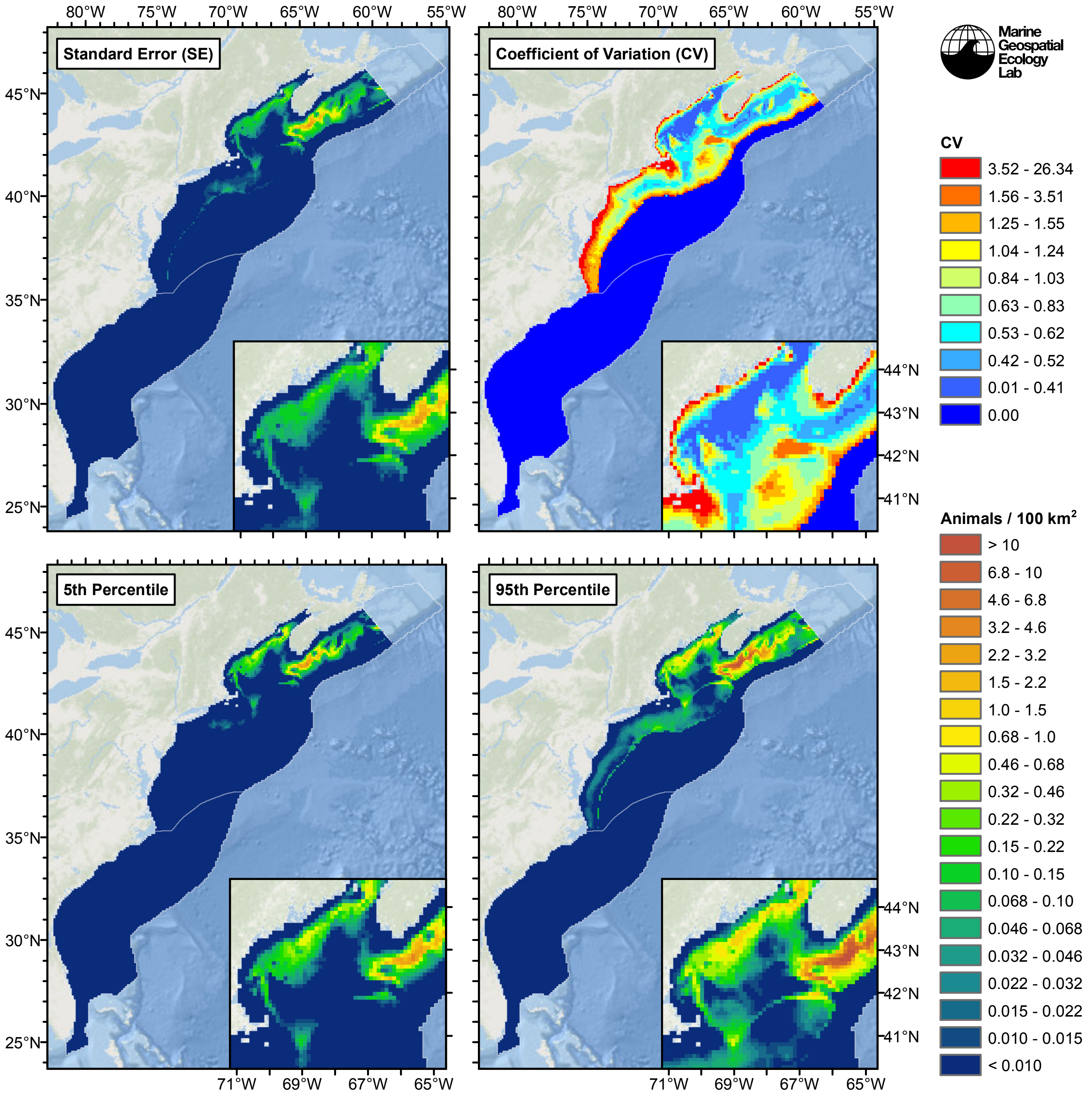

Figure 140: Estimated uncertainty for the Fall season contemporaneous model that explained the most deviance. These estimates only incorporate the statistical uncertainty estimated for the spatial model (by the R mgcv package). They do not incorporate uncertainty in the detection functions, g(0) estimates, predictor variables, and so on.

North of Gulf Stream

Statistical output

```
Rscript.exe: This is mgcv 1.8-2. For overview type 'help("mgcv-package")'.


Family: Tweedie(p=1.231)
```

```
Link function: log

Formula:
abundance ~ offset(log(area_km2)) + s(log10(Depth), bs = "ts",
    k = 5) + s(I(DistToShore/1000), bs = "ts", k = 5) + s(I(DistTo300m/1000),
    bs = "ts", k = 5) + s(SST, bs = "ts", k = 5) + s(I(DistToFront1^(1/3)),
    bs = "ts", k = 5)

Parametric coefficients:
            Estimate Std. Error t value Pr(>|t|)
(Intercept)  -21.736      3.607  -6.026 1.73e-09 ***
---
Signif. codes:  0 '***' 0.001 '**' 0.01 '*' 0.05 '.' 0.1 ' ' 1

Approximate significance of smooth terms:
                             edf Ref.df      F  p-value
s(log10(Depth))          3.6531      4 17.516 2.38e-15 ***
s(I(DistToShore/1000))   0.9515      4  2.794 0.000447 ***
s(I(DistTo300m/1000))    3.8183      4 12.342 1.32e-10 ***
s(SST)                   1.0056      4  3.522 0.000102 ***
s(I(DistToFront1^(1/3))) 2.1673      4  1.600 0.034814 *
---
Signif. codes:  0 '***' 0.001 '**' 0.01 '*' 0.05 '.' 0.1 ' ' 1

R-sq.(adj) =  0.0277   Deviance explained = 44.4%
-REML = 571.86  Scale est. = 28.857    n = 12828

All predictors were significant. This is the final model.
Creating term plots.
Diagnostic output from gam.check():

Method: REML   Optimizer: outer newton
full convergence after 17 iterations.
Gradient range [-0.0001115175,2.906641e-05]
(score 571.8587 & scale 28.85658).
Hessian positive definite, eigenvalue range [0.4185059,316.554].
Model rank =  21 / 21

Basis dimension (k) checking results. Low p-value (k-index<1) may
indicate that k is too low, especially if edf is close to k'.

                            k'   edf k-index p-value
s(log10(Depth))          4.000 3.653   0.840    0.01
s(I(DistToShore/1000))   4.000 0.951   0.893    0.12
s(I(DistTo300m/1000))    4.000 3.818   0.830    0.00
s(SST)                   4.000 1.006   0.863    0.01
s(I(DistToFront1^(1/3))) 4.000 2.167   0.908    0.57

Predictors retained during the model selection procedure: Depth, DistToShore, DistTo300m, SST,
DistToFront1

Predictors dropped during the model selection procedure: Slope, DistTo125m
```

Model term plots

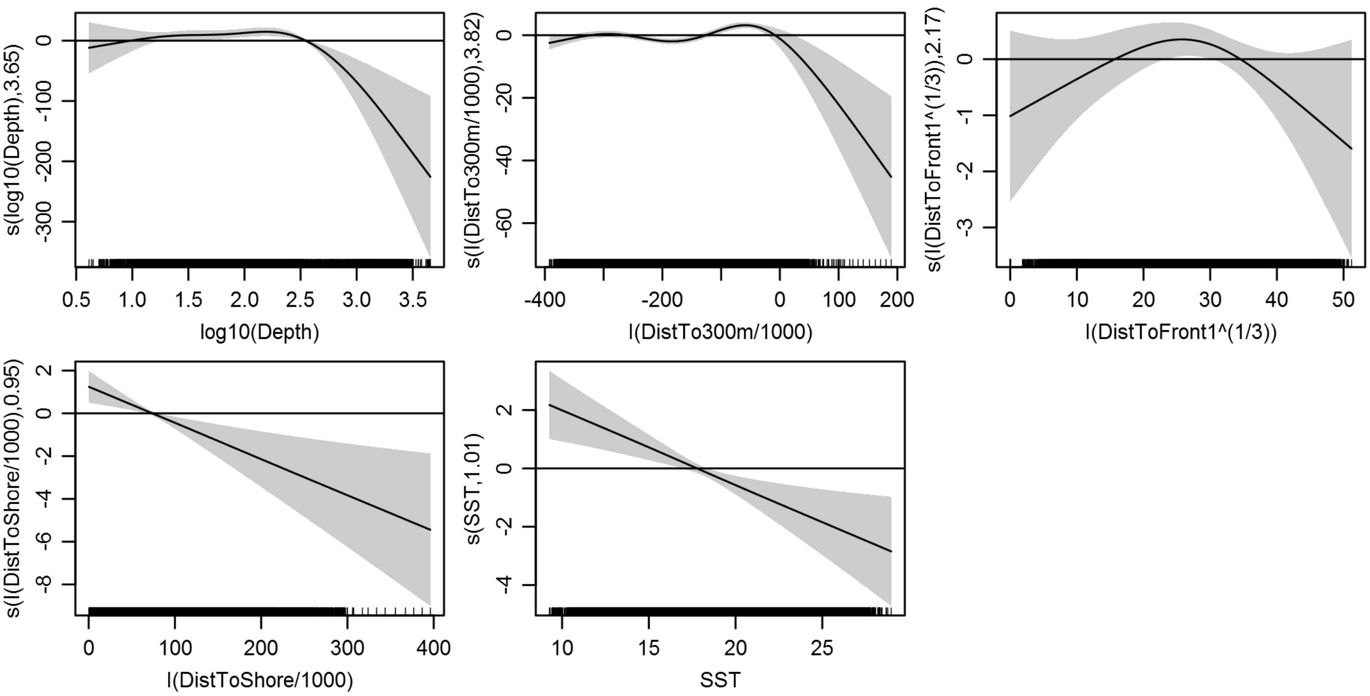

Diagnostic plots

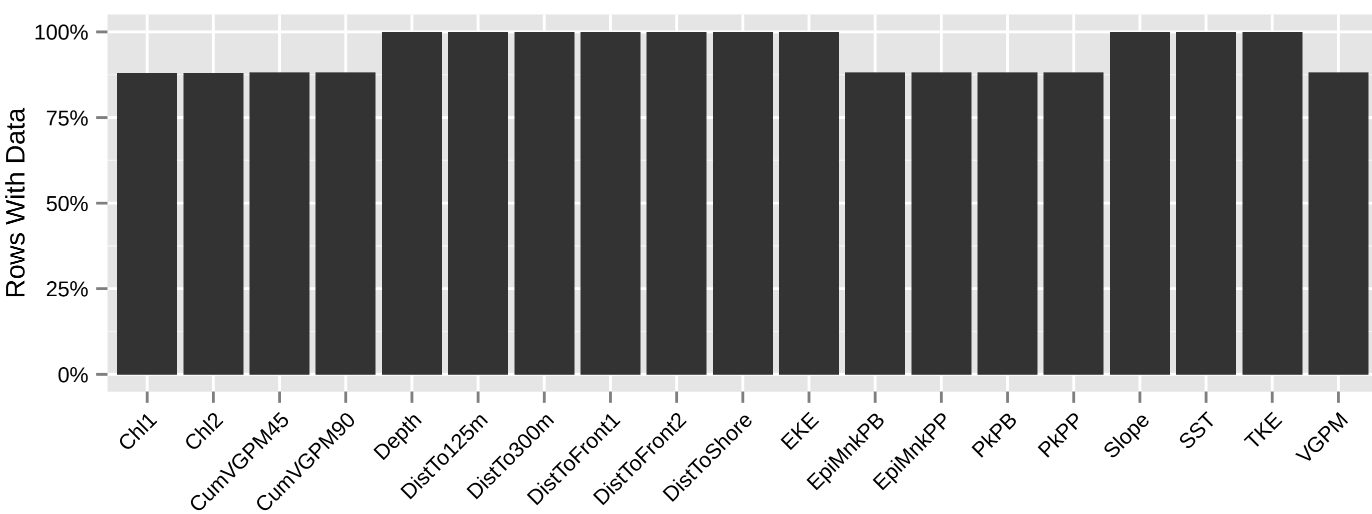

Figure 141: Segments with predictor values for the North Atlantic right whale Contemporaneous model, Fall season, North of Gulf Stream. This plot is used to assess how many segments would be lost by including a given predictor in a model.

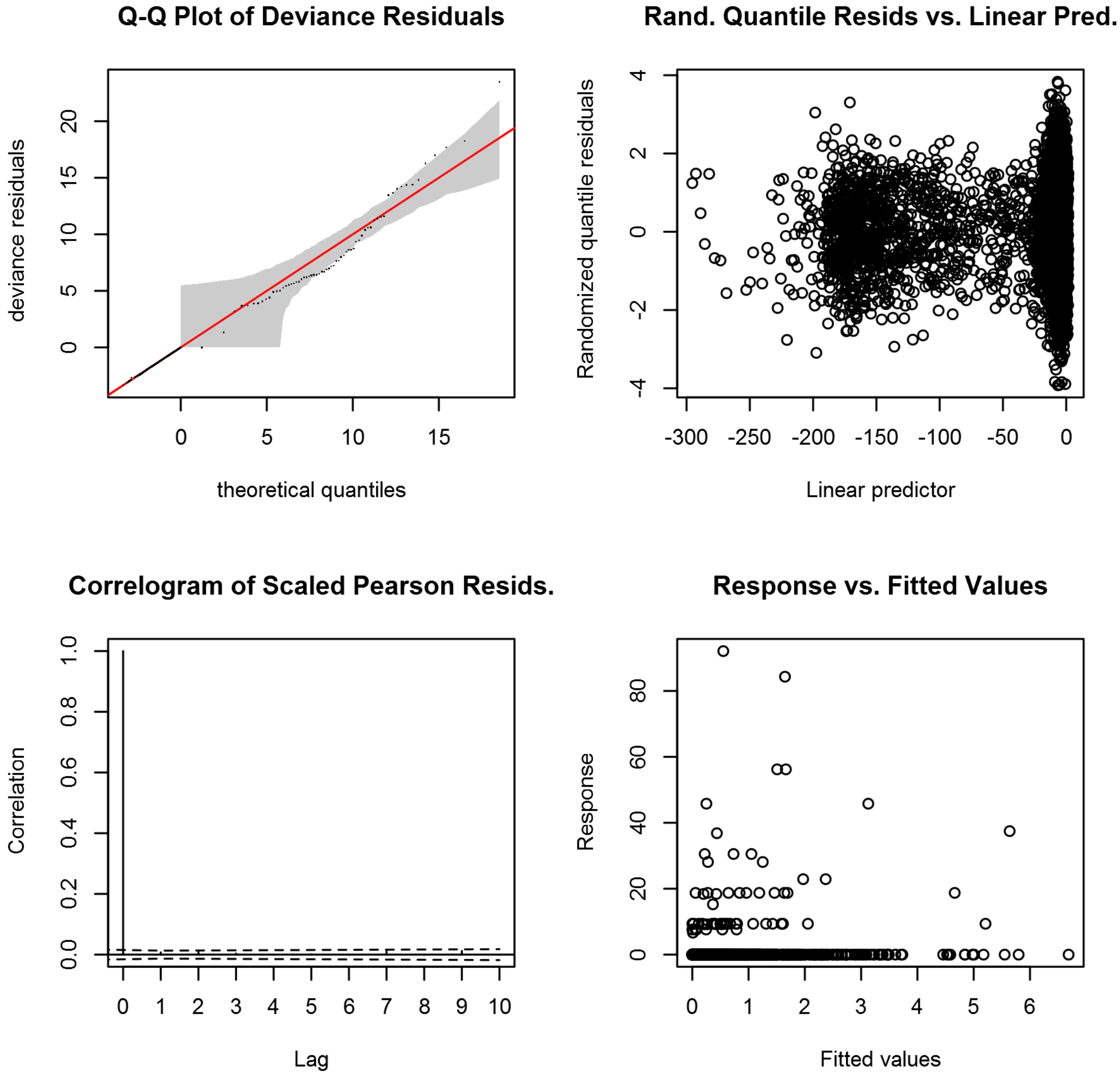

Figure 142: Statistical diagnostic plots for the North Atlantic right whale Contemporaneous model, Fall season, North of Gulf Stream.

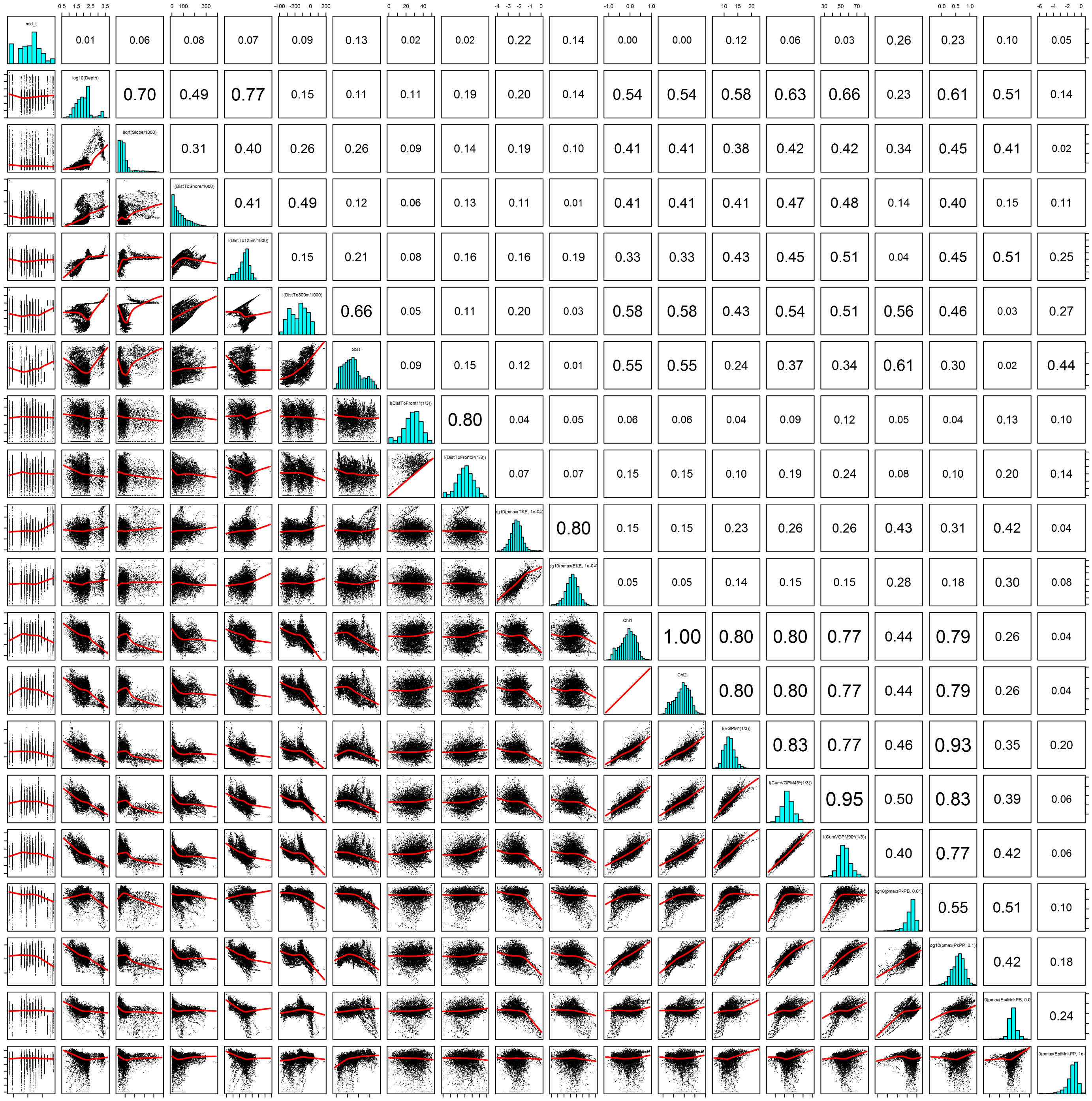

Figure 143: Scatterplot matrix for the North Atlantic right whale Contemporaneous model, Fall season, North of Gulf Stream. This plot is used to inspect the distribution of predictors (via histograms along the diagonal), simple correlation between predictors (via pairwise Pearson coefficients above the diagonal), and linearity of predictor correlations (via scatterplots below the diagonal). This plot is best viewed at high magnification.

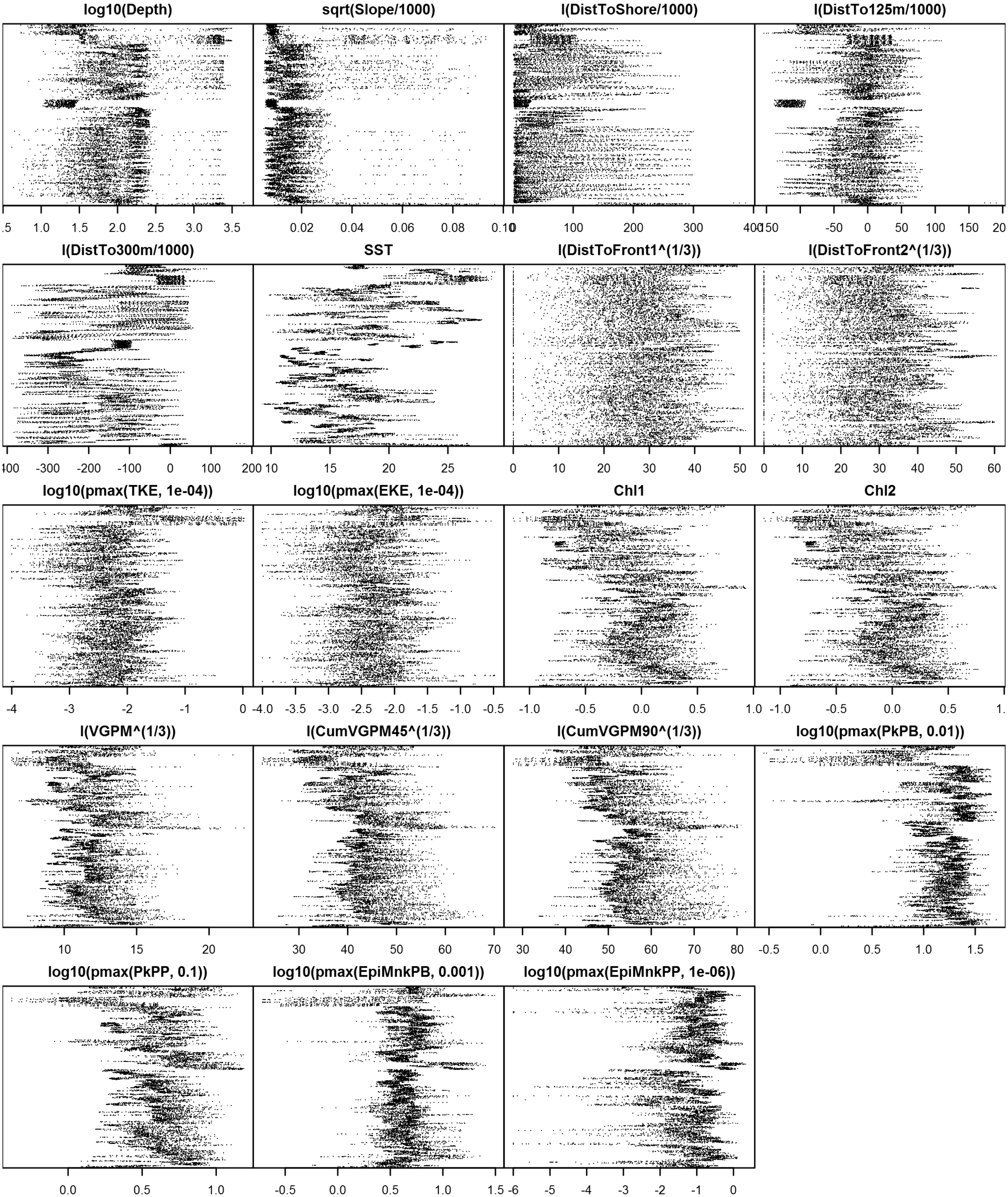

Figure 144: Dotplot for the North Atlantic right whale Contemporaneous model, Fall season, North of Gulf Stream. This plot is used to check for suspicious patterns and outliers in the data. Points are ordered vertically by transect ID, sequentially in time.

South of Gulf Stream

Density assumed to be 0 in this region.

Northern Scotian Shelf

Density was not modeled for this region.

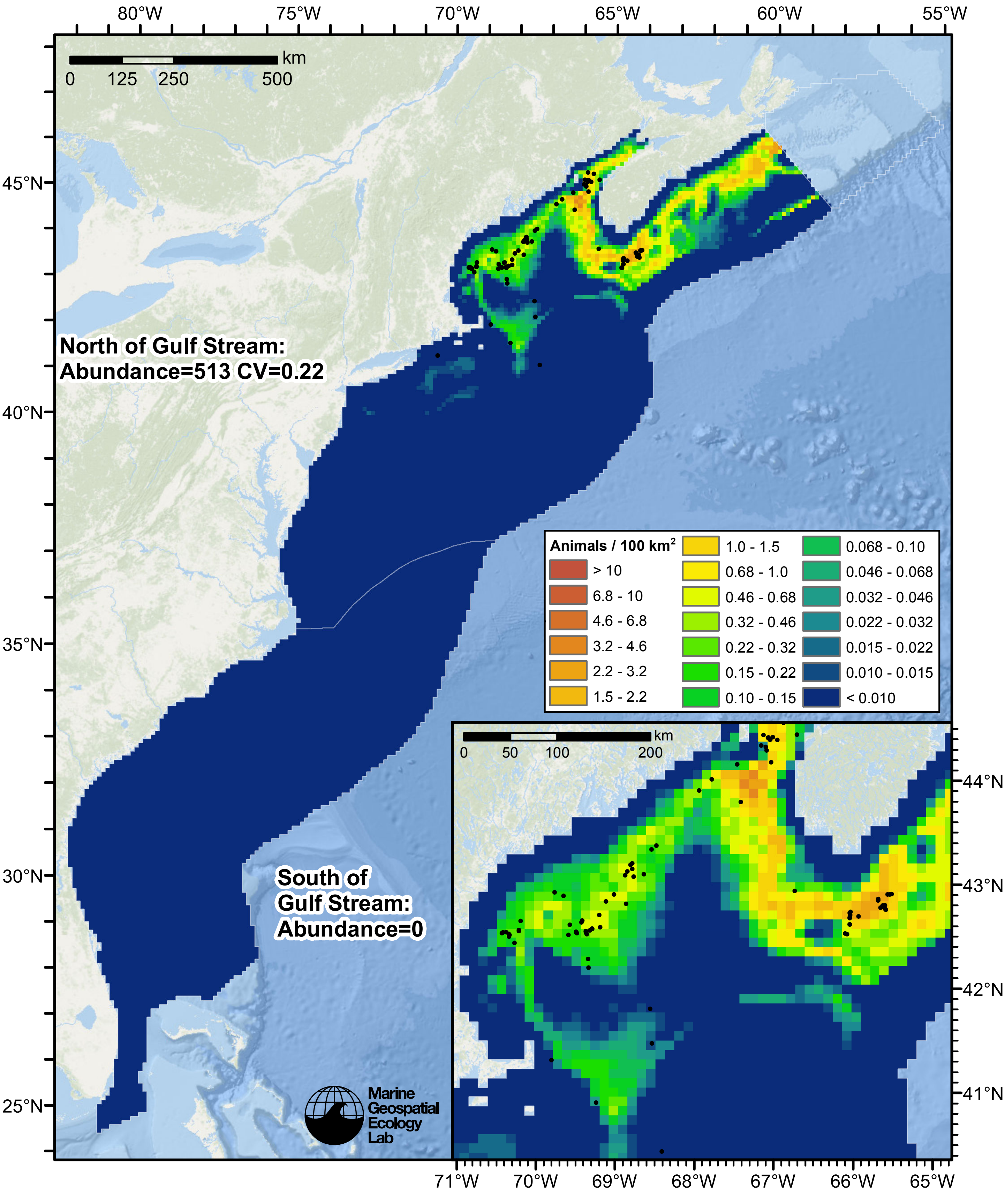

Figure 145: North Atlantic right whale density predicted by the Fall season climatological same segments model that explained the most deviance. Pixels are 10x10 km. The legend gives the estimated individuals per pixel; breaks are logarithmic. The same scale is used for all seasons. Abundance for each region was computed by summing the density cells occuring in that region.

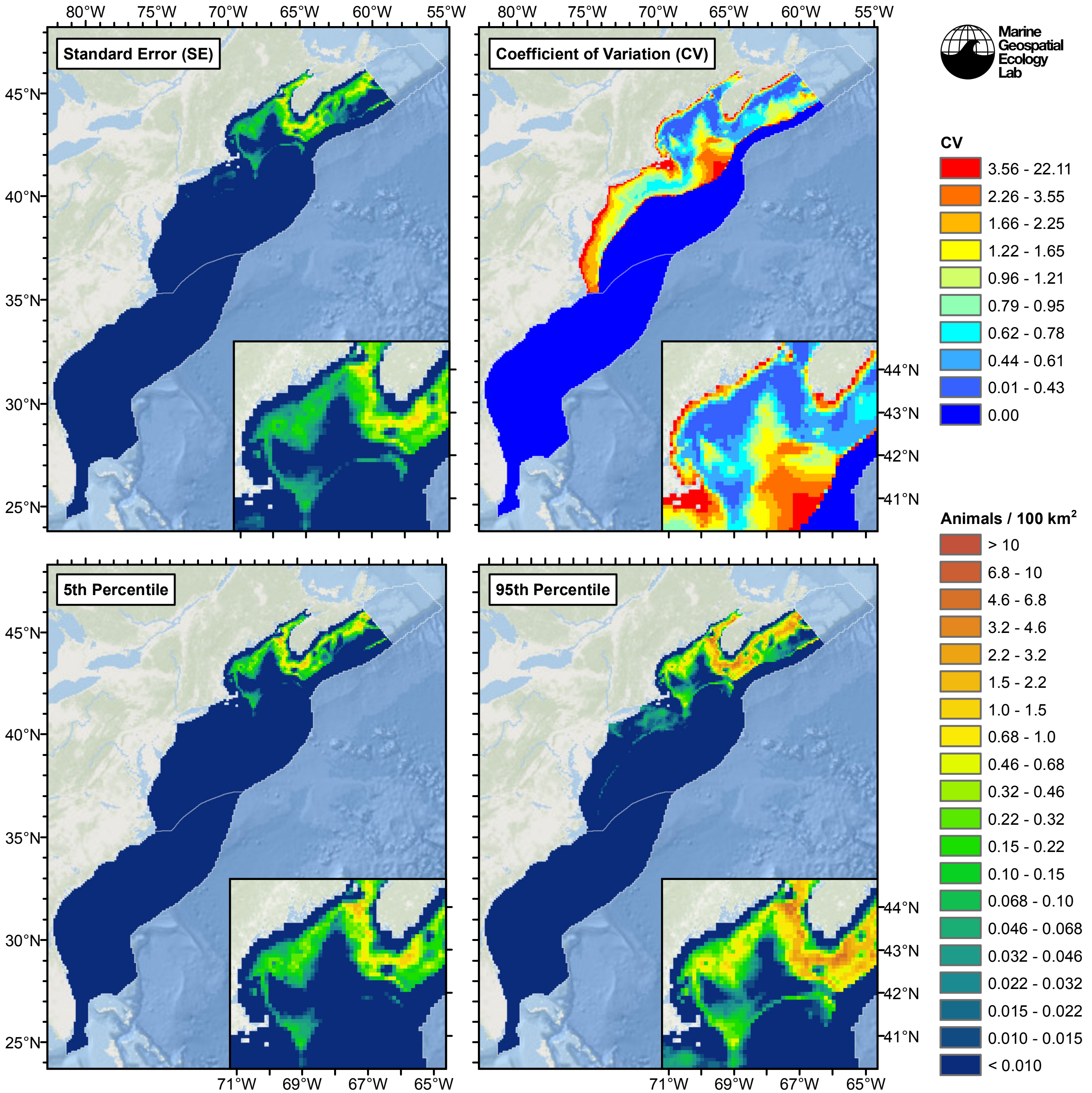

Figure 146: Estimated uncertainty for the Fall season climatological same segments model that explained the most deviance. These estimates only incorporate the statistical uncertainty estimated for the spatial model (by the R mgcv package). They do not incorporate uncertainty in the detection functions, g(0) estimates, predictor variables, and so on.

North of Gulf Stream

Statistical output

```
Rscript.exe: This is mgcv 1.8-2. For overview type 'help("mgcv-package")'.


Family: Tweedie(p=1.246)
```

```
Link function: log

Formula:
abundance ~ offset(log(area_km2)) + s(log10(Depth), bs = "ts",
    k = 5) + s(I(DistToShore/1000), bs = "ts", k = 5) + s(I(DistTo125m/1000),
    bs = "ts", k = 5) + s(I(DistTo300m/1000), bs = "ts", k = 5) +
    s(ClimSST, bs = "ts", k = 5) + s(I(ClimDistToFront1^(1/3)),
    bs = "ts", k = 5) + s(log10(pmax(ClimPkPB, 0.01)), bs = "ts",
    k = 5)

Parametric coefficients:
            Estimate Std. Error t value Pr(>|t|)
(Intercept)  -19.761      3.037  -6.507 7.98e-11 ***
---
Signif. codes:  0 '***' 0.001 '**' 0.01 '*' 0.05 '.' 0.1 ' ' 1

Approximate significance of smooth terms:
                                  edf Ref.df      F  p-value
s(log10(Depth))                3.6186      4 12.037 5.31e-11 ***
s(I(DistToShore/1000))         2.2499      4  2.281 0.008097 **
s(I(DistTo125m/1000))          1.0765      4  3.985 3.43e-05 ***
s(I(DistTo300m/1000))          0.9226      4  1.965 0.002534 **
s(ClimSST)                     0.9665      4  3.043 0.000234 ***
s(I(ClimDistToFront1^(1/3)))   2.5467      4  3.952 0.000305 ***
s(log10(pmax(ClimPkPB, 0.01))) 0.9682      4  5.903 4.98e-07 ***
---
Signif. codes:  0 '***' 0.001 '**' 0.01 '*' 0.05 '.' 0.1 ' ' 1

R-sq.(adj) =  0.0217   Deviance explained =   45%
-REML = 554.76  Scale est. = 29.584    n = 11305

All predictors were significant. This is the final model.
Creating term plots.
Diagnostic output from gam.check():

Method: REML   Optimizer: outer newton
full convergence after 21 iterations.
Gradient range [-7.536926e-05,9.078616e-05]
(score 554.7563 & scale 29.58447).
Hessian positive definite, eigenvalue range [0.3253809,291.6269].
Model rank =  29 / 29

Basis dimension (k) checking results. Low p-value (k-index<1) may
indicate that k is too low, especially if edf is close to k'.

                                  k'   edf k-index p-value
s(log10(Depth))                4.000 3.619   0.801    0.00
s(I(DistToShore/1000))         4.000 2.250   0.862    0.04
s(I(DistTo125m/1000))          4.000 1.076   0.854    0.01
s(I(DistTo300m/1000))          4.000 0.923   0.855    0.01
s(ClimSST)                     4.000 0.966   0.802    0.00
s(I(ClimDistToFront1^(1/3)))   4.000 2.547   0.876    0.08
s(log10(pmax(ClimPkPB, 0.01))) 4.000 0.968   0.859    0.03
```

Predictors retained during the model selection procedure: Depth, DistToShore, DistTo125m, DistTo300m, ClimSST, ClimDistToFront1, ClimPkPB

Predictors dropped during the model selection procedure: Slope, ClimTKE

Model term plots

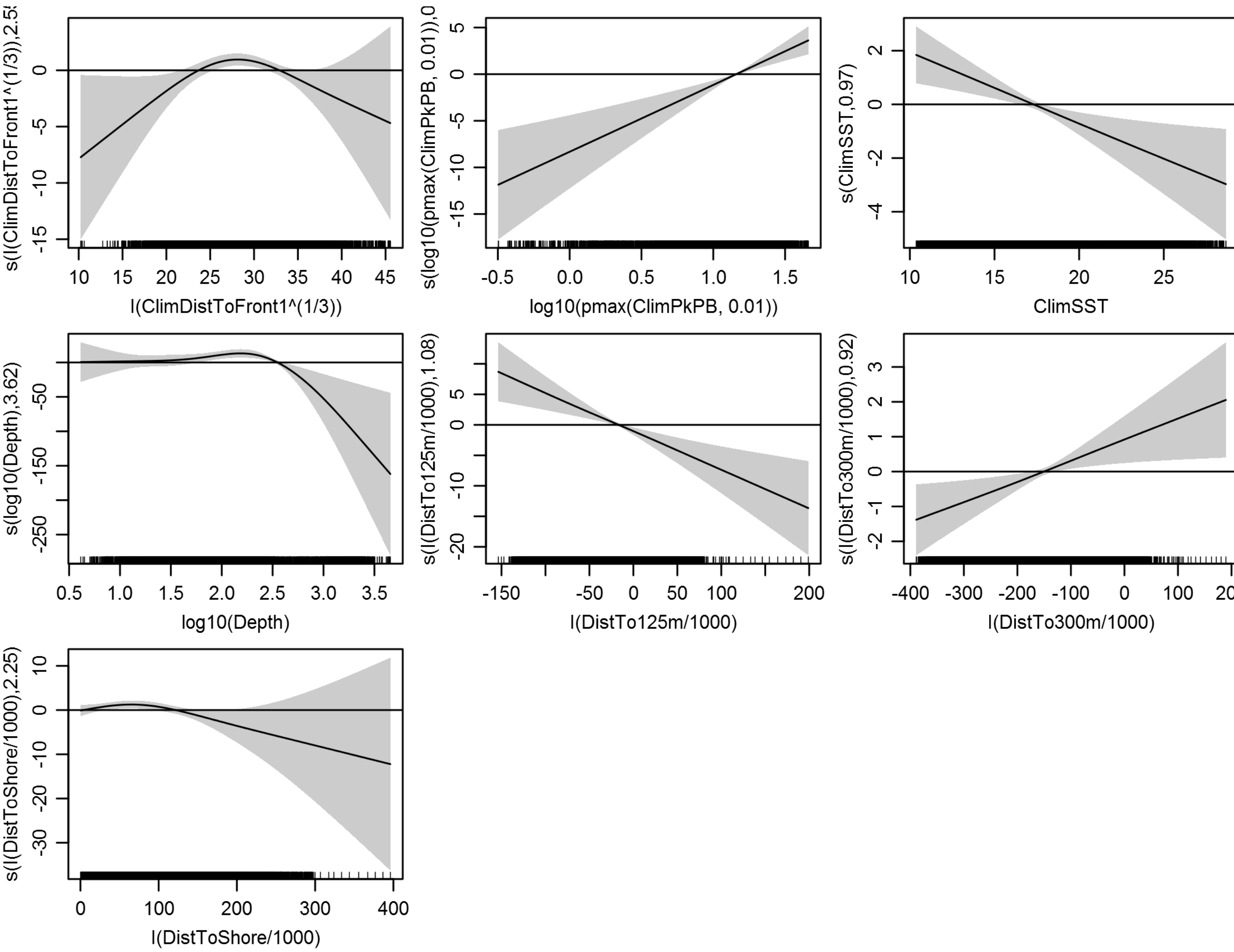

Diagnostic plots

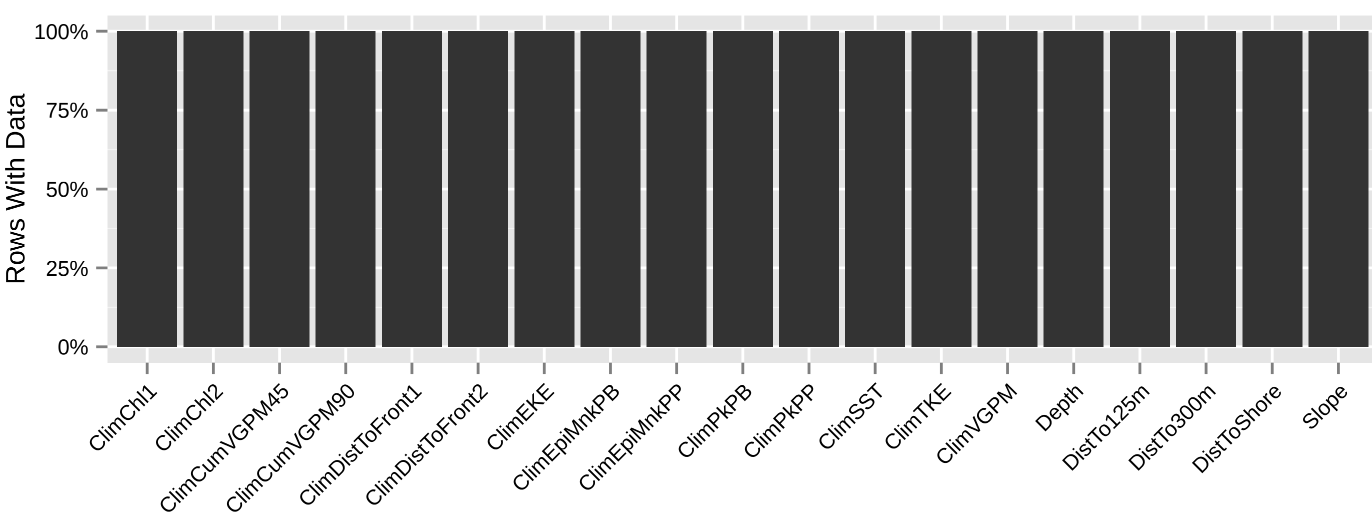

Figure 147: Segments with predictor values for the North Atlantic right whale Climatological model, Fall season, North of Gulf Stream. This plot is used to assess how many segments would be lost by including a given predictor in a model.

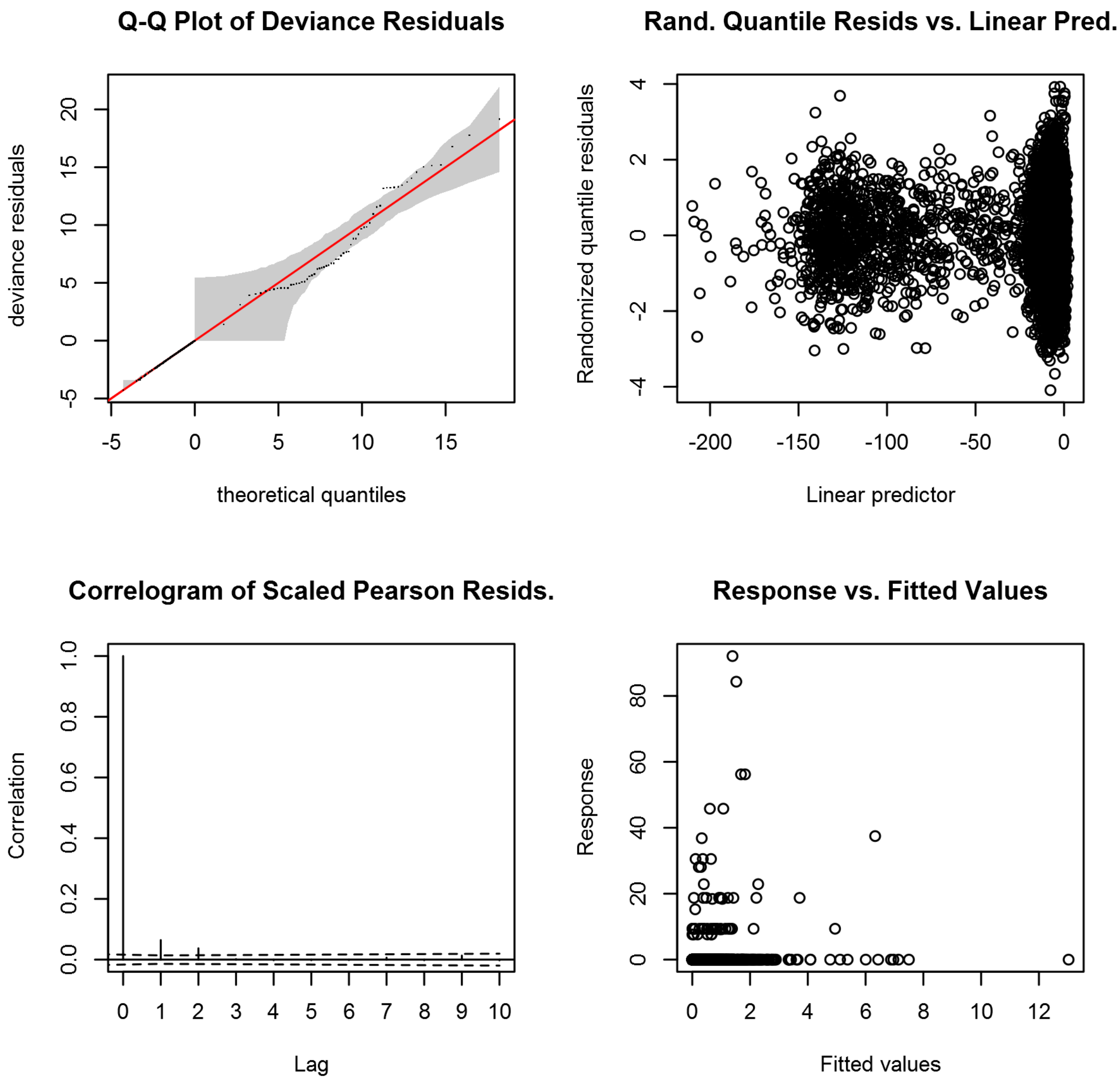

Figure 148: Statistical diagnostic plots for the North Atlantic right whale Climatological model, Fall season, North of Gulf Stream.

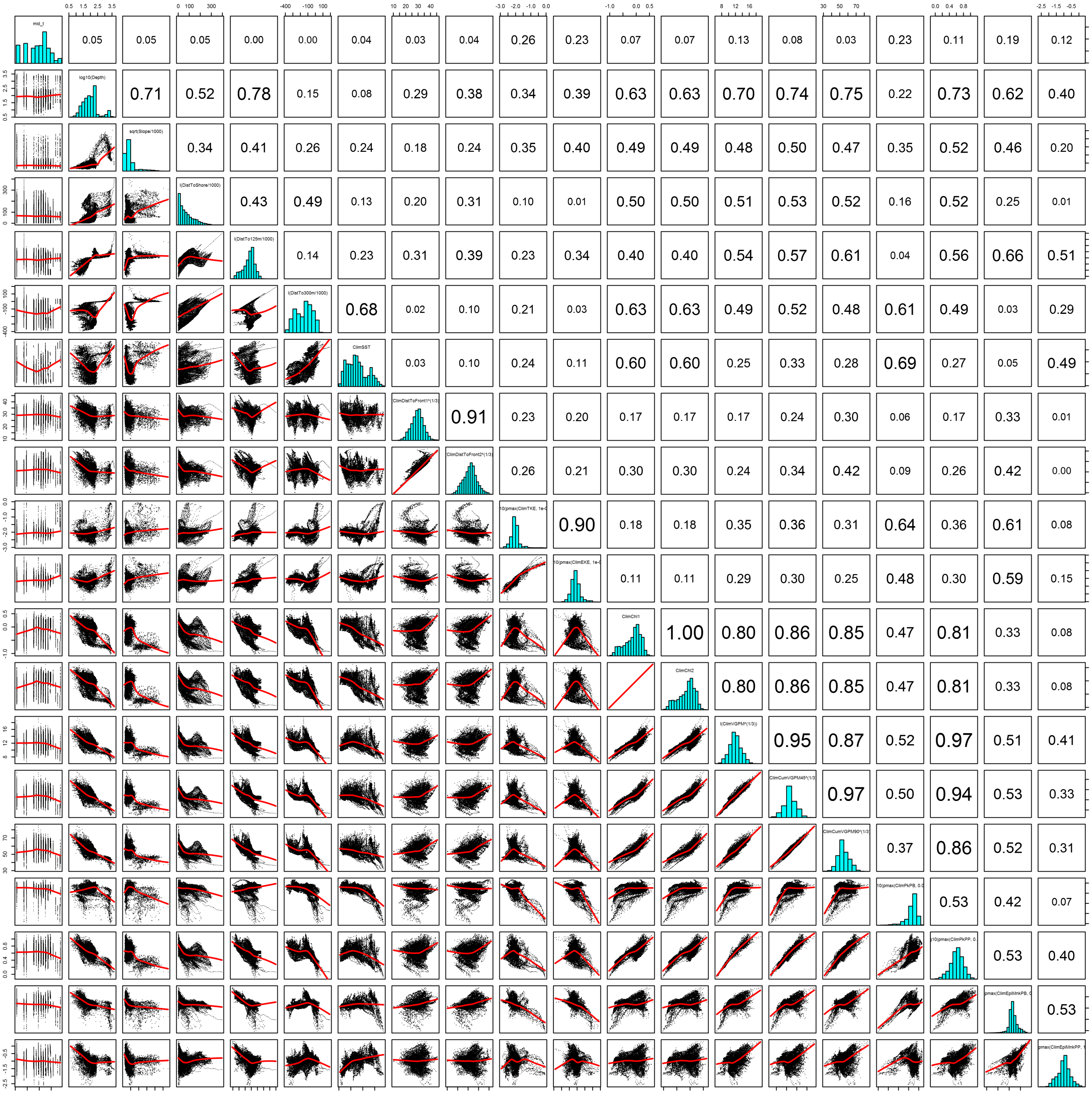

Figure 149: Scatterplot matrix for the North Atlantic right whale Climatological model, Fall season, North of Gulf Stream. This plot is used to inspect the distribution of predictors (via histograms along the diagonal), simple correlation between predictors (via pairwise Pearson coefficients above the diagonal), and linearity of predictor correlations (via scatterplots below the diagonal). This plot is best viewed at high magnification.

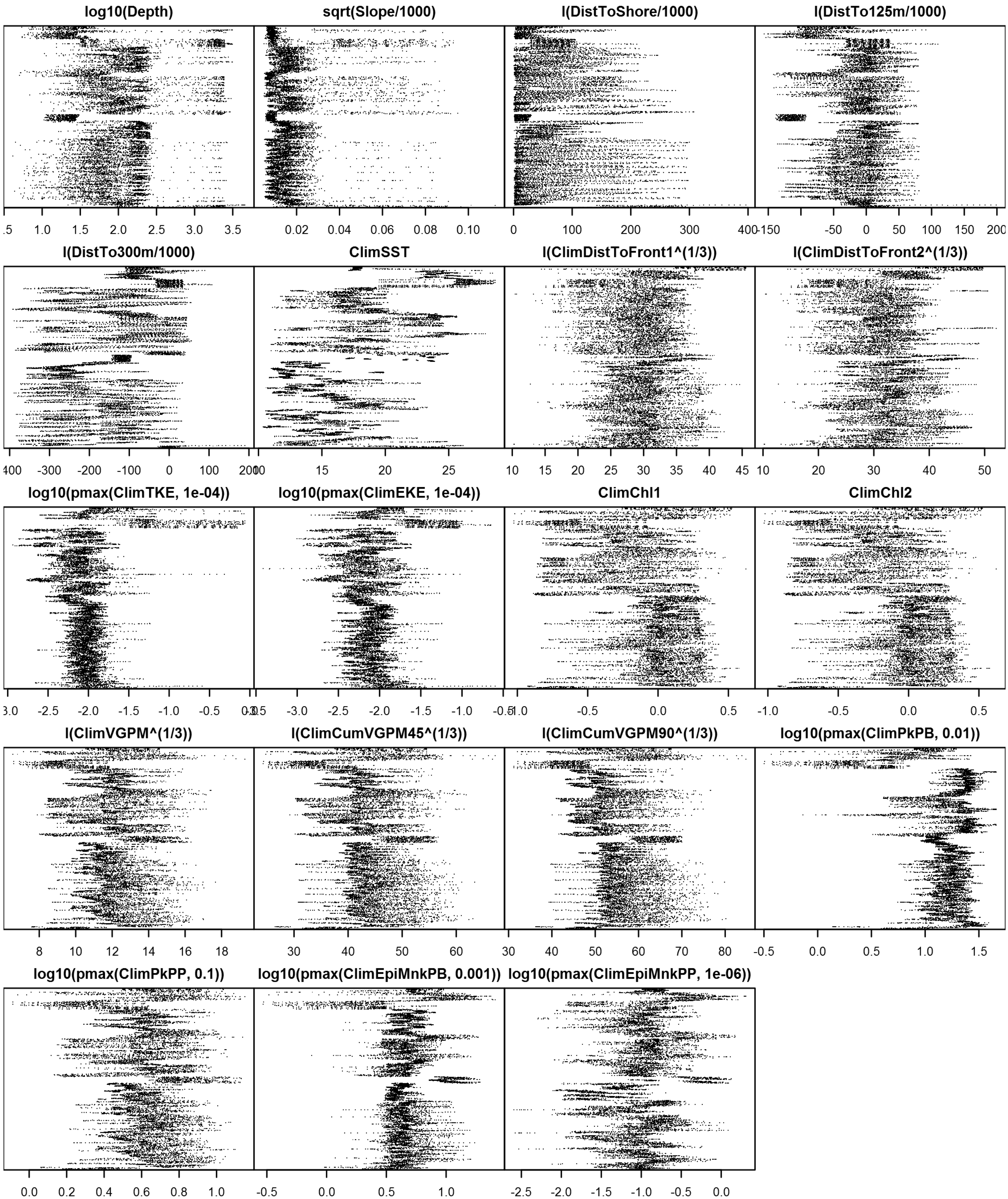

Figure 150: Dotplot for the North Atlantic right whale Climatological model, Fall season, North of Gulf Stream. This plot is used to check for suspicious patterns and outliers in the data. Points are ordered vertically by transect ID, sequentially in time.

South of Gulf Stream

Density assumed to be 0 in this region.

Northern Scotian Shelf

Density was not modeled for this region.

Model Comparison

Spatial Model Performance

The table below summarizes the performance of the candidate spatial models that were tested. For each season, the first model contained only physiographic predictors. Subsequent models added additional suites of predictors of based on when they became available via remote sensing.

For each model, three versions were fitted; the % Dev Expl columns give the % deviance explained by each one. The "climatological" models were fitted to 8-day climatologies of the environmental predictors. Because the environmental predictors were always available, no segments were lost, allowing these models to consider the maximal amount of survey data. The "contemporaneous" models were fitted to day-of-sighting images of the environmental predictors; these were smoothed to reduce data loss due to clouds, but some segments still failed to retrieve environmental values and were lost. Finally, the "climatological same segments" models fitted climatological predictors to the segments retained by the contemporaneous model, so that the explantory power of the two types of predictors could be directly compared. For each of the three models, predictors were selected independently via shrinkage smoothers; thus the three models did not necessarily utilize the same predictors.

Predictors derived from ocean currents first became available in January 1993 after the launch of the TOPEX/Poseidon satellite; productivity predictors first became available in September 1997 after the launch of the SeaWiFS sensor. Contemporaneous and climatological same segments models considering these predictors usually suffered data loss. Date Range shows the years spanned by the retained segments. The Segments column gives the number of segments retained; % Lost gives the percentage lost.

Season	Predictors	Climatol % Dev Expl	Contemp % Dev Expl	Climatol Same Segs % Dev Expl	Segments	% Lost	Date Range
Winter							
	Phys	16.3			8937		2000-2013
	Phys+SST	17.5	21.1	17.5	8937	0.0	2000-2013
	Phys+SST+Curr	20.1	21.1	20.1	8937	0.0	2000-2013
	Phys+SST+Curr+Prod	22.0	22.0	22.0	8937	0.0	2000-2013
Spring							
	Phys	24.8			9594		1999-2012
	Phys+SST	31.7	26.7	31.7	9594	0.0	1999-2012
	Phys+SST+Curr	31.7	25.9	31.7	9594	0.0	1999-2012
	Phys+SST+Curr+Prod	32.3	29.7	32.3	9594	0.0	1999-2012
Summer							
	Phys	29.5			24619		1995-2013
	Phys+SST	30.1	29.8	30.1	24619	0.0	1995-2013
	Phys+SST+Curr	31.2	30.0	31.2	24619	0.0	1995-2013
	Phys+SST+Curr+Prod	33.8	30.8	32.1	23886	3.0	1998-2013
Fall							

Phys	34.3			12828		1995-2013
Phys+SST	45.0	44.4	45.0	12828	0.0	1995-2013
Phys+SST+Curr	44.1	44.4	44.1	12828	0.0	1995-2013
Phys+SST+Curr+Prod	46.1	43.9	45.0	11305	11.9	1998-2013

Table 34: Deviance explained by the candidate density models.

Abundance Estimates

The table below shows the estimated mean abundance (number of animals) within the study area, for the models that explained the most deviance for each model type. Mean abundance was calculated by first predicting density maps for a series of time steps, then computing the abundance for each map, and then averaging the abundances. For the climatological models, we used 8-day climatologies, resulting in 46 abundance maps. For the contemporaneous models, we used daily images, resulting in 365 predicted abundance maps per year that the prediction spanned. The Dates column gives the dates to which the estimates apply. For our models, these are the years for which both survey data and remote sensing data were available.

The Assumed g(0)=1 column specifies whether the abundance estimate assumed that detection was certain along the survey trackline. Studies that assumed this did not correct for availability or perception bias, and therefore underestimated abundance. The In our models column specifies whether the survey data from the study was also used in our models. If not, the study provides a completely independent estimate of abundance.

Season	Dates	Model or study	Estimated abundance	CV	Assumed g(0)=1	In our models
Winter						
	2000-2013	Climatological model	330	0.15	No	
	2002-2013	Contemporaneous model*	535	0.45	No	
	2000-2013	Climatological same segments model	345	0.16	No	
Spring						
	1999-2012	Climatological model*	416	0.12	No	
	1999-2012	Contemporaneous model	410	0.12	No	
	1999-2012	Climatological same segments model	416	0.12	No	
Summer						
	1995-2013	Climatological model*	379	0.07	No	
	1998-2013	Contemporaneous model	364	0.06	No	
	1995-2013	Climatological same segments model	366	0.07	No	
	2013	North Atlantic Right Whale Consortium 2014 Annual Report Card (Pettis and Hamilton 2014)	522		None	None
	2012	Minimum stock size in 2012, from 2013 NOAA Stock Assessment Report (Waring et al. 2014)	455		None	None
Fall						
	1995-2013	Climatological model*	334	0.25	No	
	1995-2013	Contemporaneous model	489	0.29	No	
	1995-2013	Climatological same segments model	513	0.22	No	

Table 35: Estimated mean abundance within the study area. We selected the model marked with * as our best estimate of the abundance and distribution of this taxon. For comparison, independent abundance estimates from NOAA technical reports and/or the scientific literature are shown. Please see the Discussion section below for our evaluation of our models compared to the other estimates. Our coefficients of variation (CVs) underestimate the true uncertainty in our estimates, as they only incorporated the uncertainty of the GAM stage of our models. Other sources of uncertainty include the detection functions and g(0) estimates. It was not possible to incorporate these into our CVs without undertaking a computationally-prohibitive bootstrap; we hope to attempt that in a future version of our models.

Density Maps

Climatological Model

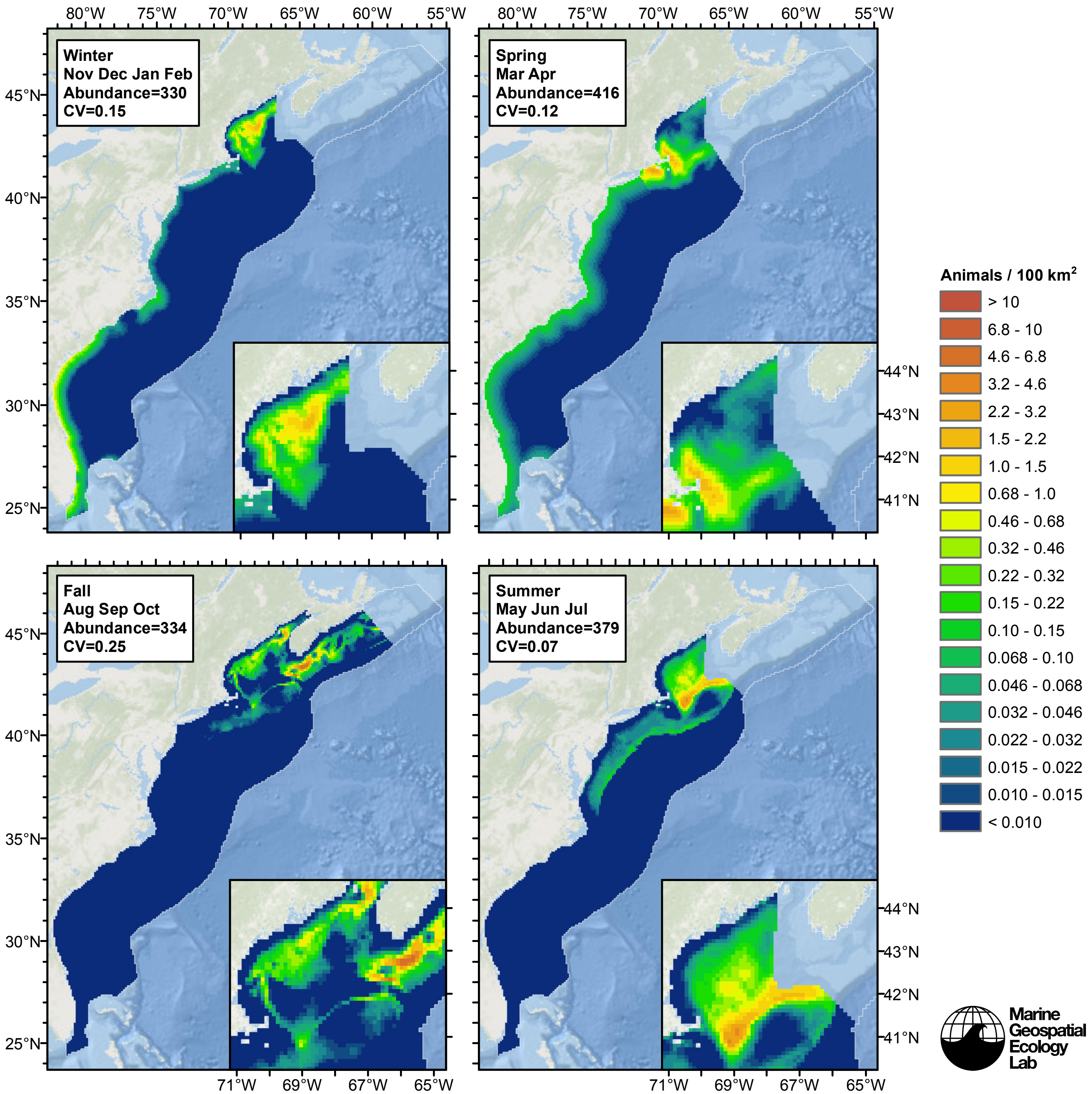

Figure 151: North Atlantic right whale density and abundance predicted by the climatological model that explained the most deviance. Regions inside the study area (white line) where the background map is visible are areas we did not model (see text).

Contemporaneous Model

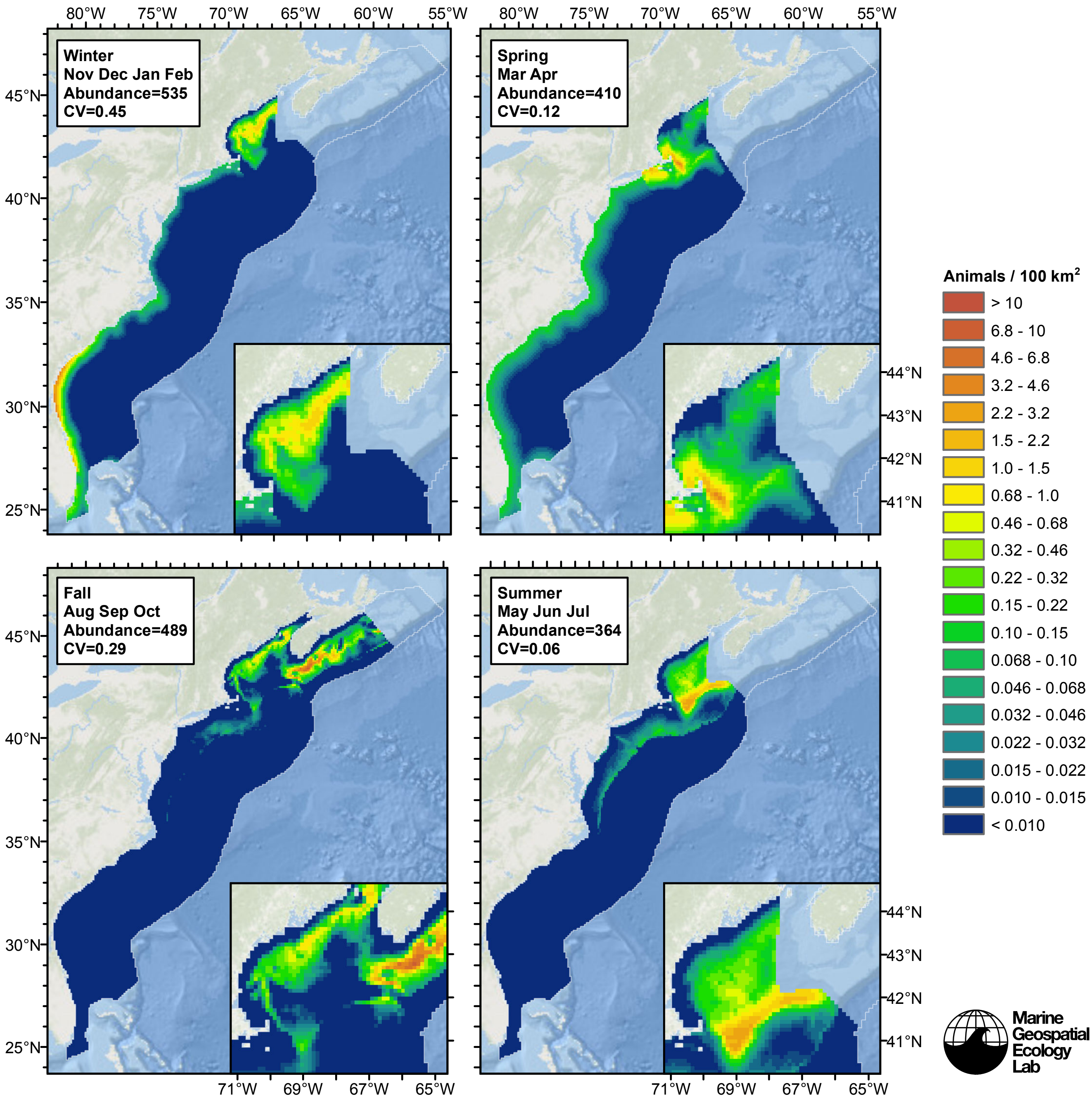

Figure 152: North Atlantic right whale density and abundance predicted by the contemporaneous model that explained the most deviance. Regions inside the study area (white line) where the background map is visible are areas we did not model (see text).

Climatological Same Segments Model

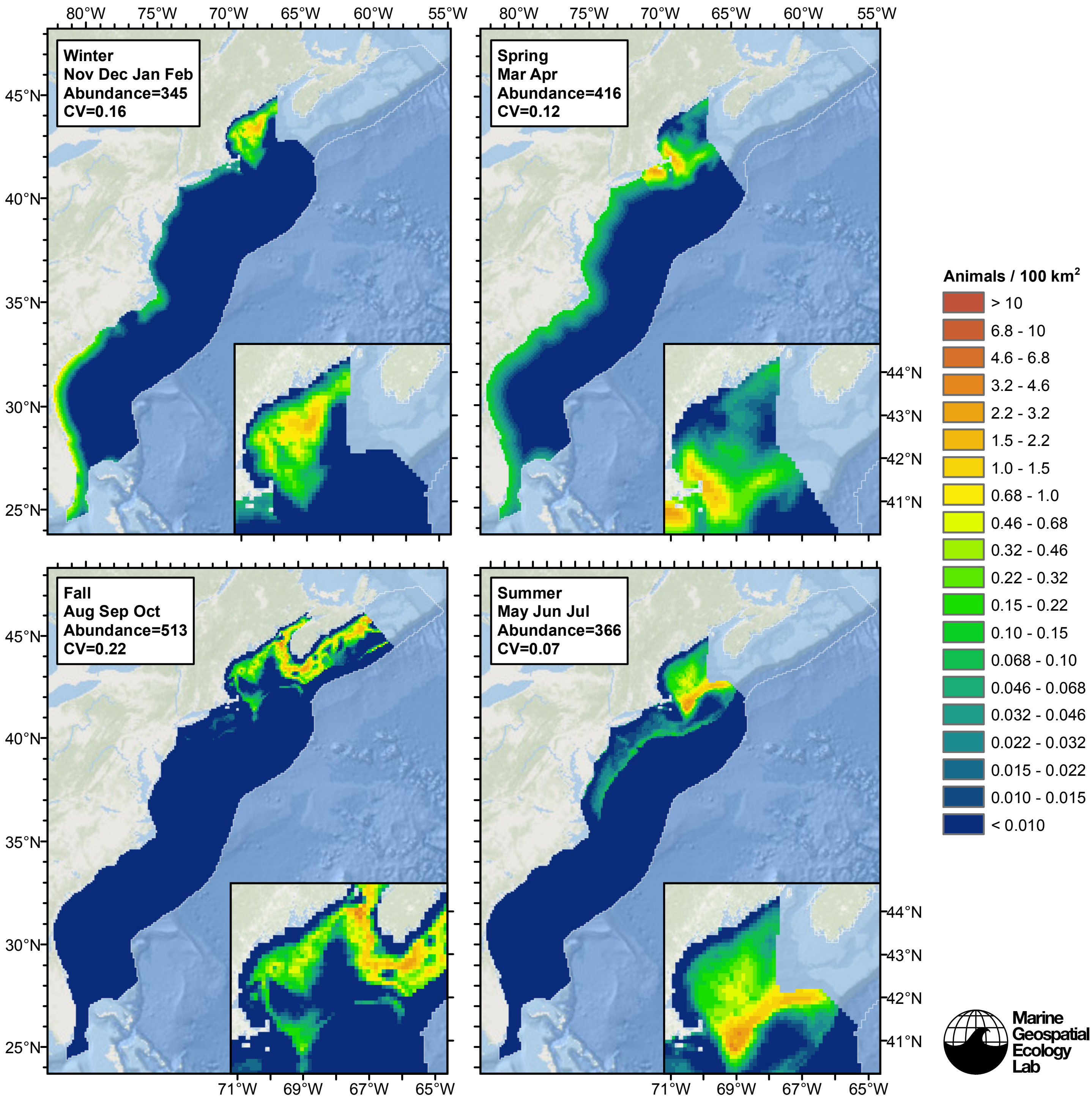

Figure 153: North Atlantic right whale density and abundance predicted by the climatological same segments model that explained the most deviance. Regions inside the study area (white line) where the background map is visible are areas we did not model (see text).

Temporal Variability

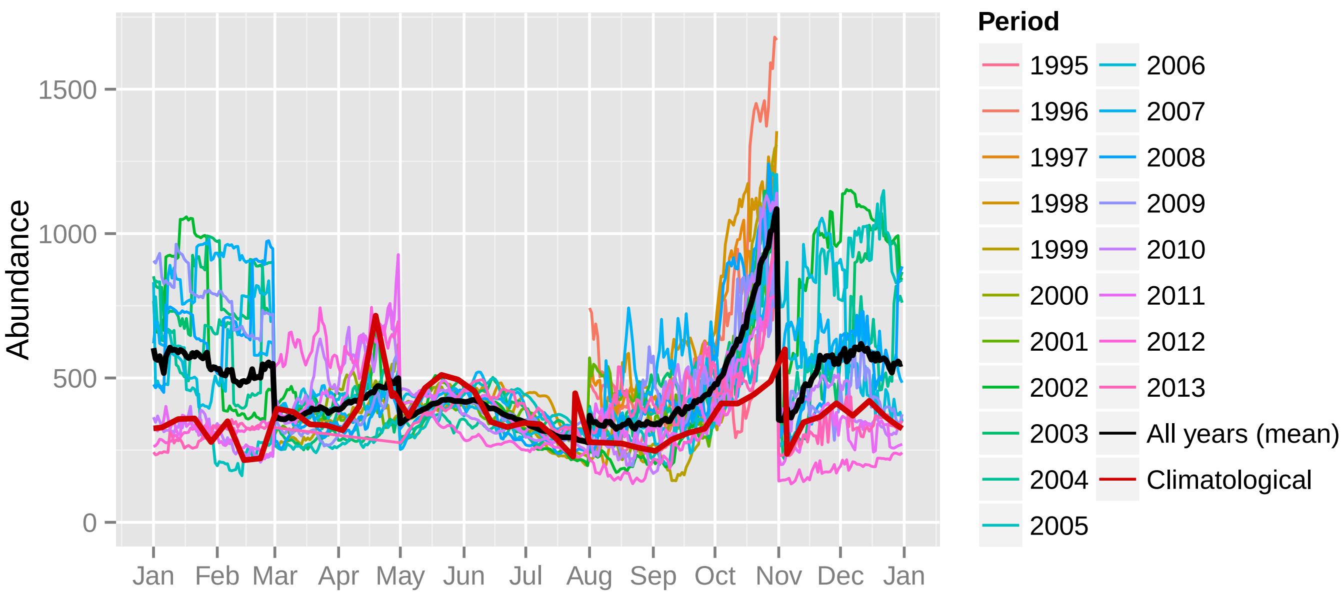

Figure 154: Comparison of North Atlantic right whale abundance predicted at a daily time step for different time periods. Individual years were predicted using contemporaneous models. “All years (mean)” averages the individual years, giving the mean annual abundance of the contemporaneous model. “Climatological” was predicted using the climatological model. The results for the climatological same segments model are not shown.

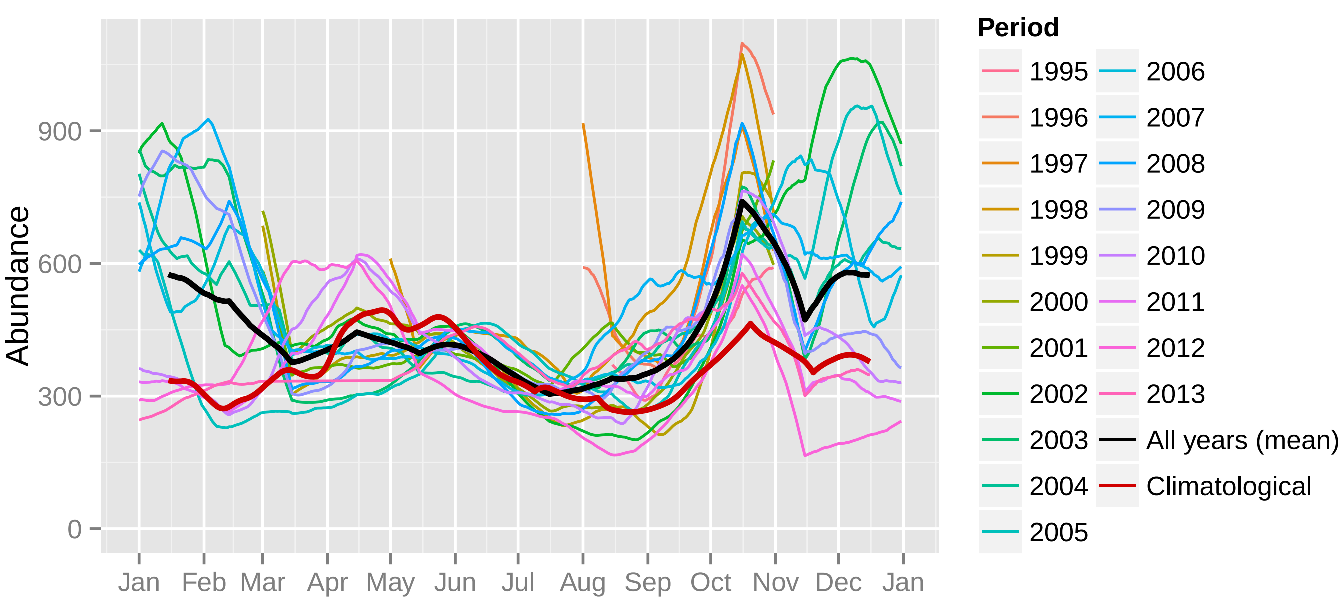

Figure 155: The same data as the preceding figure, but with a 30-day moving average applied.

Climatological Model

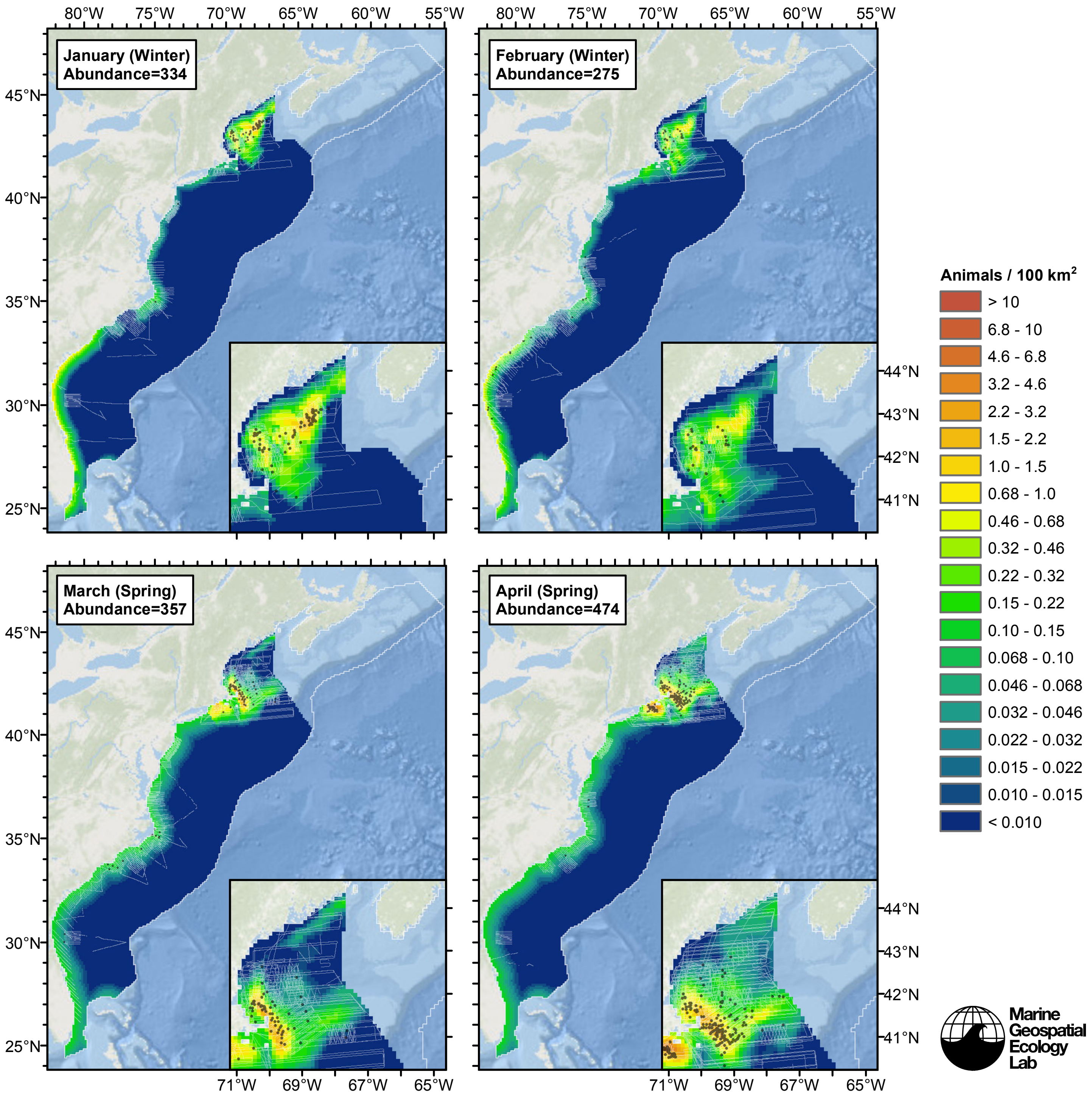

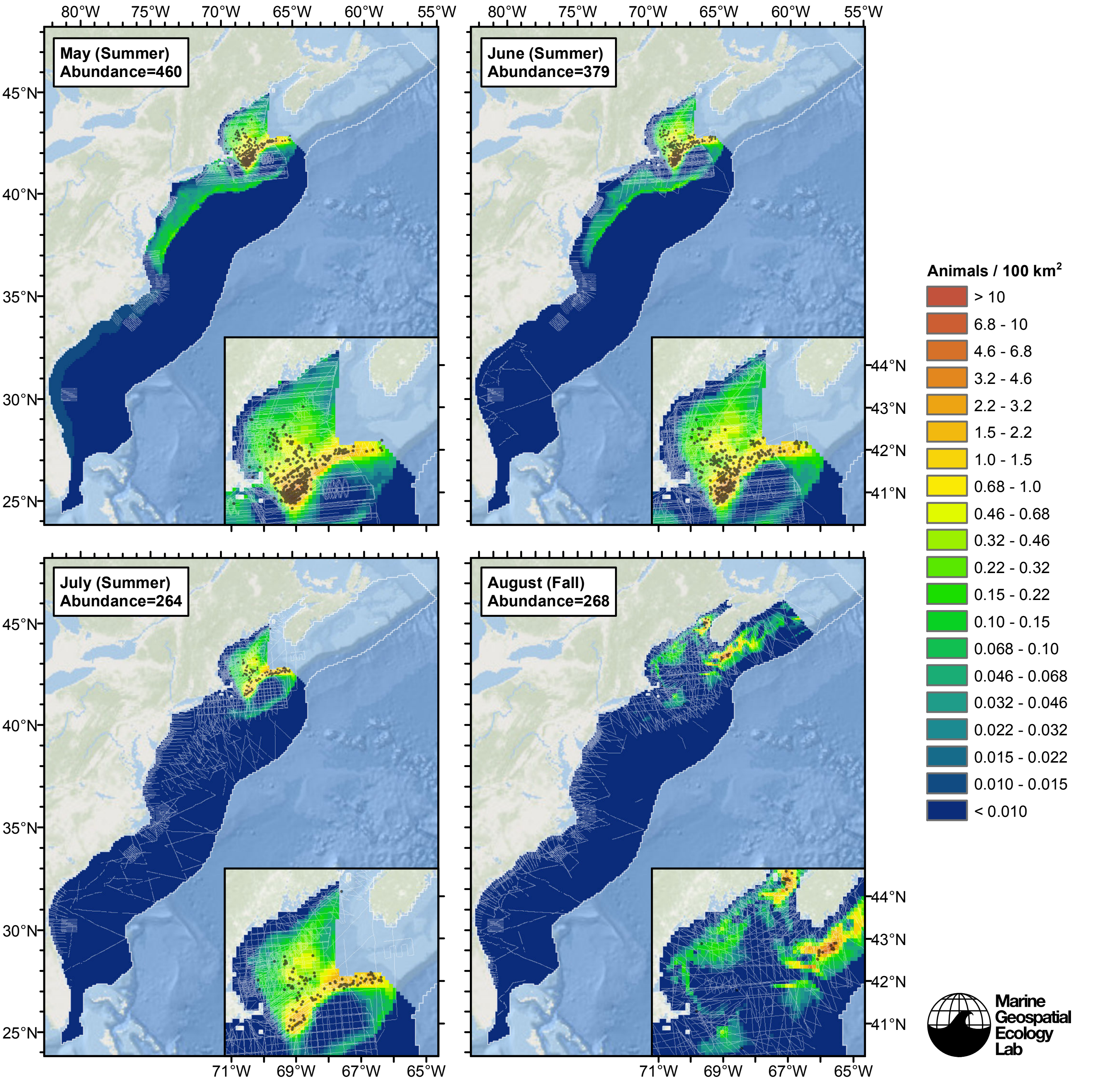

May (Summer)
Abundance=460
June (Summer)
Abundance=379
July (Summer)
Abundance=264
August (Fall)
Abundance=268
80°W
75°W
70°W
65°W
60°W
55°W
45°N
40°N
35°N
30°N
25°N
44°N
43°N
42°N
41°N
71°W
69°W
67°W
65°W
Animals / 100 km²
> 10
6.8 - 10
4.6 - 6.8
3.2 - 4.6
2.2 - 3.2
1.5 - 2.2
1.0 - 1.5
0.68 - 1.0
0.46 - 0.68
0.32 - 0.46
0.22 - 0.32
0.15 - 0.22
0.10 - 0.15
0.068 - 0.10
0.046 - 0.068
0.032 - 0.046
0.022 - 0.032
0.015 - 0.022
0.010 - 0.015
< 0.010
Marine
Geospatial
Ecology
Lab

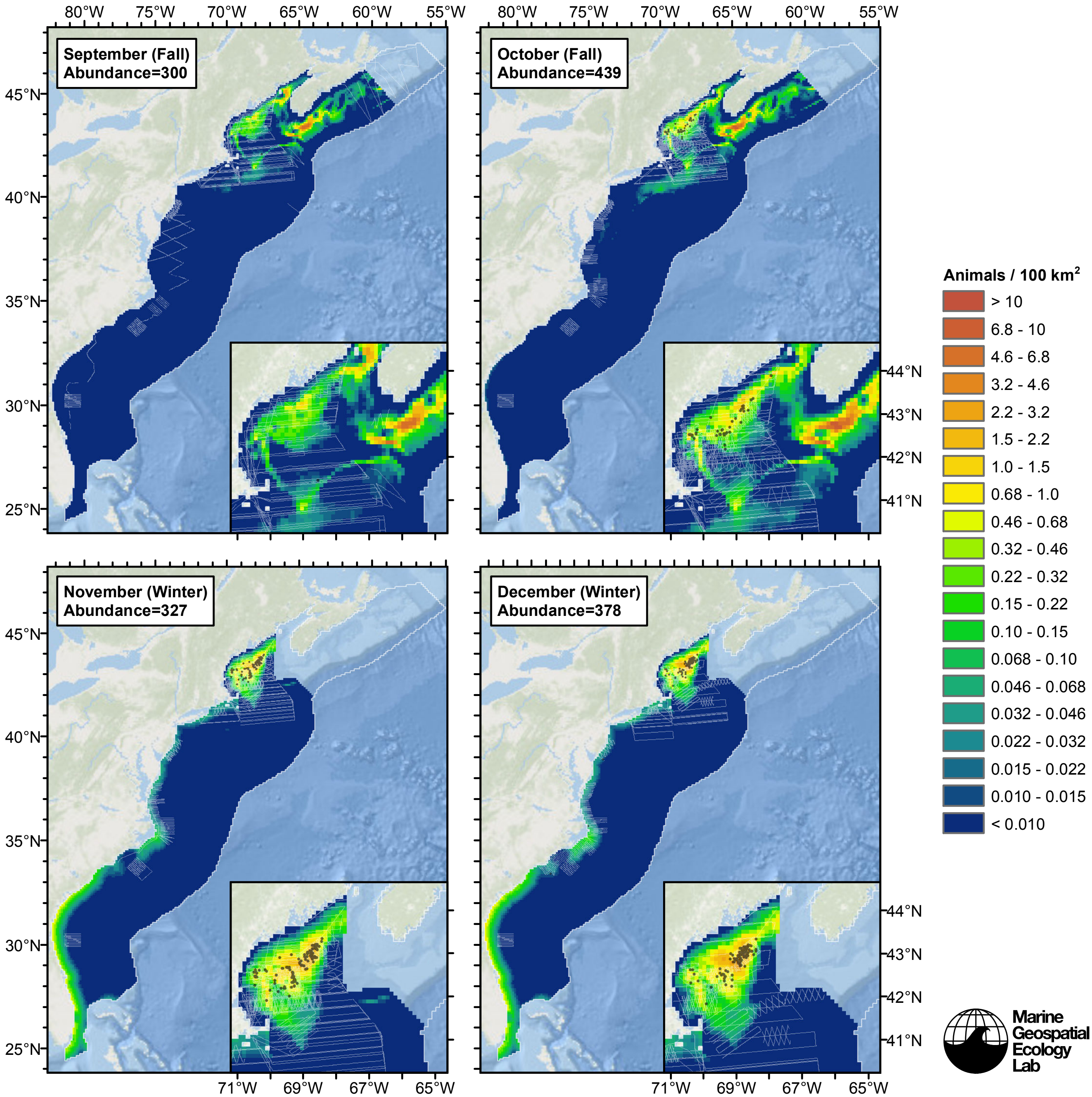

September (Fall)
Abundance=300
October (Fall)
Abundance=439
November (Winter)
Abundance=327
December (Winter)
Abundance=378
80°W
75°W
70°W
65°W
60°W
55°W
45°N
40°N
35°N
30°N
25°N
44°N
43°N
42°N
41°N
71°W
69°W
67°W
65°W
Animals / 100 km²
> 10
6.8 - 10
4.6 - 6.8
3.2 - 4.6
2.2 - 3.2
1.5 - 2.2
1.0 - 1.5
0.68 - 1.0
0.46 - 0.68
0.32 - 0.46
0.22 - 0.32
0.15 - 0.22
0.10 - 0.15
0.068 - 0.10
0.046 - 0.068
0.032 - 0.046
0.022 - 0.032
0.015 - 0.022
0.010 - 0.015
< 0.010
Marine Geospatial Ecology Lab

Contemporaneous Model

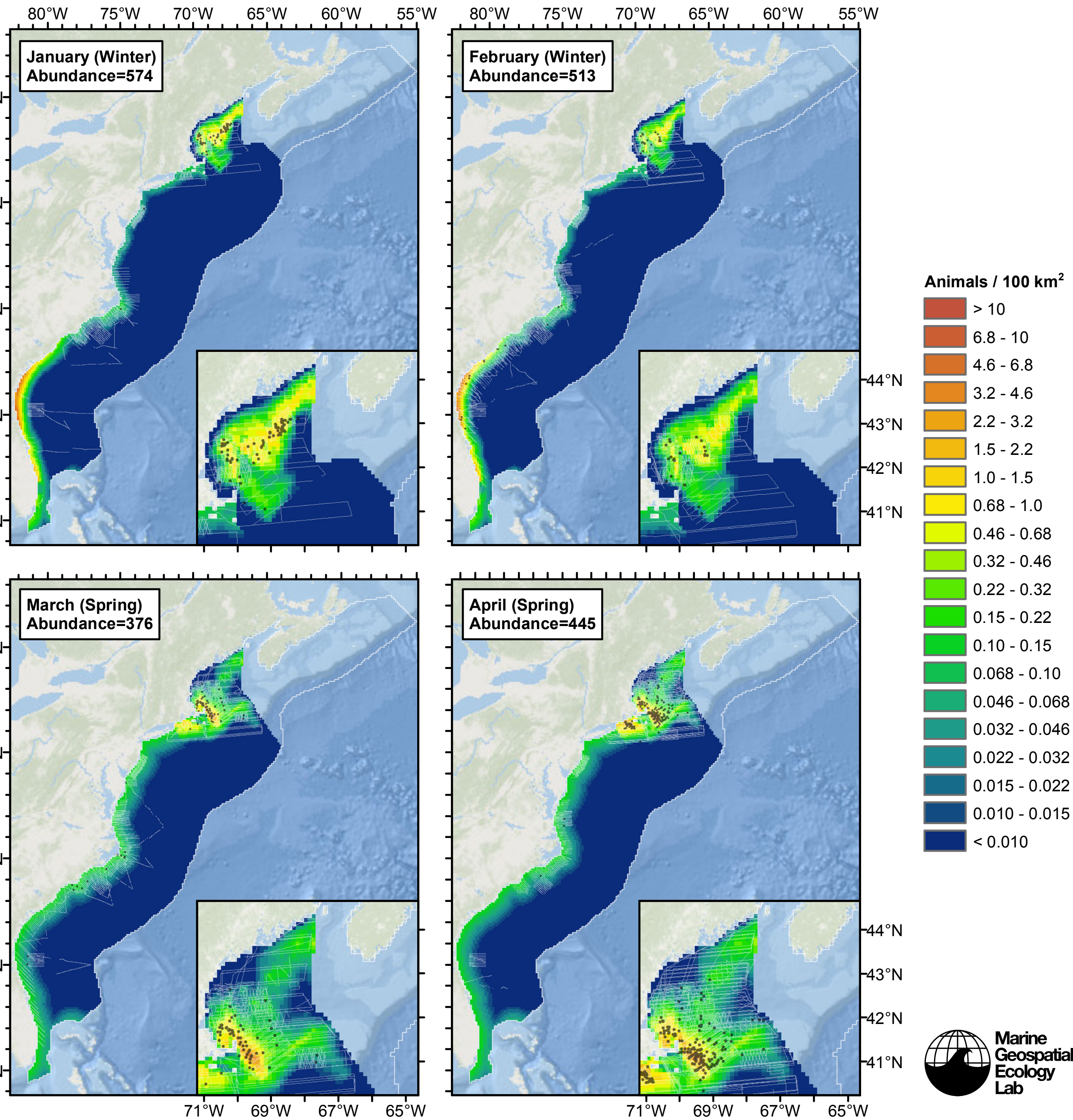

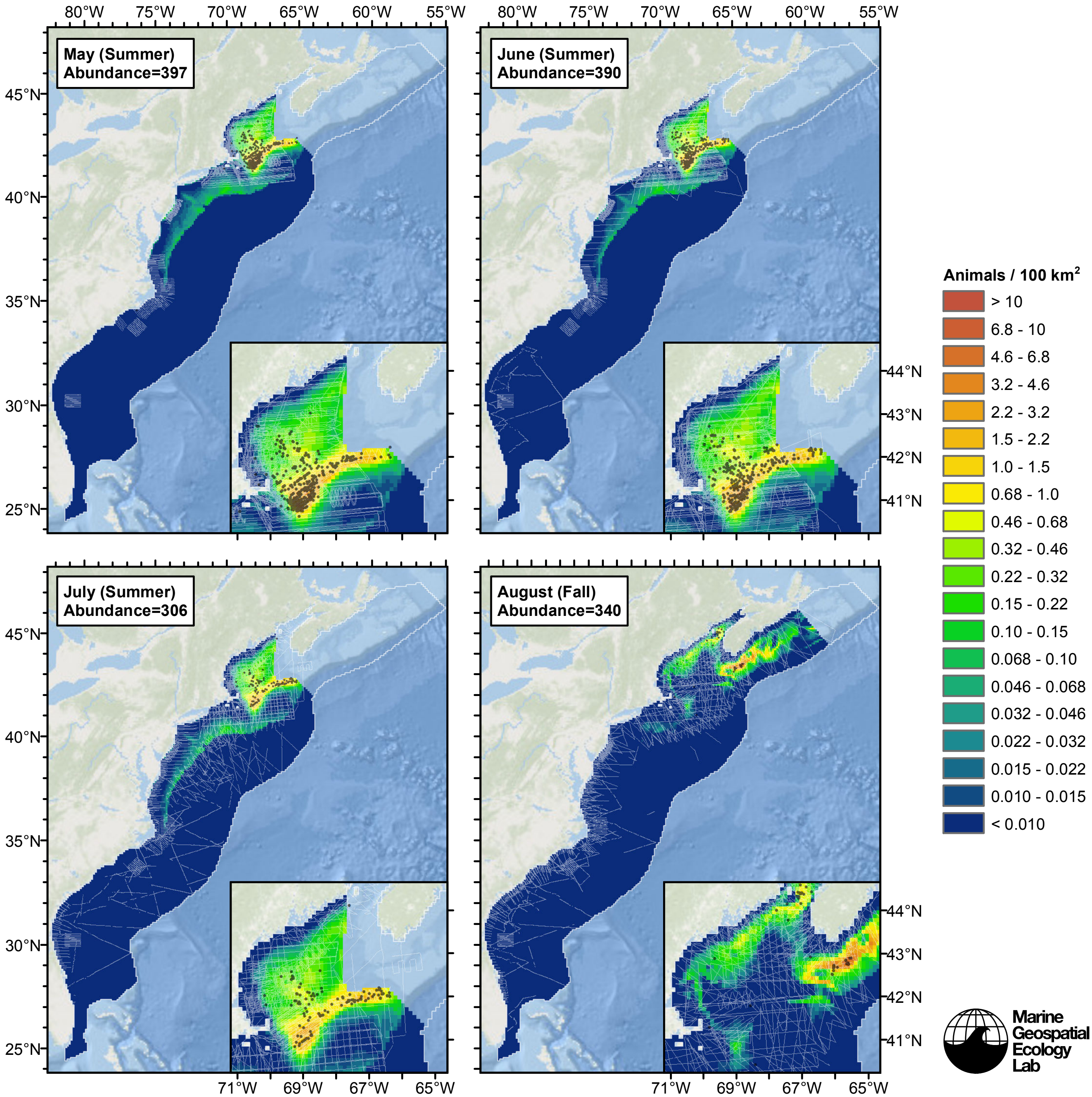
May (Summer)
Abundance=397
June (Summer)
Abundance=390
July (Summer)
Abundance=306
August (Fall)
Abundance=340
80°W
75°W
70°W
65°W
60°W
55°W
45°N
40°N
35°N
30°N
25°N
44°N
43°N
42°N
41°N
71°W
69°W
67°W
65°W
Animals / 100 km^2
> 10
6.8 - 10
4.6 - 6.8
3.2 - 4.6
2.2 - 3.2
1.5 - 2.2
1.0 - 1.5
0.68 - 1.0
0.46 - 0.68
0.32 - 0.46
0.22 - 0.32
0.15 - 0.22
0.10 - 0.15
0.068 - 0.10
0.046 - 0.068
0.032 - 0.046
0.022 - 0.032
0.015 - 0.022
0.010 - 0.015
< 0.010
Marine
Geospatial
Ecology
Lab

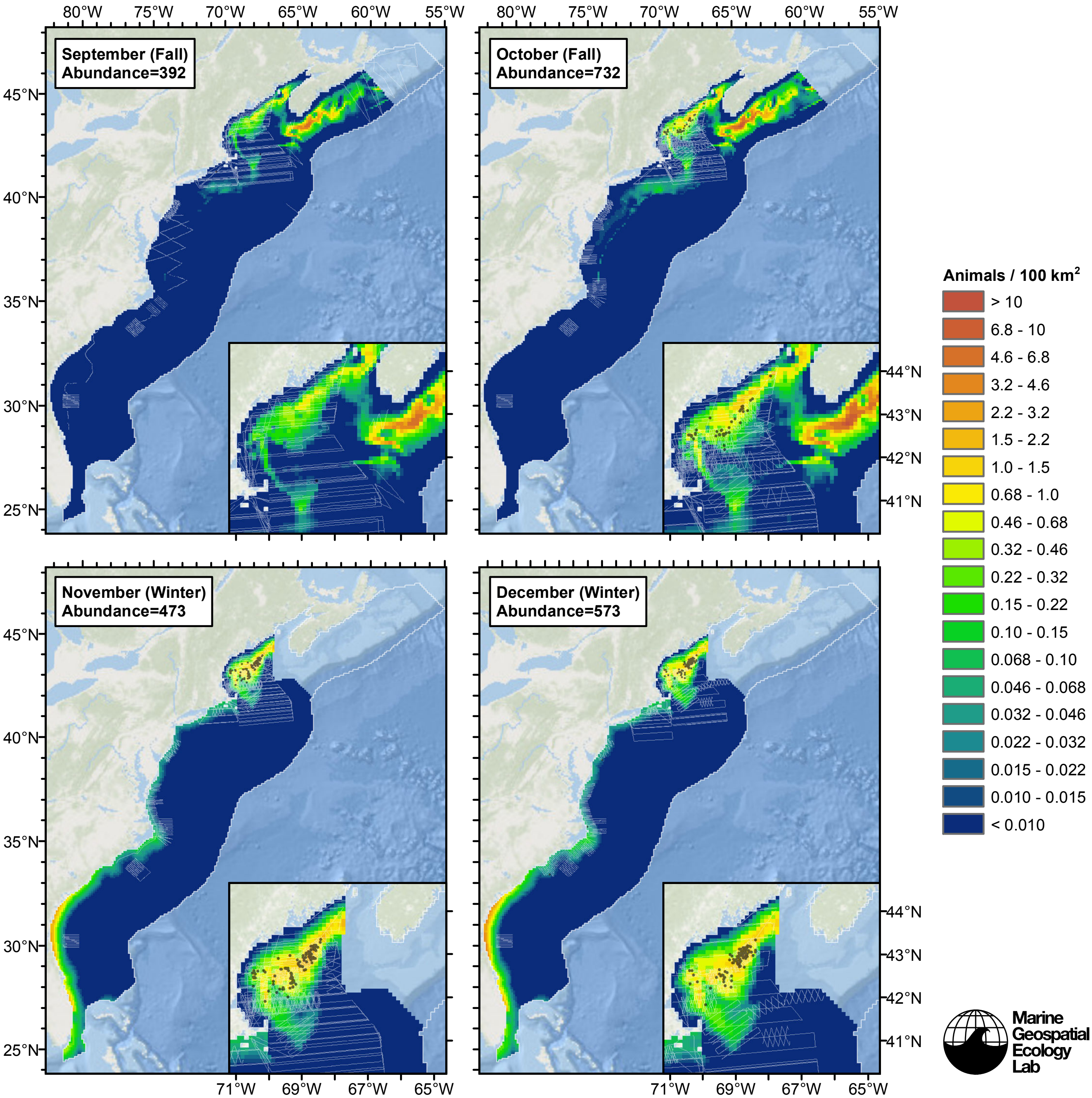
September (Fall)
Abundance=392
October (Fall)
Abundance=732
November (Winter)
Abundance=473
December (Winter)
Abundance=573
80°W
75°W
70°W
65°W
60°W
55°W
45°N
40°N
35°N
30°N
25°N
44°N
43°N
42°N
41°N
71°W
69°W
67°W
65°W
Animals / 100 km²
> 10
6.8 - 10
4.6 - 6.8
3.2 - 4.6
2.2 - 3.2
1.5 - 2.2
1.0 - 1.5
0.68 - 1.0
0.46 - 0.68
0.32 - 0.46
0.22 - 0.32
0.15 - 0.22
0.10 - 0.15
0.068 - 0.10
0.046 - 0.068
0.032 - 0.046
0.022 - 0.032
0.015 - 0.022
0.010 - 0.015
< 0.010
Marine
Geospatial
Ecology
Lab

Climatological Same Segments Model

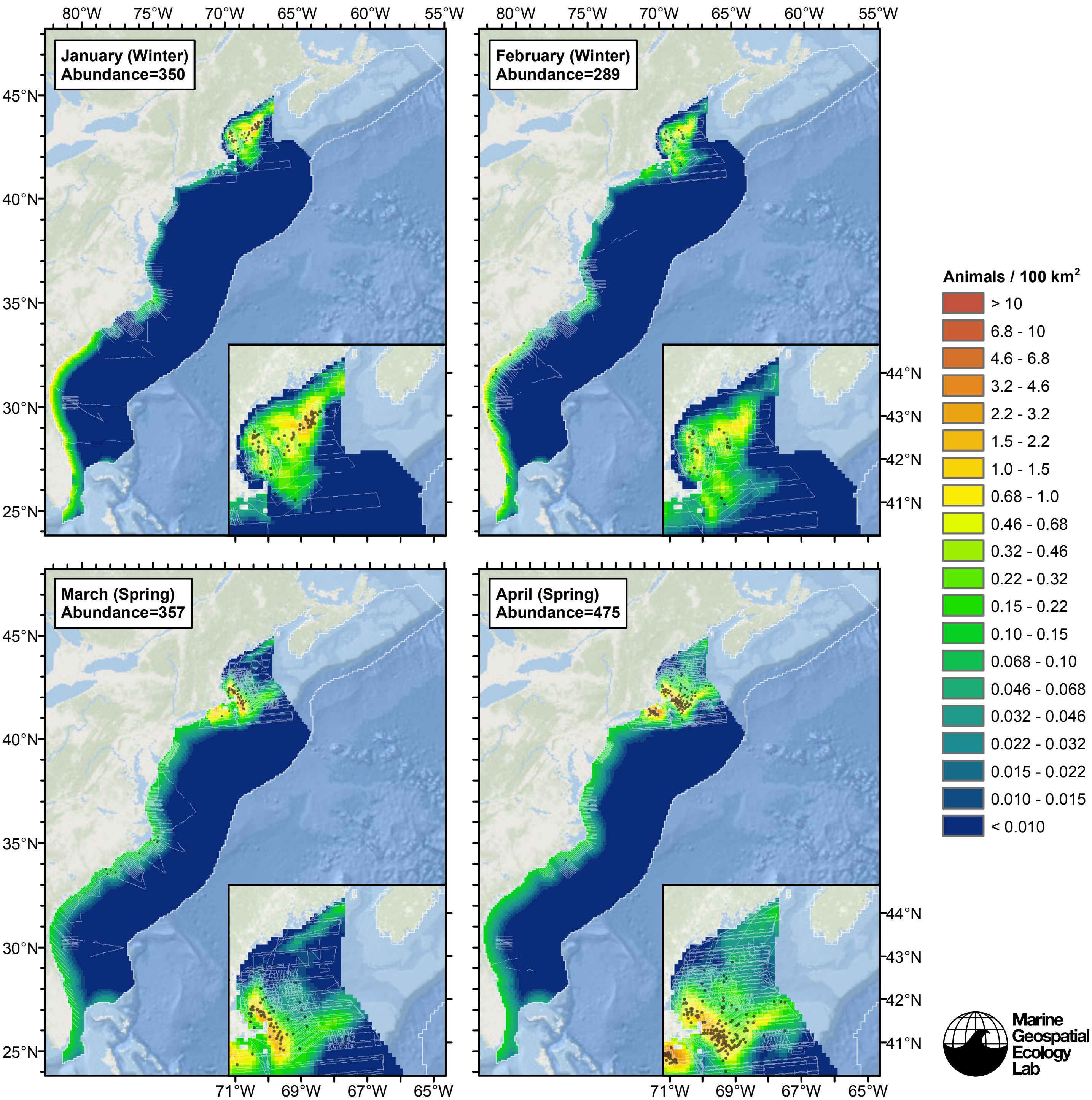

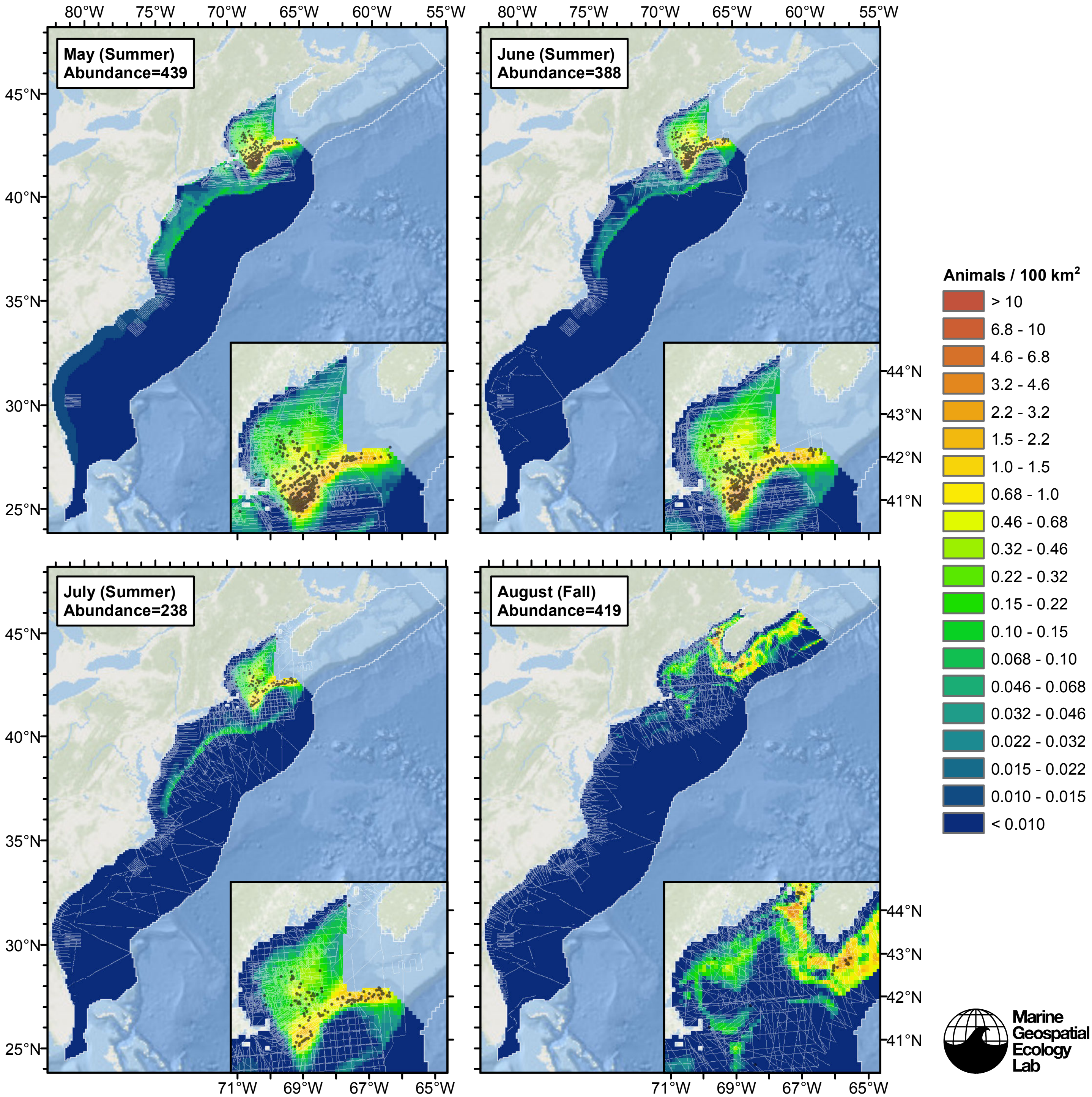
May (Summer)
Abundance=439
June (Summer)
Abundance=388
July (Summer)
Abundance=238
August (Fall)
Abundance=419
80°W
75°W
70°W
65°W
60°W
55°W
45°N
40°N
35°N
30°N
25°N
44°N
43°N
42°N
41°N
71°W
69°W
67°W
65°W
Animals / 100 km^2
> 10
6.8 - 10
4.6 - 6.8
3.2 - 4.6
2.2 - 3.2
1.5 - 2.2
1.0 - 1.5
0.68 - 1.0
0.46 - 0.68
0.32 - 0.46
0.22 - 0.32
0.15 - 0.22
0.10 - 0.15
0.068 - 0.10
0.046 - 0.068
0.032 - 0.046
0.022 - 0.032
0.015 - 0.022
0.010 - 0.015
< 0.010
Marine Geospatial Ecology Lab

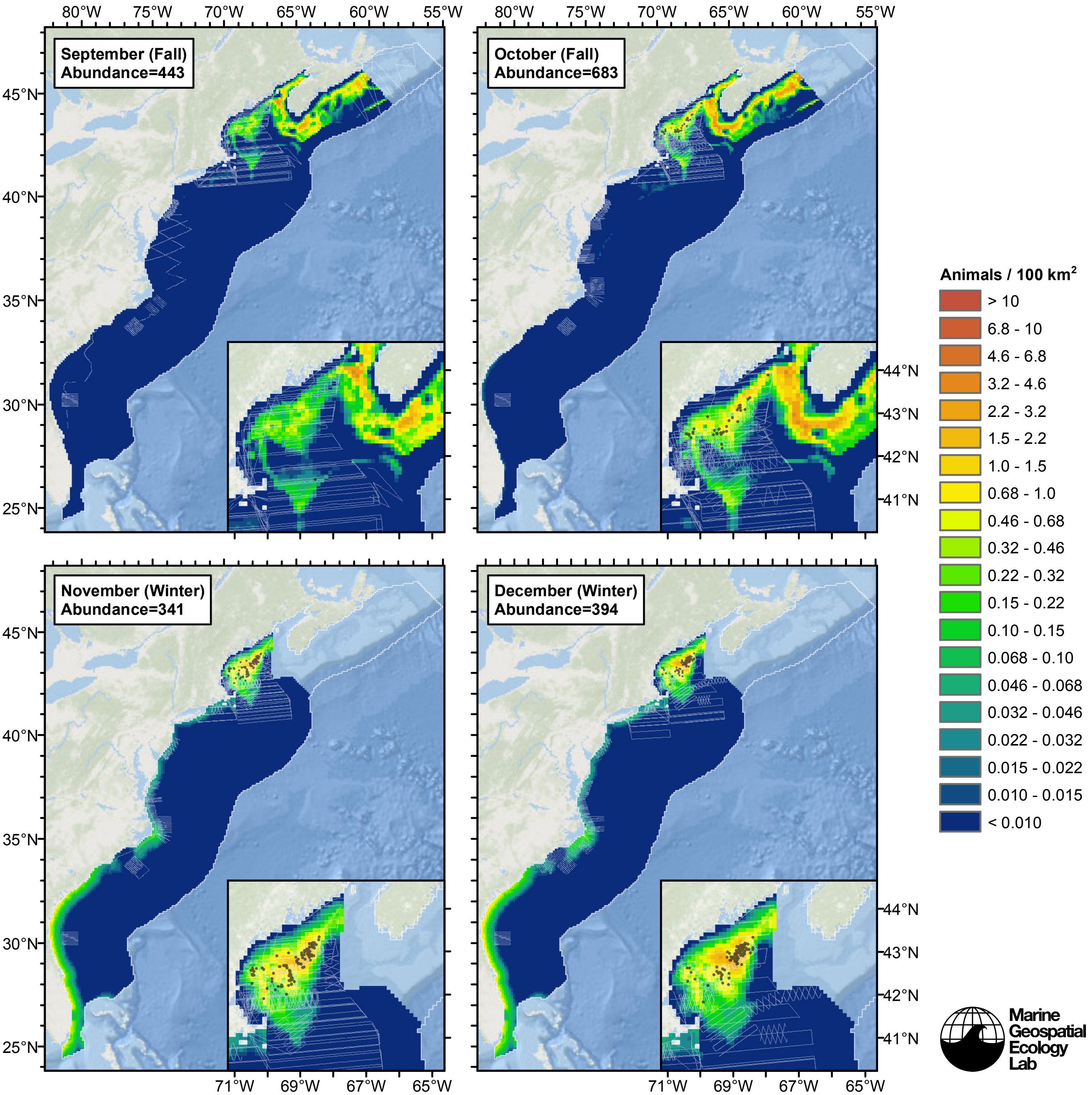

Discussion

Winter

In the Feeding Grounds region, all three models predicted a mean abundance of 163-166 whales, with highest abundance in the central Gulf of Maine, peaking in November and December and diminishing through February (see Temporal Variability section). The central Gulf of Maine is a known wintertime aggregation area where right whales may gather to mate (Cole et al. 2013). All three models explained the same amount of deviance, 22%.

In the Calving and Migration Area, the models showed less agreement. The two models with climatological predictors predicted 167 and 183 whales in this area, while the contemporaneous-predictor model predicted 369. The climatological-predictor model that considered all segments explained 12.4% of the deviance; the one that considered only the contemporaneous-predictor model's segments explained 14.7%. The contemporaneous-predictor model explained 12.3%.

Cole et al. (2013) estimated from photographic ID data that during the mid-2000s, roughly half of the right whale population occupied the central Gulf of Maine during winter, with the total population in 2005 estimated to be at least 361 whales. Our climatological-predictor models generally agreed with this, with total abundance estimated at 330-345 whales, split roughly evenly between the Gulf of Maine and the Calving and Migration Area. In contrast, the contemporaneous-predictor model estimated roughly twice as many whales in the Calving and Migration Area. Despite the climatological-predictor models' better agreement with Cole et al.'s description of the distribution, we selected the contemporaneous-predictor model as our best estimate of present day right whale distribution and abundance, for three reasons:

First, the North Atlantic Right Whale Consortium's most recent "best estimate" of alive, photographically-cataloged right whales was 522 individuals (Pettis and Hamilton 2014, however note their caution that "This 'best estimate' is based upon the number of photographed whales, but it excludes potential unphotographed whales, and therefore should not be considered a 'population estimate'."). Our contemporaneous-predictor model's estimate of 535 whales was the closest to this. (But please see the discussion of the Summer model, below, for additional interpretation of the difference between the estimates.)

Second, the areas of highest abundance predicted by the contemporaneous-predictor model, near the shores of Florida and Georgia, corresponded very well to areas delineated by NOAA as right whale Critical Habitat and Seasonal Management Areas, and also to the areas of peak relative abundance predicted by Gowan and Ortega-Ortiz (2014) (see their figures 1 and 5).

Finally, the climatological-predictor models predicted near-zero abundance near Onslow Bay, North Carolina, while the contemporaneous-predictor model did not exhibit this "hole" along the migration corridor. Right whales are known to transit this area, and Hodge et al. (2015) reported acoustic detections of right whales in the northern half of Onslow Bay on 12-25% of the days of the months of December 2012 and February and March 2013. Therefore we considered this "hole" predicted by the climatological models to be in error.

We note that the Calving and Migration Area models predicted low but non-zero density of right whales all the way to the northernmost extent of these models, at Nantucket Shoals. While the relatively low level of survey effort in the northern half of the modeled area makes it difficult to assess the correctness of this prediction, the presence of right whales throughout the eastern seaboard in winter is supported by several other studies. For example, in addition to Hodge et al.'s (2015) reports of acoustic detections in Onslow Bay, Whitt et al. (2013) reported acoustic detections near New Jersey in December of 2008 and January and February of 2009. CETAP (1982) reported visual sightings south of Nantucket and Long Island in their winter season. Finally, Knowlton et al. (2002) reported sightings near Delaware Bay in December, Rhode Island in January, and New York in February. All of these results support the prediction that right whales range across the entire eastern seaboard between the southeast and Nantucket Shoals during winter.

It is also interesting to note that in all three of our models of the Calving and Migration Area, once we introduced productivity predictors into the models, these were retained while SST and wind speed were discarded. Each of three final models retained the same two predictors: distance to shore and epipelagic micronekton biomass, with abundance higher close to shore and with high biomass. We doubt that right whales are consuming epipelagic micronekton here; more likely, this predictor correlates better with some other habitat preference that is not captured as well by SST or wind speed.

Our models would be improved by inclusion of more survey data, particularly in two regions. First, right whales are known to aggregate in Cape Cod Bay in winter and early spring (Costa et al. 2006). All of the data we had for Cape Cod Bay came from the NOAA North Atlantic Right Whale Sighting Survey (NARWSS). T. Cole advised us to consider data from the Provincetown Center for Coastal Studies (CCS), who have routinely surveyed of Cape Cod Bay for more than a decade. We investigated this possibility. Unfortunately the CCS surveys did not collect sufficient information to allow us to estimate distances from the tracklines to sightings, making them unsuitable for the distance sampling methodology that we used.

Second, with so few sightings in the calving grounds, this model would clearly benefit from incorporation of aerial surveys for right whales conducted in the southeast U.S., such as those utilized by Gowan and Ortega-Ortiz (2014). These data were collected by multiple organizations and not all of them collected distances to sightings; those that did not cannot be utilized by our modeling procedure. We have opened communications with these organizations and hope to establish a collaboration that would allow us to update this model in the future using the appropriate data from the southeast. Also, the NOAA Southeast Fisheries Science Center conducted some surveys within this region as part of the AMAPPS surveys from 2010-2014. We requested these data from NOAA several times during our analysis but NOAA did not provide them before our models were finalized. Very recently (February of 2015) NOAA has started to release them, and we plan to incorporate them into the next major revision of our models.

Spring

In this season, all three models were identical in the Calving and Migration Area, and the two climatological-predictor models were also identical in the Feeding Grounds region. Therefore the choice of which model to use came down to whether the contemporaneous model performed better or worse in the Feeding Grounds than the climatological models. There, the climatological models explained slightly higher deviance (32.3% vs. 29.7%) and predicted slightly higher abundance (263 vs. 258) than the contemporaneous model. On the basis of higher explained deviance, we selected the climatological-predictor model that considered all segments as our best estimate of right whale distribution and abundance during this season.

We noted that the Calving and Migration Area model discarded the day of year predictor and retained only distance to shore. The result was a static prediction showing right whales distributed along the entire eastern seaboard during this two-month season. It is generally believed that abundance shifts north during these months as right whales migrate to the feeding grounds, but we lack the data to model this dynamic at present, at least with our current methodology. As with winter, our models could be improved by incorporation of additional survey data, particularly in the southeast.

We also believe our models could be improved with additional survey data for Cape Cod Bay, where right whales aggregate in Cape Cod Bay in winter and early spring to feed (Costa et al. 2006). As noted in our discussion of the winter models, we hoped to utilize survey data from the Provincetown Center for Coastal Studies (CCS), but the data were unsuitable for the distance sampling methodology that we used. CCS reported that they documented 45-50% of the extant photographically-cataloged right whales in Cape Cod Bay and adjacent waters during their winter/spring survey period for each of the years 2007-2010 (Stamieszkin et al. 2010). But our selected model predicted that abundance was higher north and east of Cape Cod Bay than within it. This raised the question: was our model's density prediction for Cape Cod Bay too low?

A direct comparison to the CCS results is difficult; CCS reported relative density, i.e. number of right whales identified per 100 nm of survey effort, while we reported absolute density, i.e. number of right whales per 100 square km. But CCS also reported the number of "whale days", computed as the sum of the number of days each individual was observed to be within CCB. CCS reported these results on a yearly basis for the years 1998-2007 (Jaquet et al. 2007) and 2010 (Stamieszkin et al. 2010). The range of whale days for Cape Cod Bay and just north of it (CCS survey tracks 1-15) ranged from less than 50 in 2002 to approximately 400 in 2000, with a mean of roughly 200. The total abundance estimated by our selected model for this region was roughly 8.7 animals, and the duration of our two-month "spring" season was 61 days, yielding a "whale days" estimate of 531. This suggests our model's density prediction may not be too low, at least relative to what has been reported by the CCS surveys.

This raised the question: is our model's prediction too high, or is CCS's "whale days" estimate too low? We cannot say without further detailed study. Our model was built from data spanning the entire Gulf of Maine; it seems unlikely that it would be highly accurate in any given small region, even if it was reasonable for the broad study area The CCS survey region spans only 17 of our model cells, which is quite small. On the other hand, the accuracy of the CCS residency estimates depend on the frequency with which they are able to repeat their surveys during a given year, which can depend on weather, funding, and so on. If surveying is infrequent, the residency estimates will be biased low, due to the increased time that whales occupy the Bay before they are first observed and after they are last observed.

In conclusion, we believe our model's estimates for Cape Cod Bay are reasonable when considered in the context of regional-scale patterns, but advise caution when considering the predictions at the scale of a few grid cells in isolation. We also recommend that future surveys of Cape Cod Bay be conducted in a way that facilitates analysis with distance sampling methodology. The main change required to the CCS survey protocols is that observers should measure vertical angles to sightings, so that perpendicular distances from the survey tracklines may be calculated.

In the Calving and Migration area, our model would benefit from aerial surveys conducted by NOAA as part of the AMAPPS program in portions of March or April of of 2011, 2012, 2013, and 2014. We requested these data from NOAA several times during our analysis but NOAA did not provide them before our models were finalized. Very recently (February of 2015) NOAA has started to release them, and we plan to incorporate them into the next major revision of our models.

Finally, we note that the North Atlantic Right Whale Consortium's most recent "best estimate" of alive, photographically-cataloged right whales was 522 individuals (Pettis and Hamilton 2014), which is significantly larger than our selected model's estimate of 416. Please see the discussion of the Summer model, below, for our interpretation of this difference.

Summer

In this season, the two climatological-predictor models explained more deviance than the contemporaneous-predictor model (33.8% and 31.2% vs. 30.8%, respectively). The three models predicted a similar mean abundance, ranging from 364-379 whales. Of these, 10 were from the southern on-shelf region where we estimated mean density for the region from the single sighting that occurred there. The three models all predicted high density in the Great South Channel and along the northwest edge of Georges Bank, with lower density in the central Gulf of Maine, diminishing west and north toward shore. We selected the climatological-predictor model that considered all segments as our best estimate of right whale distribution and abundance during this season, on the basis of it explaining the most deviance.

The North Atlantic Right Whale Consortium's most recent "best estimate" of alive, photographically-cataloged right whales was 522 individuals (Pettis and Hamilton 2014). The Consortium cautioned that "This 'best estimate' is based upon the number of photographed whales, but it excludes potential unphotographed whales, and therefore should not be considered a 'population estimate' ", implying that the "best estimate" may be an underestimate of the true population size. In any case, our selected model's estimate, 379, was substantially lower.

We can offer several possible explanations for this difference. First, our models were built on surveys performed over the period 1992-2014 but our methodology did not account for changes in the overall population size (e.g. by including year as a covariate); doing so would be very difficult due to the heterogeneous spatiotemporal distribution of the surveys. Using a photographic census, the North Atlantic Right Whale Consortium estimated the right whale population size to be about 300 in 1992 but over 500 in 2013 (Pettis and Hamilton 2014). By incorporating data from across this period without correcting for population growth, our model was prone to underestimate abundance for 2013 and overestimate abundance for 1992.

Second, as discussed in the g(0) Estimates section, studies of right whale diving behavior reported inconsistent dive durations on the northern feeding grounds, with mean dive durations ranging from 1.54 to 12.17 min. We assumed 5.65 min, resulting in an availability bias for aerial surveys of 0.334. Had we assumed 12.17 min, availability bias would have been 0.216, which would have increased our abundance estimate for the feeding grounds by approximately 50%.

Finally, we note that our "summer" model predicted high abundance along the northern edge of Georges Bank, right along the edge of the modeled region. Right whales have been sighted north of here in the region we were not able to model, and have been observed to move extensively about the Gulf of Maine (CETAP 1982, Baumgartner and Mate 2005). Although the population largely shifts northward later in the year, it is likely that some portion of it was north of the modeled area during our "summer" months as well, resulting in an underestimation of total abundance by the model. We recommend additional surveying in Canada in May-July, so that the timing of the northern shift can be better characterized.

Fall

In this season, the two climatological-predictor models explained more deviance than the contemporaneous-predictor model (46.1% and 45.0% vs. 43.9% abundance, respectively). The predicted mean seasonal abundance for the three models ranged from 334-513, with the climatological model fitted to all segments predicting the lowest and the other two models predicting greater abundance, mainly around Nova Scotia. We selected the climatological model that considered all segments as our best estimate of right whale distribution and abundance during this season, on the basis of it explaining the most deviance.

In New England and Canada, the model predicted a patchy distribution that matched known aggregations, including the lower Bay of Fundy and Roseway Basin (Winn et al. 1986), Jeffreys Ledge (Weinrich et al. 2000), and the central Gulf of Maine (Cole et al. 2013), with lower density predicted in the Great South Channel. The model predicted patches of moderate to high density northeast of Roseway Basin throughout the middle of the Scotian Shelf. No sightings were reported in this area, but surveying was very sparse and only occurred in August. Mellinger et al. (2007) reported acoustic detections of right whales southwest of Emerald Bank in August-December 2004 and late June to mid-August 2005, when the study ended, and concluded that the peak number of whales occurred in this region between August and October. To better characterize the possible distribution of right whales on the Scotian Shelf during late summer and fall, we recommend additional surveying and acoustic monitoring of the Scotian Shelf region during the months of August through November.

The model predicted right whales were virtually absent south of New York. Other evidence suggests otherwise. Whitt et al. (2013) reported acoustic detections of right whales off New Jersey in August-December 2008 and August-November 2009, peaking in September both years; shipboard surveys conducted at the same time did not report any sightings in the months of August-October. Hodge et al. (2015) reported acoustic detections of right whales south of Cape Lookout, North Carolina on 3-5% of the days of the months of June, July, and September 2012. Near the Georgia-South Carolina border, they reported detections every month between June 2012 and March 2013, with detections of on 5-10% of the days in August-October. Norris et al. (2014) reported acoustic detections of right whales at the shelf break off Jacksonville, Florida in September of 2010. Finally, Knowlton et al. (2002) reported sightings in September and October near eight ports from New York to Savannah aggregated from various sources (none utilized in our model).

Until sightings of right whales are obtained by visual line-transect surveys in the mid-Atlantic and southeast, our modeling approach will have no means by which to estimate non-zero density in this region. Given the critical status of the North Atlantic right whale population, we recommend additional surveying be conducted throughout the U.S. EEZ south of 40 N in

September and October. Surveys should be conducted with a protocol that is compatible with distance sampling (Buckland et al. 2001), which requires collection of data sufficient to estimate perpendicular distances to sightings. We also recommend that acoustic monitoring be expanded, and that researchers utilizing this technology design their studies to facilitate density estimation. This may require additional investment in methodological development.

Finally, we note that the North Atlantic Right Whale Consortium's most recent "best estimate" of alive, photographically-cataloged right whales was 522 individuals (Pettis and Hamilton 2014), which is significantly larger than our selected model's estimate of 334. Please see the discussion of the Summer model, above, for our interpretation of this difference.

References

Barlow J (1999) Trackline detection probability for long diving whales. In: Marine Mammal Survey and Assessment Methods (Garner GW, Amstrup SC, Laake JL, Manly BFJ, McDonald LL, Robertson DG, eds.). Balkema, Rotterdam, pp. 209-221.

Baumgartner MF, Mate BR (2003) Summertime foraging ecology of North Atlantic right whales. Marine Ecology Progress Series 264: 123-135.

Baumgartner MF, Mate BR (2005) Summer and fall habitat of North Atlantic right whales (Eubalaena glacialis) inferred from satellite telemetry. Canadian Journal of Fisheries and Aquatic Sciences 62: 527-543.

CETAP (1982) A characterization of marine mammals and turtles in the mid-and north Atlantic areas of the US outer continental shelf. Final Report. Bureau of Land Management, Washington, DC. Ref. AA551-CT8-48.

Carretta JV, Lowry MS, Stinchcomb CE, Lynn MS, Cosgrove RE (2000) Distribution and abundance of marine mammals at San Clemente Island and surrounding offshore waters: results from aerial and ground surveys in 1998 and 1999. Administrative Report LJ-00-02, available from Southwest Fisheries Science Center, P.O. Box 271, La Jolla, CA USA 92038. 44 p.

Chelton DB, Schlax MG, Samelson RM (2011) Global observations of nonlinear mesoscale eddies. Prog. Oceanogr. 91: 167-216.

Cole TVN, Hamilton P, Henry AG, Duley P, Pace RM, et al. (2013) Evidence of a North Atlantic Right Whale Eubalaena Glacialis Mating Ground. Endangered Species Research 21: 55-64.

Costa AD, Durbin EG, Mayo CA (2006) Variability in the nutritional value of the major copepods in Cape Cod Bay (Massachusetts, USA) with implications for right whales. Marine Ecology 27: 109-123.

Dawicki, S. (2011) High Number of North Atlantic Right Whales Sighted off Rhode Island. Press release SS11.02, April 29, 2011. U.S. Department of Commerce, National Oceanic and Atmospheric Administration.

Firestone J, Lyons SB, Wang C, Corbett JJ (2008) Statistical modeling of North Atlantic right whale migration along the mid-Atlantic region of the eastern seaboard of the United States. Biological Conservation 141: 221-232.

Good CP (2008) Spatial Ecology of the North Atlantic Right Whale (Eubalaena Glacialis). PhD Thesis, Duke University, Durham, North Carolina.

Gowan TA, Ortega-Ortiz JG (2014) Wintering Habitat Model for the North Atlantic Right Whale (Eubalaena glacialis) in the Southeastern United States. PLoS ONE 9(4): e95126.

Hain JHW, Ellis SL, Kenney RD, Slay CK (1999) Sightability of right whales in coastal waters of the southeastern United States with implications for the aerial monitoring program. Marine Mammal Survey and Assessment Methods. Rotterdam: Balkerma. pp. 191-207.

Hiby L (1999) The objective identification of duplicate sightings in aerial survey for porpoise. In: Marine Mammal Survey and Assessment Methods (Garner GW, Amstrup SC, Laake JL, Manly BFJ, McDonald LL, Robertson DG, eds.). Balkema, Rotterdam, pp. 179-189.

Hodge K, Muirhead C, Morano J, Clark C, Rice A (2015) North Atlantic right whale occurrence near wind energy areas along the mid-Atlantic US coast: implications for management. Endangered Species Research 28: 225-234.

Jaquet N, Mayo CA, Osterberg D, Browning CL, Marx MK (2007) Surveillance, monitoring and management of North Atlantic right whales in Cape Cod Bay and adjacent waters. PCCS/DMF annual report. Provincetown Center for Coastal Studies, Provincetown, MA.

Keller CA, Garrison L, Baumstark R, Ward-Geiger LI, Hines L (2012) Application of a habitat model to define calving habitat of the North Atlantic right whale in the southeastern United States. Endangered Species Research 18: 73-87.

Kenney RD, Winn HE, Macaulay MC (1995) Cetaceans in the Great South Channel, 1979-1989: right whale (Eubalaena glacialis). Continental Shelf Research 15: 385-414.

Knowlton AR, Ring JB, Russell B (2002) Right whale sightings and survey effort in the Mid Atlantic Region: Migratory corridor, time frame, and proximity to port entrances. Report submitted to the NMFS Ship Strike Working Group, Silver Spring, Maryland. Available online: http://www.nero.noaa.gov/shipstrike/midatanticreportrFINAL.pdf

Mellinger DK, Nieukirk SL, Matsumoto H, Heimlich SL, Dziak RP, et al. (2007) Seasonal Occurrence of North Atlantic Right Whale (Eubalaena glacialis) Vocalizations at Two Sites on the Scotian Shelf. Marine Mammal Science 23: 856-867.

Mitchell E, Kozicki VM, Reeves RR (1986) Sightings of Right Whales, Eubalaena glacialis, On The Scotian Shelf, 1966-1972. Rep. Int. Whal. Comm. Spec. Issue 10: 83-107.

Nieukirk S (1992) Satellite Monitored Dive Characteristics of the Northern Right Whale, Eubalaena glacialis. Master's Thesis, Oregon State University. Available online: http://ir.library.oregonstate.edu/xmlui/handle/1957/36164

Norris TF, Oswald JO, Yack TM, Ferguson EL (2014) An Analysis of Marine Acoustic Recording Unit (MARU) Data Collected off Jacksonville, Florida in Fall 2009 and Winter 2009-2010. Final Report. Submitted to Naval Facilities Engineering Command (NAVFAC) Atlantic, Norfolk, Virginia, under Contract No. N62470-10-D-3011, Task Order 021, issued to HDR Inc., Norfolk, Virginia. Prepared by Bio-Waves Inc., Encinitas, CA. 21 November 2012. Revised January 2014.

Palka DL (2005b) Shipboard surveys in the northwest Atlantic: estimation of g(0). In: Proceedings of a Workshop on Estimation of g(0) in Line-Transect Surveys of Cetaceans (Thomsen F, Ugarte F, Evans PGH, eds.). European Cetacean Society's 18th Annual Conference; Kolmarden, Sweden; Mar. 28, 2004. pp. 32-37.

Palka DL (2006) Summer Abundance Estimates of Cetaceans in US North Atlantic Navy Operating Areas. US Dept Commer, Northeast Fish Sci Cent Ref Doc. 06-03: 41 p.

Pettis HM, Hamilton PK (2014) North Atlantic Right Whale Consortium 2014 annual report card. Report to the North Atlantic Right Whale Consortium, November 2014.

Schick RS, Halpin PN, Read AJ, Slay CK, Kraus SD, et al. (2009) Striking the right balance in right whale conservation. Canadian Journal of Fisheries and Aquatic Sciences 66: 1399-1403.

Stamieszkin K, Ganley L, Mayo CA, Leeney RH, Marx MK (2010) Surveillance, Monitoring and Management of North Atlantic Right Whales in Cape Cod Bay and Adjacent Waters - 2010 Final Report. Provincetown Center for Coastal Studies, Provincetown, MA.

Waring GT, Josephson E, Maze-Foley K, Rosel PE, eds. (2014) U.S. Atlantic and Gulf of Mexico Marine Mammal Stock Assessments – 2013. NOAA Tech Memo NMFS NE 228; 464 p.

Weinrich MT, Kenney RD, Hamilton PK (2000) Right whales (Eubalaena glacialis) on Jeffreys Ledge: A habitat of unrecognized importance? Marine Mammal Science 16: 326-337.

Whitt AD, Dudzinski K, Laliberte JR (2013) North Atlantic right whale distribution and seasonal occurrence in nearshore waters off New Jersey, USA, and implications for management. Endangered Species Research 20: 59-69.

Winn HE, Goodyear JD, Kenney RD, Petricig RO (1995) Dive patterns of tagged right whales in the Great South Channel. Continental Shelf Research 15: 593-611.

Winn HE, Price CA, Sorensen PW (1986) The Distributional Biology of the Right Whale (Eubalaena glacialis) in the Western North Atlantic. Rep. Int. Whal. Comm. Spec. Issue 10: 129-138.